Interim Report

I-A2049-20

SOLUTION OF THE STABILITY PROBLEM FOR 360° SELF-ACTING, GAS-LUBRICATED BEARINGS OF INFINITE LENGTH

by

V. Castelli
H. G. Elrod, Jr.

March 1963

Prepared under
Contract Nonr-2342(00)(FBM)
Task NR 062-316

Jointly Supported by

Department of Defense
Atomic Energy Commission
Maritime Administration
National Aeronautics and Space Administration

Administered by
Office of Naval Research
Department of the Navy

THE FRANKLIN INSTITUTE
LABORATORIES FOR RESEARCH AND DEVELOPMENT
PHILADELPHIA PENNSYLVANIA

THE FRANKLIN INSTITUTE • *Laboratories for Research and Development*

I-A 2049-20

Interim Report

SOLUTION OF THE STABILITY PROBLEM FOR 360° SELF-ACTING, GAS-LUBRICATED BEARINGS OF INFINITE LENGTH

by

V. Castelli
H. G. Elrod, Jr.

March 1963

Prepared under
Contract Nonr-2342(00)(FBM)
Task NR 062-316

Jointly Supported by

Department of Defense
Atomic Energy Commission
Maritime Administration
National Aeronautics and Space Administration

Administered by
Office of Naval Research
Department of the Navy

ABSTRACT

This is an investigation of the stability of self-acting, gas-lubricated bearings. Two approaches to the solution are presented and their results are compared. Also, the relation is discussed between the present work and other, more simplified, methods available in the literature. The particular case of a 360° journal bearing of infinite length is treated, and the changes necessary to use the same theories with other geometries are pointed out. Available experimental results are collected and compared with theory.

ACKNOWLEDGEMENT

This research was performed under Contract Nonr-2342(00) administered by the Office of Naval Research, and supported jointly by the Department of Defense, Atomic Energy Commission, and Maritime Administration. The authors are indebted to Captain W. T. Sawyer and Mr. S. W. Doroff, Office of Naval Research, for their assistance and cooperation.

This effort was conducted at The Franklin Institute in the Friction and Lubrication Branch under the management of W. W. Shugarts, Jr., who provided continuous cooperation and assistance. The authors are grateful for the encouragement and technical advice offered by Professor D. D. Fuller, who is responsible for the initiation and coordination of the entire gas bearing research at The Franklin Institute. Special recognition is due to Messrs. S. Malanoski and C. H. Stevenson for their indispensable technical help in coordinating and carrying out many phases of the program, and to Mr. W. Ruegner who programmed the Univac I finite-orbit solution.

Mr. James C. Reid of Bureau of Ships and the extremely helpful staff of the Applied Mathematics Laboratory of the David Taylor Model Basin made the execution of this program possible by making available their high speed electronic computers.

The authors are thankful to Dr. W. A. Gross, Ampex Corporation, Redwood City, California, and Dr. J. S. Ausman, Litton Industries, Inc., Woodland Hills, California, for helpful discussions and constructive criticism.

TABLE OF CONTENTS

TABLE OF CONTENTS (cont'd.)

I. INTRODUCTION

1. Instabilities of Gas-Lubricated Bearings and Related Problems - Review of Pertinent Literature

The development of fluid-film journal and thrust bearings coincided with the advent of the first engines in the latter half of the nineteenth century. Since then, many contributions have been made to practical bearing development, such as those of Towers, Michell, and Kingsbury and to theoretical bearing analysis by Petrov, Reynolds, Sommerfeld, and Harrison. In time, the demands on the performance of bearings have gradually climbed to high levels, especially during the rapid developments following World War II. Recent progress in modern technology has stimulated intensive research and development effort in bearings lubricated, not only by conventional liquid lubricants such as oil or water, but also by so-called "exotic" lubricants and gases.

Apparently Hirn was first in pointing out the feasibility of gaseous lubrication back in 1854. Harrison produced the first theoretical solutions for simple cases of the governing equations (infinitely long slider and journal bearings). Gas bearings are now being successfully utilized in applications where conventional lubricants and rolling element bearings cannot operate. Examples would be high temperature and cryogenic apparatus, inertial guidance components, low friction sensing elements such as glaucoma detectors and stress-strain testing machines, nuclear reactor circulators, and many others.

These applications take advantage of some peculiar properties of gas bearings such as the availability of the lubricant (often the ambient medium itself), low friction level, nearly total absence of contamination and of apparent inertia. However, together with these advantages there are many drawbacks, such as no boundary lubrication, need for extremely accurate machining and for very stable materials, low load-carrying capacity, a friction-to-load ratio higher than for liquids, susceptibility to dust or other impurities in the gas, and, most serious of all, frequent and seemingly unpredictable failures due to dynamic instability and system resonance.

According to their principle of operation, gas-lubricated bearings can be divided into two groups:

1. Externally pressurized bearings, in which the load-carrying capacity is due to the pressure of gas fed by a source and which then escapes through the narrow slit of the bearing clearance.

2. Self-acting bearings, in which the load-carrying capacity is generated by the relative motion of the bearing surfaces.

The phase shift between the line of displacement and load direction combined with a very low level of damping cause both these two apparently dissimilar types of bearings to be susceptible to self-excited instability. Namely, externally pressurized bearings are prone to the so-called "air hammer" phenomenon. This is also often encountered in valves and pressure regulators, and has been the subject of both experimental and theoretical work by Comolet [7], Fisher, Cherubim, and Fuller [13], Robinson and Sterry [29], Allen, Stokes, and Whitley [1], Rothe [30], Licht, Fuller, and Sternlicht [19], Richardson [27], [28], Licht, Fuller and Sternlicht [19], Licht [21], and Licht and Elrod [20].

The present investigation is concerned with the self-excited instability which arises in self-acting gas-lubricated journal bearings, and which is often referred to as "half-frequency whirl". The reason for this name is that this instability is characterised by orbital motion of the shaft in the direction of its rotation and at approximately half the rotational frequency (actually always somewhat less than half). This type of instability is generally very destructive since, for values of the rotational speed higher than the threshold, the orbital amplitude grows extremely rapidly until contact between shaft and bearing is achieved. Due to the poor boundary lubrication properties of gases, instantaneous failure is likely to occur. In general terms the likelihood of stability increases with decreasing load, speeds, and clearances.

Experimental evidence on the existence of this phenomenon and some of its characteristics can be found in numerous publications. Many of these are concerned with production and development and make an effort to classify and find remedies for instabilities. In this category are the work of Brix [3], Cole and Kerr [6], Drescher [9], Sixsmith [32], and Whitley and Betts [34]. Other experimentalists have been interested in establishing a more general body of knowledge and have often resorted to semi-empirical approaches. In this category, are the valuable contributions of Elwell [12], Elwell, Hooker, Sternlicht [11], Fisher, Cherubim, and Fuller [13], and others.

Due to severe mathematical difficulties, it was not until very recently that some conclusive theoretical work was performed. In the case of cylindrical journal bearings of perfect geometry and infinite length, concurrently with the present work three other approaches were attempted by Rentzepis and Sternlicht [26], Cheng [5], and Ausman [2]. Other valuable contributions in this general field were made by Gross, [15], [17], Pan and Sternlicht [24], and others. All these authors found it expedient to introduce into their analyses several severe approximations, the exact consequences of which have not yet been established. Namely, Rentzepis and Sternlicht neglected the effect of fluid film history, (time dependent terms). Cheng used approximate Galerkin analytical expressions for both steady-state pressure and transient distributions, and Ausman made certain severe assumptions on the relation between shaft velocity components. These assumptions can be justified only intuitively, and in a limited number of cases.

All above-mentioned analyses investigate stability with respect to small perturbations from equilibrium. No acceptable approach has yet been devised to solve the complete non-linear case of finite oscillations of the shaft center. Due to the fact that non-linearity exists in the space terms of the governing equations, even the attainment of steady state solutions necessitated the use of numerical methods, such as for the infinite-length complete journal bearing by Elrod and Burgdorfer [10], finite length complete journal bearings by Raimondi [25], flat and crowned sliders by Gross [16], and finite length partial cylindrical bearings by Stevenson and Castelli [33].

2. Purpose and Outline of the Present Investigation

The present work is concerned with establishing the ranges of parameters corresponding to stable operation in self-acting gas bearings. Even though the treatment included is limited to journal bearings of infinite length, the validity and effectiveness of the approaches employed can be extended without any difficulty in principle to many other bearing geometries. Two methods of attack are used, both of which take account of the time-dependent (history) terms in the equations of compressible lubrication, but which differ in the handling of non-linearities.

a) Small Perturbation Method:

Non-linearities are eliminated by restricting the analysis to possible shaft motions only while in a very narrow range about an equilibrium position. Recently, this approach was successfully employed by Licht and Elrod [20], in the study of "air-hammer" in externally pressurized gas bearings. This method of attack was outlined in a previous report [5].

b) Orbit Program:

The complete non-linear equations pertinent to the case are integrated by numerical methods to obtain the shaft-center orbits corresponding to any specified set of geometrical, running, and initial conditions. This solution, obtained by means of a high speed digital computer program provides an idealized experimental rig which operates obeying exactly the assumed governing equations. The importance of the orbit program is not to be underestimated since detailed information from actual experiments is at the present moment extremely difficult to obtain. The attainment of exact data is impeded by interference from extraneous factors, limitations on measurements, and dimensional requirements at the limit of present technological capabilities. Since it is expensive to establish complete stability maps by using the orbit program, its main value at present consists of serving as a check on the range of applicability of approximate methods, which then can be used for the determination of the thresholds over all ranges of parameters.

II. DEFINITION OF THE PROBLEM AND BASIC EQUATIONS

1. Reynolds' Equation

The following equations apply to the behavior of the gas in the clearance space:

Equation of Continuity,

Equation of Momentum,

Equation of Energy,

Equation of State.

As it is common in lubrication theory, the ratio of the clearance to any characteristic linear dimension of the bearing can always be taken much smaller than unity. Also the pressure gradient is locally tangent to the film so that no pressure variations exist across the clearance. The effects of fluid inertia and gravity are neglected in comparison to forces due to viscous stresses. The fluid is taken to be Newtonian with constant viscosity and with a molecular mean free path small with respect to the clearance. Due to the small thickness of the film and the presence of metal boundaries it is customary to assume an isothermal flow; this assumption is supported by an order of magnitude analysis presented by Elrod and Burgdorfer [10]. The rotating member is assumed to be absolutely rigid and to possess a large enough polar moment of inertia to keep the rotational speed essentially constant.

The general lubrication equation, known as "Reynolds' equation", is derived from these assumptions in Appendix 1.

$$\frac{1}{R^2}\frac{\partial}{\partial\theta}\left(P\frac{h^3}{\mu}\frac{\partial P}{\partial\theta}\right)+\frac{\partial}{\partial\beta}\left(P\frac{h^3}{\mu}\frac{\partial P}{\partial\beta}\right)=6\Omega\left[\frac{2}{\Omega}\frac{\partial(Ph)}{\partial t}+\frac{\partial(Ph)}{\partial\theta}\right] \tag{1}$$

Figure 1 represents the particular geometry treated in this work and suggests the following choices of dimensionless parameters

$$X=\frac{x_1}{c}, \tag{2a}$$

$$Y=\frac{y_1}{c}, \tag{2b}$$

$$H=\frac{h_1}{c}=\frac{c+x_1\sin\theta+y_1\cos\theta}{c}=1+X\sin\theta+Y\cos\theta \tag{2c}$$

Then it is natural to adopt the following parameters

$$\Lambda=\frac{6\mu\Omega R^2}{Pa\ c^2} \tag{2d}$$

$$T=\frac{\Omega}{2}t \tag{2e}$$

$$P = \frac{P_1}{P_a} \tag{2f}$$

$$\eta = \frac{\beta}{R} \tag{2g}$$

Definitions (2a through f) enable us to write Reynolds' equation in the form

$$\frac{\partial}{\partial\theta}\left(PH^3\frac{\partial P}{\partial\theta}\right) + \frac{L^2}{R^2}\frac{\partial}{\partial\eta}\left(PH^3\frac{\partial P}{\partial\eta}\right) = \Lambda\left[\frac{\partial(PH)}{\partial\theta} + \frac{\partial(PH)}{\partial T}\right] \tag{3}$$

for a bearing of finite length, which reduces to

$$\frac{\partial}{\partial\theta}\left(PH^3\frac{\partial P}{\partial\theta}\right) = \Lambda\left[\frac{\partial(PH)}{\partial\theta} + \frac{\partial(PH)}{\partial T}\right] \tag{4}$$

for our case.

Another commonly used form of Reynolds' equation is obtained by adopting

$$\psi = PH \tag{5}$$

as independent variable; the equivalent of equation (4) is:

$$\frac{\partial}{\partial\theta}\left(\psi H\frac{\partial\psi}{\partial\theta} - \psi^2\frac{\partial H}{\partial\theta}\right) = \Lambda\left(\frac{\partial\psi}{\partial\theta} + \frac{\partial\psi}{\partial T}\right) \tag{6}$$

Equation (6) is especially suitable for numerical treatment due to the fact that $\psi(\theta)$ is a much smoother function than $P(\theta)$, especially for large values of the bearing running parameter Λ, and lower truncation errors are thus ensured. For the case of isothermal films ψ physically represents the local mass content of the bearing clearance.

The definition of reference pressure P_a in the case of bearings of infinite length might give rise to ambiguities, and in this work it shall be handled in the following way: Consider an infinite bearing as the central region of a very long but finite bearing so that the gas film is in communication with the ambient. The ambient pressure can then be chosen as a meaningful reference. Perform now a cyclic integration in θ of equation (3). Due to the periodic nature of P and H and with $H = H(\theta,T)$ only, we have

$$\frac{L^2}{ZR^2}\oint\frac{\partial^2}{\partial\eta^2}\quad P^2H^3\quad d\theta = \Lambda\oint\frac{\partial(PH)}{\partial T}\,d\theta \tag{7}$$

or

$$\frac{\partial^2}{\partial\eta^2}\oint P^2H^3d\theta = \frac{2R^2\Lambda}{L^2}\frac{\partial}{\partial T}\oint PHd\theta \tag{8}$$

at steady state

$$\frac{\partial}{\partial T} = 0$$

and

$$\frac{\partial^2}{\partial\eta^2} \oint P^2H^3 d\theta = 0 \tag{9}$$

or

$$\oint P^2H^3 d\theta = A\eta + B \tag{10}$$

where A and B are constants.

Since the integral in (10) has the same value at both ends of the bearing, it must be that

$A = 0$

and

$$B = \oint P^2H^3 d\theta \text{ is dependent of } \eta. \tag{11}$$

The numerical value of B can now be obtained at one of the bearing ends of the bearing where, by definition $P = 1$.

$$B = \oint H^3 d\theta = \oint(1 + X \sin\theta + Y \cos\theta)^3 \; d\theta = 2\pi \left[1 + \frac{3}{2}(X^2 + Y^2)\right] \tag{12}$$

Equations (11) and (12) are called the "mass content rule" and were first introduced by Elrod and Burgdorfer [10]. For bearings which are of infinite length in the mathematical sense this rule can be applied also in non-steady conditions since $\partial/\partial\eta = 0$. Its validity can be extended to very long but finite bearings by adopting the following model: Consider the bearing is finite but long enough to have small η-derivatives everywhere. At zero speed the local mass content is everywhere the same; after starting, it will vary slowly to its steady state distribution. The bearing under study should then be of sufficient length to make the time constant of this process large in comparison to the period of any oscillation about the steady-state position (see eq. (8)). Use of equation (4) will now ensure the absence of any axial "leaks" and still retain meaningful relation to practical situations.

2. Equations of Motion

With the assumption of inflexible shaft, constant alignment, rigid bearing mount, and large polar moments of inertia, the equations of motion of the shaft reduce to those which apply to a point mass (namely the shaft center) as affected by the integrated pressure and viscous effects.

The fluid film exerts two types of forces on the shaft: normal pressure and tangential viscous stress. The pressure force has the following load carrying components per unit axial length.

$$\text{Pressure Force } F \begin{cases} \text{x-component} = F_x = R \oint p_1 \sin\theta \; d\theta \\ \\ \text{y-component} = F_y = R \oint p_1 \cos\theta \; d\theta \end{cases} \tag{13}$$

The frictional forces due to the viscous shear stress on the surface of the rotating shaft can be resolved into two parts:

a) a torque about the center of the shaft

$$\text{Friction Torque} = R^2 \oint S_f(\theta)\, d\theta \tag{14}$$

This term will not appear in this analysis because the assumption of constant angular velocity takes the place of the third equation of motion (balance of moments about the shaft center).

b) a resultant force through the shaft center which, in turn, can be decomposed into the components

$$\text{Friction force } K \begin{cases} \text{x-comp} = K_x = R \oint S_f \cos\theta\, d\theta \\ \text{y-comp} = K_y = -R \oint S_f \sin\theta\, d\theta \end{cases} \tag{15}$$

The expression for the shear stress is (see expression for μ in Appendix 1)

$$S_f = \mu \left.\frac{\partial \mu}{\partial \gamma}\right|_{\substack{\text{on shaft}\\ \text{surface}}} = \frac{h_1}{2R} \frac{\partial p_1}{\partial \theta} + \frac{\mu \Omega R}{h_1} - \frac{\mu}{h_1} \frac{\partial}{\partial \theta} \dot{h}_1 =$$

$$= \frac{c p_a}{2R} H \frac{\partial P}{\partial \theta} + \frac{\mu \Omega R}{cH} - \frac{\mu}{H} \frac{\partial}{\partial \theta} \dot{H} \tag{16}$$

Performing the integrations indicated in equations (15) we obtain (see Appendix 2):

$$\frac{K_x}{F} = \frac{c}{2R} \left[\frac{F_x}{F} + \frac{RP_a}{F} \left(-X \oint P \cos 2\theta\, d\theta + Y \oint P \sin 2\theta\, d\theta \right) + \right.$$
$$\left. - \frac{2}{3}\pi \frac{RP_a}{F} \Lambda \frac{Y(1 - \sqrt{1-\epsilon^2})}{\epsilon^2 \sqrt{1-\epsilon^2}} \right] \tag{17a}$$

$$\frac{K_y}{F} = \frac{c}{2R} \left[\frac{F_y}{F} + \frac{RP_a}{F} \left(X \oint P \sin 2\theta\, d\theta + Y \oint P \cos 2\theta\, d\theta \right) + \right.$$
$$\left. - \frac{2}{3}\pi \frac{RP_a}{F} \Lambda \frac{X(1 - \sqrt{1-\epsilon^2})}{\epsilon^2 \sqrt{1-\epsilon^2}} \right] \tag{17b}$$

It is evident that all terms in square brackets but the last are of order 1. Utilizing results obtained by Elrod and Burgdorfer [10] it is also possible to show that at least for values of ϵ up to 0.9, the last terms are also of order 1. Therefore the net force due to friction is of order c/R in comparison with the normal pressure forces. To retain consistency with the approximations made up to this point, the effect of the friction force will be neglected.

Then the equations of Motion reduce to

$$M \frac{d^2x_1}{dt^2} = F_x = R \oint p_1 \sin\theta \, d\theta \tag{18}$$

$$M \frac{d^2y_1}{dt^2} = F_y + W = R \oint p_1 \cos\theta \, d\theta + W \tag{19}$$

where W is the external load per unit axial length, and M is the rotor mass per unit axial length.

Transforming equations (18) and (19) into dimensionless form,

$$\frac{d^2X}{dT^2} = B \oint P \sin\theta \, d\theta \tag{20}$$

$$\frac{d^2Y}{dT^2} = B \oint P \cos\theta \, d\theta + B\,L \tag{21}$$

where

$$B = \frac{RP_a}{Mc\left(\frac{\Omega}{2}\right)^2} \tag{22}$$

and

$$L = \frac{W}{RP_a} \tag{23}$$

The problem studied in this report is then defined to be the determination of the stability threshold for the system described by equations (4) (or (6)), (20) and (21).

III. SMALL PERTURBATION TECHNIQUE

1. Linearization of the Equations

We shall treat now the system of equations (4), (20), and (21) as they are rewritten below for the purpose of ready visualization.

$$\begin{cases} \dfrac{\partial}{\partial\theta}\left(PH^3\dfrac{\partial P}{\partial\theta}\right) = \Lambda\left(\dfrac{\partial PH}{\partial\theta} + \dfrac{\partial PH}{\partial T}\right) & (24,a) \\[2ex] \dfrac{d^2X}{dT^2} = B\oint P\sin\theta\, d\theta & (24,b) \\[2ex] \dfrac{d^2Y}{dT^2} = B\oint P\cos\theta\, d\theta + B\,L. & (24,c) \end{cases}$$

Setting

$$\frac{d^2X}{dT^2} = \frac{d^2Y}{dT^2} = \frac{\partial PH}{\partial T} = 0$$

and assigning numerical values to L and Λ, we can, at least in principle, find a solution to system (24) in the form of values for X and Y, and a distribution $P(\theta)$; we shall call this an "equilibrium" solution and denote its coordinates by a subscript zero. Symbolically,

$$\Lambda,\ L \rightarrow X_o,\ Y_o,\ P_o(\theta). \tag{25}$$

Physically, this process is equivalent to giving the shaft a steady load, spinning it at a fixed rotational speed, and, by adding sufficient external damping, if necessary, letting it reach an equilibrium position.

Let us now consider small deviations from this equilibrium state, so that in system (24) we can use the following expressions:

$$X(T) = X_o + x(T) \tag{26,a}$$

$$Y(T) = Y_o + y(T) \tag{26,b}$$

$$P(\theta,T) = P_o(\theta) + p(\theta,T) \tag{26,c}$$

Limiting ourselves to cases for which x, y, and p and their derivatives are small in comparison to 1, 1, and P_0 respectively, we undertake the problem of determining for what range of values of the parameter B the perturbation quantities x, y, and p have an exponentially decaying behavior in time.

Introduction of definitions (26) into system (24), use of the above-mentioned relation between Λ, L, X_o, Y_o, and P_o, and the neglect of powers and crossproducts of perturbation terms as quantities of higher order, yields a corresponding set of linear equations

$$\frac{\partial^2 p}{\partial \theta^2} + f_2(\theta)\frac{\partial p}{\partial \theta} + f_3(\theta)\,p + f_4(\theta)\frac{\partial p}{\partial T} = f_5(\theta)\frac{dx}{dT} + f_6(\theta)\frac{dy}{dT} + f_7(\theta)\,x + f_8(\theta)\,y, \tag{27,a}$$

$$\frac{d^2 x}{dT^2} = B \oint p \sin\theta \, d\theta, \tag{27,b}$$

$$\frac{d^2 y}{dT^2} = B \oint p \cos\theta \, d\theta, \tag{27,c}$$

where

$$f_2(\theta) = 2\frac{P_o'}{P_o} + 3\frac{H_o'}{H_o} - \frac{\Lambda}{P_o H_o^{\,2}}, \tag{28,a}$$

$$f_3(\theta) = \frac{\Delta P_o'}{P_o^{\,2} H_o^{\,2}} - \left(\frac{P_o'}{P_o}\right)^2, \tag{28,b}$$

$$f_4(\theta) = -\frac{\Lambda}{P_o H_o^{\,2}}, \tag{28,c}$$

$$f_5(\theta) = \frac{\Lambda \sin\theta}{H_o^{\,3}}, \tag{28,d}$$

$$f_6(\theta) = \frac{\Lambda \cos\theta}{H_o^{\,3}}, \tag{28,e}$$

$$f_7(\theta) = \left\{-\frac{2\Lambda P_o'}{P_o H_o^{\,3}} + \frac{3H_o' P_o'}{H_o^{\,2}} - \frac{3\Delta H_o'}{H_o^{\,4}}\right\}\sin\theta + \left\{\frac{\Lambda}{H_o^{\,3}} - \frac{3P_o'}{H_o}\right\}\cos\theta, \tag{28,f}$$

$$f_8(\theta) = \left\{ -\frac{2\Lambda P_o'}{P_o H_o^3} + \frac{3H_o' P_o'}{H_o^2} - \frac{3\Lambda H_o'}{H_o^4} \right\} \cos\theta + \qquad (28,g)$$

$$- \left\{ \frac{\Lambda}{H_o^3} - \frac{3P_o'}{H_o} \right\} \sin\theta,$$

where a prime denotes differentiation with respect to θ.

The system of governing equations is now linear and the stability threshold can be determined by one of the well known standard methods such as the Routh-Hurwitz criterion.

2. Determination of the Stability Threshold

Taking the time Laplace transform as defined by

$$\bar{Q}(\theta, s) = \int_0^\infty Q(\theta, T) e^{-sT} \, dT \qquad (29)$$

of equations (27), we obtain

$$\frac{\partial^2 \bar{p}}{\partial \theta^2} + f_2(\theta) \frac{\partial \bar{p}}{\partial \theta} + [f_3(\theta) + s f_4(\theta)] \bar{p} =$$

$$= [s f_5(\theta) + f_7(\theta)] \bar{x}(s) + [s f_6(\theta) + f_8(\theta)] \bar{y}(s), \qquad (30,a)$$

$$s^2 \bar{x} = B \oint \bar{p} \sin\theta \, d\theta, \qquad (30,b)$$

$$s^2 \bar{y} = B \oint \bar{p} \cos\theta \, d\theta. \qquad (30,c)$$

The solution of system (30) is subject to the condition that $\bar{p}(\theta, s)$ be periodic with period 2π, or

$$\bar{p}(\theta, s) = \bar{p}(\theta + 2\pi, s). \qquad (31)$$

Since the coefficients $f_i(\theta)$, $i = 2, \ldots, 8$ of equation (30,a) are periodic with period 2π, condition (31) reduces to

$$\bar{p}(a, s) = \bar{p}(a + 2\pi, s) \qquad (32,a)$$

$$\left.\frac{\partial \bar{p}}{\partial \theta}\right|_{\theta = a} = \left.\frac{\partial \bar{p}}{\partial \theta}\right|_{\theta = a + 2\pi} \qquad (32,b)$$

where a is an arbitrary number which will be chosen to be zero. Therefore, the conditions to be associated with system (30) are

$$\begin{cases} \bar{p}(\theta, s) = \bar{p}(2\pi, s) & (33,a) \\ \left.\frac{\partial \bar{p}}{\partial \theta}\right|_{\theta = 0} = \left.\frac{\partial \bar{p}}{\partial \theta}\right|_{\theta = 2\pi} & (33,b) \end{cases}$$

Since $\bar{x}$ and $\bar{y}$ are independent of θ, the solution of equation (30,a) is of the form

$$\bar{p}(\theta, s) = S(\theta, s)\ \bar{x}(s) + Q(\theta, s)\ y(s). \qquad (34)$$

Substitution of (34) into (30,b) and (30,c) will produce a system of two equations in $\bar{x}$ and $\bar{y}$, the determinant of the coefficients of which equated to zero is the so-called "characteristic" equation of the system.

$$\begin{cases} A_{11}\ \bar{x} + A_{12}\ \bar{y} = 0 \\ A_{21}\ \bar{x} + A_{22}\ \bar{y} = 0 \end{cases} \qquad (35)$$

$$\begin{vmatrix} A_{11} & A_{12} \\ A_{21} & A_{22} \end{vmatrix} = 0 \quad \text{"characteristic equation"} \qquad (36)$$

The sign of the real part of the zeroes of equation (36) indicates a decaying or growing exponential response of the system to a perturbation from equilibrium. Therefore, a negative real part denotes stability and a positive real part denotes instability and, in principle, the problem is solved.

Two difficulties arise in the practical execution of this scheme; on one hand, the coefficients f_i (θ), $i = 2, \ldots, 8$ are not known analytically but only numerically, and, on the other hand, the general form of the solution of an equation of the type of (30,a) is not known analytically but for a few particular cases. Both of these facts make it impossible to obtain analytical expressions for $S(\theta, s)$ and $Q(\theta, s)$.

As a consequence the dependence of S and Q on s cannot be kept explicit and the problem must be solved by trial and error. In order to simplify and reduce the volume of computations, and since the determination of the instability threshold, rather than of the actual response is the object of this analysis, only values of s on the imaginary axis are used. We may thus assume a value of zero for the real part of "s" and determine by trial-and-error the value of its imaginary part which will allow a single value of the dynamical parameter "B" to satisfy both the real and imaginary components of the characteristic equation. The following procedure is adopted:

a) Assign a value of $s = i\omega$ and solve equation (30,a) with conditions (33).

b) Obtain the characteristic equation, and solve for the values of the parameter B which are the zeroes of its real and imaginary parts. Check if the same value of B satisfies both real and imaginary parts. If not, go to a new guess of s.

c) When a solution is found, and B is the threshold value of the dynamical parameter, ω is the corresponding dimensionless frequency.

The actual solution is derived from the following manipulations.

Substituting expression (34) for $\bar{p}$ into equation (30,a) and separating the coefficients of $\bar{x}$ and $\bar{y}$, we have

$$S'' + f_2 S' + (f_3 + s f_4) S = s f_5 + f_7 \qquad (37,a)$$

$$Q'' + f_2 Q' + (f_3 + s f_4) Q = s f_6 + f_8 \qquad (37,b)$$

Now let

$$s = i\omega \qquad (38)$$

$$S = S_R + i S_N \qquad (39,a)$$

and

$$Q_E = Q_R + i Q_N \qquad (39,b)$$

and separate real from imaginary components. System (37) then becomes

$$\begin{cases} S_R'' + f_2 S_R' + f_3 S_R - \omega f_4 S_N = f_7 & (40,a) \\ S_N'' + f_2 S_N' + f_3 S_N + \omega f_4 S_R = \omega f_5 & (40,b) \end{cases}$$

$$\begin{cases} Q_R'' + f_2 Q_R' + f_3 Q_R - \omega f_4 Q_N = f_8 & (41,a) \\ Q_N'' + f_2 Q_N' + f_3 Q_N + \omega f_4 Q_R = \omega f_6 & (41,b) \end{cases}$$

The conditions on the solution of these equations are

$$\begin{cases} S_R(0) = S_R(2\pi) & (42,a) \\ S_R'(0) = S_R'(2\pi) & (42,b) \\ S_N(0) = S_N(2\pi) & (42,c) \\ S_N'(0) = S_N'(2\pi), & (42,d) \end{cases}$$

$$\begin{cases} Q_R(0) = Q_R(2\pi) & (43,a) \\ Q_R'(0) = Q_R'(2\pi) & (43,b) \\ Q_N(0) = Q_N(2\pi) & (43,c) \\ Q_N'(0) = Q_N'(2\pi) & (43,d) \end{cases}$$

Several methods of solution were tried for equations (40 through 43,d). A discussion of these methods can be carried out for any system of the type

$$\begin{cases} z''(x) + p(x)z'(x) + q(x)z(x) = r(x) & (44,a) \\ z(a) - z(b) = 0 & (44,b) \\ z'(a) - z'(b) = 0 & (44,c) \end{cases}$$

The solution of system (44) is unique because the corresponding homogeneous system

$$\begin{cases} z'' + pz' + qz = 0 \\ z(a) - z(b) = 0 \\ z'(a) - z'(b) = 0 \end{cases}$$

is "incomplete" and admits no non-trivial solution unless p or q contain a free parameter which is free to assume eigenvalues.

One well known method of solution of system (44) consists of obtaining two independent solutions of the homogeneous part of eq. (44,a) by solving the following system numerically:

$$\begin{cases} z_1'' + pz_1' + qz_1 = 0 \\ z_1(a) = 0 \\ z_1'(a) = 1 \end{cases} \qquad (45)$$

and

$$\begin{cases} z_2'' + pz_2' + qz_2 = 0 \\ z_2(a) = 0 \\ z_2'(a) = 1 \end{cases} \qquad (46)$$

Then the solution of [44a] is:

$$z = Az_1 + Bz_2 - z_1 \int_o^x \frac{z_2 r(x)}{W(x)} dx + z_2 \int_o^x \frac{z_1 r(x)}{W(x)} dx \qquad (47)$$

where A, B are constants

and $W(x)$ is the Wronskian of z_1 and z_2.

A and B are determined by using (44,b) and (44,c). A stable "self-starting" method such as that of Runge-Kutta-Gill [31] can be used for the solution of systems (45) and (46) but losses of accuracy in the numerical process can arise due to the fact that z_1, and z_2, have rather violent exponential behavior and assume values which span a range of $10^6 - 10^7$. When this "explosion" happens, it is very difficult to apply the boundary conditions and retain more than one or two significant figures. This inconvenience was actually encountered, since the problem was initially programmed according to this scheme. Attempts to improve the accuracy were frustrated especially in cases involving large values of Λ and ϵ.

A second method consists of solving system (44) by numerical relaxation or by adding a time derivative such as would be met in a diffusion equation and numerically develop an asymptotic solution. This method was also actually tried with very little success. The basic reason is the following: On one hand, the problem has "cyclic" boundary conditions only, therefore, there exists no a priori knowledge of the general level of the numerical values of the solution. On the other hand, due to the absence of actual boundaries where the values of dependent variable or its derivative are fixed, the numerical relaxation or diffusion process possesses very little internal damping so that it is very difficult to control numerical stability. As a consequence, extremely small "steps" are required to preserve numerical stability with consequently very long computation times to close the wide gap between inaccurate "starting guesses" and the final solution.

A third method was then developed. It consists of performing the following steps:

a) Solve the two problems

$$\begin{cases} z_I'' + pz_I' + qz_I = 0 \\ z_I(a) = M \\ z_I(b) = M \end{cases} \tag{48}$$

and

$$\begin{cases} z_{II}'' + pz_{II}' + qz_{II} = r \\ z_{II}(a) = M \\ z_{II}(b) = M \end{cases} \tag{49}$$

where M is an arbitrary number.

b) Form

$$z = z_{II} + Cz_I, \tag{50}$$

and impose condition (44,c)

$$z'(a) = z'(b)$$

to determine C.

We have

$$C = \frac{z_{II}'(b) - z_{II}'(a)}{z\,'(a) - z\,'(b)} \tag{51}$$

Then, since condition (44,b) is satisfied by z_I, z_{II}, and any linear combination of the two and since z as defined in equation (50) satisfies (44,a), we can say that

$$z(x) = z_{II}(x) + \frac{z_{II}'(b) - z_{II}'(a)}{z_I'(a) - z_I'(b)}\, z_I(x) \tag{52}$$

is the solution of system (44). Due to the fact that the solution of system (44) is unique the final result is independent of the choice of M as it can also be easily shown by direct substitution.

This method has been found to present several advantages over the previous two. In contrast with the first method, it does not let the solutions assume values which are too extraneous to the problem because the "two point" fictitious boundary conditions satisfied by z_I and z_{II} more closely represent the physical situation than those of systems (45) and (46). Moreover, it involves the least amount of computations and no numerical stability problem. Indeed, problems of the type of systems (48) or (49) can be numerically solved in the following way:

Divide the interval a-b of interest in N + 1 equal sub-intervals and write the differential equations at each of the N points dividing the intervals. Replace the dependent function and its derivatives by finite difference approximations; the simplest, and, most often, sufficiently accurate of these approximations are obtained with the so-called "three-point central difference" formulae, according to which

$$z'(x_i) \simeq \frac{z(x_{i+1}) - z(x_{i-1})}{2(b-a)/N} \tag{53}$$

$$z''(x_i) \simeq \frac{z(x_{i+1}) - 2\,z(x_i) + z(x_{i-1})}{(b-a)^2/N^2} \tag{54}$$

The solution gives rise to N linear algebraic equations in N unknowns

$$\begin{bmatrix} a_{11} & a_{12} & 0 & 0 & 0 & . & . & 0 \\ a_{21} & a_{22} & a_{23} & 0 & 0 & . & . & 0 \\ 0 & a_{32} & a_{33} & a_{34} & 0 & . & . & 0 \\ . & . & . & . & . & . & . & . \\ 0 & . & . & . & 0 & a_{N-1,N-2} & a_{N-1,N-1} & a_{N-1,N} \\ 0 & . & . & . & 0 & 0 & a_{N,N-1} & a_{NN} \end{bmatrix} \begin{bmatrix} z(x_1) \\ z(x_2) \\ z(x_3) \\ . \\ z(x_{N-1}) \\ z(x_N) \end{bmatrix} = \begin{bmatrix} R_1 \\ R_2 \\ R_3 \\ . \\ R_{N-1} \\ R_N \end{bmatrix} \tag{55}$$

Here the R_i's are known.

A matrix such as that of the coefficients of equations (55) is called "Tridiagonal" and any algebraic system of N equations with tridiagonal matrix can be easily solved by 3N explicit equation, in one unknown each. It is evident, then, that no numerical stability problem is encountered because no iterations are necessary, and that no error due to truncation of an asymptotic process ensues.

In the particular case under consideration, we are not dealing with one equation, but with two systems of two equations (system (40) and (41), with conditions (42) and (43)); however, no additional difficulty in principle is encountered. Indeed the algebraic equations resulting from reducing the equations from differential to finite difference form are of the type

$$\begin{aligned} a_i\, x_{i-1} + b_i\, x_i + c_i\, x_{i+1} + d_i y_i &= e_i \\ f_i\, y_{i-1} + g_i\, y_i + h_i\, y_{i+1} + i_i x_i &= j_i \end{aligned} \tag{56}$$

where x_o, y_o, x_{N+1}, y_{N+1}, are known.

The recurrence scheme which can be shown to lead to the solution of (56) is the following:

a) Let $A_1 = B_1 = D_1 = E_1 = 0$

and $C_1 = x_o$; $F_1 = y_o$

b) Use the recurrence relations

$$A_{i+1} = \frac{-Y_i c_i}{W_i Y_i - X_i Z_i}; \quad C_{i+1} = \frac{R_i Y_i - Z_i S_i}{W_i Y_i - X_i Z_i}; \quad E_{i+1} = \frac{-W_i h_i}{W_i Y_i - X_i Z_i};$$

$$B_{i+1} = \frac{Z_i h_i}{W_i Y_i - X_i Z_i}; \quad D_{i+1} = \frac{X_i c_i}{W_i Y_i - X_i Z_i}; \quad F_{i+1} = \frac{W_i S_i - R_i X_i}{W_i Y_i - X_i Z_i}; \tag{57}$$

for

$i = 1 \rightarrow N$

where

$$\begin{aligned} W_i &= b_i + a_i A_i \\ Z_i &= d_i + a_i B_i \\ R_i &= e_i - a_i C_i \\ X_i &= i_i + f_i D_i \\ Y_i &= g_i + f_i E_i \\ S_i &= j_i - f_i F_i \end{aligned} \tag{58}$$

c) Then the desired solutions are given by the recurrence relations

$$\begin{cases} x_i = A_{i+1}\, x_{i+1} + B_{i+1}\, y_{i+1} + C_{i+1} \\ y_i = D_{i+1}\, x_{i+1} + E_{i+1}\, y_{i+1} + F_{i+1} \end{cases} \tag{59}$$

$i = N \rightarrow 1$

which is started using the knowledge of x_{N+1} and y_{N+1}. Proof of the validity of this solution is given in Appendix 3. The method of solution for systems with simple tridiagonal matrices can be obtained from this procedure as a particular case.

At this point the solutions for $S_{R,N}$ and $Q_{R,N}$ (and therefore for $\bar{P}$) are available, and we can substitute in equations (30,b) and (30,c) to obtain the characteristic equation.

Define:

$$\oint S_{R,N} \begin{Bmatrix} \sin\theta \\ \cos\theta \end{Bmatrix} d\theta = \begin{Bmatrix} I_{R,N} \\ J_{R,N} \end{Bmatrix}, \tag{60,a}$$

$$\oint Q_{R,N} \begin{Bmatrix} \sin\theta \\ \cos\theta \end{Bmatrix} d\theta = \begin{Bmatrix} K_{R,N} \\ L_{R,N} \end{Bmatrix}. \tag{60,b}$$

The imaginary and real part of the characteristic equation are:

$$(I_R L_N - K_R J_N + I_N L_R - K_N J_R)\frac{B}{\omega^2} + (I_N + L_N) = 0 \tag{61,a}$$

$$(I_R L_R - I_N L_N - K_R J_R + K_N J_N)\left(\frac{B}{\omega^2}\right)^2 + (I_R + L_R)\frac{B}{\omega^2} + 1 = 0. \tag{61,b}$$

For one particular case it is possible to carry out the solution analytically. This is the case of an unloaded bearing, for which L = 0, and correspondingly,

$\epsilon_o = 0; \quad P_o(\theta) = 1.$

Then equations (40) and (41) become

$$\left\{\begin{aligned} S_R'' - \Lambda S_R' + \omega\Lambda S_N &= \Lambda\cos\theta \\ S_N'' - \Lambda S_N' - \omega\Lambda S_R &= \omega\Lambda\sin\theta \end{aligned}\right. \tag{62}$$

$$\left\{\begin{aligned} Q_R'' - \Lambda Q_R' + \omega\Lambda Q_N &= -\Lambda\sin\theta \\ Q_R'' - \Lambda Q_R' - \omega\Lambda Q_N &= \omega\Lambda\cos\theta \end{aligned}\right. \tag{63}$$

with boundary conditions (42) and (43). These equations can be solved analytically and yield

$$\left.\begin{aligned} S_R &= A\cos\theta + B\sin\theta \\ S_N &= C\cos\theta + D\sin\theta \end{aligned}\right\} \tag{64}$$

$$\left.\begin{aligned} Q_R &= B\cos\theta - A\sin\theta \\ Q_N &= D\cos\theta - C\sin\theta \end{aligned}\right\} \tag{65}$$

where

$$A = \Lambda\,[\Lambda^2(\omega^2 - 1) - 1]\,/\,\mathrm{Den},$$

$$B = -\Lambda^2\,[\Lambda^2(1 - \omega^2)^2 + (1 + \omega^2)]\,/\,\mathrm{Den},$$

$$C = 2\omega\,\Lambda^2/\mathrm{Den},$$

$$D = \omega\Lambda\,[\Lambda^2(1 - \omega^2) - 1]\,/\,\mathrm{Den},$$

$$\mathrm{Den} = (1 + \Lambda^2)^2 + \omega^2\Lambda^2\,[2(1 - \Lambda^2) + \omega^2\Lambda^2].$$

Evaluation and solution of the characteristic equation give the following results:

a) root of (61,a)

$$\frac{B_a\,\pi}{\omega^2} = -\frac{D \cdot \mathrm{Den}}{B \cdot D + A \cdot C} \tag{66}$$

b) roots of (61,b)

$$B_{\substack{b1\\b2}}\,\frac{\pi}{\omega^2} = \mathrm{Den}\,\frac{-B \pm \sqrt{D^2 - A^2 + C^2}}{B^2 - D^2 + A^2 - C^2} \qquad (67,a)\ (67,b)$$

3. Presentation and Discussion of Results

Because of the need for accurate steady state solutions, it was chosen to evaluate the stability threshold for all the solutions presented by Elrod and Burgdorfer [10]. The pressure distributions are available as functions discretized at 60 points and with an accuracy of six significant figures. The Univac I Computer CIO Program is still available at The Franklin Institute if runs for different parameters or more accuracy are required.

Let us define now

$$\nu = \frac{K}{p_a c}\,\frac{\sqrt{1 - \epsilon^2}}{\Lambda} \tag{68}$$

where "K" is the value of the product PH at a stationary point for the pressure, and

$$\epsilon = \sqrt{X^2 + Y^2} = \text{eccentricity ratio}$$

Any two of the four parameters ν, Λ, ϵ, L completely define the problem. A list of the computed cases is shown in Table 1. For each run a set of ω's from 0.0 to 2.0 was tried and results were plotted as shown by Figures 8 and 9. Intermediate results such as the functions of S_R, S_N, Q_R, Q_N were printed out and plotted. An example is shown by Figure 7. It can be seen that the functions are cyclic as required by the boundary conditions thus confirming the validity of the adopted methods.

Figure 10 contains a plot of the three roots (66), (67,a), (67,b). It is impossible to distinguish them from the ones obtained by the numerical procedure. From this figure it is also evident that the only points at which B_a meets any of the other two roots is at $\omega = 1$ and with a threshold value of the stability parameter equal to infinity. This is then a proof of the fact that at least in the small, unloaded bearings of infinite length are always unstable.

The complete results are presented as plotted in five different manners in Figures 2 through 6 and listed in Table 1a. Figure 2 presents the value of the parameter B at the threshold of instability which is associated with every computed point on a plot of C_L = (2L) vs Λ with lines of constant ν and ϵ_o. Figure 3 contains lines of constant ϵ_o, in a plot of Λ vs. $\omega_1{}^* = \sqrt{4/(LB)}$ and reproduces some of Cheng's [5] results. Figure 5 presents the results as plotted for $\omega_1{}^*$ vs. C*, where

$$\omega^* = \left(\frac{4\Lambda}{B^2}\right)^{0.2} = \frac{3}{2}\left(\frac{\mu M^2}{P_a{}^3}\right)^{0.2} \cdot \Omega \tag{69}$$

$$C^* = \left(\frac{2}{B\,\Lambda^2}\right)^{0.2} = M\left(\frac{P_a}{72\mu^2}\right)^{0.2} \cdot \frac{C}{R} \tag{70}$$

The parameters ω^* and C*, suggested by Rentzepis and Sternlicht, are physically very meaningful because they separate the effects of running speed and clearance. In this figure a comparison with sample Rentzepis and Sternlicht results is made. Figure 6 presents a comparison with some sample threshold values obtained by Ausman. The parameters used are Δ, ϵ_o, and

$$\Omega_a = \frac{M\,c\,\Omega^2}{2\,\pi\,R\,p_a} = \frac{2}{\pi\,B} \tag{71}$$

Strictly speaking, conclusions as to on which side of the stability threshold the stability region is located cannot be reached by the results of the small perturbation analysis, as so far described, but can actually be obtained several ways. First, practical experience shows that higher rotational speeds, larger clearance to diameter ratios, and larger masses, are all unstabilizing factors, thus leading to the conclusion that values of B between zero and the threshold correspond to instability. Second, it would be possible to obtain a solution for a value of "s" close to one of the computed intersections of the roots of the characteristic equation with the imaginary axis and observe the sign of the real part of s in conjunction with the variation of the value of the stability parameter B. In such a case it should be that a decreased value of B corresponds to a positive real part of "s". Third, the evaluation of the finite response orbit by direct integration, which is presented in section V of this work, can provide the answer by evaluating the journal orbit corresponding to values of B on either side of the threshold.

IV. FINITE SHAFT ORBIT EVALUATION

1. Finite Difference Form of Pertinent Equations.

This approach consists of taking the chosen set of governing equations, assuming that all functions involved are "well behaved" and smooth, and replacing the continuous character of the functions over the intervals of interest by their values at discrete points. The additional approximation of replacing derivatives at each point by algebraic combinations of the values of the functions at neighboring points reduces the problem from differential to algebraic. A set of integro-differential equations can be discretized by means of various techniques leading to more or less convenient algebraic schemes of solution. The choice of a technique is based mainly on three considerations: computation time, accuracy, and numerical stability. The last of these should not be confused with the stability of the system represented by the equations in question, but consists of a phenomenon which directly results from the discretization of the problem. Therefore, it does not exist in the differential system. Indeed the representation of a function by values at a finite number of points can only adequately represent harmonics whose wave-length is large in comparison to the point spacing. All higher harmonics are actually destroyed and replaced by a random distribution of round-off errors. As the function is operated upon by the system of equations in question (for example, as time goes on in a diffusion equation), the influence of the false higher harmonics leads to errors in the lower components. If the chosen process is not able to dampen out these errors, the true solution is soon obliterated and the phenomenon of numerical instability is said to have set in. Semantically, the term suggests the violently oscillating and diverging behavior of the values of the dependent variables as observed in this phenomenon. In a diffusion equation numerical instability can be generally avoided by adopting sufficiently small time steps. One can also intuitively see how a smaller size of discrete interval will increase the accuracy of the approximation. Therefore, in general, both the requirements of stability and higher accuracy can be met at the expense of longer computation time.

In writing the approximations to the derivatives of the department functions, one can achieve higher accuracy by involving more than the point itself and its two immediate neighbors. However, even with 5-point formulae, great complications are usually encountered in the treatment of the boundaries and initial conditions, as well as because of the presence of an increased number of unknowns in each equation. The treatments presented in this work are all concerned with three-point formulae.

In the integration of Reynolds' equation by numerical methods, either $\psi = PH$ or $\pi = P^2H^2$ was chosen as dependent variable, for two important reasons. First both $\psi(\theta)$ and $\pi(\theta)$ are smoother functions than $P(\theta)$ and finite difference approximations of them lead to smaller truncation errors. Second if $P(\theta)$ is the dependent variable, Reynolds' equation requires a knowledge of $\frac{\partial H}{\partial \tau}$, that is to say, a knowledge of the motion of the shaft. This requirement is inconvenient since, in most cases, the motion of the shaft is the output, rather than the input, to the problem. Therefore, the two forms of Reynolds' equation of interest are

$$\frac{\partial}{\partial \theta}\left[\psi H \frac{\partial \psi}{\partial \theta} - \psi^2 \frac{\partial H}{\partial \theta}\right] = \Lambda \left[\frac{\partial \psi}{\partial \theta} + \frac{\partial \psi}{\partial \tau}\right] \tag{72}$$

and

$$\frac{\partial}{\partial \theta}\left[\frac{H}{2}\frac{\partial \pi}{\partial \theta} - \pi \frac{\partial H}{\partial \theta}\right] = \frac{2\Lambda}{\sqrt{\pi}}\left[\frac{\partial \pi}{\partial \theta} + \frac{\partial \pi}{\partial \tau}\right] \tag{73}$$

For the purpose of general argument let us call the dependent variable ν and divide the θ - axis in intervals $\Delta\theta$ and the T-axis in intervals $\Delta\tau$. Then any of the modes of the space-time grid can be characterized by the pair of integers (i,j) where

$$\theta = i\,\Delta\theta \tag{74}$$

and

$$\tau = j\,\Delta\tau \tag{75}$$

Take:

$$\nu(\theta,\tau) = \eta\,\nu_i^{j+1} + (1-\eta)\,\nu_i^j \tag{76}$$

$$\frac{\partial\nu(\theta,\tau)}{\partial\theta} = \frac{\eta\,(\nu_{i+1}^{j+1} - \nu_{i-1}^{j+1}) + (1-\eta)\,(\nu_{i+1}^{j} - \nu_{i-1}^{j})}{2\,\Delta\theta} \tag{77}$$

$$\frac{\partial^2\nu}{\partial\theta^2}(\theta,\tau) = \frac{\xi\,(\nu_{i+1}^{j+1} - 2\,\nu_i^{j+1} + \nu_{i-1}^{j+1}) + (1-\xi)\,(\nu_{i+1}^{j} - 2\,\nu_i^{j} + \nu_{i-1}^{j})}{\Delta\theta^2} \tag{78}$$

$$\frac{\partial\nu}{\partial t}(\theta,\tau) = \frac{\nu_i^{j+1} - \nu_i^j}{\Delta\tau} \tag{79}$$

In the typical case of a progressive time integration, η and ξ represent the percentage of participation of the function at time $\tau = (j+1)\,.\,\Delta\tau$ as compared with time $\tau = j\,.\,\Delta\tau$. It is to be noticed that all values of ν_i^{j+1} are unknown for any i and that, therefore, if η and ξ are different from zero the finite difference equations replacing equations (72) and (73) contain three unknowns $(\nu_{i+1}^{j+1}, \nu_i^{j+1}, \nu_{i-1}^{j+1})$ while only for $\eta = \xi = o$ the number of unknowns is reduced to one (ν_i^{j+1}). According to the values adopted for η and ξ the following schemes are commonly used:

a) $\eta = \xi = o$. Explicit integration.

The finite difference problem is reduced in N algebraic equations in one unknown each of which can be explicitly solved for. This is by far the simplest scheme from the computational point of view.

b) $\eta = \xi = 1$. Implicit integration.

The system now contains N non-linear algebraic equations in 3 unknowns each. The solution of such a scheme can imply serious difficulties.

c) $\eta = \xi = ½$. Semi-implicit integration.

This method was first used by Crank-Nicolson [8] and possesses very attractive features which will be discussed later. However, it also involves the solution of a system of non-linear algebraic equations.

d) $\nu = o$, $\xi = 1$. Lee's Integration. (33)

It has some of the advantages of implicit schemes and results in a linear set of N algebraic equations in three unknowns each.

Other combinations of values of η and ξ can be used with special advantages to be derived in particular cases.

As far as the equations of motion are concerned, the linearity simplifies the problem considerably.

$$\begin{cases} \dfrac{d^2 X}{d T^2} = B \oint P \sin \theta \, d \theta & (80) \\ \dfrac{d^2 Y}{d T^2} = B \oint P \cos \theta \, d \theta + BL & (81) \end{cases}$$

The integrals on the right-hand side can be approximated by the trapezoidal rule, for it is well known that nothing is gained in applying more complex quadrature rules to cyclic integrations unless variable intervals and weights are used. The equations of motion reduce to:

$$\Delta \dot{X} = B \cdot \Delta \theta \cdot \Delta T \cdot \sum_{i=1}^{N} P_i^{\,j} \sin (i \, \Delta \theta) \tag{82,a}$$

$$\Delta X = \dot{X} \cdot \Delta T \tag{82,b}$$

$$\Delta \dot{Y} = B \cdot \Delta T \cdot \Delta \theta \cdot \sum_{i=1}^{N} P_i^{\,j} \cos (i \, \Delta \theta) \tag{83,a}$$

$$\Delta Y = \dot{Y} \cdot \Delta T \tag{83,b}$$

The evaluation of the orbits of the shaft can then be carried out by taking a set of running conditions, such as values for Λ, L, B, taking a set of initial conditions, such as P_i° (i = 1, ..., N), X_o, Y_o, $\dot{X}_o$, $\dot{Y}_o$. We use equations (82) and (83) and obtain X_2, Y_2, $\dot{X}_2$, $\dot{Y}_2$; go back to Reynolds' equation, and so on.

2. Choice of an Integration Method

A discussion of the relative merits of methods a, b, c, d has been published in May 1962 by Michael [23] of International Business Machines, San Jose, California. Pertinent considerations in the choice of a method are accuracy and stability. Let us discuss them separately.

a) Accuracy Considerations

The truncation errors connected with the integration schemes presented above are

a) $O\,[\,(\Delta\theta)^2 + \Delta T\,]$,

b) $O\,[\,(\Delta\theta)^2 + \Delta T\,]$,

c) $O\,(\,(\Delta\theta)^2 + (\Delta T)^2\,]$,

d) $O\,[\,(\Delta\theta)^2 + \Delta T\,]$·

We see that the error contributed by the θ-discretization is the same in all methods and can be reduced by using a finer grid size. As for the influence of the time step size ΔT, we see that the Crank-Nicolson method is better but that this advantage is soon lost if an increased ΔT is used, as allowed by the greater stability of this method (see section on "Stability Considerations"). Even though the order of magnitude of the error at each iteration is readily definable, it is difficult to estimate the effect of error propogation.

Some physical considerations might help in connection with this discussion. Knowing that Reynolds' equation obeys the principles of conservation of mass and since all the streamlines have been assumed to close on themselves and to be on a plane normal to the shaft axis. It is necessary that the mass content of any given axial length of bearing be conserved in time. An accumulation of error would show an effect on the mass content, since all other distributions are damped out in the diffusion process. In an infinite bearing, therefore, error propagation and accumulation can be monitored by periodic checking of the integral

$$\oint P H \, d\theta \qquad \text{or} \qquad \oint \psi \, d\theta$$

In addition, corrections can be performed by multiplying the pressure distribution by a factor which makes the mass content reassume the original value.

It is very doubtful whether considerations of accuracy alone will ever provide a strong enough argument in favor of any one of the proposed methods. Obviously, though, the choice of space step and time step size will be quite important in setting the general level of accuracy of the approximation. It will be shown later that the adopted method provides an accurate enough approximation to the exact solution.

b) Numerical Stability Considerations

The condition for numerical stability of a difference equation representing a diffusion process can be obtained by several methods. In many problems, it is very complicated to find analytically a sufficient criterion for stability which gives threshold values reasonably close to the actual ones. Then, in order not to waste computation time by following a safe, but very conservative criterion, it is convenient to proceed by trial and error. The following procedure will be followed to find a threshold value of the ratio $q = \frac{\Delta T}{(\Delta \theta)^2}$ setting the upper limit of the size of ΔT which will ensure numerical stability for a finite difference scheme using a space interval equal to $\Delta \theta$.

To analyze this problem, let us consider the differential equation in question as a linearized system of the type

$$\frac{\partial \psi}{\partial T} = \frac{1}{\Lambda} \left[H \psi \frac{\partial^2 \psi}{\partial \theta^2} - \psi^2 \frac{\partial^2 H}{\partial \theta^2} + H \left(\frac{\partial \psi}{\partial \theta} \right)^2 - \psi \frac{\partial \psi}{\partial \theta} \frac{\partial H}{\partial \theta} - \Lambda \frac{\partial \psi}{\partial \theta} \right] \tag{84}$$

Define now

$$F_1 = \partial \left(\frac{\partial \psi}{\partial T} \right) \Big/ \partial \psi, \tag{85,a}$$

$$F_2 = \partial \left(\frac{\partial \psi}{\partial T} \right) \Big/ \partial \left(\frac{\partial \psi}{\partial \theta} \right), \tag{85,b}$$

$$F_3 = \partial \left(\frac{\partial \psi}{\partial T}\right) \Big/ \partial \left(\frac{\partial^2 \psi}{\partial \theta^2}\right), \tag{85,c}$$

which are evaluated somewhere in the interval in accordance with the mean value theorem. In the following F_1, F_2, F_3 will be regarded as constant with the justification that the solution components causing instability vary at a much greater rate than these terms.
In infinite difference form we have

$$\frac{\nu_i^{j+1} - \nu_i^j}{\Delta T} = F_1 \left[\eta\, \nu_i^{j+1} + (1-\eta)\, \nu_i^j\right] + \frac{F_2}{2\,\Delta\theta}\left[\eta\,(\nu_{i+1}^{j+1} - \nu_{i-1}^{j+1}) + (1-\eta)\,(\nu_{i+1}^{j} - \nu_{i-1}^{j})\right] + \frac{F_3}{\Delta\theta^2}\left[\xi\,(\nu_{i+1}^{j+1} - 2\,\nu_i^{j+1} + \nu_{i-1}^{j+1}) + (1-\xi)\,(\nu_{i+1}^{j} - 2\,\nu_i^j + \nu_{i-1}^j)\right]. \tag{86}$$

If V_i^j is the exact solution to the set of finite difference equations (86) over the space and time grid, then the actual solution can be represented as the sum of the exact solution and the deviations ϵ_i^j.

$$\nu_i^j = V_i^j + \epsilon_i^j \tag{87}$$

Substitution of (87) into (86) and use of the fact that V_i^j satisfies (86) exactly, yield an equation in the disturbance

$$\frac{\epsilon_i^{j+1} - \epsilon_i^j}{\Delta T} = F_1\left[\eta\ \epsilon_i^{j+1} + (1-\eta)\,\epsilon_i^j\right] + \frac{F_2}{2\,\Delta\theta}\left[\eta\,(\epsilon_{i+1}^{j+1} - \epsilon_{i-1}^{j+1}) + (1-\eta)\,(\epsilon_{i+1}^{j} - \epsilon_{i-1}^{j})\right] + \frac{F_3}{\Delta\theta^2}\left[\xi\,(\epsilon_{i+1}^{j+1} - 2\,\epsilon_i^{j+1} + \epsilon_{i-1}^{j+1}) + (1-\xi)\,(\epsilon_{i+1}^{j} - 2\,\epsilon_i^j + \epsilon_{i-1}^j)\right] \tag{88}$$

The form of (88) is the same as that of (86) because of the fact that (86) is linear.

Equation (88) can be satisfied by

$$\epsilon\ (\theta,\ T) = \sum_{n=1}^{N} A_n\ e^{a_n T + \sqrt{-1}\, b_n\, \theta} \tag{89}$$

where every term of the series represents a solution. Substituting equation (89) into (88), we have for a representative term:

$$e^{a_n(T+\Delta T)+\sqrt{-1}\,b_n\theta} - e^{a_n T+\sqrt{-1}\,b_n\theta} =$$

$$= F_1\,\Delta T\left\{\eta\, e^{a_n(T+\Delta T)+\sqrt{-1}\,b_n\theta} + (1-\eta)\, e^{a_n T+\sqrt{-1}\,b_n\theta}\right\} +$$

$$+\frac{F_2\,\Delta T}{2\,\Delta\theta}\left\{\eta\left[e^{a_n(T+\Delta T)+\sqrt{-1}\,b_n(\theta+\Delta\theta)} - e^{a_n(T+\Delta T)+\sqrt{-1}\,b_n(\theta-\Delta\theta)}\right]+\right.$$

$$\left.+(1-\eta)\left[e^{a_n T+\sqrt{-1}\,b_n(\theta+\Delta\theta)} - e^{a_n T+\sqrt{-1}\,b_n(\theta-\Delta\theta)}\right]\right\}+$$

$$+F_3\frac{\Delta T}{\Delta\theta^2}\left\{\xi\left[e^{a_n(T+\Delta T)+\sqrt{-1}\,b_n(\theta+\Delta\theta)} - 2\,e^{a_n(T+\Delta T)+\sqrt{-1}\,b_n\theta}+\right.\right.$$

$$\left.+e^{a_n(T+\Delta T)+\sqrt{-1}\,b_n(\theta-\Delta\theta)}\right]+$$

$$+(1-\xi)\left[e^{a_n T+\sqrt{-1}\,b_n(\theta+\Delta\theta)} - 2\,e^{a_n T+\sqrt{-1}\,b_n\theta}+\right.$$

$$\left.\left.+e^{a_n T+\sqrt{-1}\,b_n(\theta-\Delta\theta)}\right]\right\} \tag{90}$$

or

$$e^{a_n\Delta T} - 1 =$$

$$= F_1\,\Delta T\left\{\eta\, e^{a_n\Delta T} + (1-\eta)\right\} +$$

$$+\frac{F_2\,\Delta T}{2\,\Delta\theta}\left\{\eta\left[e^{a_n\Delta T+\sqrt{-1}\,b_n\Delta\theta} - e^{a_n\Delta T-\sqrt{-1}\,b_n\Delta\theta}\right]+\right.$$

$$\left.+(1-\eta)\left[e^{\sqrt{-1}\,b_n\Delta\theta} - e^{-\sqrt{-1}\,b_n\Delta\theta}\right]\right\}+$$

$$+F_3\frac{\Delta T}{\Delta\theta^2}\left\{\xi\left[e^{a_n\Delta T+\sqrt{-1}\,b_n\Delta\theta} - 2\,e^{a_n\Delta T} + e^{a_n\Delta T-\sqrt{-1}\,b_n\Delta\theta}\right]+\right.$$

$$\left.+(1-\xi)\left[e^{\sqrt{-1}\,b_n\Delta\theta} - 2 + e^{-\sqrt{-1}\,b_n\Delta\theta}\right]\right\} \tag{91}$$

Collecting terms and using the complex exponential definition of the functions sin $(b_n \Delta \theta)$ and cos $(b_n \Delta \theta)$, we have

$$- e^{a_n \Delta T} \cdot \Big\{ - 1 + \eta F_1 \Delta T + \eta F_2 \sqrt{q \Delta T} \cdot (\sqrt{-1} \sin b_n \Delta \theta) +$$

$$+ 2 \xi F_3 q \quad 1 - \cos b_n \Delta \theta \Big] \Big\} =$$

$$= 1 + (1 - \eta) F_1 \Delta T + (1 - \eta) F_2 \sqrt{q \Delta T} (\sqrt{-1} \sin b_n \Delta \theta) +$$

$$+ 2 (1 - \xi) F_3 q \quad 1 - \cos b_n \Delta \theta \Big] \Big\} \tag{92}$$

$e^{a_n \Delta T}$ represents the ratio of error growth over one step ΔT and is dependent on the pertinent values of the coefficients b_n. A sufficient condition for stability is obviously that

$$\left| e^{a_n \Delta T} \right| \leq 1 \tag{93}$$

or

$$\left| \frac{1 - 4 (1 - \xi) F_3 q \sin^2 \frac{b_n \Delta \theta}{2} + O (\Delta T)}{- 1 - 4 \xi F_3 q \sin^2 \frac{b_n \Delta \theta}{2} + O (\Delta T)} \right| < 1 \tag{94}$$

or

$$\left| \frac{1 - 4 (1 - \xi) F_3 q \sin^2 \frac{b_n \Delta \theta}{2}}{1 + 4 \xi F_3 q \sin^2 \frac{b_n \Delta \theta}{2}} \right| < 1 \tag{95}$$

Referring to equation (84), we see that

$$F_3 = \partial \left(\frac{\partial \psi}{\partial T} \right) \Big/ \partial \left(\frac{\partial^2 \psi}{\partial \theta^2} \right) = \frac{H \psi}{\Lambda} \tag{96}$$

and by the physical nature of H, ψ, and Λ we know that

$$F_3 > 0 \tag{97}$$

Then:

a) For $\xi = o$ (explicit integration)

$$-1 < 1 - 4\frac{H\psi}{\Lambda} q \sin^2 \frac{b_n \Delta\theta}{2} < 1$$

or

$$1 - 4\frac{H\psi}{\Lambda} q \sin^2 \frac{b_n \Delta\theta}{2} > -1$$

The condition for numerical stability is

$$\frac{\Delta T}{(\Delta\theta)^2} = q < \frac{\Lambda}{2 H\psi} = \frac{\Lambda}{2 P H^2} \tag{98}$$

b) and d) $\xi = 1$ (implicit and Lee's Integration)

$$-1 < \frac{1}{1 + 4 F_3 q \sin^2 \frac{b_n \Delta\theta}{2}} > 1 \tag{99}$$

always satisfied.

c) $\xi = \frac{1}{2}$ (Crank-Nicolson Integration)

$$-1 < \frac{1 - 2\frac{H\psi}{\Lambda} q \sin^2 (\frac{b_n \Delta\theta}{2})}{1 + 2\frac{H\psi}{\Lambda} q \sin^2 (\frac{b_n \Delta\theta}{2})} < 1 \tag{100}$$

always satisfied.

We conclude then that the implicit, Lee's and Crank-Nicolson integration methods are stable regardless of the relative sizes of ΔT and $\Delta\theta$ whereas the explicit method must use values of ΔT limited by

$$\Delta T < \frac{(\Delta\theta)^2 \Lambda}{2 P H^2}$$

Difficulties seem to arise from the fact that this stability analysis gives a result dependent on the value of ψ which is unknown. The obtained bound on ΔT, however, is extremely useful in practice because the upper bound of ψ is either known by experience or could be calculated from the developing pressure profile and used to adjust the adopted value of ΔT.

At this point, it is important to notice that the apparent unbounded stability of methods b), c) and d) is probably not actual because, for large enough values of ΔT, most of linearizing assumptions made in this development cease to be valid. It is definitely true, however, that for these methods, ΔT can be allowed to assume values one or two orders of magnitude larger than those for the explicit method. Even considering the sharp contrast between the stability characteristic of explicit and implicit integration procedures, no general recommendations can be made on choice of a method without consideration of the particular problem at hand. Indeed, all implicit methods involve the solution of systems of simultaneous algebraic equations, entailing long computation times (partly overshadowing the advantages of improved stability), more complex programs (with proportionate debugging times), and the possibility of larger errors.

The solution of simultaneous algebraic equations can be very simple in a few particular cases, one of which consists of a set of linear equations with a tridiagonal matrix, mentioned in section IV. This matrix is actually encountered in the case of a slider or any one dimensional problem with two-point space boundary conditions. If the bearing is a complete cylinder, the matrix of the coefficient is tridiagonal but for the addition of the (I, N) and (N, 1) elements which already greatly complicate the solution. If the system of algebraic equations is non-linear, then relaxation methods must be used with ensuing long computations and possible truncation errors.

For cases in which the fluid film equation is coupled with the dynamical equations of motion of the bearing component parts, the problem of numerical stability must be studied for the whole system. Since any possible motion of the parts is contained in the variable ψ, the numerical stability condition for the finite difference form of Reynolds' equation must still be satisfied. It is possible, however, that more stringent restrictions must be imposed on the size of the time step ΔT so that the number of points that go into describing an orbit is sufficiently large to confine the error to high order harmonics. An accurate prediction of this limiting value of ΔT is made difficult by the fact that, in the equation of motion, all points influence the orbit of the center of the shaft at the same time. It will be seen that the response of the shaft center to a general set of initial conditions is composed of two main parts: a transient with dimensionless frequencies often much larger than unity, and a smooth orbit with frequency slightly below unity. In most cases of small initial disturbances, the transient response dies out and conclusions regarding system stability can be drawn from the smooth orbit. However, the integration procedure must be stable while the transient is being felt if a valid solution is desired for the following orbit. Since the number of points necessary to describe the transient is generally rather large, it happens that values of ΔT must be used which are of the same order of magnitude as those imposed by numerical stability conditions for explicit integration methods. It is then a waste to program the lengthy Lee and Crank-Nicolson procedures if their chief advantage is not exploited over most of the work. The Crank-Nicolson method has the added disadvantage that the error involved in each step increases as the square of the time step ΔT. Michael [23] indicates that this is not a problem in the range of ΔT characteristic of the situation at hand but it is possible that his conclusions were not obtained from a general enough set of tests to be valid in all cases.

Procedures b), c) and d) bring about considerable saving in cases where the relative motion of the surfaces is imposed as a smooth and relatively slowly varying function of time, and in the particular case of no motion. Indeed, in computational experiments designed to assess the relative value of the most common integration procedures, it was found that the explicit method had approximately the same speed as a relaxation procedure for the solution of steady state pressure distribution problems, whereas the Crank-Nicolson method was in the average 50-60 times faster in number of steps and 20-25 times faster in actual computation time. A very adequate relative evaluation of these methods is presented by Michael [23]. Forsythe and Wasow [14] treat this subject in general and have some reservations about the usefulness of the Crank-Nicolson method. Because of the number of assumptions that must be made in evaluating error bonds and stability characteristics of these methods especially in non-linear cases, it is quite possible that Reynolds' equation offers a particularly favorable application to some method which is only of limited general value.

In conclusion, the explicit method was used in orbit calculations because of the large number of points generally necessary to describe the journal path. The Crank-Nicolson method is advised for all calculations of steady pressure distributions or cases of smooth enough motion (by being externally imposed or for cases of large external damping).

3. Description of Special Features of Numerical Procedures.

In comparison to the computation time necessary to perform the iteration of Reynolds' equation, even when as few as 30 circumferential points are used, the dynamic equations are treated in zero time for all practical purposes. Many complex features can therefore be incorporated with an insignificant sacrifice in computer time.

One obvious generalization is the consideration of an arbitrary rotating unbalance force. It has been noticed by some experimental investigators that, in the case of gas bearings working with light external loadings, a limited amount of unbalance prevents failure by half-frequency whirl. Unbalance forces, of course, can always be made large enough to cause failure. Provision for the unbalance feature is incorporated in the program.

A second special feature was incorporated for the sole purpose of shortening computation time in evaluations of the stability threshold. When the value of the stability parameter B is close to the instability threshold the rate of convergence or divergence of the journal center orbit is small. If the orbit is now perturbed by transient oscillations of higher frequency, it becomes difficult to estimate whether the case is stable or unstable before a large number of orbits have been accumulated. Since most conclusions are drawn from the behavior of the shaft after the high frequency transient subsides, a discriminating artificial damper is applied to the shaft. This device operates as a linear viscous damper and acts with a force which is proportional to the vectorial difference between the actual journal center velocity and the velocity corresponding to half-frequency circular or elliptic whirl. The artificial damper is applied at the beginning of an orbit and is taken off after a specifiable number of steps as dictated by experience. The purpose is to smooth out the high frequency transient response in as small a number of steps as possible. It could be interpreted as letting the computer find by itself a set of "smooth" initial conditions.

The orbit programs are all versatile enough to accept changes of physical and running parameters while in orbit, thus being able to follow an acceleration procedure such as at "start-up" or a load variation in time.

Numerical instability detectors and automatic time step changes are also incorporated.

Some of the outputs are included in this paper. The pressure distributions are obtained only at intervals of time which are specified by the input. This selection is made in order to eliminate wasteful output time, but the possibility of following the pressure history is left. This feature is particularly important in connection with the assessment of the relative value and range of application of approximate theories. For example, the question of the relative size of the term $H \frac{\partial P}{\partial T}$ with respect to $P \frac{\partial H}{\partial T}$ and other terms in Reynolds' equation can be settled by direct computation from the values of the pressure at every point of the θ, T grid.

4. Presentation and Discussion of Results.

The whirl problem in cylincrical journal bearings was attacked in steps in order to acquire familiarity with available numerical techniques and develop and debug any new methods that might become necessary. The first problem solved was the case of the flat slider of infinite lateral extent with compressible lubrication. The geometry under consideration is shown in Fig. 11. This problem can be solved exactly by analytical methods and can provide an instructive check on the accuracy of the numerical techniques.

For this case, at steady state, Reynolds' equation is

$$\frac{d}{d\theta}\left(P H^3 \frac{dP}{d\theta}\right) = \Lambda \frac{d(PH)}{d\theta} \tag{101}$$

with $\theta = \beta + \alpha H$ (straight line) and can be solved by the following procedure:

let $\psi = P H$ and integrate once

$$\psi H^2 \frac{d(\psi/H)}{d\theta} = \Lambda\psi + \text{const.} \tag{102}$$

or, since $d\theta = \alpha\, d H$

$$\Lambda\alpha\psi + \psi^2 + C = \psi H \frac{d\psi}{dH}, \tag{103}$$

This equation can be separated as

$$\frac{\psi\, d\psi}{C + \Lambda\alpha\psi + \psi^2} = \frac{dH}{H}; \tag{104}$$

Now let $-\Lambda\alpha = q_1 + q_2$,

and $C = q_1 \cdot q_2$

Then:

$$\frac{\psi}{C + \Lambda\alpha\psi + \psi^2} = \frac{1}{(q_1 - q_2)}\left[\frac{\psi}{\psi - q_1} - \frac{\psi}{\psi - q_2}\right] \tag{105}$$

Integration of (104) yields:

$$\frac{\left|\psi - q_1\right|^{q_1}}{\left|\psi - q_2\right|^{q_2}} = E\, H^{(q_1 - q_2)} \tag{106}$$

where E, q_1, and q_2 can be found from the conditions

P leading edge = 1

P trailing edge = 1

$$q_1 + q_2 = -\Lambda\alpha \qquad (107)$$

Figures 12 and 13 show results of computations for two slider bearing cases. These calculations were made first by desk calculator, and later with the help of an IBM 650 computer. The initial pressure distribution was taken to be ambient throughout so that this situation resembles the problem of a suddenly accelerated wall. Besides the steady-state results and the exact solution, Figures 12 and 13 present pressure distribution curves at intermediate values of time corresponding to explicit integration. It should be noticed that high accuracy can be obtained by this procedure, but at the expense of a very large number of steps (in the neighborhood of 150-200 to reduce the truncation error to a fraction of 10^{-3}). The Crank-Nicolson method applied to the same cases achieves the same results in approximately 10 steps. Figure 12 also shows results obtained by Gross [16] by relaxation methods. This plot was drawn taking points from graphical data, so that the apparent slight discrepancy between Gross' results and the exact solution might be due to reading errors, rather than high truncation values. It is remarkable, though, that the computing times quoted by Gross as necessary for relaxation solutions are commensurate with explicit integration times.

After the successful completion of many slider-bearing runs, the complete journal-bearing dynamic problem was programmed for a Univac I computer at the Franklin Institute. The first successful set of orbits were obtained with programs employing P, PH, and P^2H^2 as independent variables. It was learned that the use of P was definitely detrimental to the accuracy of the solution, especially when high values of the running parameter Λ were involved. With an average speed of 5 seconds per time step it soon became a problem to keep computer time down to reasonable levels. Indeed, it had been hoped that fifteen time steps would suffice to describe one half-frequency orbit since at the time there was no published evidence on the existence of high frequency transients. It became then necessary to evaluate approximately 200 points per half-frequency orbit. Moreover, because of the very limited fast memory capacity of the Univac I computer, no more sophisticated integration methods could be used.

Fortunately then, the Bureau of Ships, U. S. Navy Department made available some time on their Remington Rand LARC and IBM 7090 high-speed computers at the David Taylor Model Basin in Washington. The LARC was chosen first, but the program had to be written in machine language, since no working pseudo-code was available at the time. Consequent debugging difficulties discouraged further use of that machine.

All subsequent work was conducted on the IBM 7090. The FORTRAN pseudo-code connected with the very efficient Bell system BE-SYS-3 and the very helpful staff of the Applied Mathematics Laboratory of D.T.M.B. made programming, debugging, and running very simple and expeditious. The remarkably high internal speed of this modern computer (access time of 2.4 microseconds, floating add time 14.4 microseconds) made possible an increase in integration frequency to 1600-2000 steps/minute for a 30 point space grid. Thus, seven or eight half-frequency orbits can be obtained in one minute; this is generally sufficient to decide the stability of a case.

A very useful feature of the D.T.M.B. facility is the availability of a General Dynamics CHARACTRON which can be programmed automatically by the IBM 7090 to plot any array of X-Y pairs on a cathode-ray tube and issue a microfilm photograph of it. This eliminated most of the cumbersome hand plotting that was previously necessary.

The first check on the 7090 program was provided by a duplication of Univac results. The only existing differences consisted of machine round-off errors which are due to the fact that the actual 7090 word length is one digit shorter, and that the Univac program was written in fixed point.

One of the interesting results obtained with the shaft position held fixed was the slight overshoot of the pressure distribution over and under the steady state pressure profile. This behavior is shown in Figure 14 and seems to be dependent on the running parameter Λ. Namely high values of Λ will correspond to more ample and prolonged oscillations. Figure 14 represents pressure profiles at equally spaced time intervals. Since each time interval corresponds to 100 steps, it can be seen once again that the explicit method is rather inefficient in obtaining steady state results.

One of the most important tests to perform on the finite-orbit technique is to examine if two different values of the time-step size ΔT, both such as to ensure numerical stability, produce the same orbit under the same initial and running conditions. This is clearly shown in tabulations and orbit plots of Figures 15 through 20. Figure 19 contains 100 X-Y pairs for a bearing running under the conditions of Run 13 and with

$B = .45$

$\Delta T = .026$

started from the steady state position of $X_o = .1563$, $Y_o = .57928$ and with

$\dot{X}_o = .01$

$\dot{Y}_o = .01$

The listing of every step on Figure 19 corresponds to every second step on Figure 20 which is for the same case with $\Delta T = .013$. It can be seen that agreement to approximately five figures is attained. Figures 17 and 18 show the same results for the pressure profiles, although data for exactly double the number of steps are not available. Other pieces of evidence to the same extent are available for examination in the A2049 file of The Franklin Institute.

Another important verification of the validity of the finite orbit program is furnished by the agreement between steady-state positions and pressure profiles obtained by Elrod and Burgdorfer [10] and the values resulting from the settling of the shaft center at an equilibrium point in stable cases. The validity of this argument is particularly evident when one notices that Elrod and Burgdorfer obtained their results by imposing the geometrical configuration and obtained the load magnitude, Λ, and mass content as results, whereas the orbit program imposes the load, Λ, and the mass content and finds a geometrical configuration corresponding to them. Thus the two methods are completely independent.

Choosing as a sample comparison Elrod and Burgdorfer's case of

$\nu = 0.5$

$\epsilon = 0.6$

and the corresponding orbit program for

$\Lambda = 1.460$

$L = 1.9934$

we obtain the values of Table II for ψ = PH distributions at equilibrium. Elrod and Burgdorfer use sets of points which are evenly spaced in the distorted spatial variable β related to θ by

$$\cos\theta = \frac{\epsilon - \cos\beta}{\epsilon\cos\beta - 1} \tag{108}$$

Therefore, a direct numerical comparison of the two distributions is not possible without interpolation. Figure 21 contains the two plots of those distributions and shows conclusively excellent agreement. The orbit which approaches this equilibrium point is shown in Figure 22. It should be pointed out now that in all CHARACTRON-plotted orbits only one out of every four X-Y pairs is registered and a straight line drawn between consecutive points. As a result some orbits appear to be less smooth than they are actually produced by the computer integration.

The foregoing proofs of accuracy of the numerical procedure are deemed to have sufficiently established the validity of the results which are hereinafter discussed.

Concerning the general behavior of the solutions - it was previously mentioned that, for values of the stability parameter above the critical (stable), the response is composed of two simultaneous parts: a rather smooth precession in the same direction as the rotation of the journal at a frequency slightly below $\Omega/2$ and a higher frequency component. The frequency of the overriding component is directly related to the value of B. Indeed, there is evidence to show that, at least for cases far from the instability threshold, the overriding frequency increases proportionately to the square root of B. Instability sets in when the value of B is low enough to give rise to overriding components, the frequency of which is commensurate with $\Omega/2$. It would then appear as though the actual bearing response is the overriding oscillation with its frequency and damping characteristics directly controlled by the film parameters, while the half-frequency component is a pseudo-natural frequency to which the bearing cannot react. Then, when the bearing-response frequency is of the order of $\Omega/2$, the resonance is excited and divergence occurs. For unstable cases, the rate of divergence is also controlled by the value of B and the half frequency component disappears. Therefore, frequencies much below $\Omega/2$ are possible in a bearing, although it is very difficult to obtain experimental evidence of them - probably due to the fact that the rate of divergence is so rapid that failure would always ensue.

If this model is accepted for the phenomenon of self-excited instability, a parallel can be drawn with the commonly known case of "oil whip". This term refers to the resonance of the elastic response frequency of a shaft with the half frequency component of complete oil journal bearings.

This interpretation would then attribute the overriding response to the "squeeze-film" effect due to the trapping of gas between the moving shaft and the bearing. It can be easily visualized that trapped gas gives rise to an elastic restoring force which, coupled with the mass of journal through the parameter B, has a characteristic response frequency. Trapping, however, is not complete and escaping gas produced the viscous shear damping that slowly eliminates the overriding response. In long journal bearings gas can escape only in the circumferential direction whereas more and more axial flow is possible as the bearing length decreases. This justifies the high level of damping of short journal bearings.

The effect of load can also be justified by means of this interpretation. Indeed, keeping Λ constant and increasing the load L causes an increase of eccentricity ratio, thus magnifying the elastic to damping ratio of the squeeze-film effect. Thus, for any given value of B, the film response frequency is higher and the threshold of instability occurs at a lower value of B. In fact, load is seen to have a stabilizing influence, all other parameters being kept the same.

The damping characteristics of the film show a dependence on the bearing parameter Λ. Namely, high values of Λ give rise to smaller damping with consequent prolonged duration of the transient responses.

Many other bearing response characteristics might be derived from examination of the orbit program results. Much material is already available at The Franklin Institute for anyone interested in further studies, and plans have been made to exploit extensively the orbit program within the same O.N.R. contract that is responsible for its creation. Here we shall discuss results of the finite orbit program which are pertinent to the definition of the stability region of infinite gas bearing, so that a check may be provided to the conclusions derived from the small perturbation approach of Section IV.

A set of nine cases was run corresponding to Runs 7, 8, 12, 13, 16, 17, 18, 19, 20. These are in excellent agreement with the small perturbation results. Perhaps the term "excellent agreement" should be qualified. Indeed, several factors contribute to some uncertainty in the determination of the threshold of instability by means of the finite orbit program. First, for values of B close to the threshold the rate of convergence or divergence is so low that increasingly higher numbers of orbits are necessary to interpret each case as the threshold is second, the threshold value of B is not unique since the size of the initial disturbance has an effect on the result. Indeed, the case studied to-date show once again that perturbation analyses of stability problems are only able to produce necessary, but not sufficient, criteria for stability. For certain ranges of values of B the system is stable with respect to small disturbances while it is unstable for large ones. This phenomenon is widely known and has often been proven experimentally. Licht's test apparatus, still operational at The Franklin Institute [22], very clearly demonstrates that non-linear effects are often sufficient to overpower linear ones and cause a disturbance-dependent correction to the stability limit defined by small perturbation techniques.

Evidence of the occurrence of this phenomenon in the present case is provided by the contrast between Figures 23.1 a, b, c and figures 39 a, b. Both sets of figures refer to Run 6 with B = 10 and the same initial position and velocity. However, in the Figure 23.1 series, the initial pressure distribution is closer to the steady state than in the Figure 39 series. As the figures show and the numerical results confirm, the orbit of Figures 24.1 a, b, c (smaller perturbation) is convergent and the orbit of Figures 39 a, b (larger perturbation) is divergent.

The above-mentioned reasons contributed to the formation of the following policy in the running of finite orbit cases: the threshold value of B was defined within limits which are narrow enough for practical purposes but not further; small perturbations of equilibrium conditions were used in order to provide a check on the accuracy of the linearized theory of Section IV. A study of the non-linearity effects aimed at developing sufficient stability criteria on a quantitative, rather than qualitative basis was not undertaken, because presently outside the means of the project.

From a qualitative point of view it can be said that stable operation was always observed for values of B larger than a threshold 10 to 15% higher than that predicted by the linearized theory. In using such numbers, however, one should remember that no systematic study of this effect has been made, and that these limits might well be exceeded for some combination of running parameters.

One more interesting non-linear effect has not been studied in detail; the occurrence of limit cycle or "stable orbits". Experimental evidence indicates that stable finite orbits actually occur in rotating machinery. For long complete gas journal bearings evidence is not plentiful because, after the inception of half-frequency whirl, expensive bearing failure usually occurs almost immediately. Actual machines are never completely rid of unbalance and bearing-surface out-of-roundness, so that dynamic stabilizing effects from these agencies (in the form of squeeze film forces and phase angle shifts) can help establish an orbital equilibrium which would be impossible for a perfect shaft. On the other hand, it can be very expensive to make a systematic study of limit cycles by means of the orbit program because it is very difficult to distinguish between the tendency toward an orbit from simple slow convergence or divergence.

The results of the above-mentioned runs designed to check the accuracy of the small perturbation program are condensed in Table III. For the purpose of better visualization these results have been plotted on stability maps of the type of Figure 4. For the sake of clarity the stability map has been split in two: Figure 23 for ϵ_o = 0.2, 0.6, 0.9 and Figure 24 for ϵ_o = 0.4, 0.8. The points corresponding to a given case lie on a Λ = constant line and are represented by a triangle if the orbit is stable and a dot if the orbit is unstable.

A series of orbits as obtained from the CHARACTRON is shown in Figures 25 through 34. Unfortunately, the scaling routine uses a minimum plot size of 0.2 x 0.2 in X and Y so that the orbits representing the system response to small disturbances appear as smeared dots and conclusions on stability have to be drawn from the numerical list of X-Y pairs. Such a situation is shown by Figures 27 a, b, and c and is true for all points which are close to the stability threshold. The reader will remember that, within certain limits, the disturbance size plays a role in the definition of instability and therefore will understand why such small orbits were necessary. Since no definition is offered by such plots, only one sample run is shown. Figures 25 a through 41 b are illustrations of orbits with the particular features discussed in this section.

Figures 25a through 34 b are illustrations of stable and unstable orbits for Runs 7, 8 and 12.

Figures 35 a through 37 b are orbits corresponding to Runs 17 and 16 and show the long duration of transients in cases of high values of Λ.

Figures 38 a and b show the response of Run 17 when an arbitrary amount of unbalance mass U_1 is attached at a radius R_1 from the shaft center so that

$$\frac{4U_1 R_1}{Mc} = 2$$

The striking feature of this orbit is that it is very similar to one which was experimentally obtained by Elwell [12] of the General Electric Company. This orbit should be interpreted only from a qualitative standpoint since no systematic study of the effect of unbalance has been carried out.

Figures 28 a, b, 39 a, b, and 40 b, are illustrations of possible limit cycles arising from two of the attached runs.

Figures 41 a, b, show an orbit which has grown to cover nearly the entire clearance area. It can be seen that the divergence rate decreases once the amplitude of oscillation becomes large enough to boost the effect of squeeze film forces.

V. DISCUSSION

1. General Discussion and Comparison with the Results of Other Investigators

The success of the two techniques presented in this paper, and the results they have produced, will help settle a number of questions which have been puzzling research engineers for some time.

It was previously mentioned that one of the major obstacles encountered in the study of gas bearing dynamic problems has been the treatment of the "history" effect. Obviously, this effect prevents the use of field charts of gas film forces expressed as instantaneous functions of position and velocity. Thanks to the orbit pressures, it is now possible to evaluate the relative magnitude of terms in Reynolds' equation. Figures 42a through 42k, and 43, and 44 all concern Run 17 with B = 10 and contain respectively: the PH distributions at every time step, the values of X, Y, $\dot{X}$, $\dot{Y}$, at every time step, and the orbit covered by 300 steps. It will be of interest to evaluate

$$H \frac{dP}{dT}$$

as compared with

$$P \frac{dH}{dT}$$

For that purpose we can use the fact that

$$H \frac{dP}{dT} = \frac{dPH}{dT} - P \frac{dH}{dT} \tag{109}$$

$$\frac{H \frac{dP}{dT}}{P \frac{dH}{dT}} \cong \frac{\Delta PH}{P\Delta H} - 1 =$$

$$= \frac{(\Delta \psi)/\psi}{(\Delta H)/H} - 1 =$$

$$= \frac{\Delta(\ln \psi)}{\Delta(\ln H)} - 1. \tag{110}$$

Some sample calculations for the point $\theta = 0°$ (last PH point) and between steps 6103 and 6118 yield the results listed in Table IV. It can be easily seen that the orders of magnitude of H $\frac{dP}{dT}$ and P $\frac{dH}{dT}$ are comparable, and no strict justification exists for neglecting either term. More pressure distributions are available both from this run and from other ones so that more extensive studies can be conducted to evaluate the magnitude of the serious terms in Reynolds' equation in various orbital conditions.

It should be pointed out that this case was chosen at random and that the relative importance of these terms might vary in other cases.

An important fact to be noticed in all orbits obtained up to the present time is that the journal center path seems to have little tendency to enclose the bearing center. This information might throw unfavorable light on approximations which assume steady orbiting of the journal center at almost constant eccentricity and angular velocity.

Comparisons with other theories show that best agreement, both in the qualitative and quantitative sense, is achieved by Cheng's analysis [5]. This was expected, because Galerkin's method yields a surprisingly good approximation to steady-state pressure distribution. The quasi-static theory of Sternlicht and Rentzepis [26] comes relatively close to the small perturbation results but it is quite inadequate at low values of C^* (high values of Λ). This may be understood when we realize that neglect of compressibility effects will lead to greater errors at high values of the compressibility parameter Λ.

Ausman's results show great discrepancy with all other theories. This fact can be attributed to two basic reasons: first, his linearized PH expansion does not give the high accuracy needed in stability calculations even at moderate values of eccentricity ratio ϵ_o; second, for the purpose of mathematical expediency, the terms

$$1 - \frac{X^2 + \sqrt{1-\epsilon^2}\, Y}{\epsilon^2} \; ; \quad 1 - \frac{\sqrt{1-\epsilon^2}\, X^2 + Y^2}{\epsilon^2} \quad \text{and} \quad (1 - \sqrt{1-\epsilon^2})\,\frac{XY}{\epsilon^2}$$

are arbitrarily taken to be constant in time. It is also possible that some errors in calculations have been made in the evaluation of the preliminary stability maps received by the authors.

2. Practical Value of this Investigation and Sample Problem

It is well recognized in practice and it has been the result of all theories that, for the same dimensionless load, the shorter the bearing the higher the instability threshold speed. This effect is amenable to intuitive justification when we consider that, for a short bearing, the same load produces larger eccentricities ratios in steady state operation. Then the squeeze-film effects produce both higher overriding response frequencies and larger damping due to axial inflow and outflow. By the reasoning presented in Section V.4, these effects correspond to higher threshold speeds. Therefore, from this practical point of view, the results of any accurate theory based on bearings of infinite axial length give conservative stability criteria.

Unfortunately, a pessimistic criterion in the present stability problem is often not adequate for practical applications. The tendency to whirl is so pronounced that using pessimistic criteria could, in many applications, rule out a considerable portion of the useful range of operating parameters. However, extension of the treatments presented in this paper to finite-length bearings is not expected to present any difficulties in principle.

The orbit program can be very useful for practical applications since it takes into account non-linearity and will give valid answers for real situations. Extension of this program to the finite-bearing case is being carried out at Columbia University by the author.

A typical design problem for a long bearing will require the determination of the clearance ratio C/R which will allow stable operation of a bearing carrying a dimensionless load L at an eccentricity ratio not larger than ϵ and at rotational speed Ω.

The combination of minimum load and maximum ϵ lead to the specification of a minimum Λ from Elrod and Burgdorfer results of Figure 2. Having evaluated ω^* from known physical parameters and Ω, we can enter Figure 5 and determine the maximum C^* corresponding to Λ and ω^*. The conversion from the maximum value of C^* to the maximum value of C/R is obvious from the definition of C^*.

As a numerical example let us consider an air bearing to operate with a unit load

$$L = 2 \text{ at } \epsilon = 0.8$$

From Figure 2 this corresponds to

$$\Lambda = 0.7$$

Then

$$\omega_1{}^* = 4.2 \text{ from Figure 4}$$

or

$$B = \frac{4}{L(\omega_1{}^*)^2} = 0.113$$

We can now compute

$$C^* = \left(\frac{2}{B\Lambda^2}\right)^{0.2} = 2.05$$

If the load was due to gravity

$$C^* = \left(\frac{M P_a}{72\mu^2}\right)^{0.2} \frac{C}{R} = \left(\frac{L R P_a{}^2}{72\ g\ \mu^2}\right)^{0.2} \frac{C}{R}$$

Then, for R = 2 in,

$$C^* = 1.336 \times 10^3 \frac{C}{R}$$

which yields

$$\left(\frac{C}{R}\right)_{stable} \leq \frac{2.05}{1.336} 10^{-3} = 1.53 \times 10^{-3}$$

From

$$\Lambda = \frac{6\,\mu\,\omega\,R^2}{P_a C^2}, \quad \omega_{cr} = \frac{\Lambda\, P_a C_{cr}{}^2}{6\mu R_{cr}{}^2} = 1490 \ \frac{\text{rad}}{\text{sec}} \simeq 14{,}200 \text{ RPM}$$

3. Concluding Remarks and Recommendations

The experience of all experimental investigators in the gas bearing field has been that instability is the major problem to overcome. Stability maps for the idealized model treated in this paper, even with eventual extension to finite-length bearings, certainly represent a forward step in understanding the mechanism of this phenomenon, but should not be interpreted as the final answer. In fact, strictly speaking, the dynamics of the shaft in its bearings cannot be studied separately from the rest of the system. Bearing supports, machine frame, driving mechanisms, unbalance, shaft flexibility are elements which operate in direct coupling with the rotor-bearing system. Obviously, it would be extremely costly and somewhat wasteful to develop a general theory taking all factors into account. It is possible, however, to construct computer programs similar to the orbit program, but generalized to include the above-mentioned effects. Runs would then be made only for the purpose of aiding the design of particular machines. This tool would be of extreme practical value because their low level of internal damping makes gas bearings susceptible to harmful resonances with natural frequencies of some other members of the machine structure.

With the present stability theories now at hand, it would seem quite appropriate that extensive sets of accurate experiments be run to give a firmer footing for further theoretical efforts. Furthermore, instrumentation and machining techniques have now been developed which are capable of handling physical dimensions in microinches with a fair degree of reliability, so that such experimentation is definitely possible.

Dudley D. Fuller
D. D. Fuller
Project Engineer

Reviewed by

W. Shugarts Jr
W. Shugarts, Jr., Manager
Friction and Lubrication Laboratory

N R Droulard
N. R. Droulard
Technical Director

F L Jackson
F. L. Jackson
Director of Laboratories

REFERENCES

1. Allen, D. S., Stokes, P. J., and Whitley, S., "The Performance of Externally Pressurized Bearings Using Simple Orifice Restrictors," ASLE Paper No. 602C-17, presented at the joint ASME/ASLE Lubrication Conference, Boston, Mass., October 1960.

2. Ausman, S., "Linearized PH Stability Theory for Translatory Half-Speed Whirl of Long Self-Acting Gas-Lubricated Journal Bearings, Report 2011-009, Litton Systems, Inc., May 22, 1962.

3. Brix, V. H., "Shaft Stability in Gas Film Bearings," Engineering 187, Feb. 6, 1959, pp. 178-182.

4. Castelli, V. F., Elrod, H. G., "Perturbation Analysis of the Stability of Self-Acting, Gas Lubricated Journal-bearings". The F. I. Lab Interim report no. I-A2049-11, Feb. 1960.

5. Cheng, H. S., "The Dynamic of the Infinitely Long, Self-Acting, Gas-Lubricated Journal Bearings Under a Steady Load". Ph D. Thesis, University of Pennsylvania, 1961.

6. Cole, J. A., and Kerr, J., "Observations on the Performance of Air Lubricated Bearings," Paper 95, Hydrodynamic Lubrication, Conference on Lubrication & Wear, London, 1st-3rd Oct. 1957, The Institution of Mechanical Engineers, 1 Birdroge Walk, London, SW 1.

7. Comolet, R., "Ecoulement d'un Fluide entre Deux Plans Paralleles. Contributions a l'Etude des Buteis d'Air," Publications Scientifiques et Techniques de l'Air, No. 334, September 1957.

8. Crank, J., and Nicolson, P., "A Practical Method for Numerical Evaluation of Solution of Partial Differential Equations of the Heat-Conduction Type," Proc. Cambridge Philos. Soc. 43 (1947), pp. 50-67.

9. Drescher, H., "Gleitlager Mit Lufschmierung (Sliding Bearings with Air Lubrication)," V.D.I. Zeit, Vol. 95, No. 35, Dec. 11, 1953, pp. 1182-1190. Bu Ships Translation 549, also referenced as AEC Translation 3495 Available Library of Congress or John Crerar Library. Abstract in Engineers Digest, Vol. 15, No. 3, March 1954, pp. 103-107.

10. Elrod, H. G., and Burgdorfer, A., "Refinements of the Theory of the Infinitely-Long, Self-Acting, Gas-Lubricated Journal Bearing," First Intern. Symp. Gas-Lubricated Bearings, Washington, D.C., Oct. 26-28, 1959, pp. 93-118 (Also F. I. Interim Report No. I-A2049-10, Jan. 1960; OTS No. AEC-4688; ASTIA No. AD-232 705).

11. Elwell, R. C., Hooker, R. J. and Sternlicht, B., "Gas Bearing Stability Study - Vertical Rotor Investigation," General Electric Co., General Engng. Lab., Contract No. NONR-2844(00), Task NR 097-348, ASTIA No. AD 237 432; May 1960, p. 64.

12. Elwell, R. C., "Observations on the Performance of Self-Acting Gas Journal Bearings," General Electric Co., Schenectady, N. Y., ONR Contract No. NONR 2844(00) March 3, 1961; ASTIA No. AD 253-820; p. 31.

13. Fischer, G. K., Cherubim, V. L., and Fuller, D. D., "Some Instabilities and Operating Characteristics of High Speed Gas-Lubricated Journal Bearings," ASME Paper 58-A-231.

14. Forsythe, G. E., and Wasow, W. R., "Finite-Difference Methods for Partial Differential Equations," Wiley (1960).

REFERENCES (Cont.)

15. Gross, W. A., "Film Lubrication IV. Compressible Lubrication of Infinitely Long Slider and Journal Bearings, RV-RR-117-4, 6/25/58, IBM Report.

16. Gross, W. A., "A Gas Film Lubrication Study, Part 1, Some Theoretical Analyses of Slider Bearings," IBM Journal of Research and Development, Vol. 3, No. 3, July 1959, pp. 237–249.

17. Gross, W. A., "Film Lubrication-VIII. Unsteady Bearing Films and Bearing Systems," IBM Research Lab., San Jose, Calif., Report No. RV 117-8, May 1, 1960, p. 89.

18. Lees, M., "Approximate Solutions of Parabolic Equations", Journ. Soc., Indust. App. M&T 7 (1959).

19. Licht, L., Fuller, D. D., Sternlicht, B., "Self-Excited Vibrations of an Air-Lubricated Thrust Bearing, Trans. ASME, Vol. 80, No. 2, 1958, pp. 411-414.

20. Licht, L., and Elrod, H. G., "A Study of the Stability of Externally Pressurized Gas Bearings," The F. I. Lab. Interim Report I-A2049-4, Nov. 1958. Contract NONR 2342(00) Task NR. 097-343. AEC U 3913, OTS. ASTIA No. AD-206762.

21. Licht, L., "Air-Hammer Instability in Pressurized Journal-Gas Bearings," Paper No. 60-WA-10, presented at the ASME Winter Annual Meeting, N. Y., December 1960 (To be published Trans. ASME).

22. Franklin Institute, Licht, L., and Elrod, H. G., "An Analytical and Experimental Study of the Stability of Externally-Pressurized, Gas-Lubricated Thrust Bearings," F. I. Labs. Res. Devel., Tech. Report No. I-A2049-12, Feb. 1961, p. 209.

23. Michael, W. A., "Approximate Methods for Time Dependent Gas Film Lubrication Problems; IBM Research Report RV-205, May 1, 1962.

24. Pan, C. H. T., and Sternlicht, B., "On the Translatory Whirl Motion of a Vertical Rotor in Plain Cylindrical Gas-Dynamic Journal Bearings," G. E. Tech. Report for ONR, Cont. No. NONR 2844(00) May 8, 1961, p. 23.

25. Raimondi, A. A., "A Numerical Solution for the Gas Lubricated Full Journal Bearing of Finite Length," Trans. ASLE, Vol. 4, No. 1, April 1961, pp. 131-155.

26. Rentzepis, G. M. and Sternlicht, B., "On the Stability of Rotors in Cylindrical Journal Bearings," G. E. Tech. Report for ONR, Cont. No. NONR A2844(00), May 15, 1961, p. 35, AD 251014.

27. Richardson, H. H., "Static and Dynamic Characteristics of Compensated Gas Bearings," Trans. ASME, Vol. 80, No. 7, 1958, pp. 1503-1509.

28. Richardson, H. H., "A Dynamic Analysis of Ext. Press. Air Bearings," MIT Dept. of M.E., MS Thesis, Cambridge, Mass., Jan. 1955.

29. Robinson, C. H., and Sterry, F., "The Static Strength of Pressure Fed Gas Journal Bearings," Atomic Energy Res. Est. Rep. No. AERE-ED/R 1672, 1958, Harwell, England.

30. Rothe, H. C., "Air Bearings for Guidance Components of Ballistic Missiles and their Prod. Aspects, Paper presented at the First Int. Symposium on Gas-Lubricated Bearings, Washington, D.C., October, 1959.

REFERENCES (Cont.)

31. Ralston, A. and Wilf, H. S., "Mathematical Methods for Digital Computers," 1960, Wiley & Sons, New York.

32. Sixsmith, H., "The Theory and Description of a Gas-Lubricated Bearing of High Stability," First International Symposium, Gas-Lubricated Bearings, Washington, D.C., Oct. 26-28, 1959, pp. 418-434.

33. Stevenson, C. H. and Castelli, V., "Static Characteristics of Gas-Lubricated, Self-Acting Cylindrical Partial Arc Journal Bearings, F. I. Interim Report, I-A2049-18. (To Be Published).

34. Whitley, S. and Betts, C., "A Study of Gas-Lubricated Hydrodynamic Full Journal Bearings," Brit. J. Appl. Physics, Vol. 10, No. 10, Oct. 1959, pp. 455-463.

NOMENCLATURE

Symbol	Definition	Pg. of first appearance
B	$R\,P_a\,(ME\,\frac{\Omega^2}{4})$ Dimensionless Stability Parameter	8
C	Radial Clearance	4
C*	$(2/B\Lambda^2)^{1/5} = MP_a/(72\mu^2)^{1/5} \cdot C/R$ - Dimensionless critical clearance Parameter	20
e	eccentricity	
F_x, F_y	Pressure Force Components in x, y direction	6
$H = h_1/c$	Dimensionless Film Thickness	4
h	Film Thickness	4
$I_{R,N}$	Function of s	18
$J_{R,N}$	Function of s	18
$K_{R,N}$	Function of s	18
$K_{x,y}$	Friction Force Components in x, y direction	7
L	$W/(R\,.\,P_a)$ Dimensionless Load Parameter	8
$L_{R,N}$	Function of s	18
M	Rotor Mass per Unit Axial Length	8
P	Film Pressure	4
P_a	Ambient Pressure	4
P	$\frac{P}{P_a}$ Dimensionless Pressure	4
$Q(\theta, s)$	Function of θ and s	12
q	$\frac{\Delta T}{(\Delta\theta)^2}$ Numerical Stability Parameter	24
R	Shaft Radius	4
$S(\theta, s)$	Function of θ and S	12
S_f	Viscous Shear Stress	7

NOMENCLATURE (Cont.)

Symbol	Definition	Pg. of first appearance
S	Transformed Time Variable	11
$T = (\Omega/2)^t$	Dimensionless Time Parameter	4
t	Time	4
W	External Load per Unit Axial Length	
$X = x_1/c$	Dimensionless Cartesian Coordinate of Shaft Center	4
$Y = y_1/c$	Dimensionless Cartesian Coordinate of Shaft Center	4
β	Coordinate Normal to Direction of Motion	4
ϵ	Eccentricity Ratio = e/c	7
$\eta = \beta/R$	Dimensionless Length Normal to Direction of Motion	5
η	Dimensionless Coordinates	5
θ	Angle Measured in the Direction of Journal Rotation	4
Λ	$6\Omega\mu R^2/(P_a C^2)$ Dimensionless Speed Parameter	5
μ	Dynamic Viscosity Coeff.	4
ν	$\frac{K}{P_a C} \frac{\sqrt{1-\epsilon^2}}{\Lambda}$	19
ϵ	Dimensionless Coordinate	22
PH	Dimensionless Variable	5
Ω	Angular Velocity	4
A	$M C \Omega^2/(2\pi R P_a) = 2/(\pi B)$ = Dimensionless Stability Parameter	20
ω	Complex part of s	12
$\omega_1{}^*$	$\sqrt{4/(LB)}$ = Stability Parameter	20
ω^*	$(4/\sqrt{B^2})\ 1/5 = (\frac{3}{2} \frac{\mu M^2}{P_a{}^3})^{1/5}$ Dimensionless Critical Speed Parameter	20
$(\quad)^\circ$	Parameter or Coordinate at Equilibrium Condition	9
$(\quad)'$	Differentiation with Respect to θ	10
$(\bar{\quad})$	LaPlace Transform of a Function	11

TABLE 1

Run	ν	ϵ_o	Λ	$L = 2\ C_L$	X_o	Y_o
1	1.0	.2	.9622	.4414	.14326	.13956
2		.4	.8209	.8312	.29710	.26782
3		.6	.5418	.9036	.47781	.36290
4		.8	.2052	.6078	.65156	.46418
5		.9	.0722	.3416	.71306	.54914
6	0.5	.2	1.979	.5828	.09059	.17831
7		.4	1.859	1.2734	.18840	.35285
8		.6	1.460	1.9934	.30662	.51574
9		.8	0.6348	1.9074	.45943	.65492
10		.9	0.2221	1.1866	.48334	.75920
11	0.25	.2	4.0126	0.6428	.04850	.19403
12		.4	3.9754	1.5068	.09936	.38746
13		.6	3.643	2.880	.15630	.57928
14		.8	2.379	4.894	.23701	.76409
15		.9	1.017	4.596	.30487	.84679
16	.125	.2	8.058	.6604	.02484	.19845
17		.4	8.110	1.5738	.04990	.39688
18		.6	7.781	3.162	.07641	.59512
19		.8	6.256	6.758	.10673	.79285
20		.9	4.246	10.922	.12940	.89064
21	----	0.0	1.0	0.0	0.0	0.0
22	1.0	.1	.99107	.221950	.07094	.07048
23	.5	.1	1.9957	.283682	.04485	.08937
24	.25	.1	4.0043	.30896	.02428	.09701
25	.125	.1	8.01657	.31633	.01242	.09923

TABLE 1 A

INSTABILITY THRESHOLDS

Run	B	ω_1^*
1	9.4	0.98
2	2.45	1.40
3	0.97	2.14
4	0.36	4.27
5	0.116	10.05
6	5.80	1.09
7	1.2	1.62
8	0.47	2.07
9	0.115	4.27
10	0.0021	40.1
11	5.6	1.06
12	1.15	1.52
13	0.37	1.94
14	0.114	2.68
15	0.0045	13.9
16	5.0	1.10
17	1.1	1.52
18	0.345	1.91
19	0.11	2.32
20	0.038	3.11
22	32.	.75
23	21.	.819
24	19.	.826
25	18.	.838

TABLE II

COMPARISON OF EQUILIBRIUM DISTRIBUTIONS*

Elrod & Burgdorfer		Castelli & Elrod Orbit Program	
θ (deg.)	PH	θ (deg.)	PH
194.1	0.93435	12	1.30588
187.6	0.96949	24	1.39255
180.6	1.00953	36	1.46353
173.1	1.05558	48	1.51551
164.8	1.10892	60	1.54646
155.5	1.17090	72	1.55562
144.9	1.24248	84	1.54344
132.8	1.32331	96	1.51145
118.6	1.40969	108	1.46217
102.0	1.49135	120	1.39889
82.8	1.54807	132	1.32547
61.0	1.55058	144	1.24602
37.5	1.47433	156	1.16463
13.7	1.32218	168	1.08502
350.8	1.13351	180	1.01030
330.1	0.96086	192	0.94271
312.0	0.83789	204	0.88364
296.5	0.76765	216	0.83365
283.2	0.73570	228	0.79279
271.8	0.72637	240	0.76088
261.8	0.72927	252	0.73804
253.0	0.73884	264	0.72523
245.1	0.75223	276	0.72479
237.8	0.76811	288	0.74034
231.0	0.78593	300	0.77572
224.6	0.80544	312	0.83288
218.5	0.82669	324	0.91034
212.4	0.84983	336	1.00331
206.4	0.87517	348	1.10498
200.3	0.90315	360	1.20810

*Case of

$\nu = 0.5$

$\epsilon_o = 0.6$

$\Lambda = 1.46$

$L = 1.9934$

TABLE III

Run	ΔT	X_o	Y_o	$\dot{X}_o$	$\dot{Y}_o$	B	ω_1^*	Stable?
7	.026	st.st.	st.st.	0	0	8	.627	yes
						4	.886	yes
						1.8	1.321	yes
						1.3	1.555	yes
						1.1	1.690	no
						.8	1.982	no
8	.011	st.st.	st.st.	0	0	4	.708	yes
						.8	1.584	yes
						.5	2.004	yes
						.45	2.112	no
						.2	3.167	no
12	.026	st.st.	st.st.	0	0	1.5	1.330	yes
						1.2	1.487	no
						1.0	1.629	no
13	.026	st.st.	st.st.	0	0	7.0	.445	yes
				.01	.01	0.6	1.521	yes
				.01	.01	0.45	1.757	yes
				0	0	0.3	2.152	no
				0	0	0.07	4.454	no
16	.026	st.st.	st.st.	0	0	20	.550	yes
						8	.870	yes
						7	.930	no
						5	1.101	no
						1	2.461	
17	0.026	st.st.	st.st.	0	0	10	.504	yes
						7	.603	yes
						6	.651	yes
						1	1.59	no
						0.3	2.91	no
18	.026	st.st.	st.st.	0	0	8	.398	yes
						4	.562	yes
						.8	1.258	yes
						.35	1.901	no
						.25	2.250	no
19	.026	st.st.	st.st.	0	0	0.14	1.056	yes
						0.11	1.320	no
						0.08	2.721	no
20	.026	st.st.	st.st.	0	0	0.07	2.288	yes
						.04	3.026	no
						.02	4.280	no

TABLE IV

Step	$\left(H \frac{\partial P}{\partial T}\right) / \left(P \frac{dH}{dT}\right)$
6103	
	-1.5635
6104	
	-1.5187
6105	
	-1.5012
6106	
	-1.5069
6107	
	-1.5377
6108	
	-1.6022
6109	
	-1.7278
6110	
	-1.9836
6111	
	-2.6635
6112	
	-8.0809
6113	
	+1.9262
6114	
	+0.2063
6115	
	-0.2307
6116	
	-0.4238
6117	
	-0.5282
6118	

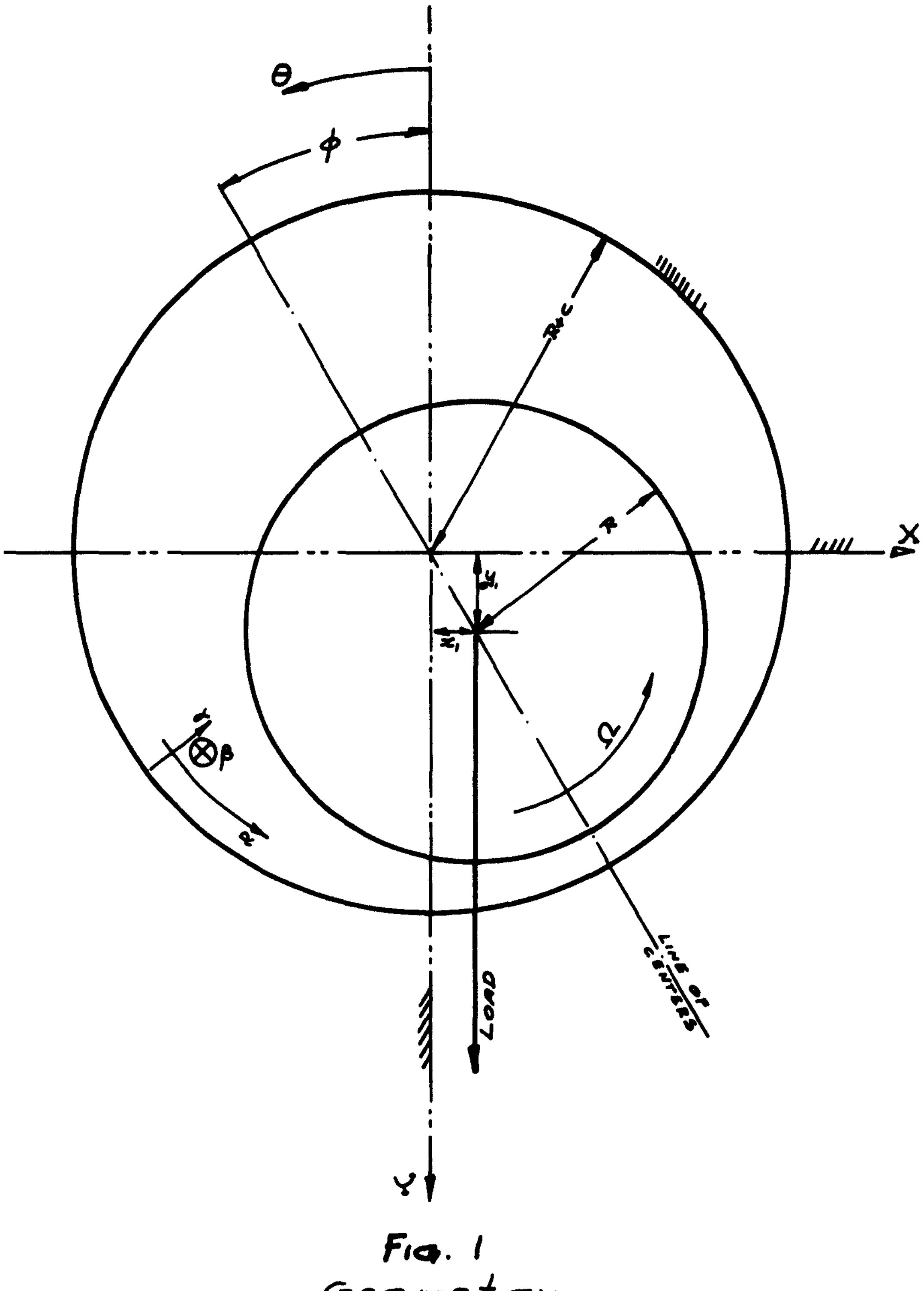

Fig. 1
Geometry

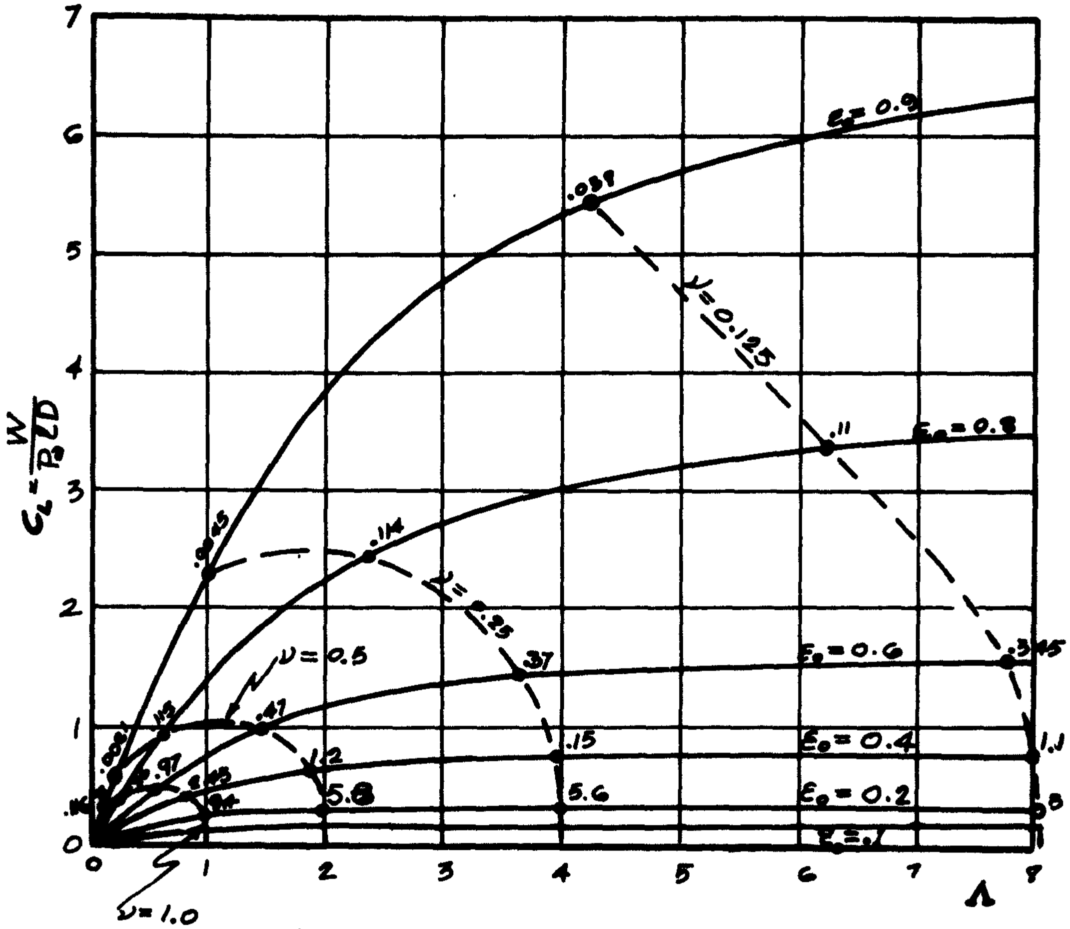

STABILITY CHART
(Numbers by the computed points are the corresponding values of B at the threshold of instability)

FIG. 2

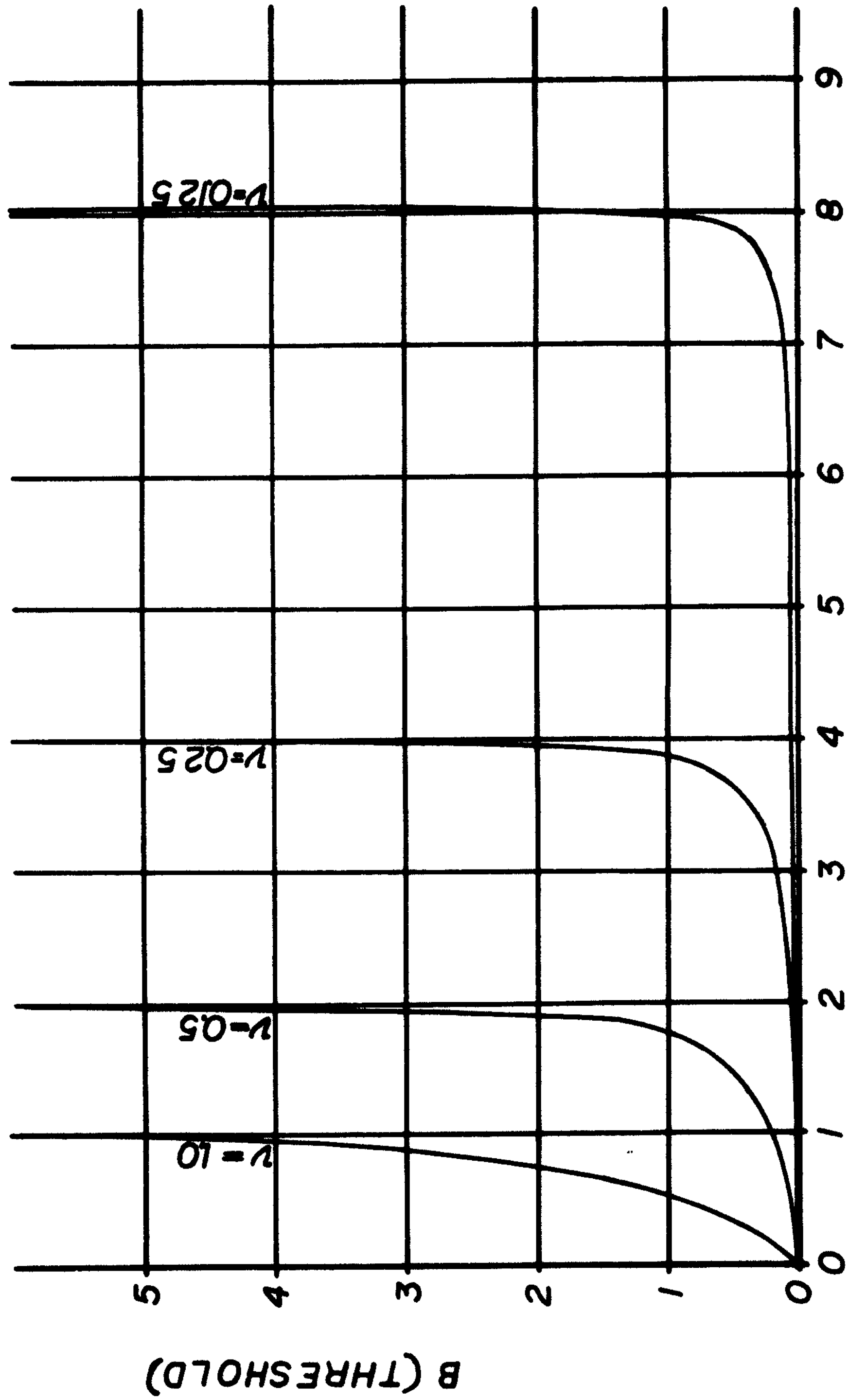

FIG. 3 ~ STABILITY MAP

$0 < B < B_{THRESHOLD}$ UNSTABLE $B_{THRESHOLD} < B$ STABLE

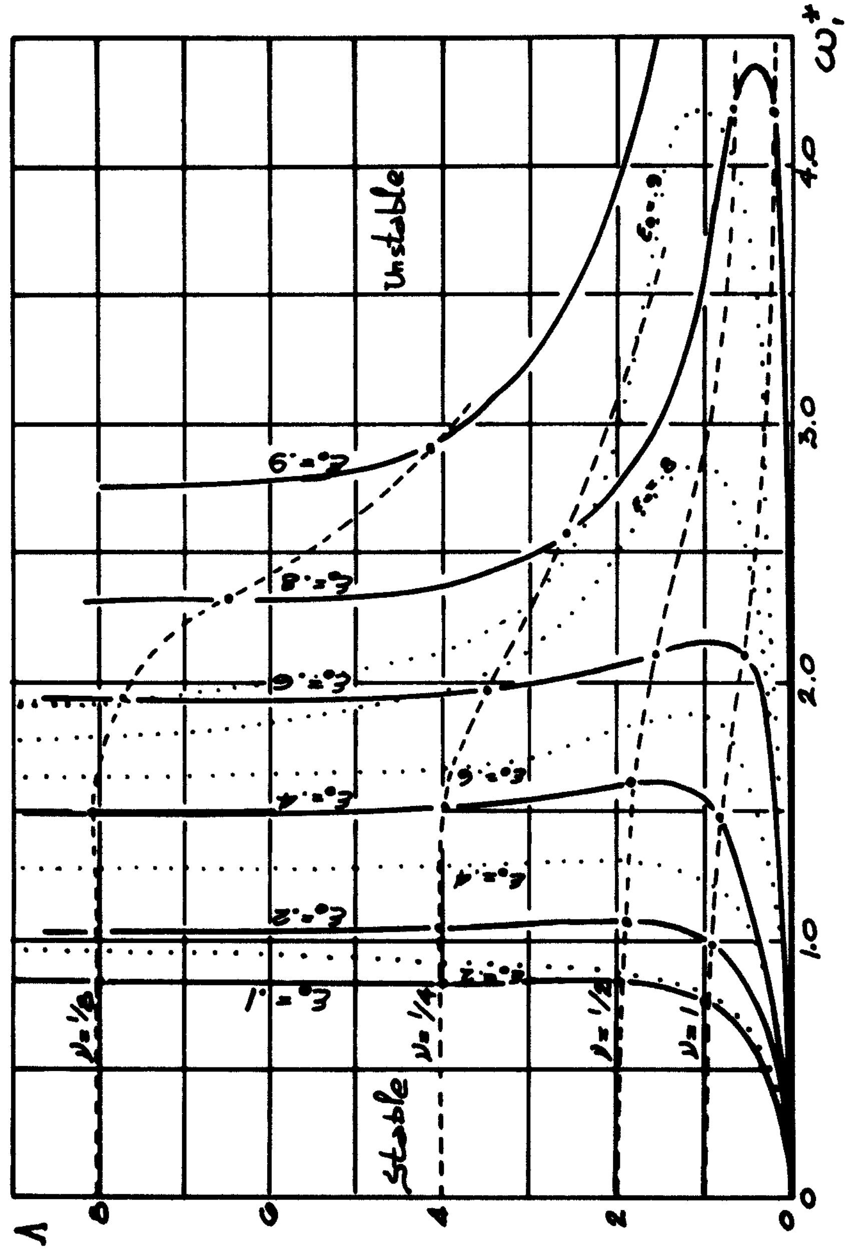

.... CHENG-TRUMPLER

———— CASTELLI-ELROD

FIG. 4

STABILITY MAP

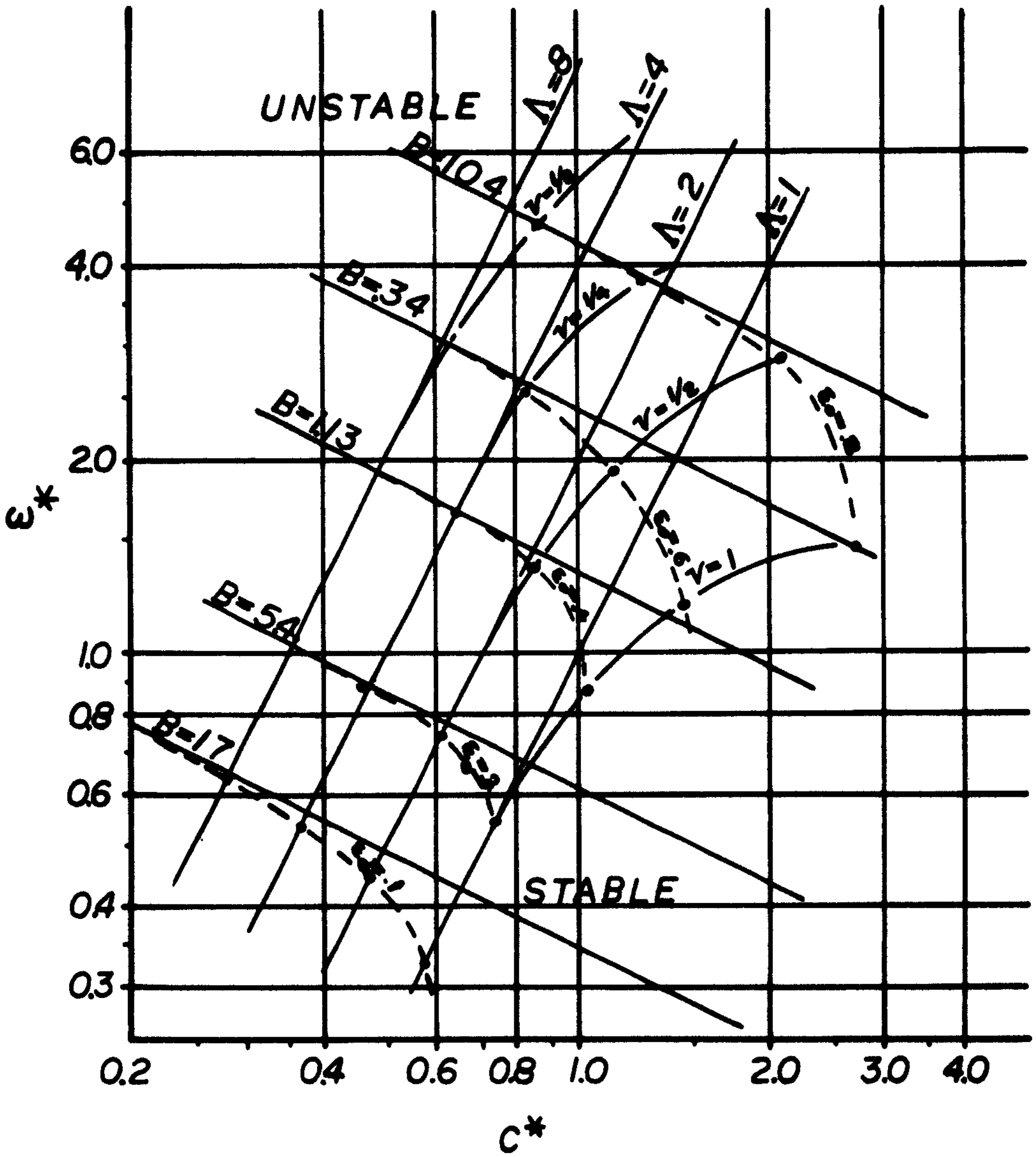

FIG. 5

STABILITY MAP

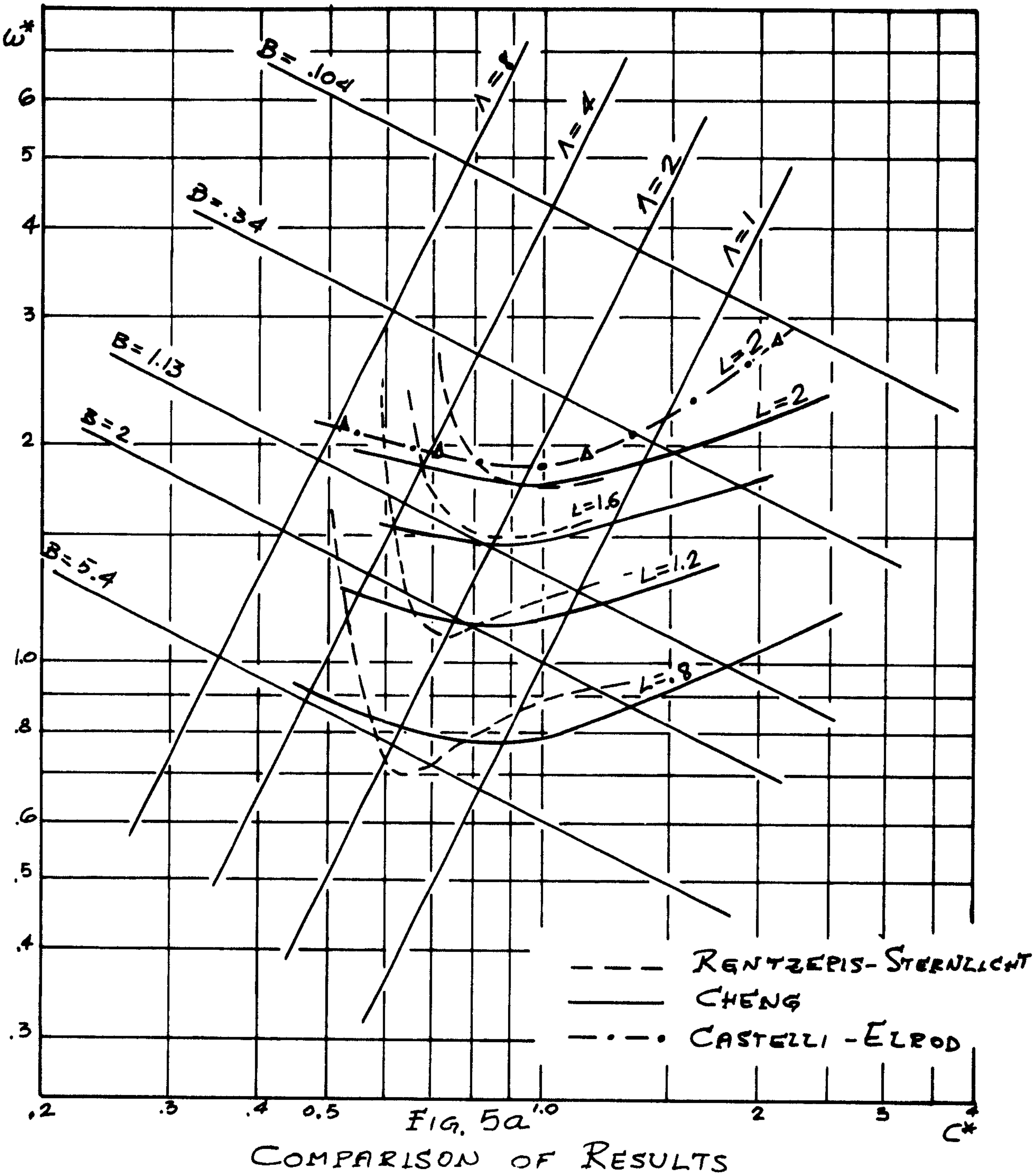

FIG. 5a

COMPARISON OF RESULTS

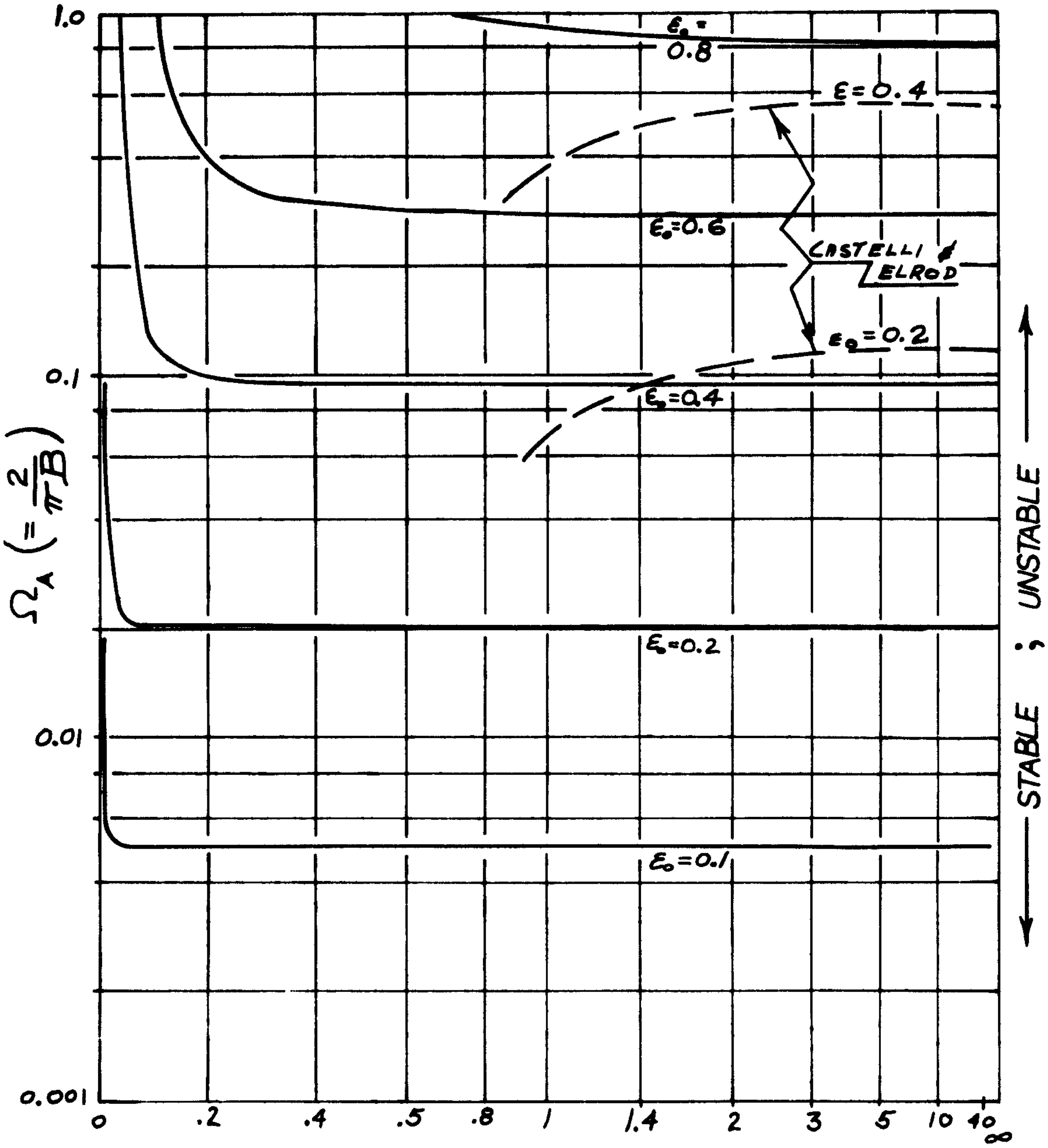

FIG. 6

AUSMAN RESULTS & COMPARISON WITH PERTURBATION

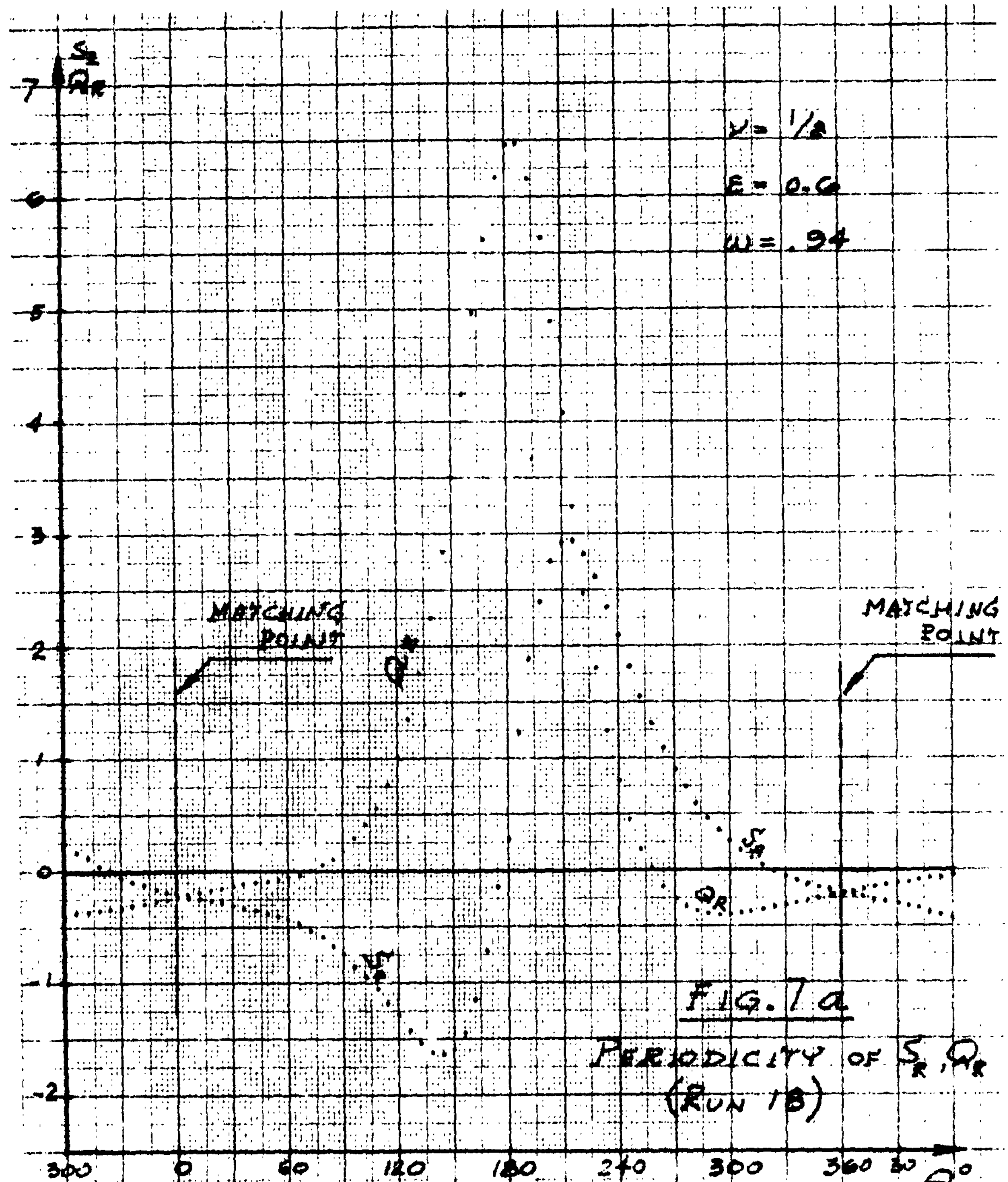

FIG. 7a
PERIODICITY OF S_R, Q_R
(RUN 1B)

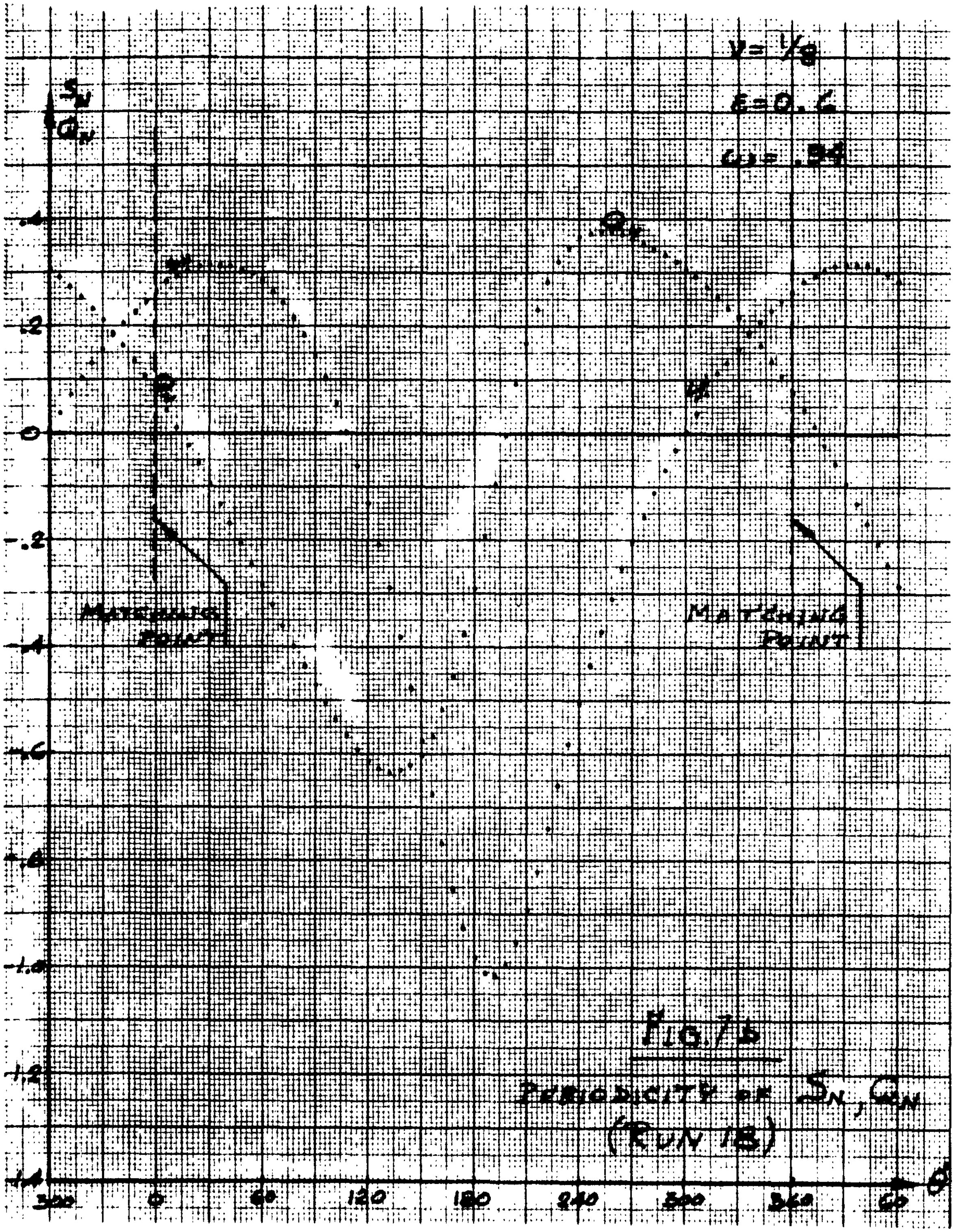

FIG. 7b

PERIODICITY OF S_N, Q_N

(RUN 18)

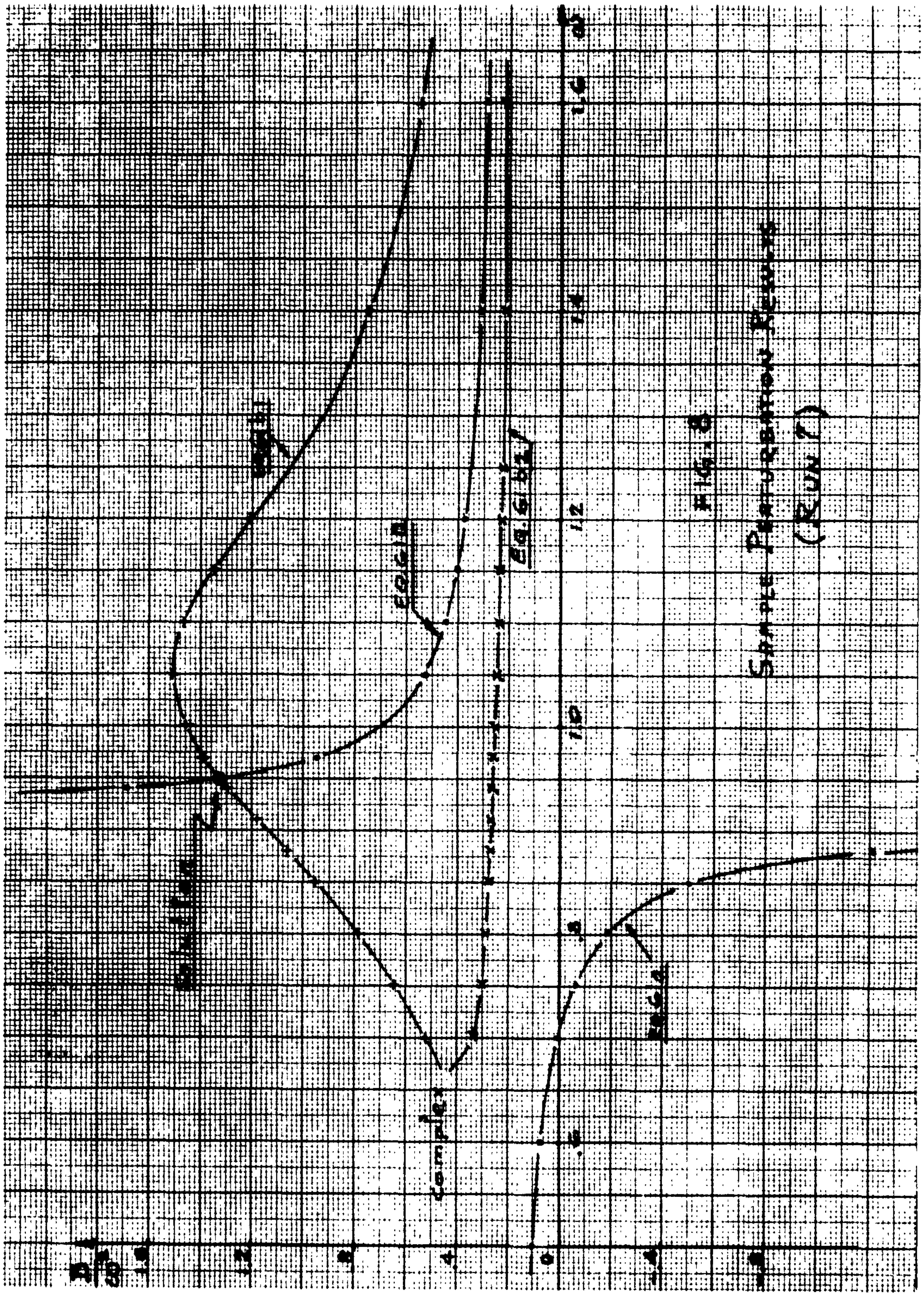

FIG. 8

SAMPLE PERTURBATION RESULTS (RUN 7)

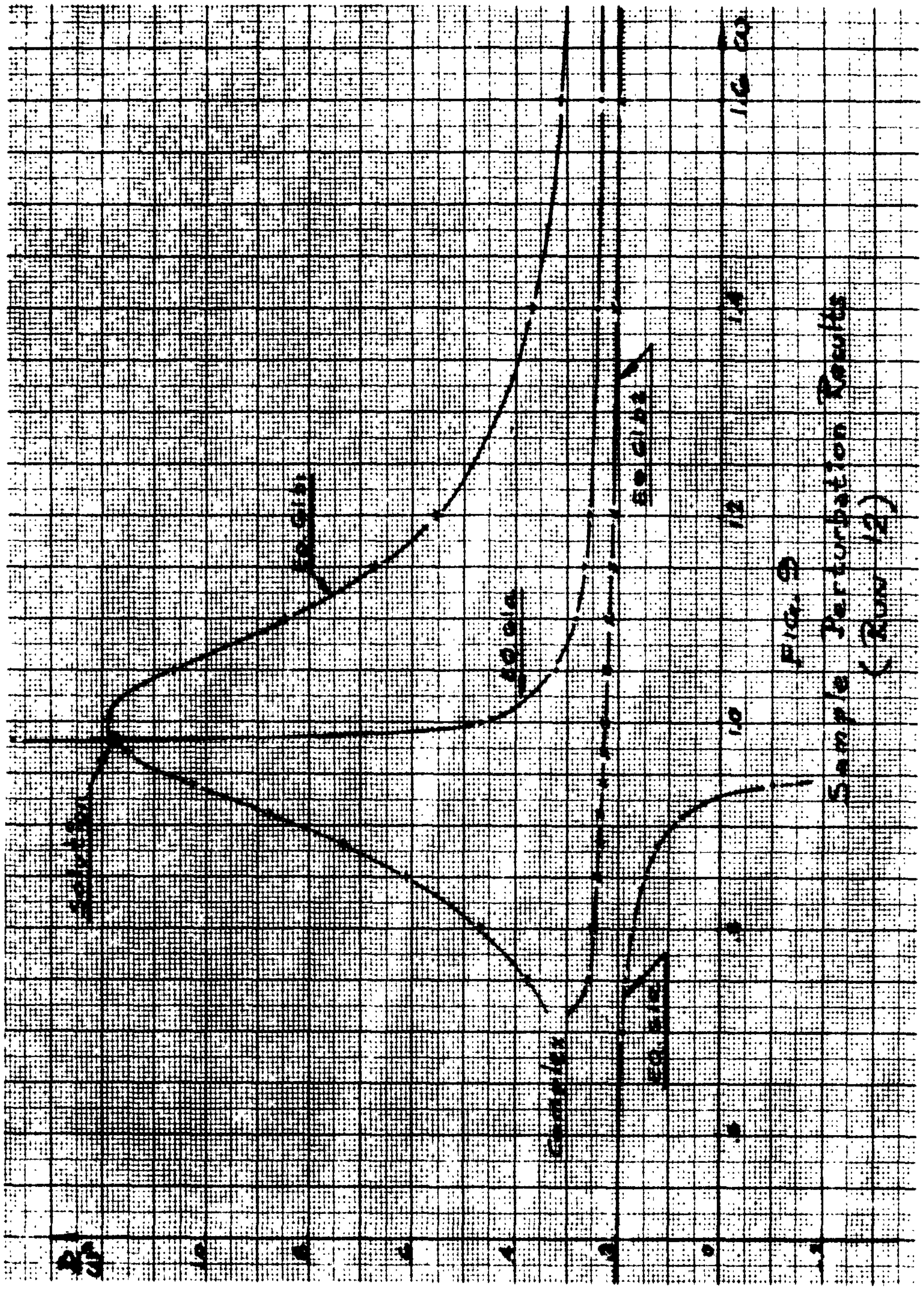

Fig. 9
Sample Perturbation Results
(Run 12)

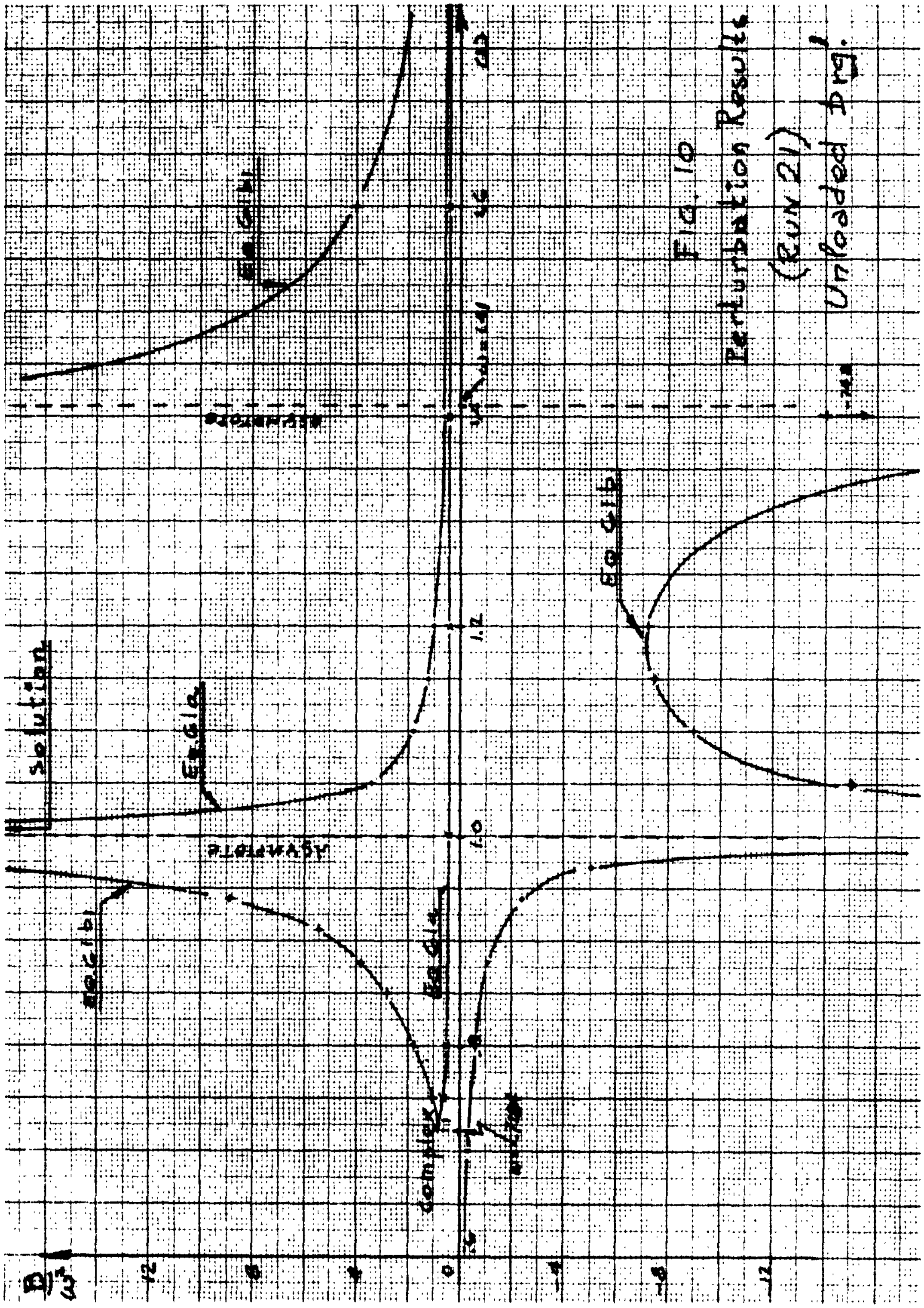

Fig. 10
Perturbation Results
(Run 21)
Unloaded Drg.

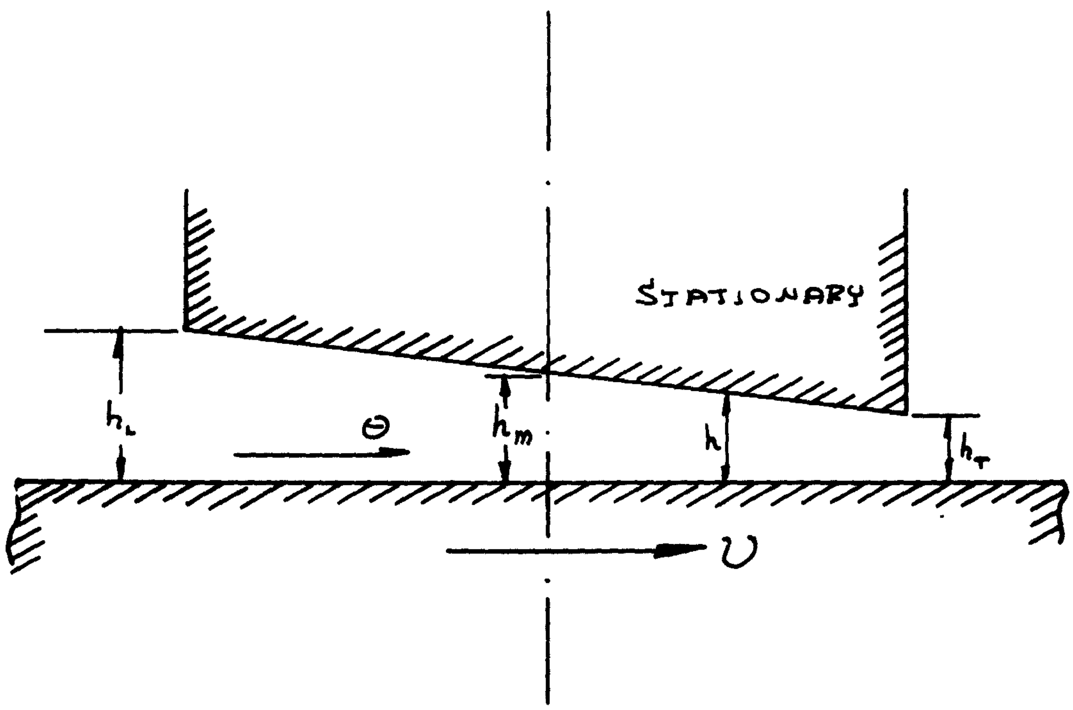

FIG. 11

SLIDER BEARING GEOMETRY

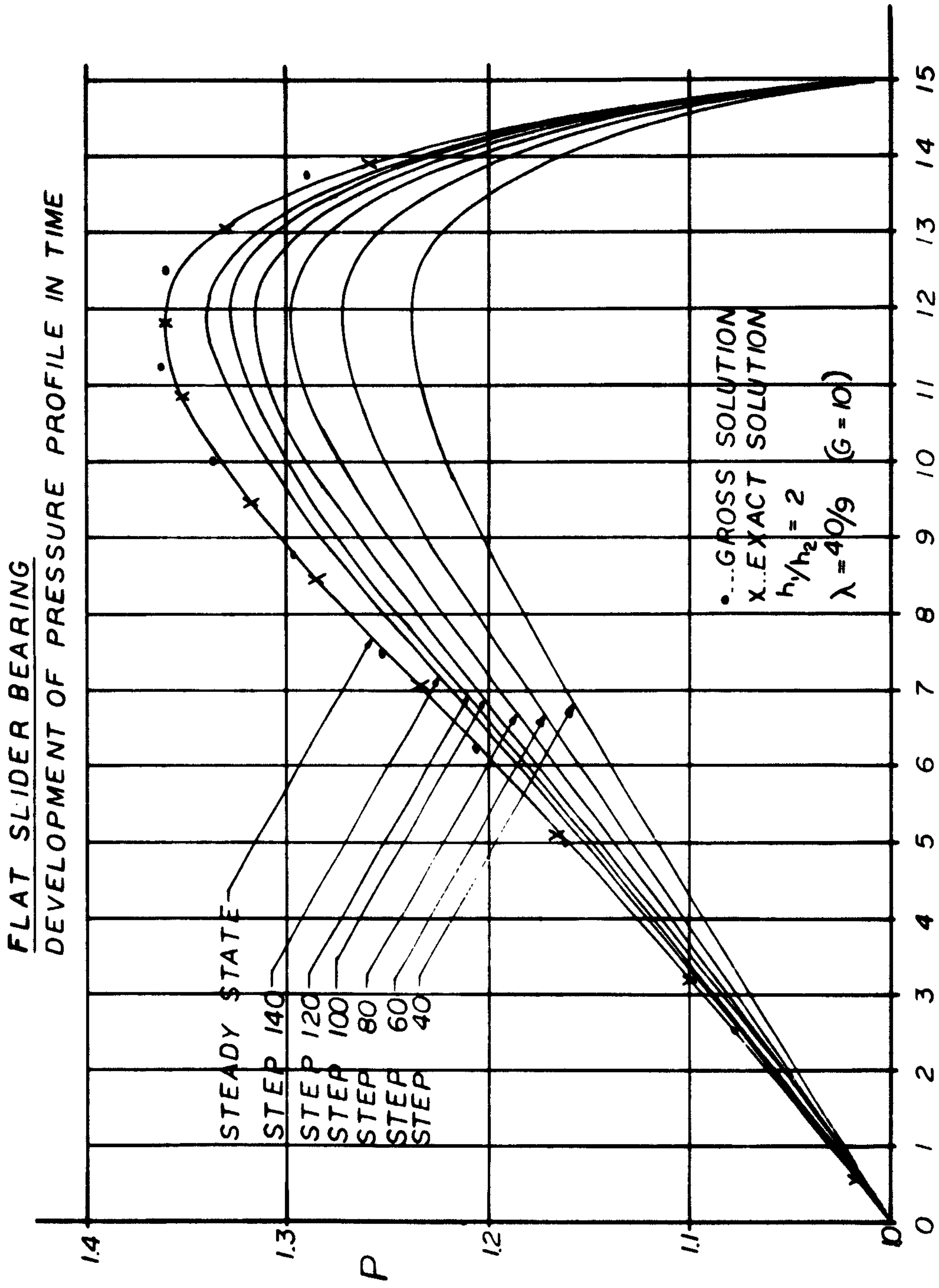
FLAT SLIDER BEARING
DEVELOPMENT OF PRESSURE PROFILE IN TIME
STEADY STATE
STEP 140
STEP 120
STEP 100
STEP 80
STEP 60
STEP 40
•...GROSS SOLUTION
X...EXACT SOLUTION
$h_1/h_2 = 2$
$\lambda = 40/9$ (G = 10)
P
1.4
1.3
1.2
1.1
0
POINT
0
1
2
3
4
5
6
7
8
9
10
11
12
13
14
15

FIG. 12

FIG. 13

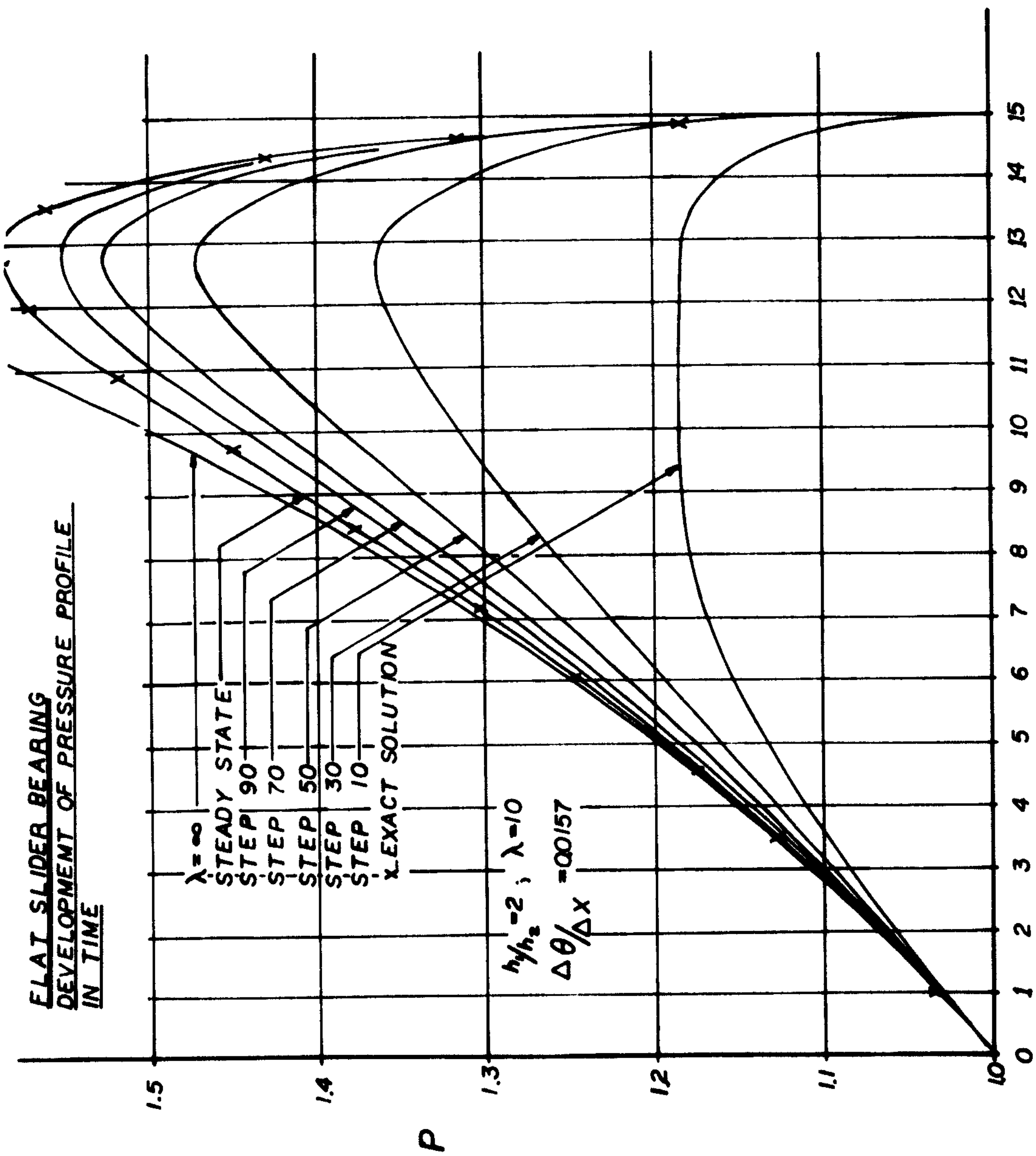
FLAT SLIDER BEARING
DEVELOPMENT OF PRESSURE PROFILE
IN TIME
λ = ∞
STEADY STATE
STEP 90
STEP 70
STEP 50
STEP 30
STEP 10
x EXACT SOLUTION
$h_1/h_2 = 2$; λ = 10
$\Delta\theta/\Delta X$ = .00157
P
POINT
1.0
1.1
1.2
1.3
1.4
1.5
0
1
2
3
4
5
6
7
8
9
10
11
12
13
14
15

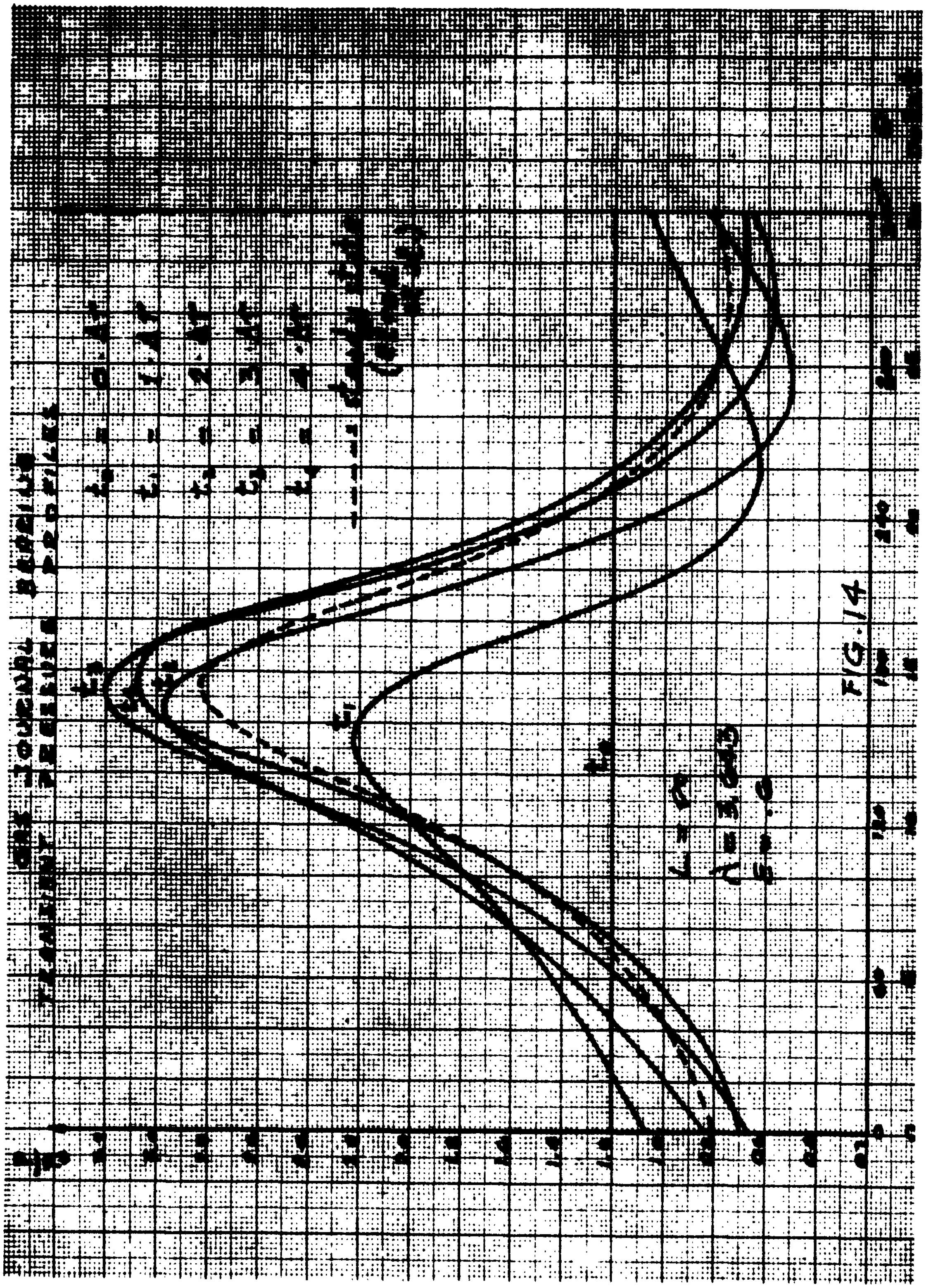

FIG. 14

Fig. 15a
Run 13
B = 0.45
ΔT = .026
1st 1000 steps

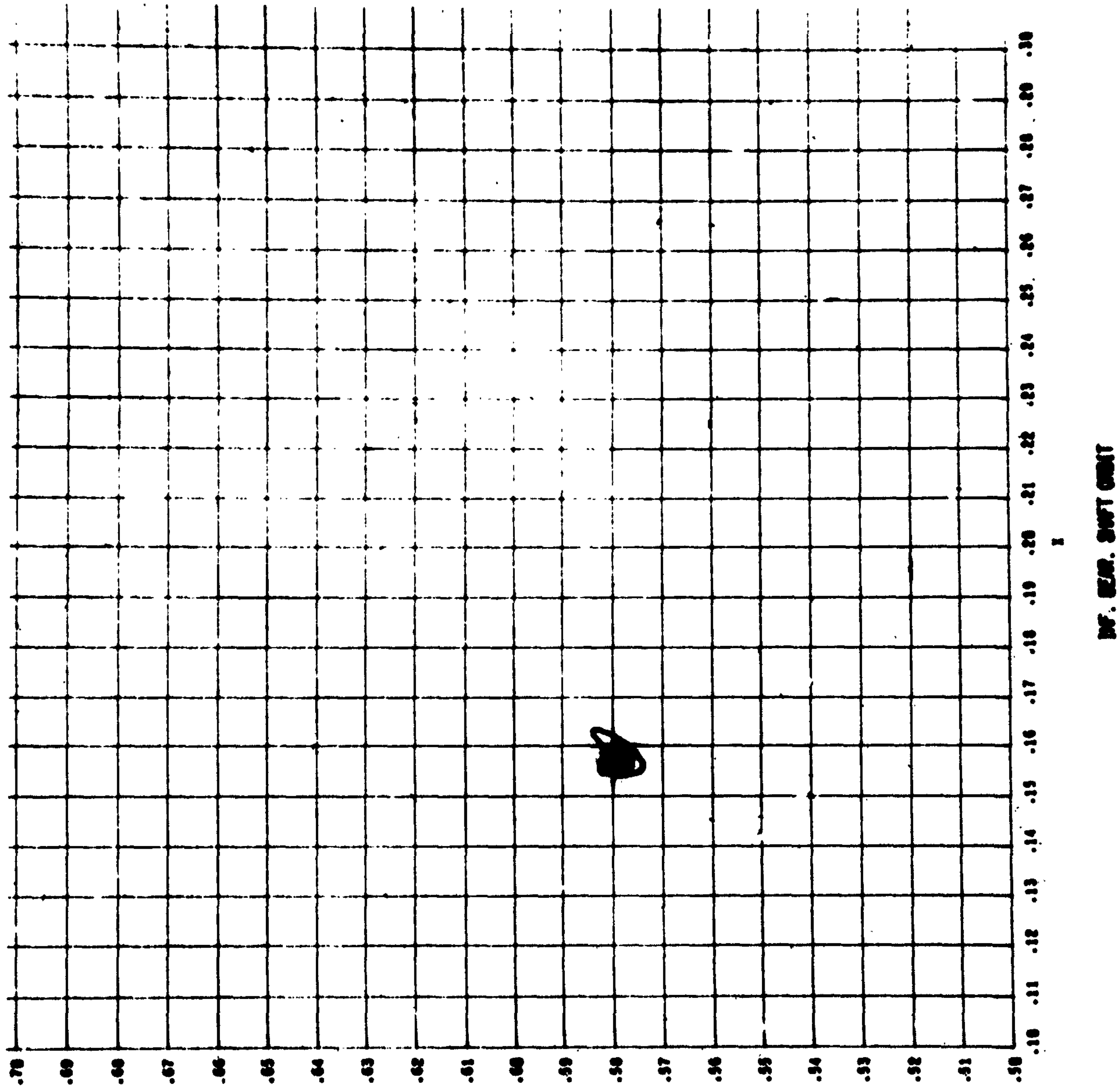

Fig. 15b
Run 13
B = 0.45
ΔT = .013
2nd 1000 steps

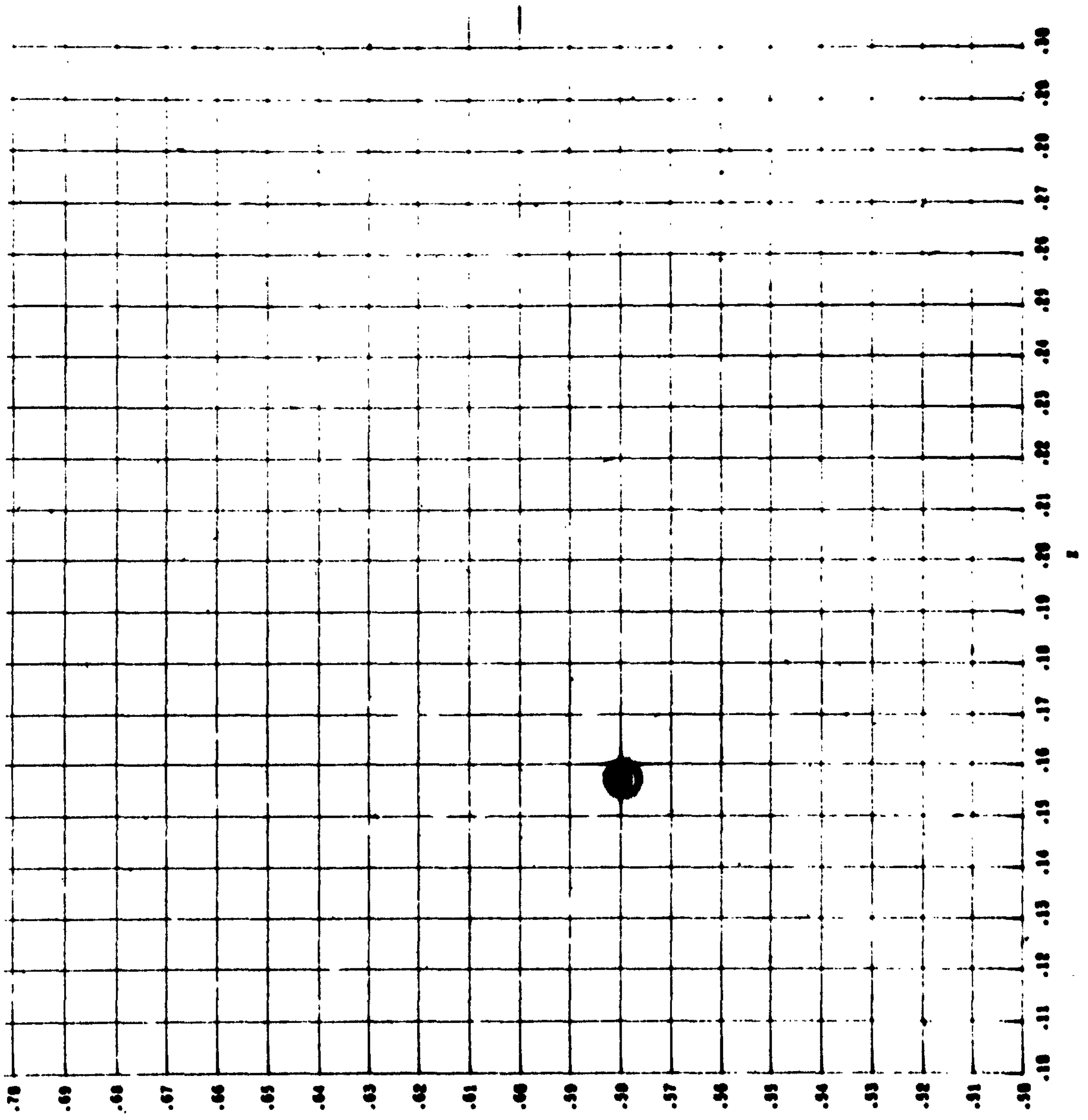

Fig. 16a
Run 13
B = 0.45
ΔT = 0.013
1st 1000 steps

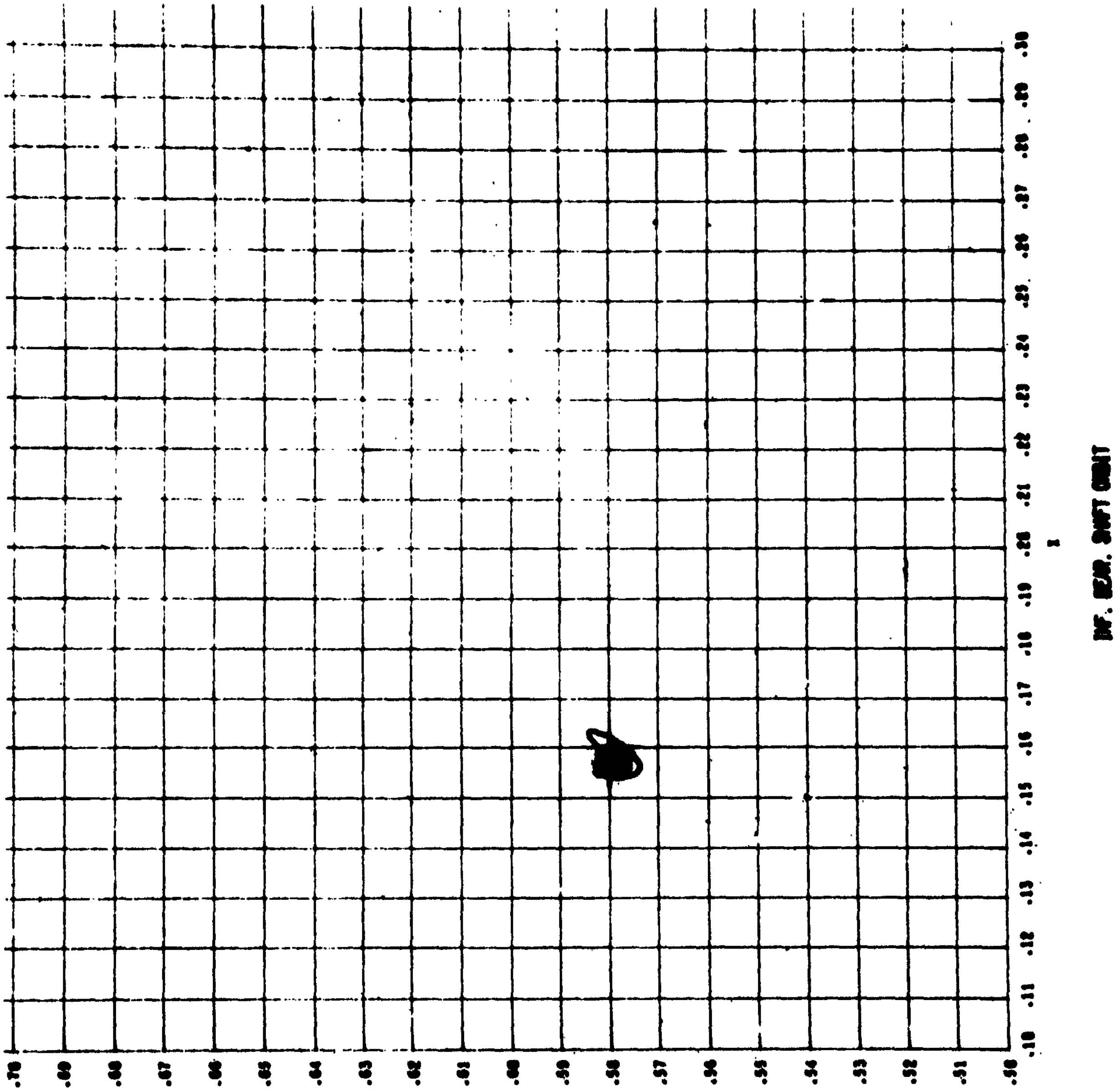

Fig. 16b
Run 13
B = 0.45
$\Delta T = 0.013$
2nd 1000 steps

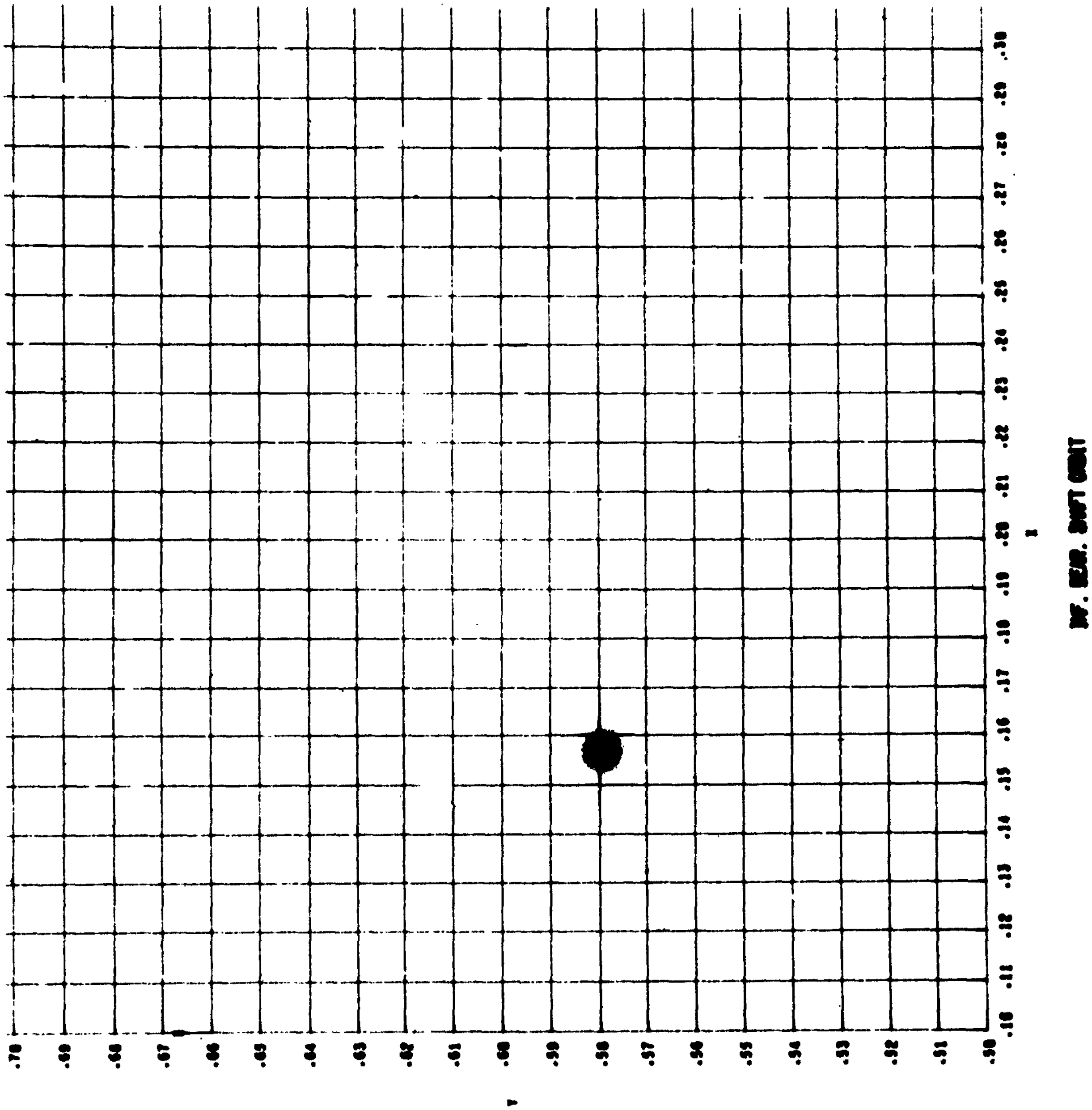

Fig. 16c
Run 16
B = 0.045
ΔT = 0.013
3rd 1000 steps

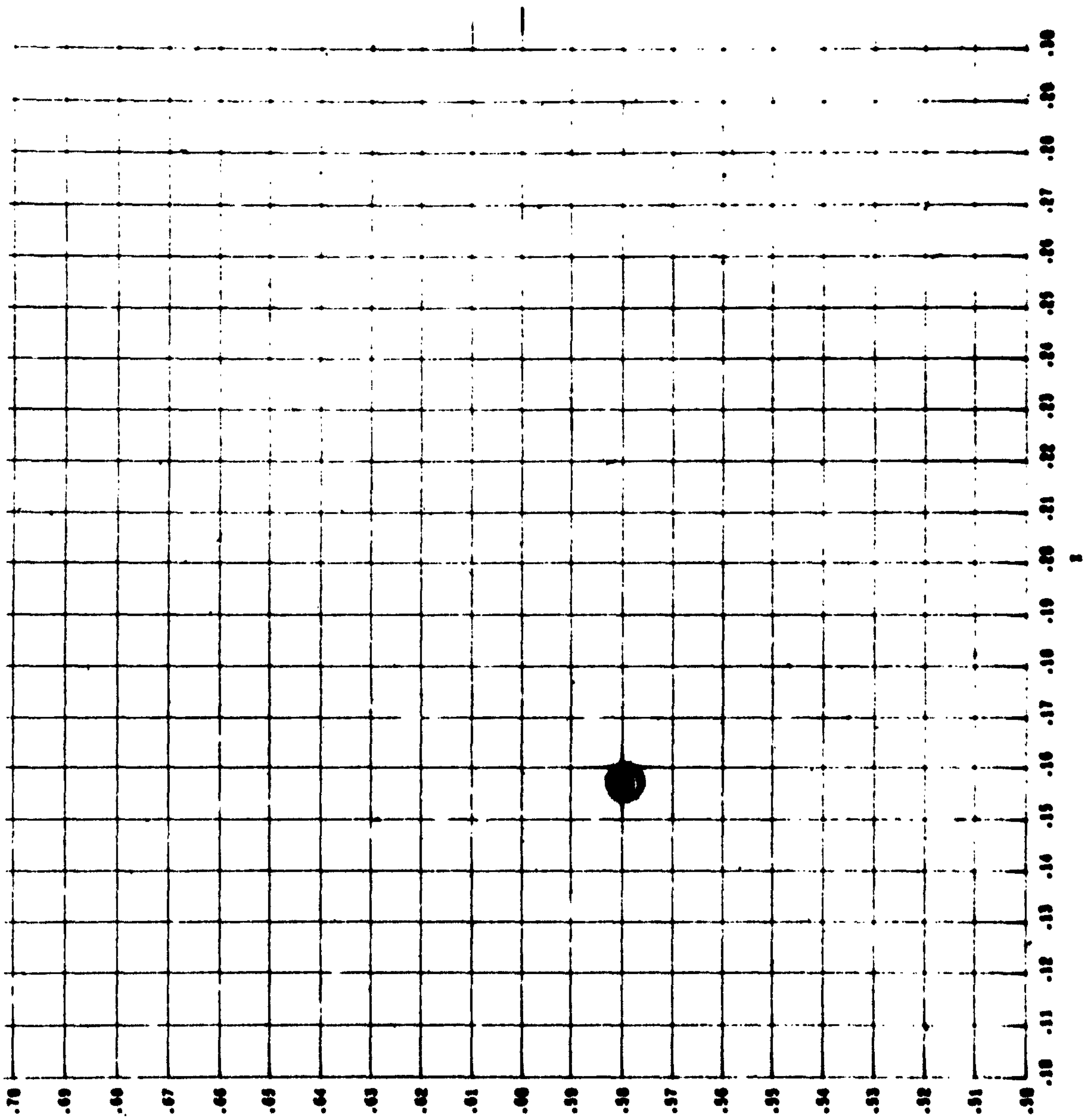

```
CASE    1, STEP    1, B= 0.4500000E-00, TIME=0.26000000E-01, X= 0.15748640, Y= 0.57952482, DT=0.26000000E-01
 LAMBDA=0.36430000E 01           W = PH  DISTRIBUTION
  1.2699358  1.3235082  1.3712435  1.4101995  1.4381336  1.4536307  1.4561485  1.4459935  1.4242401  1.3926005
  1.3532540  1.3086490  1.2612927  1.2135519  1.1674889  1.1247574  1.0865701  1.0537368  1.0267532  1.0059195
  0.9914683  0.9836916  0.9830484  0.9902061  1.0059574  1.0309757  1.0654484  1.1087195  1.1591013  1.2139444

CASE    1, STEP   51, B= 0.4500000E-00, TIME=0.13259997E 01, X= 0.16288353, Y= 0.58132542, DT=0.26000000E-01
 LAMBDA=0.36430000E 01           W = PH  DISTRIBUTION
  1.2708498  1.3249664  1.3731773  1.4125086  1.4406942  1.4563043  1.4587911  1.4484649  1.4264123  1.3943658
  1.3545320  1.3093914  1.2614856  1.2132142  1.1666683  1.1235224  1.0850009  1.0519160  1.0247594  1.0038224
  0.9893282  0.9815608  0.9809761  0.9882454  1.0041727  1.0294466  1.0642664  1.1079768  1.1588753  1.2142834

CASE    1, STEP  101, B= 0.4500000E-00, TIME=0.26259994E 01, X= 0.15534628, Y= 0.57411203, DT=0.26000000E-01
 LAMBDA=0.36430000E 01           W = PH  DISTRIBUTION
  1.2667055  1.3206729  1.3689470  1.4085510  1.4372045  1.4534537  1.4567183  1.4472688  1.4261473  1.3950376
  1.3560970  1.3117584  1.2645219  1.2167552  1.1705303  1.1275174  1.0889501  1.0556605  1.0281658  1.0067837
  0.9917599  0.9833957  0.9821568  0.9887200  1.0038951  1.0283844  1.0624150  1.1053738  1.1556085  1.2104897

CASE    1, STEP  151, B= 0.4500000E-00, TIME=0.39259990E 01, X= 0.15505200, Y= 0.58237205, DT=0.26000000E-01
 LAMBDA=0.36430000E 01           W = PH  DISTRIBUTION
  1.2685463  1.3214740  1.3686849  1.4072584  1.4349627  1.4503841  1.4529742  1.4430279  1.4216031  1.3903919
  1.3515511  1.3075052  1.2607368  1.2135888  1.1681017  1.1259101  1.0882115  1.0558037  1.0291738  1.0086150
  0.9943527  0.9866700  0.9860131  0.9930331  1.0085067  1.0330979  1.0670009  1.1095867  1.1592130  1.2132856

CASE    1, STEP  201, B= 0.4500000E-00, TIME=0.52259973E 01, X= 0.15601735, Y= 0.57855898, DT=0.26000000E-01
 LAMBDA=0.36430000E 01           W = PH  DISTRIBUTION
  1.2724197  1.3255229  1.3726851  1.4110073  1.4382895  1.4531548  1.4550931  1.4444367  1.4222782  1.3903404
  1.3508061  1.3061210  1.2587839  1.2111497  1.1652674  1.1227773  1.0848815  1.0523814  1.0257682  1.0053402
  0.9913298  0.9840285  0.9838909  0.9915712  1.0078357  1.0333169  1.0681528  1.1116404  1.1620600  1.2167531

CASE    1, STEP  251, B= 0.4500000E-00, TIME=0.65259954E 01, X= 0.15858386, Y= 0.58084965, DT=0.26000000E-01
 LAMBDA=0.36430000E 01           W = PH  DISTRIBUTION
  1.2713750  1.3251474  1.3729789  1.4119270  1.4397570  1.4550669  1.4573312  1.4468754  1.4247938  1.3928177
  1.3531444  1.3082372  1.2606147  1.2126502  1.1664085  1.1235418  1.0852588  1.0523643  1.0253502  1.0045152
  0.9900941  0.9823859  0.9818602  0.9891974  1.0052001  1.0305425  1.0653988  1.1090854  1.1598778  1.2150891

CASE    1, STEP  301, B= 0.4500000E-00, TIME=0.78259936E 01, X= 0.15894331, Y= 0.57914328, DT=0.26000000E-01
 LAMBDA=0.36430000E 01           W = PH  DISTRIBUTION
  1.2699573  1.3240299  1.3722308  1.4115879  1.4398361  1.4555459  1.4581674  1.4480072  1.4261458  1.3943072
  1.3546871  1.3097538  1.2620361  1.2139218  1.1674923  1.1244162  1.0859163  1.0528070  1.0255848  1.0045472
  0.9899237  0.9820048  0.9812521  0.9883434  1.0040892  1.0291848  1.0638363  1.1073948  1.1581630  1.2134665

CASE    1, STEP  351, B= 0.4500000E-00, TIME=0.91259892E 01, X= 0.15747739, Y= 0.57698114, DT=0.26000000E-01
 LAMBDA=0.36430000E 01           W = PH  DISTRIBUTION
  1.2674860  1.3212484  1.3692933  1.4086549  1.4370628  1.4530728  1.4561135  1.4464637  1.4251734  1.3939337
  1.3549079  1.3105338  1.2633141  1.2156167  1.1695104  1.1266593  1.0882886  1.0552201  1.0279605  1.0068178
  0.9920287  0.9838869  0.9828511  0.9895907  1.0049074  1.0294946  1.0635710  1.1065181  1.1566828  1.2114400

CASE    1, STEP  401, B= 0.4500000E-00, TIME=0.10425984E 02, X= 0.15603982, Y= 0.58039208, DT=0.26000000E-01
 LAMBDA=0.36430000E 01           W = PH  DISTRIBUTION
  1.2689497  1.3221742  1.3696403  1.4084167  1.4362645  1.4517664  1.4543731  1.4443808  1.4228513  1.3914821
  1.3524377  1.3081516  1.2611171  1.2136887  1.1679188  1.1254538  1.0875015  1.0548685  1.0280489  1.0073411
  0.9929746  0.9852361  0.9845756  0.9916487  1.0072362  1.0320041  1.0661435  1.1090154  1.1589608  1.2133654

CASE    1, STEP  451, B= 0.4500000E-00, TIME=0.11725979E 02, X= 0.15522034, Y= 0.57905324, DT=0.26000000E-01
 LAMBDA=0.36430000E 01           W = PH  DISTRIBUTION
  1.2710594  1.3242385  1.3715377  1.4100459  1.4375495  1.4526584  1.4548500  1.4444450  1.4225260  1.3908075
  1.3514656  1.3069403  1.2597270  1.2121782  1.1663416  1.1238576  1.0859286  1.0533575  1.0266368  1.0060663
```

FIG. 17
RUN 13
$\Delta T = 0.026$
PRESSURE
PROFILES

FIG. 18
RUN 13
$\Delta T = 0.013$
PRESSURE
PROFILES

```
LAMBDA=0.36430000E 01                W = PH  DISTRIBUTION
 1.2695603  1.3230985  1.3708036  1.4097350  1.4376512  1.4531380  1.4556531  1.4455028  1.4237610  1.3921386
 1.3528138  1.3082338  1.2609043  1.2131907  1.1671544  1.1244479  1.0862835  1.0534705  1.0265044  1.0056853
 0.9912457  0.9834774  0.9828388  0.9899965  1.0057422  1.0307481  1.0652014  1.1084463  1.1587964  1.213604[illegible]

CASE    1, STEP    1, B= 0.4500000E-00, TIME=0.13000000E-01, X= 0.15735640, Y= 0.57939479, DT=0.13000000E-01
LAMBDA=0.36430000E 01                W = PH  DISTRIBUTION
 1.2699360  1.3235083  1.3712437  1.4101996  1.4381337  1.4536308  1.4561486  1.4459936  1.4242402  1.39260[illegible]5
 1.3532540  1.3086490  1.2612928  1.2135520  1.1674890  1.1247575  1.0865702  1.0537369  1.0267532  1.0059195
 0.9914683  0.9836916  0.9830485  0.9902062  1.0059575  1.0309758  1.0654485  1.1087197  1.1591014  1.2139445

CASE    1, STEP   51, B= 0.4500000E-00, TIME=0.66299987E 00, X= 0.16266501, Y= 0.58402750, DT=0.13000000E-01
LAMBDA=0.36430000E 01                W = PH  DISTRIBUTION
 1.2705917  1.3243459  1.3722232  1.4112694  1.4392341  1.4546985  1.4571215  1.4468152  1.4248642  1.3929944
 1.3534016  1.3085518  1.2609691  1.2130339  1.1668177  1.1239779  1.0857259  1.0528660  1.0258873  1.0050828
 0.9906789  0.9829637  0.9823947  0.9896412  1.0055004  1.0306514  1.0652853  1.1087448  1.1593348  1.2143935

CASE    1, STEP  101, B= 0.4500000E-00, TIME=0.13129997E 01, X= 0.16294248, Y= 0.58144213, DT=0.13000000E-01
LAMBDA=0.36430000E 01                W = PH  DISTRIBUTION
 1.2708443  1.3249572  1.3731647  1.4124931  1.4406763  1.4562849  1.4587709  1.4484447  1.4263930  1.3943484
 1.3545175  1.3093805  1.2614789  1.2132123  1.1666711  1.1235297  1.0850121  1.0519304  1.0247759  1.0038403
 0.9893465  0.9815791  0.9809936  0.9882616  1.0041871  1.0294587  1.0642756  1.1079828  1.1588776  1.2142819

CASE    1, STEP  151, B= 0.4500000E-00, TIME=0.19629995E 01, X= 0.15906211, Y= 0.57540024, DT=0.13000000E-01
LAMBDA=0.36430000E 01                W = PH  DISTRIBUTION
 1.2691067  1.3233673  1.3718002  1.4114211  1.4399507  1.4559437  1.4588343  1.4489133  1.4272473  1.3955482
 1.3560033  1.3110763  1.2632969  1.2150587  1.1684539  1.1251654  1.0864319  1.0530831  1.0256284  1.0043751
 0.9895578  0.9814689  0.9805690  0.9875330  1.0031701  1.0281778  1.0627688  1.1063045  1.1570975  1.2124803

CASE    1, STEP  201, B= 0.4500000E-00, TIME=0.26129986E 01, X= 0.15538202, Y= 0.57404207, DT=0.13000000E-01
LAMBDA=0.36430000E 01                W = PH  DISTRIBUTION
 1.2667348  1.3207018  1.3689744  1.4085760  1.4372261  1.4534713  1.4567310  1.4472761  1.4261488  1.3950330
 1.3560860  1.3117413  1.2644990  1.2167275  1.1704989  1.1274837  1.0889159  1.0556276  1.0281358  1.0067583
 0.9917402  0.9833826  0.9821507  0.9887210  1.0039029  1.0283984  1.0624343  1.1053975  1.1556353  1.2105184

CASE    1, STEP  251, B= 0.4500000E-00, TIME=0.32629977E 01, X= 0.15435091, Y= 0.57845997, DT=0.13000000E-01
LAMBDA=0.36430000E 01                W = PH  DISTRIBUTION
 1.2663585  1.3197509  1.3675044  1.4066670  1.4349763  1.4509900  1.4541337  1.4446794  1.4236656  1.3927688
 1.3541348  1.3101817  1.2633910  1.2161101  1.1703887  1.1278753  1.0897836  1.0569289  1.0298153  1.0087512
 0.9939757  0.9857842  0.9846357  0.9911975  1.0062671  1.0305367  1.0642296  1.1067418  1.1564441  1.2107409

CASE    1, STEP  301, B= 0.4500000E-00, TIME=0.39129968E 01, X= 0.15499089, Y= 0.58240078, DT=0.13000000E-01
LAMBDA=0.36430000E 01                W = PH  DISTRIBUTION
 1.2685525  1.3214856  1.3687006  1.4072769  1.4349826  1.4504045  1.4529943  1.4430472  1.4216213  1.3904087
 1.3515665  1.3075189  1.2607487  1.2135984  1.1681084  1.1259132  1.0882101  1.0557971  1.0291617  1.0085972
 0.9943295  0.9866424  0.9859825  0.9930014  1.0084761  1.0330707  1.0669790  1.1095716  1.1592053  1.2132853

CASE    1, STEP  351, B= 0.4500000E-00, TIME=0.45629945E 01, X= 0.15559241, Y= 0.58150972, DT=0.13000000E-01
LAMBDA=0.36430000E 01                W = PH  DISTRIBUTION
 1.2712611  1.3241177  1.3711194  1.4093669  1.4366539  1.4515947  1.4536682  1.4431953  1.4212576  1.3895678
 1.3502996  1.3058906  1.2588326  1.2114740  1.1658576  1.1236174  1.0859487  1.0536461  1.0271934  1.0068809
 0.9929321  0.9856289  0.9854153  0.9929367  1.0089555  1.0341097  1.0685551  1.1116183  1.1616147  1.2159200

CASE    1, STEP  401, B= 0.4500000E-00, TIME=0.52129922E 01, X= 0.15606795, Y= 0.57859470, DT=0.13000000E-01
LAMBDA=0.36430000E 01                W = PH  DISTRIBUTION
 1.2724103  1.3255208  1.3726904  1.4110193  1.4383070  1.4531761  1.4551165  1.4444602  1.4223002  1.3903594
 1.3508212  1.3061315  1.2587900  1.2111518  1.1652662  1.1227738  1.0848765  1.0523756  1.0257619  1.0053333
 0.9913217  0.9840185  0.9838781  0.9915549  1.0078158  1.0332941  1.0681284  1.1116166  1.1620391  1.2167371
```

CASE NUMBER 1, B= 0.45000

STEP	X	Y	STEP	X	Y
1	0.1574864	0.5795248	51	0.1628835	0.5813254
2	0.1577459	0.5797841	52	0.1627789	0.5810893
3	0.1580045	0.5800420	53	0.1626676	0.5808479
4	0.1582617	0.5802976	54	0.1625498	0.5806020
5	0.1585170	0.5805502	55	0.1624258	0.5803520
6	0.1587700	0.5807991	56	0.1622959	0.5800987
7	0.1590202	0.5810436	57	0.1621605	0.5798428
8	0.1592672	0.5812830	58	0.1620198	0.5795848
9	0.1595105	0.5815166	59	0.1618741	0.5793254
10	0.1597497	0.5817437	60	0.1617238	0.5790654
11	0.1599845	0.5819637	61	0.1615693	0.5788053
12	0.1602143	0.5821760	62	0.1614108	0.5785458
13	0.1604389	0.5823800	63	0.1612486	0.5782876
14	0.1606578	0.5825750	64	0.1610832	0.5780313
15	0.1608707	0.5827606	65	0.1609148	0.5777775
16	0.1610772	0.5829363	66	0.1607438	0.5775269
17	0.1612770	0.5831014	67	0.1605705	0.5772800
18	0.1614698	0.5832557	68	0.1603952	0.5770374
19	0.1616552	0.5833986	69	0.1602184	0.5767999
20	0.1618331	0.5835298	70	0.1600402	0.5765678
21	0.1620030	0.5836490	71	0.1598610	0.5763417
22	0.1621649	0.5837557	72	0.1596812	0.5761223
23	0.1623184	0.5838497	73	0.1595011	0.5759099
24	0.1624633	0.5839308	74	0.1593209	0.5757052
25	0.1625995	0.5839987	75	0.1591410	0.5755084
26	0.1627267	0.5840533	76	0.1589616	0.5753202
27	0.1628448	0.5840944	77	0.1587831	0.5751408
28	0.1629537	0.5841220	78	0.1586058	0.5749708
29	0.1630532	0.5841359	79	0.1584298	0.5748104
30	0.1631433	0.5841362	80	0.1582556	0.5746601
31	0.1632239	0.5841228	81	0.1580833	0.5745200
32	0.1632949	0.5840959	82	0.1579131	0.5743906
33	0.1633563	0.5840554	83	0.1577454	0.5742720
34	0.1634080	0.5840016	84	0.1575803	0.5741645
35	0.1634501	0.5839346	85	0.1574181	0.5740683
36	0.1634826	0.5838545	86	0.1572590	0.5739836
37	0.1635055	0.5837617	87	0.1571031	0.5739105
38	0.1635189	0.5836564	88	0.1569507	0.5738490
39	0.1635228	0.5835389	89	0.1568019	0.5737994
40	0.1635174	0.5834095	90	0.1566569	0.5737616
41	0.1635028	0.5832685	91	0.1565158	0.5737356
42	0.1634790	0.5831165	92	0.1563789	0.5737215
43	0.1634462	0.5829538	93	0.1562461	0.5737193
44	0.1634047	0.5827808	94	0.1561176	0.5737287
45	0.1633545	0.5825980	95	0.1559935	0.5737498
46	0.1632958	0.5824059	96	0.1558740	0.5737824
47	0.1632290	0.5822051	97	0.1557590	0.5738264
48	0.1631540	0.5819961	98	0.1556487	0.5738816
49	0.1630713	0.5817794	99	0.1555431	0.5739477
50	0.1629811	0.5815557	100	0.1554423	0.5740246

FIG. 19
RUN 13
$\Delta T = 0.026$
ORBIT
COÖRDINATES

CASE NUMBER 1, B= 0.45000

STEP	X	Y	STEP	X	Y
1	0.1573564	0.5793948	51	0.1626650	0.5840275
2	0.1574863	0.5795247	52	0.1627276	0.5840532
3	0.1576162	0.5796544	53	0.1627879	0.5840755
4	0.1577458	0.5797839	54	0.1628459	0.5840944
5	0.1578752	0.5799130	55	0.1629017	0.5841100
6	0.1580043	0.5800416	56	0.1629551	0.5841221
7	0.1581331	0.5801697	57	0.1630061	0.5841309
8	0.1582615	0.5802971	58	0.1630549	0.5841362
9	0.1583894	0.5804238	59	0.1631012	0.5841381
10	0.1585167	0.5805497	60	0.1631452	0.5841366
11	0.1586435	0.5806746	61	0.1631868	0.5841317
12	0.1587697	0.5807985	62	0.1632261	0.5841234
13	0.1588951	0.5809213	63	0.1632629	0.5841117
14	0.1590198	0.5810429	64	0.1632974	0.5840966
15	0.1591437	0.5811633	65	0.1633294	0.5840781
16	0.1592667	0.5812822	66	0.1633590	0.5840562
17	0.1593889	0.5813998	67	0.1633863	0.5840311
18	0.1595100	0.5815158	68	0.1634111	0.5840025
19	0.1596302	0.5816302	69	0.1634335	0.5839707
20	0.1597492	0.5817429	70	0.1634535	0.5839356
21	0.1598672	0.5818538	71	0.1634711	0.5838973
22	0.1599840	0.5819628	72	0.1634864	0.5838557
23	0.1600995	0.5820700	73	0.1634992	0.5838109
24	0.1602138	0.5821751	74	0.1635096	0.5837630
25	0.1603268	0.5822781	75	0.1635177	0.5837119
26	0.1604384	0.5823790	76	0.1635234	0.5836578
27	0.1605486	0.5824777	77	0.1635267	0.5836005
28	0.1606573	0.5825741	78	0.1635277	0.5835403
29	0.1607646	0.5826681	79	0.1635263	0.5834771
30	0.1608702	0.5827597	80	0.1635226	0.5834109
31	0.1609743	0.5828488	81	0.1635166	0.5833419
32	0.1610768	0.5829353	82	0.1635084	0.5832701
33	0.1611776	0.5830193	83	0.1634978	0.5831954
34	0.1612767	0.5831006	84	0.1634850	0.5831180
35	0.1613740	0.5831791	85	0.1634699	0.5830380
36	0.1614695	0.5832549	86	0.1634526	0.5829553
37	0.1615632	0.5833278	87	0.1634331	0.5828701
38	0.1616551	0.5833979	88	0.1634115	0.5827823
39	0.1617450	0.5834650	89	0.1633876	0.5826921
40	0.1618330	0.5835291	90	0.1633616	0.5825995
41	0.1619191	0.5835903	91	0.1633336	0.5825046
42	0.1620031	0.5836483	92	0.1633034	0.5824074
43	0.1620851	0.5837033	93	0.1632712	0.5823080
44	0.1621651	0.5837551	94	0.1632369	0.5822065
45	0.1622430	0.5838038	95	0.1632006	0.5821029
46	0.1623187	0.5838492	96	0.1631624	0.5819973
47	0.1623924	0.5838915	97	0.1631222	0.5818898
48	0.1624638	0.5839304	98	0.1630801	0.5817805
49	0.1625331	0.5839661	99	0.1630360	0.5816694
50	0.1626002	0.5839985	100	0.1629902	0.5815566

FIG. 20 a
RUN 13
$\Delta T = 0.013$
ORBIT
COORDINATES

CASE NUMBER 1, R= 0.45001

TEP	X	Y	STEP	X	Y
101	0.1629425	0.5814421	151	0.1590621	0.5754002
102	0.1628930	0.5813261	152	0.1589723	0.5753068
103	0.1628417	0.5812087	153	0.1588828	0.5752156
104	0.1627888	0.5810898	154	0.1587934	0.5751267
105	0.1627341	0.5809696	155	0.1587044	0.5750401
106	0.1626777	0.5808482	156	0.1586156	0.5749559
107	0.1626198	0.5807256	157	0.1585272	0.5748741
108	0.1625603	0.5806019	158	0.1584391	0.5747947
109	0.1624992	0.5804772	159	0.1583515	0.5747179
110	0.1624366	0.5803516	160	0.1582643	0.5746436
111	0.1623725	0.5802252	161	0.1581776	0.5745719
112	0.1623070	0.5800980	162	0.1580914	0.5745028
113	0.1622401	0.5799701	163	0.1580057	0.5744363
114	0.1621718	0.5798416	164	0.1579206	0.5743726
115	0.1621022	0.5797127	165	0.1578361	0.5743116
116	0.1620314	0.5795832	166	0.1577522	0.5742533
117	0.1619593	0.5794535	167	0.1576690	0.5741978
118	0.1618859	0.5793234	168	0.1575864	0.5741451
119	0.1618115	0.5791932	169	0.1575045	0.5740953
120	0.1617359	0.5790629	170	0.1574234	0.5740482
121	0.1616592	0.5789326	171	0.1573430	0.5740041
122	0.1615815	0.5788023	172	0.1572635	0.5739629
123	0.1615028	0.5786722	173	0.1571847	0.5739245
124	0.1614231	0.5785423	174	0.1571067	0.5738891
125	0.1613426	0.5784127	175	0.1570296	0.5738566
126	0.1612611	0.5782835	176	0.1569534	0.5738271
127	0.1611788	0.5781548	177	0.1568781	0.5738005
128	0.1610958	0.5780266	178	0.1568036	0.5737769
129	0.1610120	0.5778991	179	0.1567302	0.5737563
130	0.1609274	0.5777722	180	0.1566577	0.5737386
131	0.1608423	0.5776461	181	0.1565861	0.5737239
132	0.1607565	0.5775209	182	0.1565156	0.5737122
133	0.1606701	0.5773966	183	0.1564460	0.5737035
134	0.1605831	0.5772734	184	0.1563775	0.5736977
135	0.1604957	0.5771512	185	0.1563100	0.5736949
136	0.1604078	0.5770301	186	0.1562436	0.5736950
137	0.1603195	0.5769103	187	0.1561783	0.5736982
138	0.1602309	0.5767918	188	0.1561140	0.5737042
139	0.1601419	0.5766747	189	0.1560508	0.5737132
140	0.1600526	0.5765590	190	0.1559888	0.5737251
141	0.1599630	0.5764449	191	0.1559278	0.5737398
142	0.1598732	0.5763323	192	0.1558680	0.5737575
143	0.1597833	0.5762213	193	0.1558094	0.5737780
144	0.1596932	0.5761121	194	0.1557518	0.5738013
145	0.1596030	0.5760046	195	0.1556955	0.5738275
146	0.1595128	0.5758989	196	0.1556403	0.5738565
147	0.1594225	0.5757952	197	0.1555863	0.5738882
148	0.1593323	0.5756934	198	0.1555334	0.5739226
149	0.1592421	0.5755936	199	0.1554818	0.5739598
50	0.1591521	0.5754958	200	0.1554313	0.5739996

FIG. 20b
RUN 13
$\Delta T = 0.013$
ORBIT
COÖRDINATES

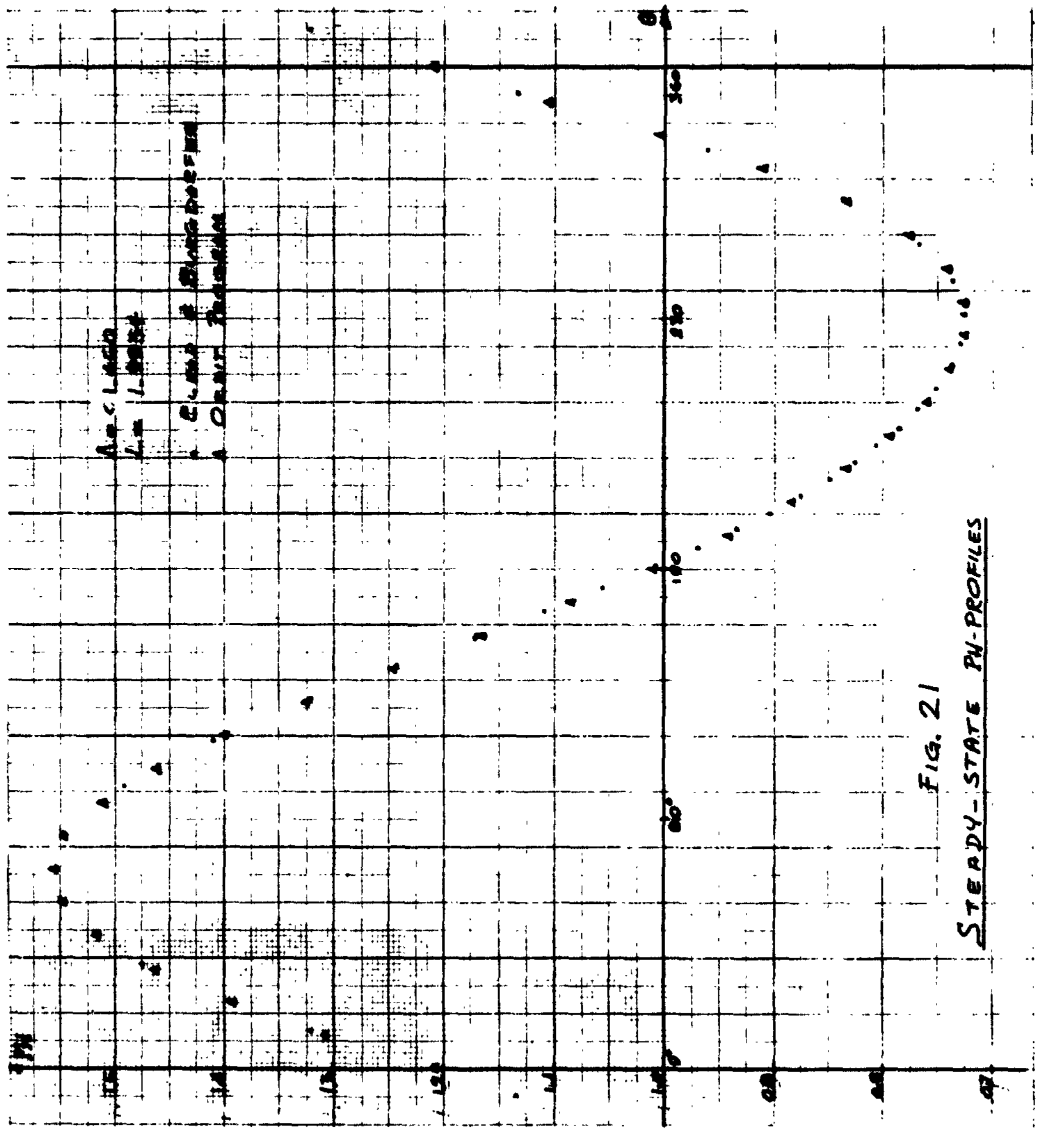

FIG. 21

STEADY-STATE PU-PROFILES

Fig. 22a
Run 8
B = 4;
ΔT = 0.011
1st 1000 steps
Convergent Case

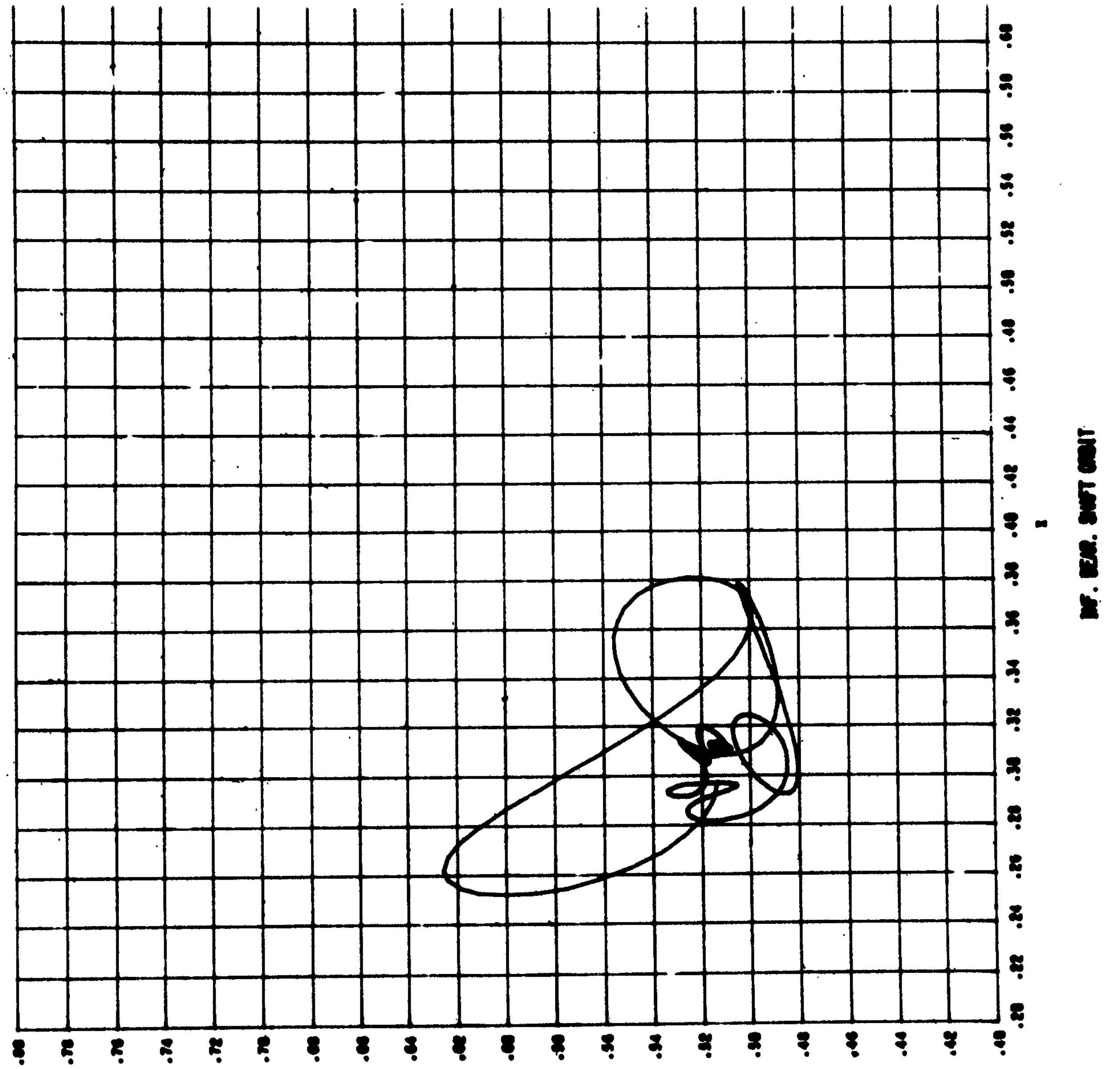

Fig. 22b
Run 8
B = 4;
$\Delta T = 0.011$
2nd 1000 steps

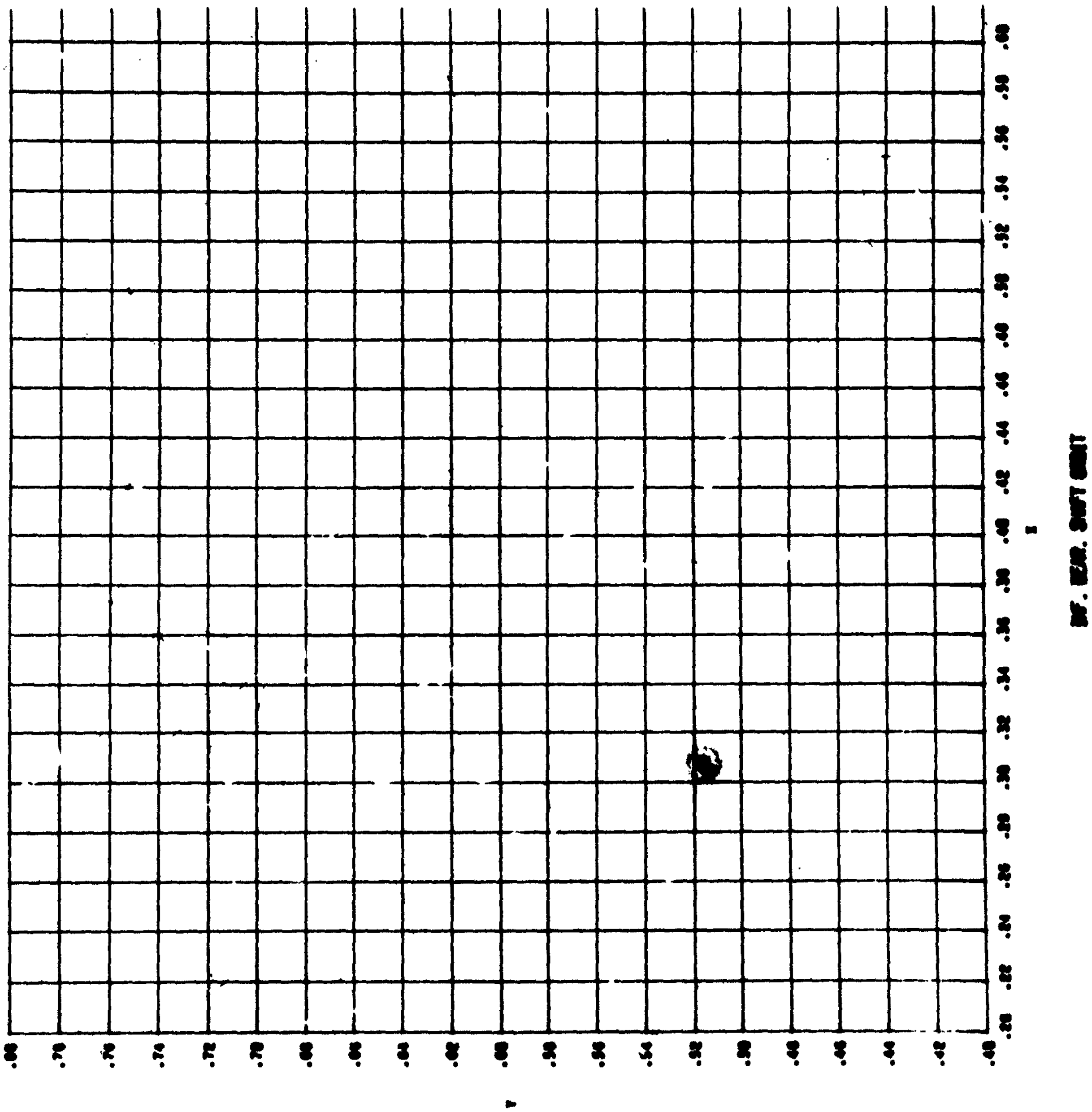

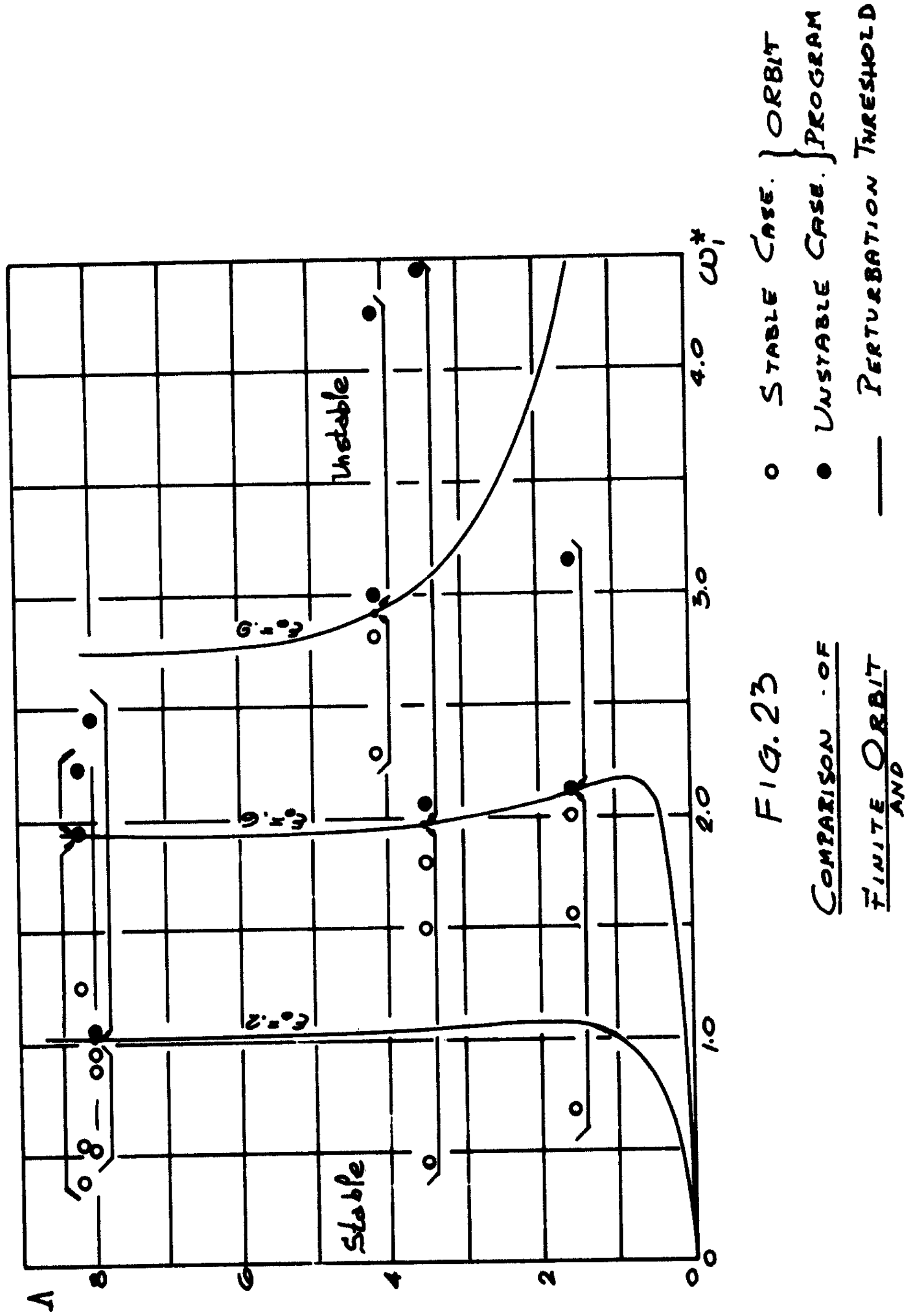

FIG. 23

COMPARISON OF FINITE ORBIT AND PERTURBATION RESULTS

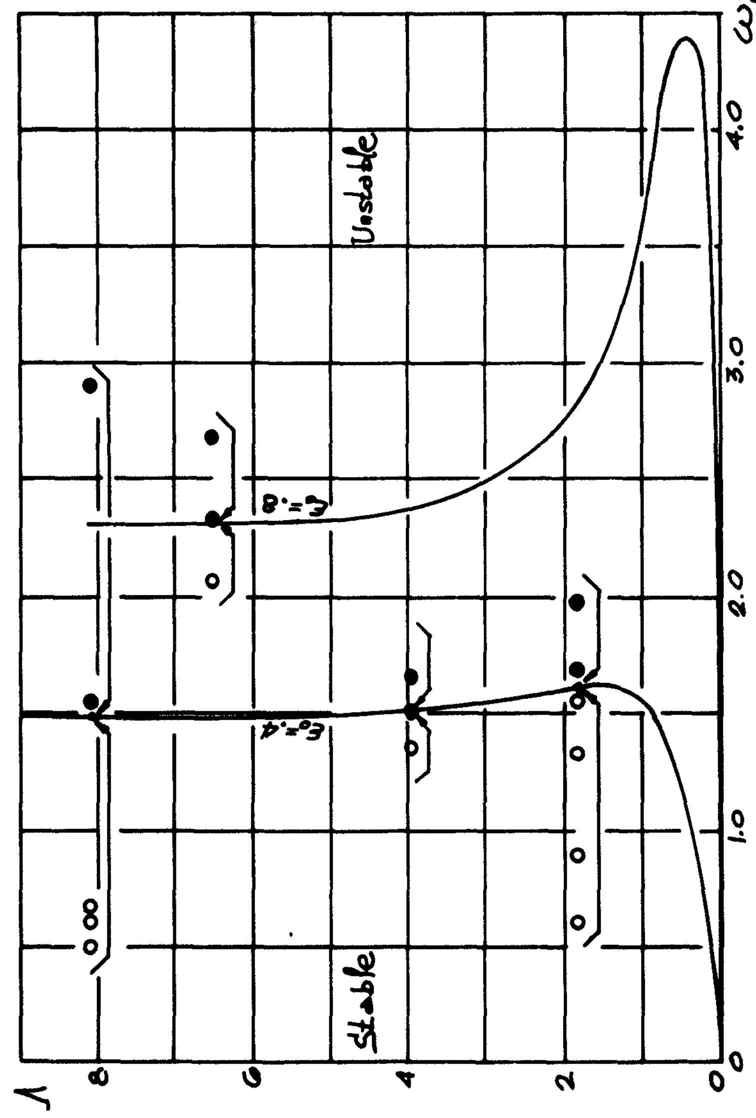

FIG. 24

COMPARISON OF FINITE ORBIT AND PERTURBATION RESULTS

Fig. 24.1a
Effect of
Size of
Disturbance
Run 6

$\Lambda = 1.979$

$\epsilon_o = 0.2$

$X_o = .09059$

$Y_o = .17831$

$L = \frac{W}{PaR} = 1.1656$

$B = 10$

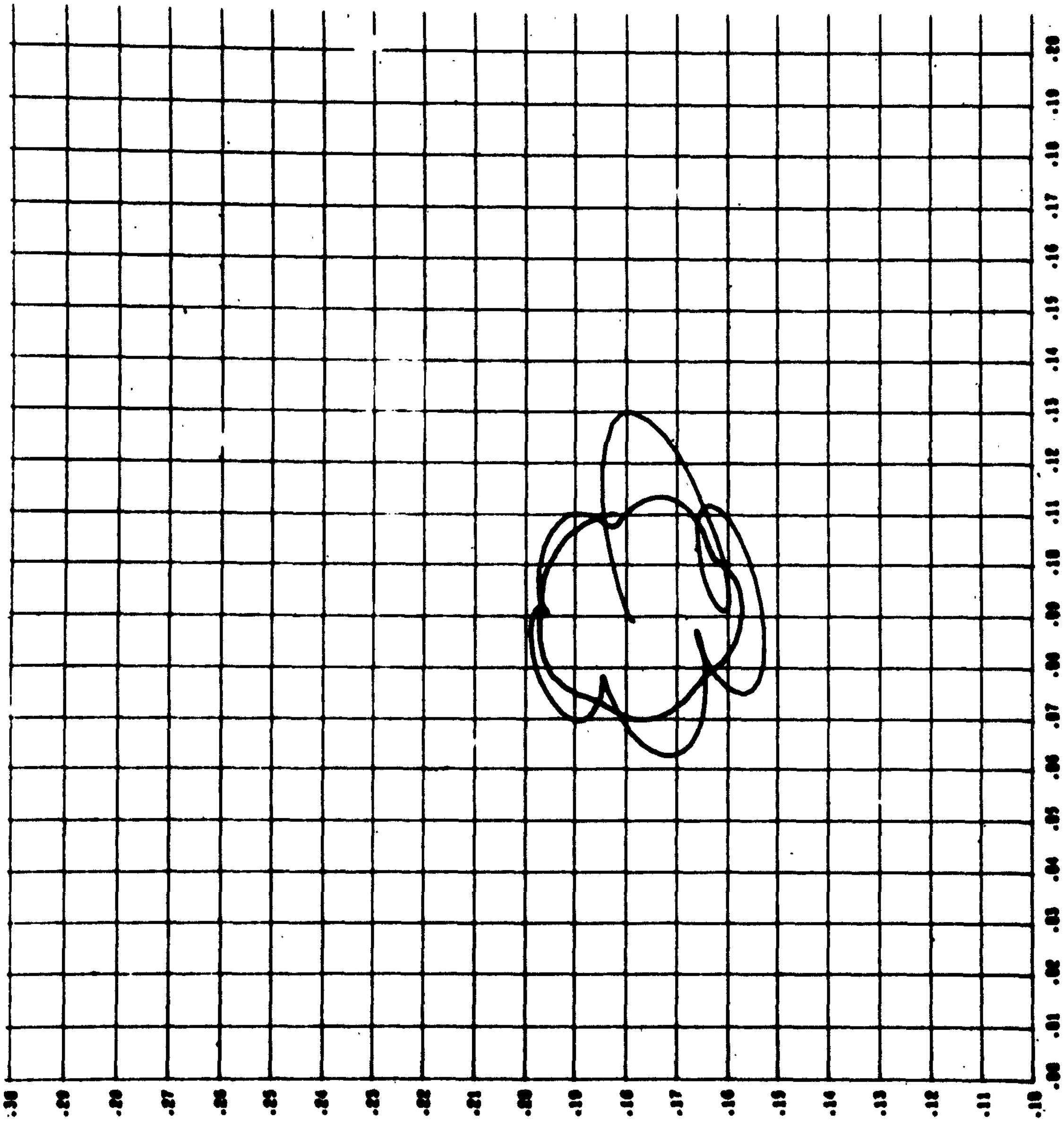

Fig. 24.1b
Effect of
Size of
Disturbance
Continued
from
Fig. 24.1a

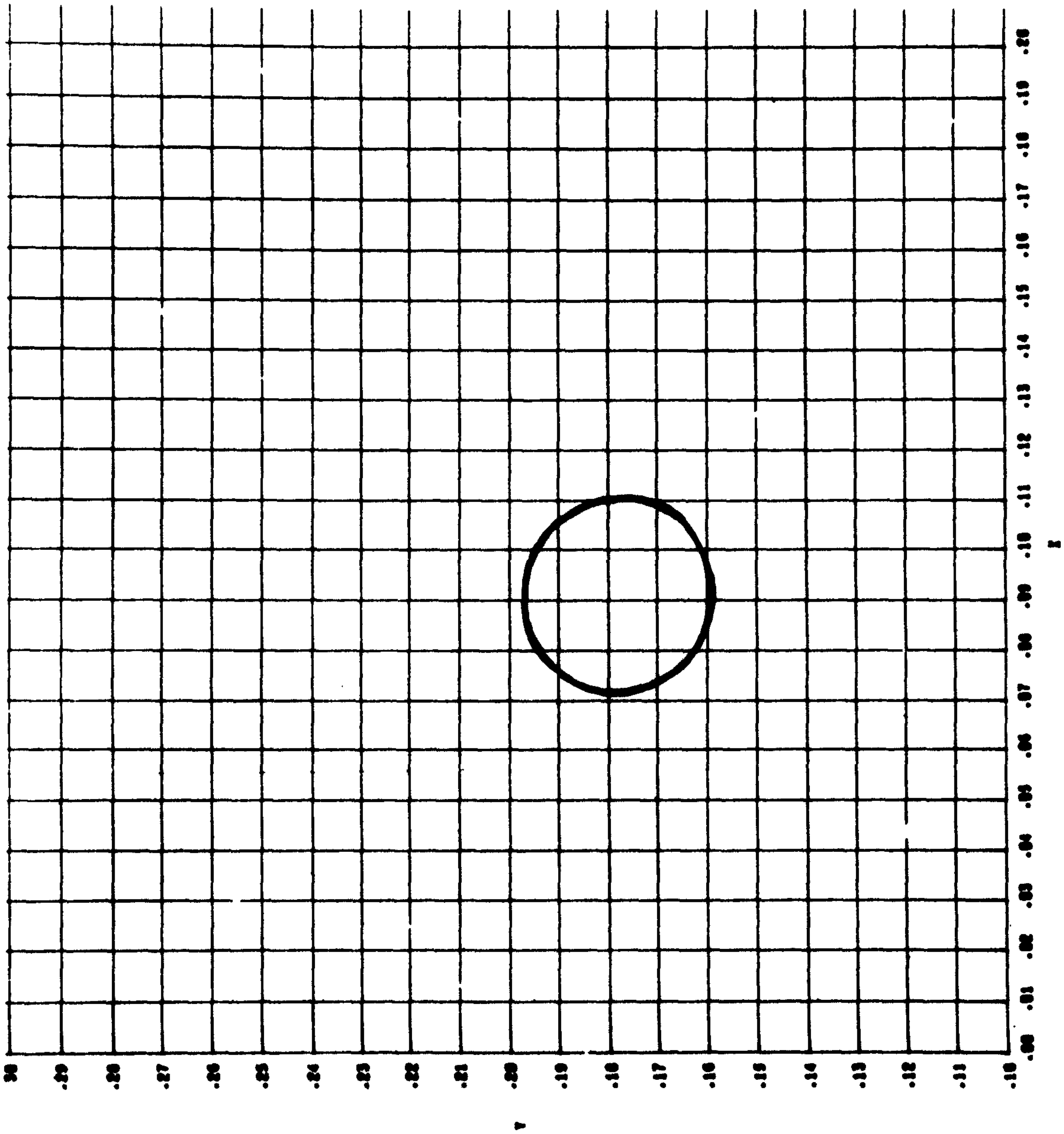

Fig. 24.1c
Effect of
Size of
Disturbance
Continued
from
Fig. 24.1b

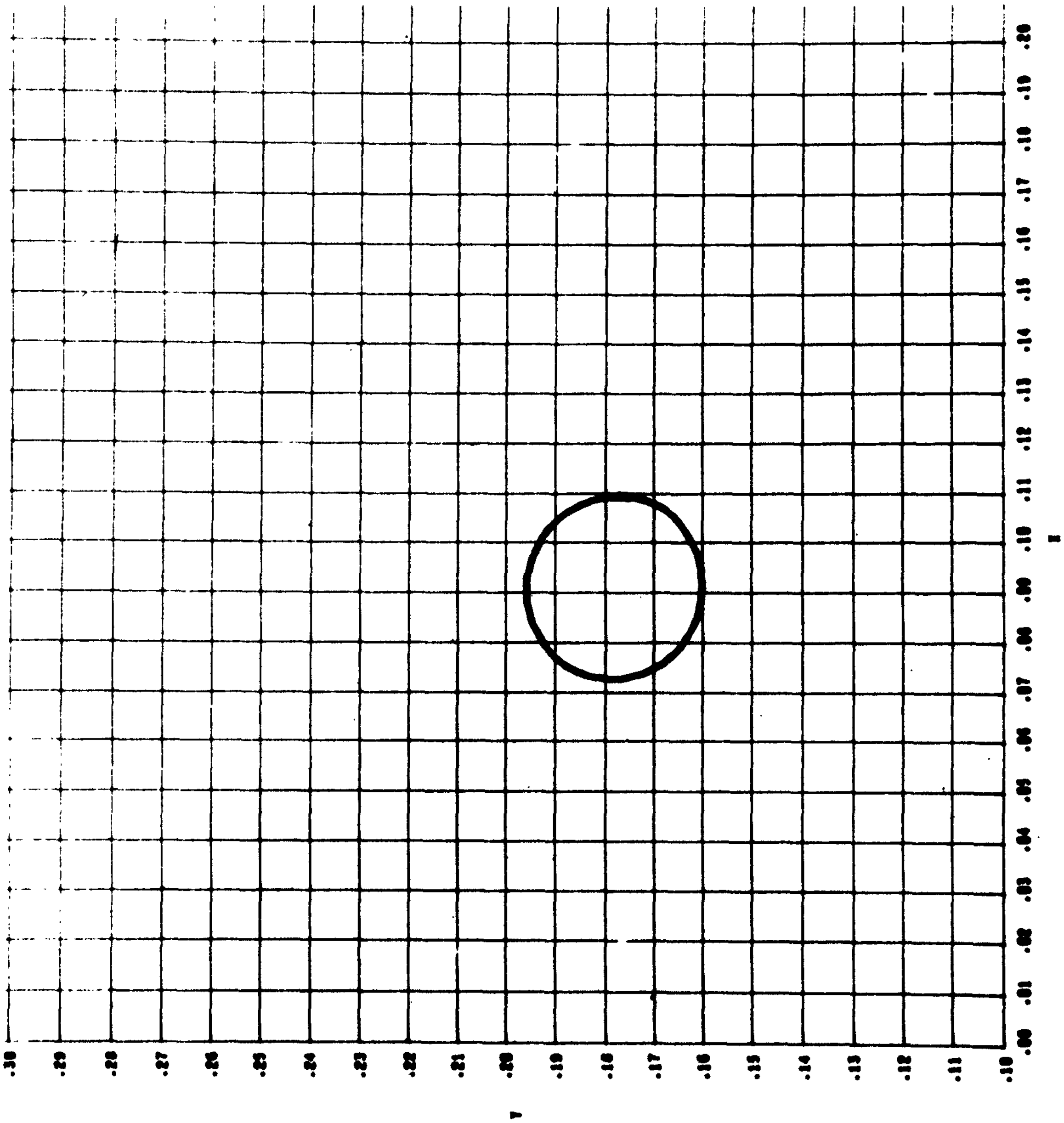

Fig. 25a
Run 7
$B = 8$;
$\Delta T = 0.026$
1st 1000 steps

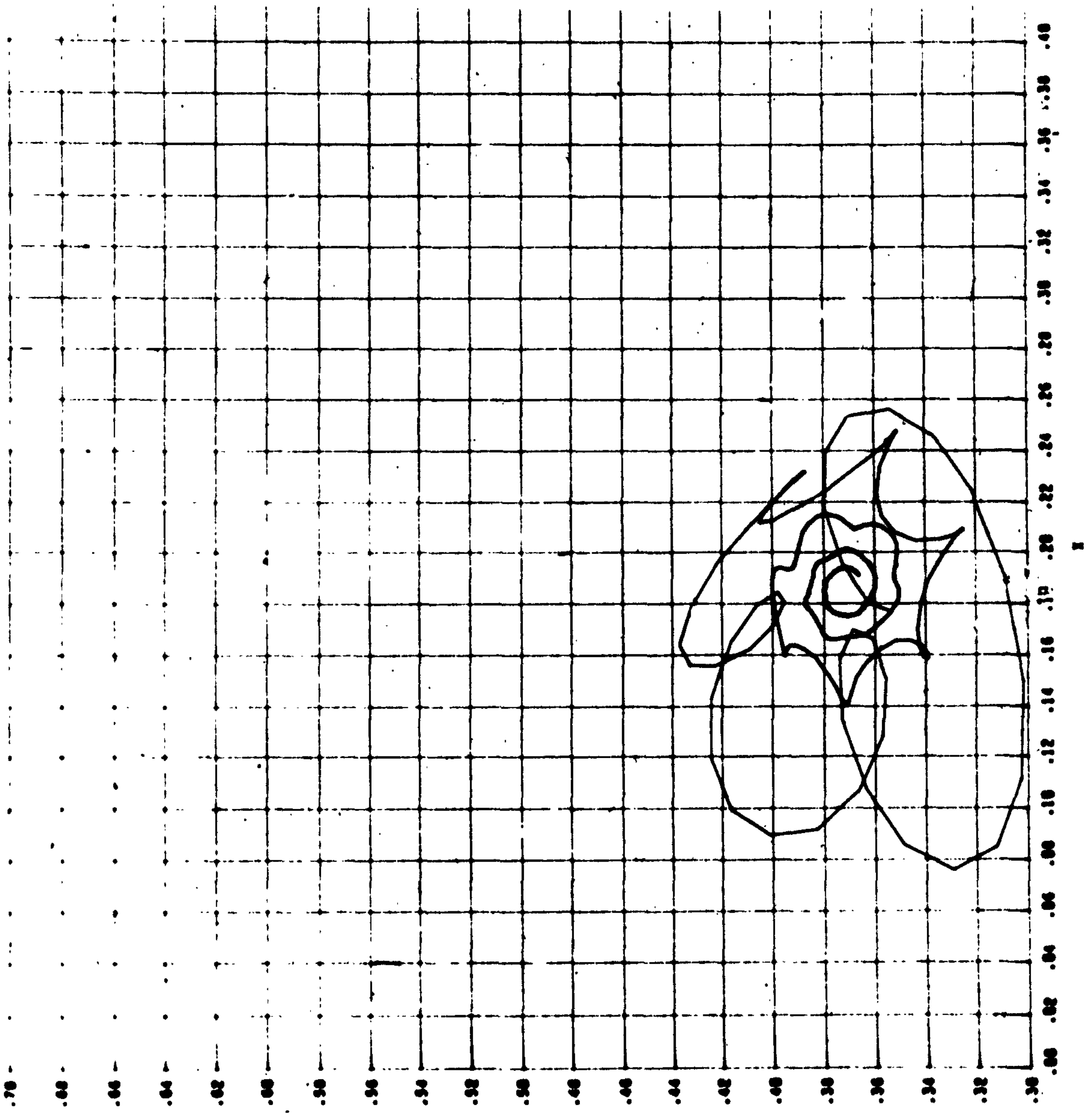

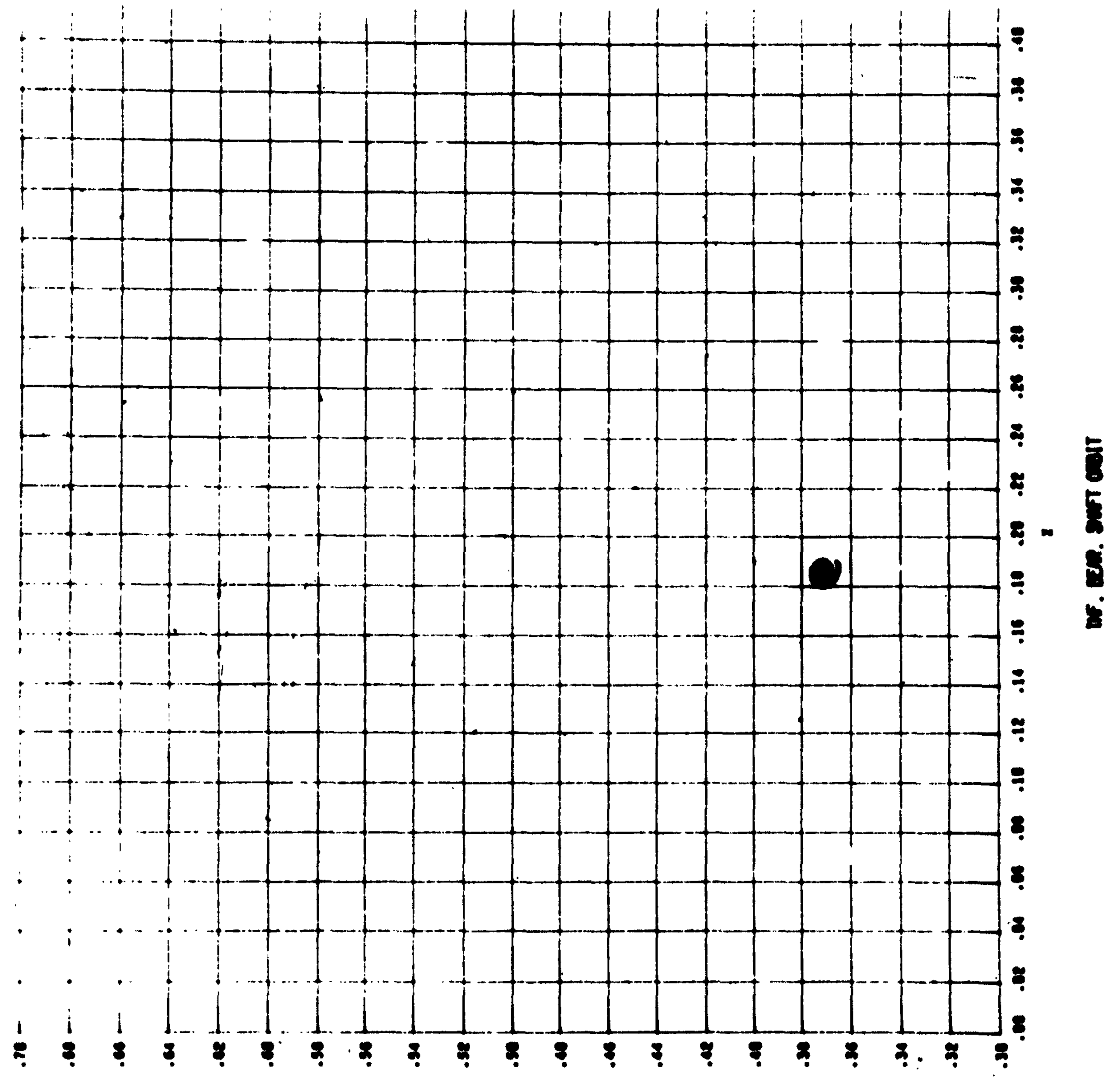

Fig. 25b
Run 7
B = 8;
$\Delta T = 0.026$
2nd 1000 steps

Fig. 26a
Run 7
B = 4;
$\Delta T = 0.026$
1st 1000 steps

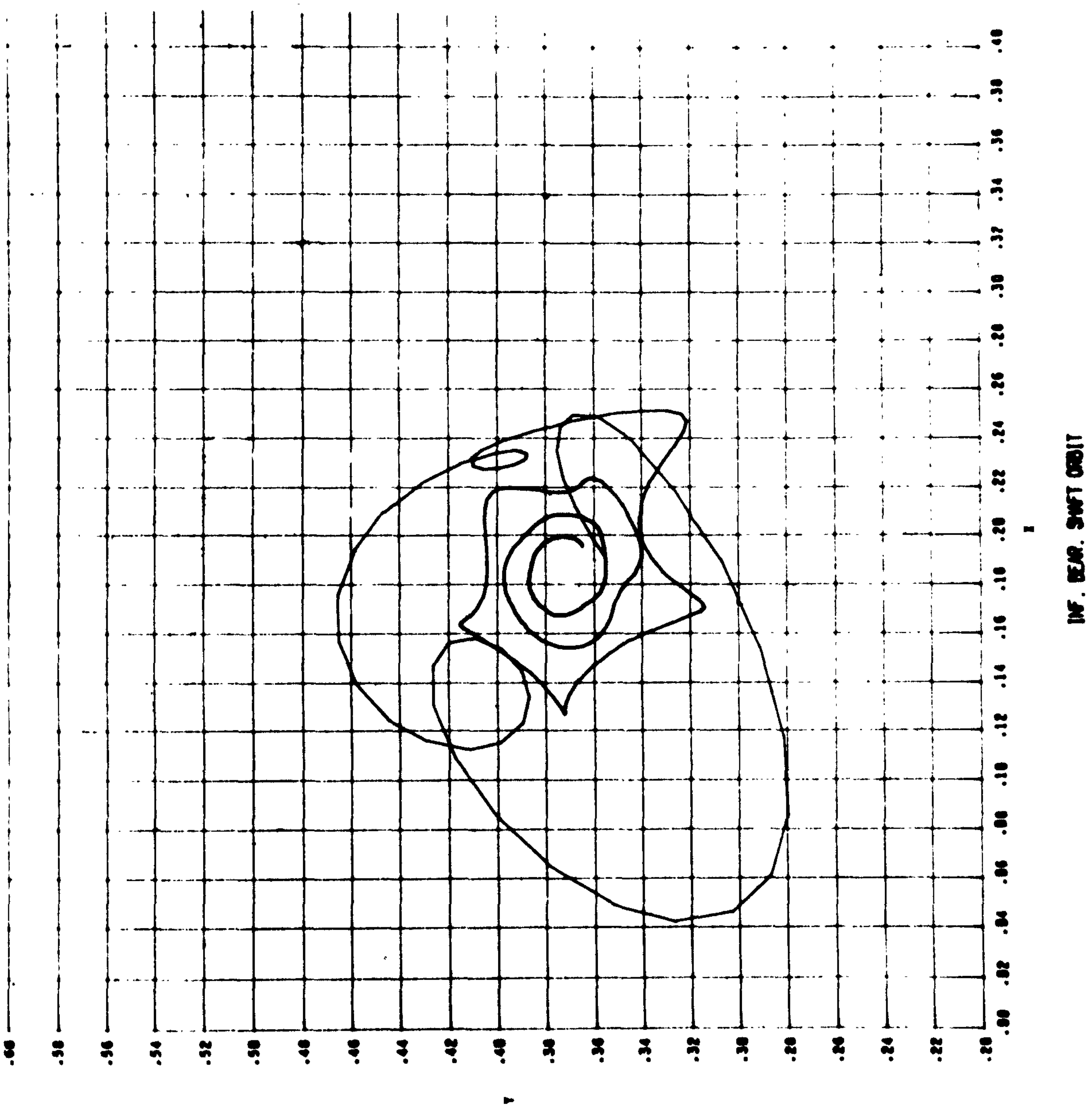

Fig. 26t
Run 7
B = 4;
$\Delta T = 0.026$
2nd 1000 steps

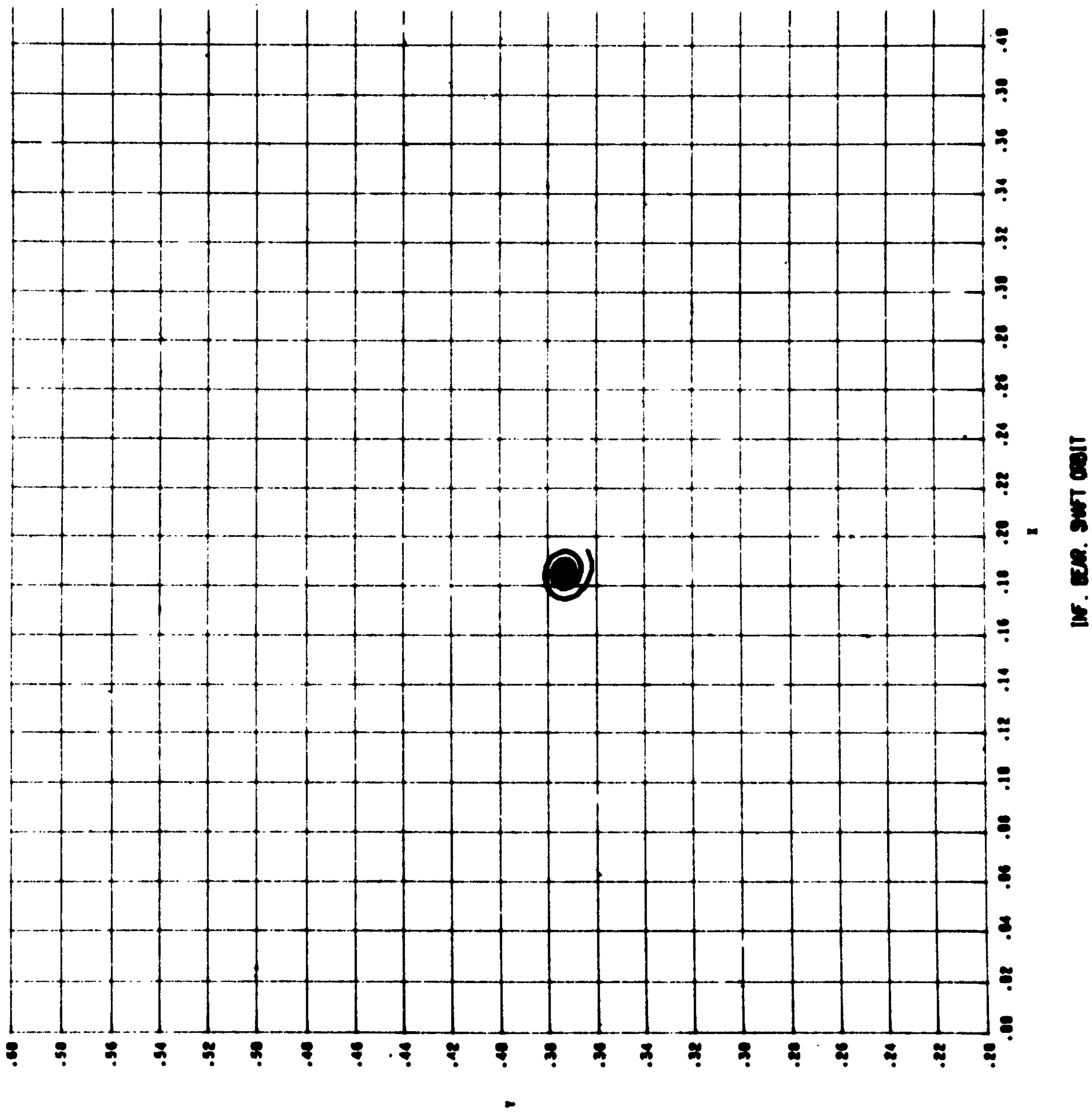

Fig. 27a
Run 7
B = 1.8
$\Delta T = 0.013$
1st 1000 steps
Sample Orbit
with
Small
Perturbation

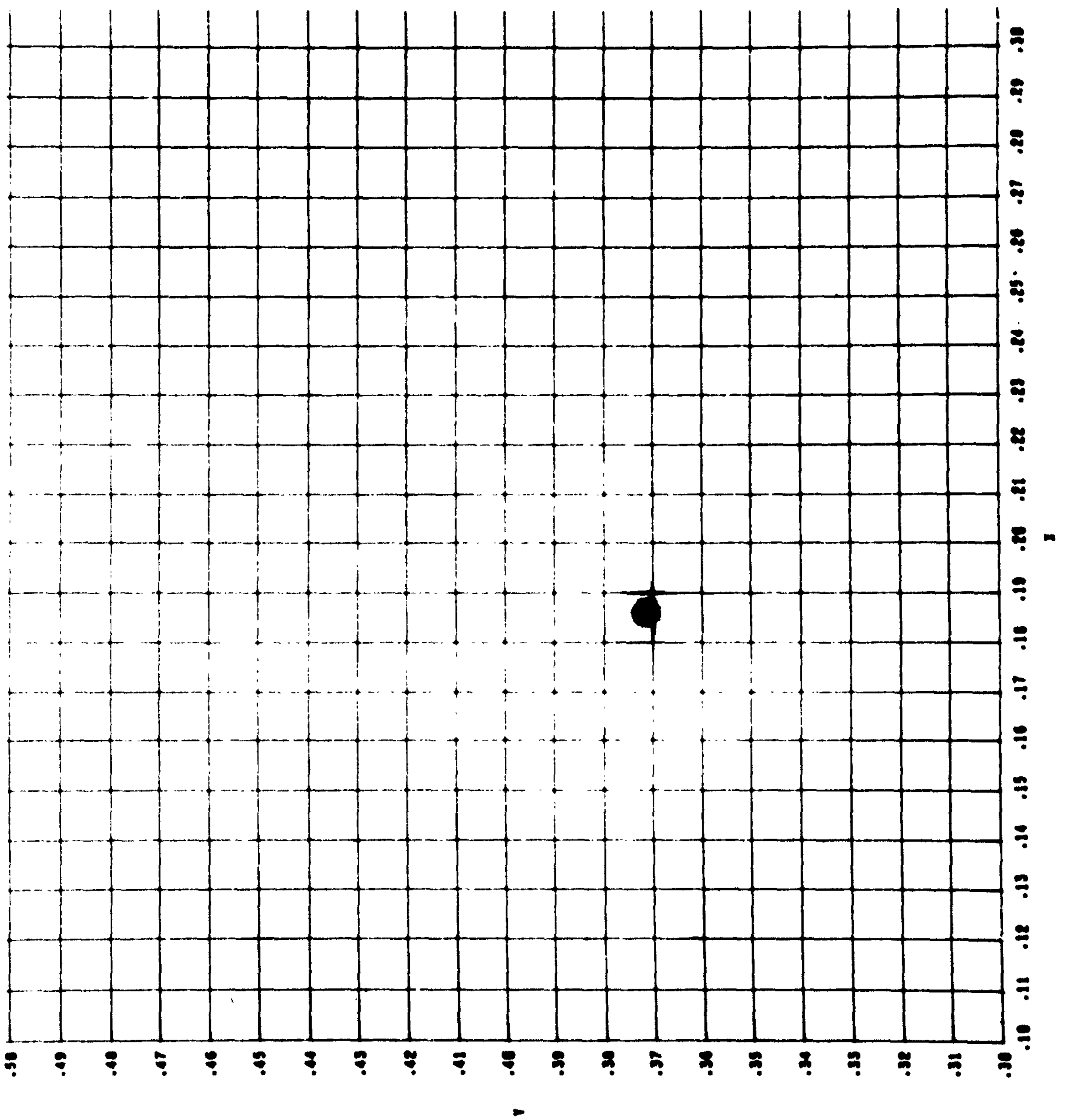

Fig. 27b
Run 7
B = 1.8
$\Delta T = 0.013$
2nd 1000 steps
Sample Orbit
with
Small
Perturbation

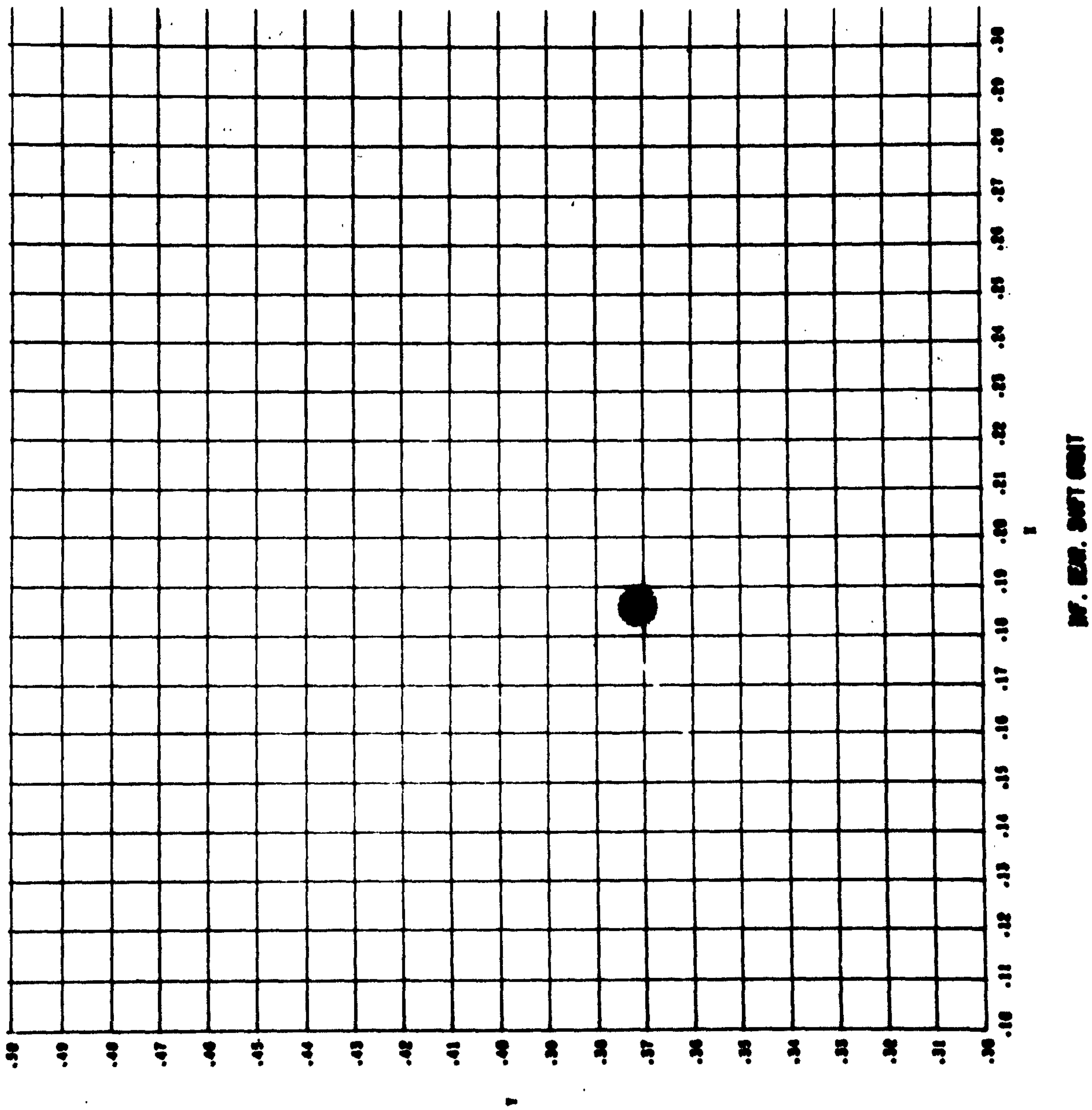

Fig. 27c
Run 7
B = 1.8
$\Delta T = 0.013$
3rd 1000 steps
Sample Orbit
with
Small
Perturbation

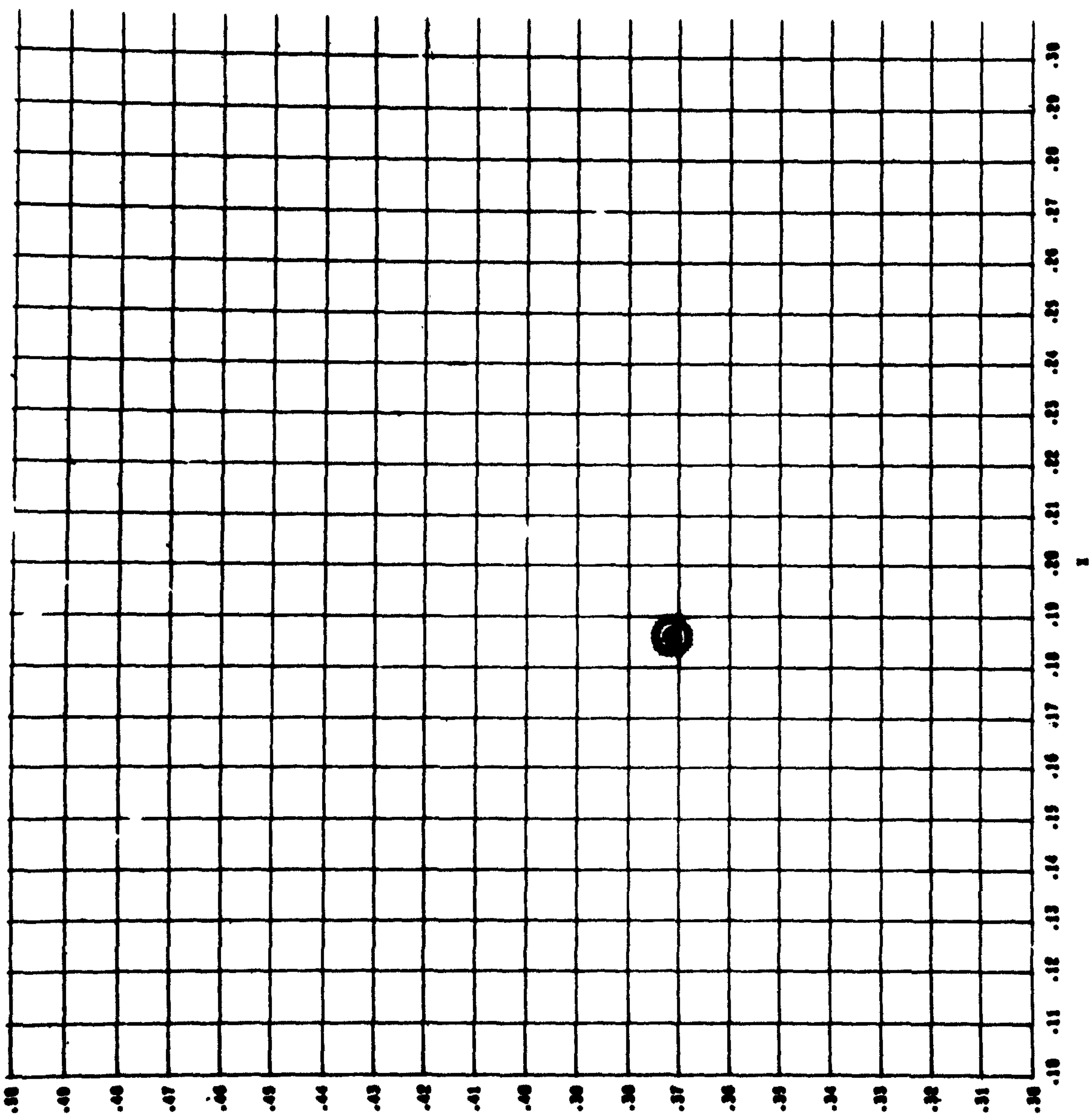

Fig. 28a
Run 7
B = .8;
$\Delta T = 0.026$
1st 1000 steps

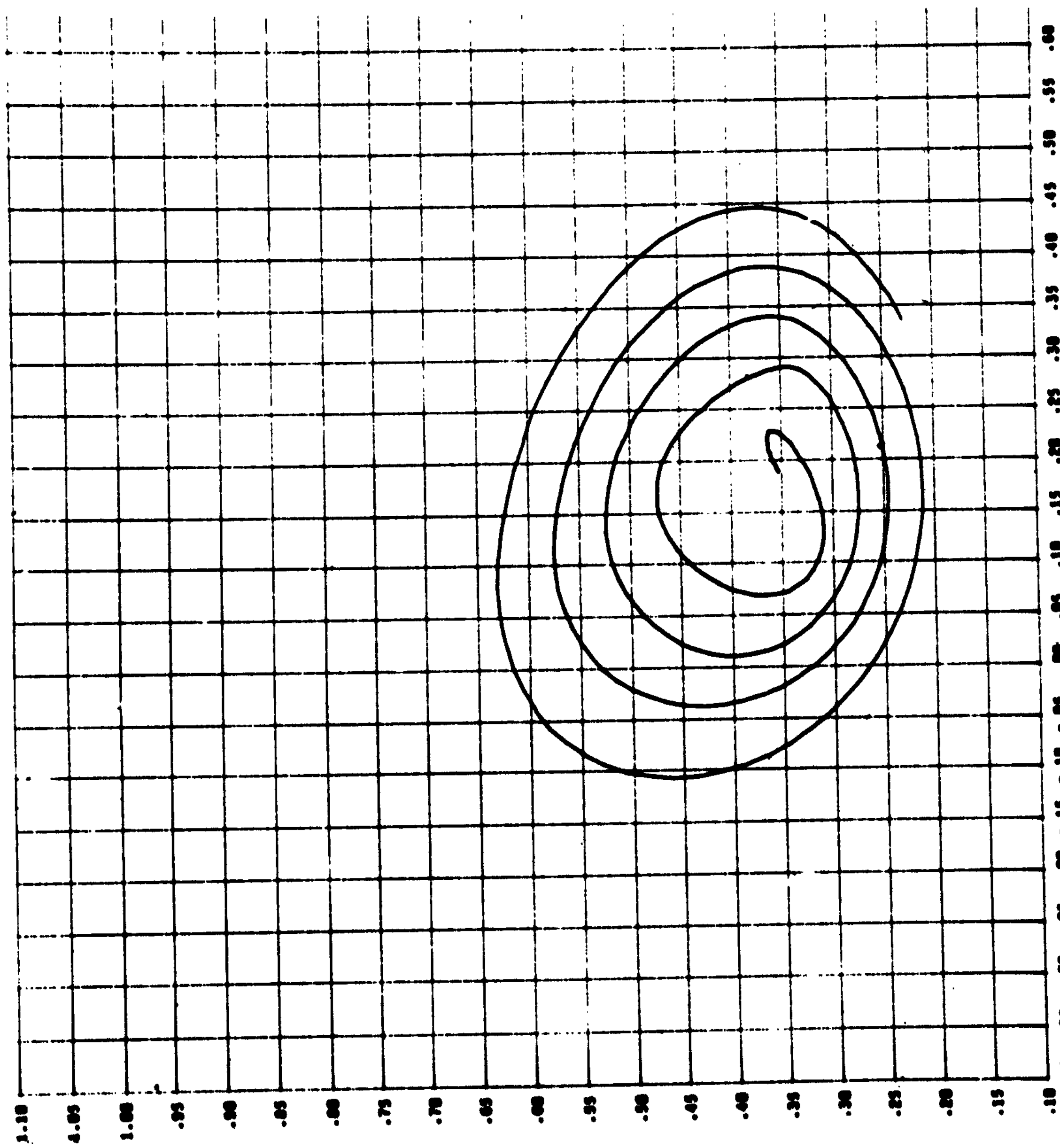

Fig. 28b
Run 7
B = .8;
$\Delta T = 0.026$
2nd 1000 steps

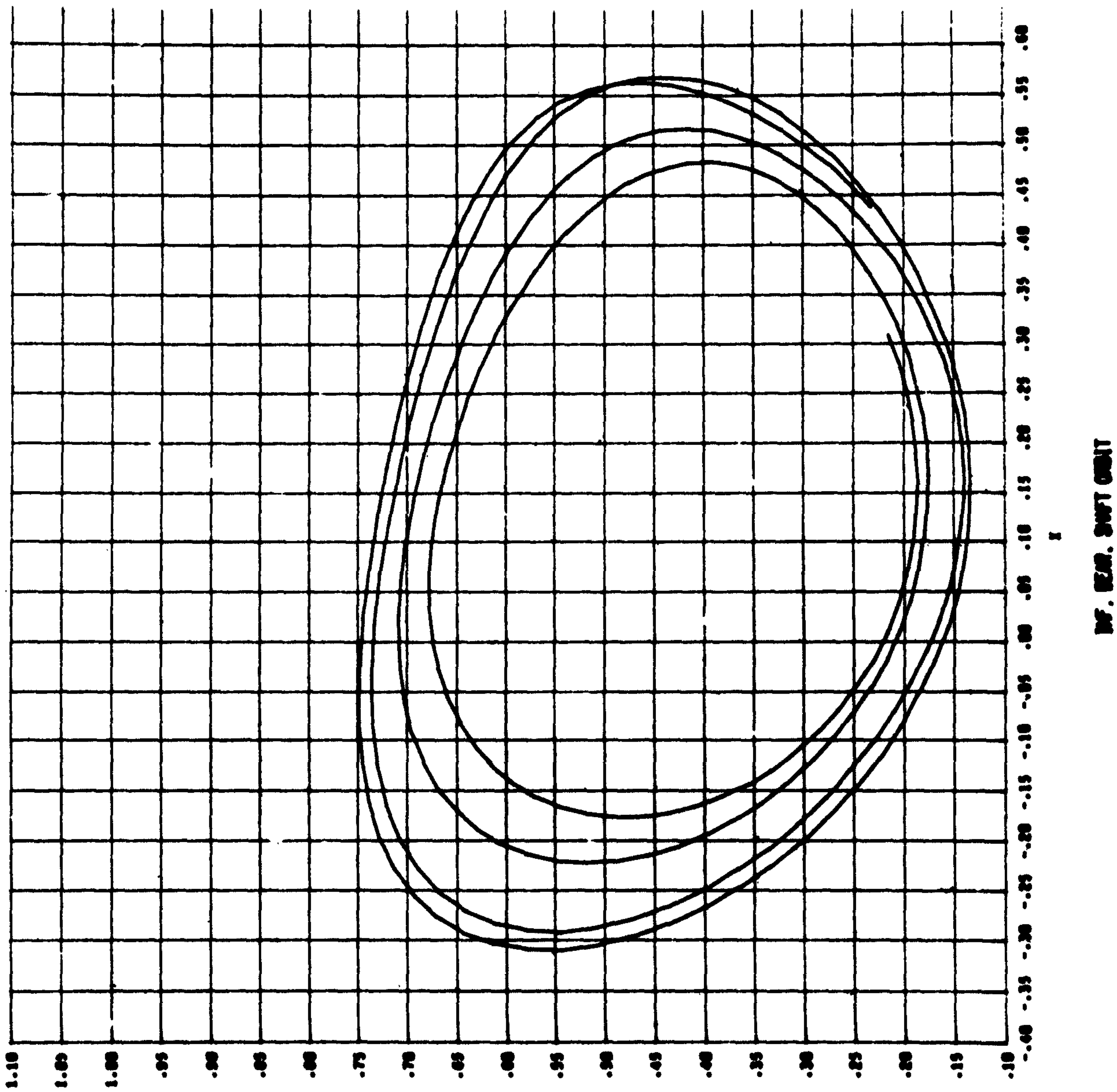

Fig. 29a
Run 8
B = 4;
$\Delta T = 0.011$
1st 1000 steps

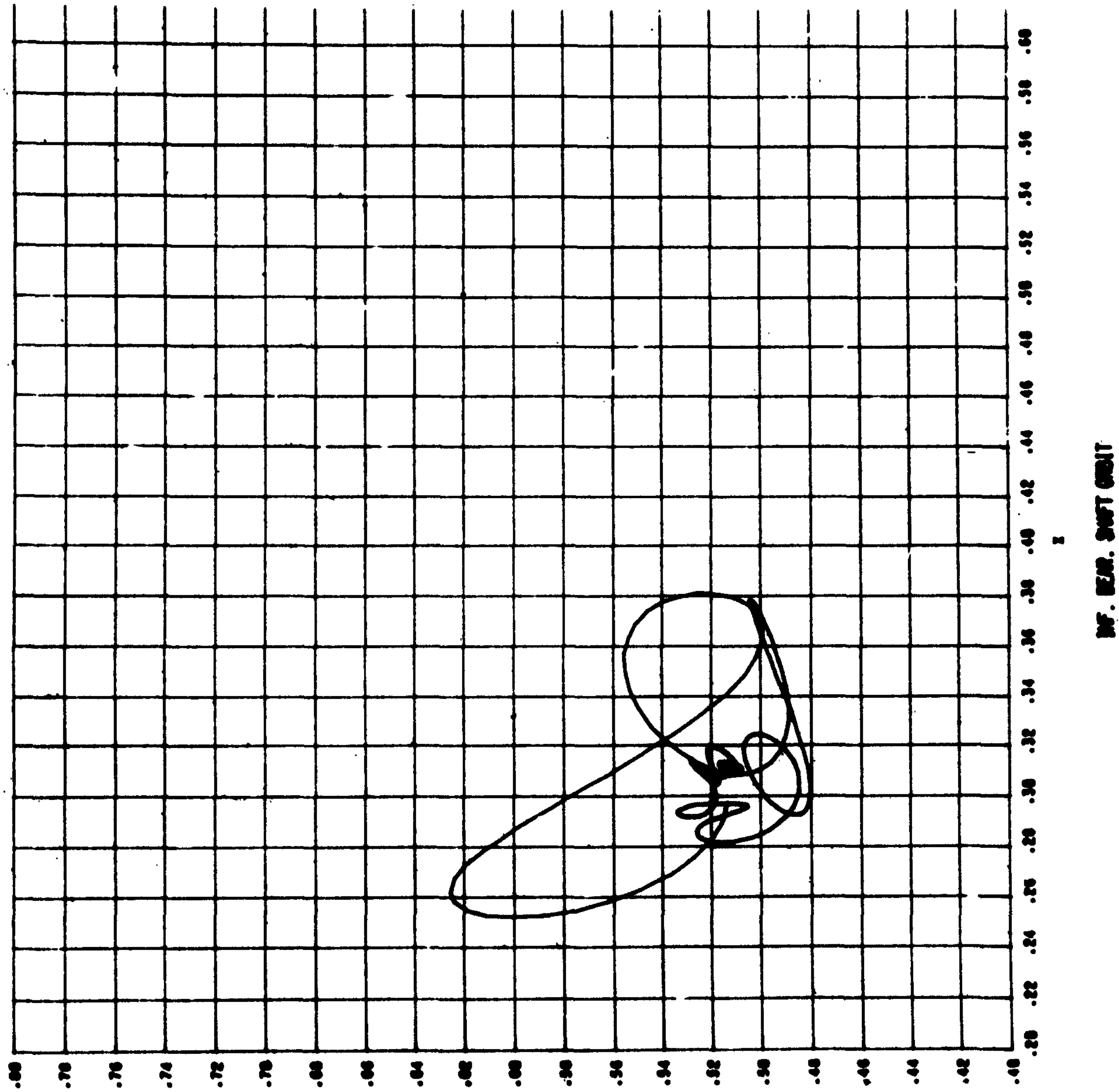

Fig. 29b
Run 8
B = 4;
$\Delta T = 0.011$
2nd 1000 steps

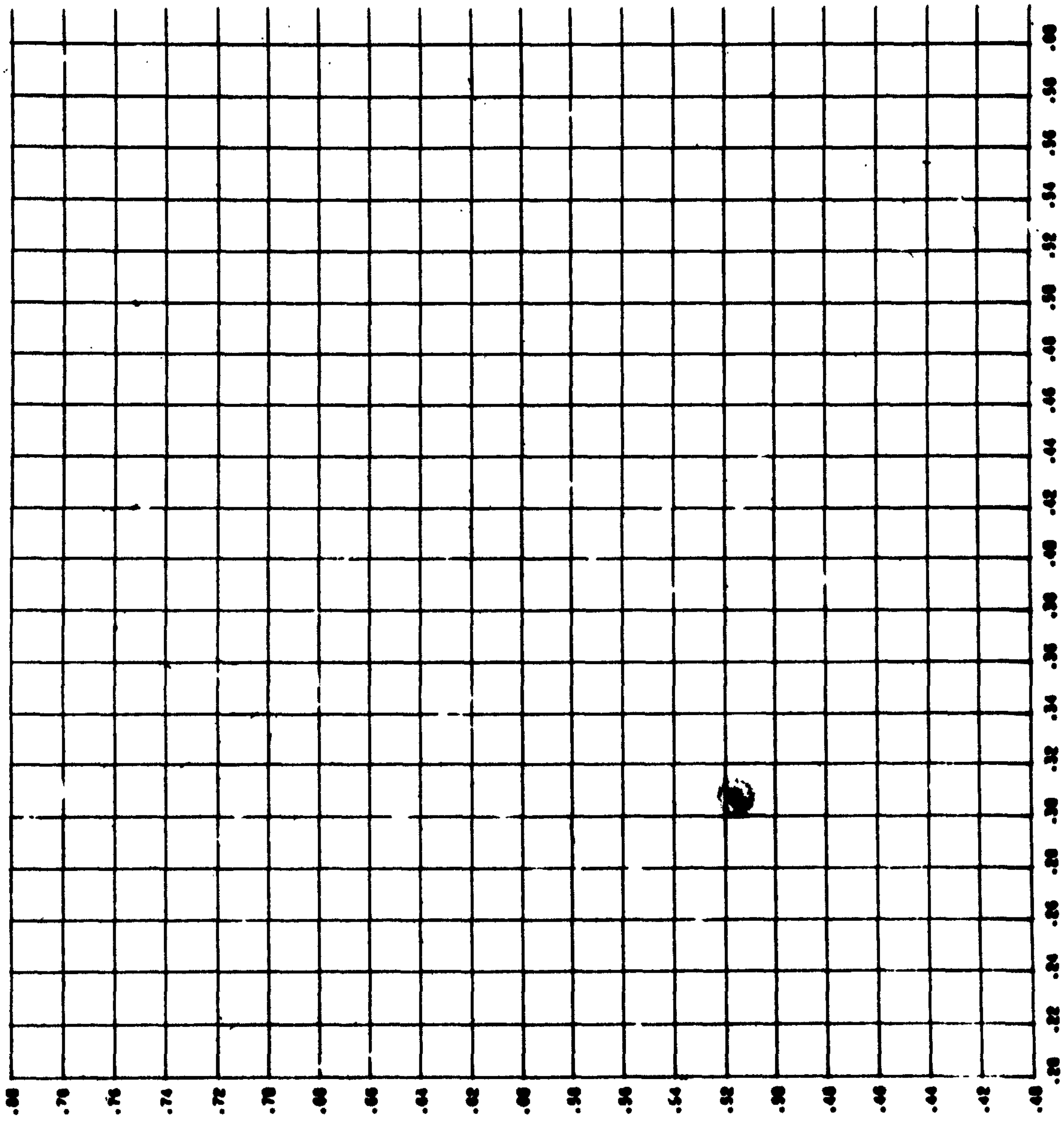

Fig. 30a
Run 8
B = .8;
ΔT = .011
1st 1000 steps

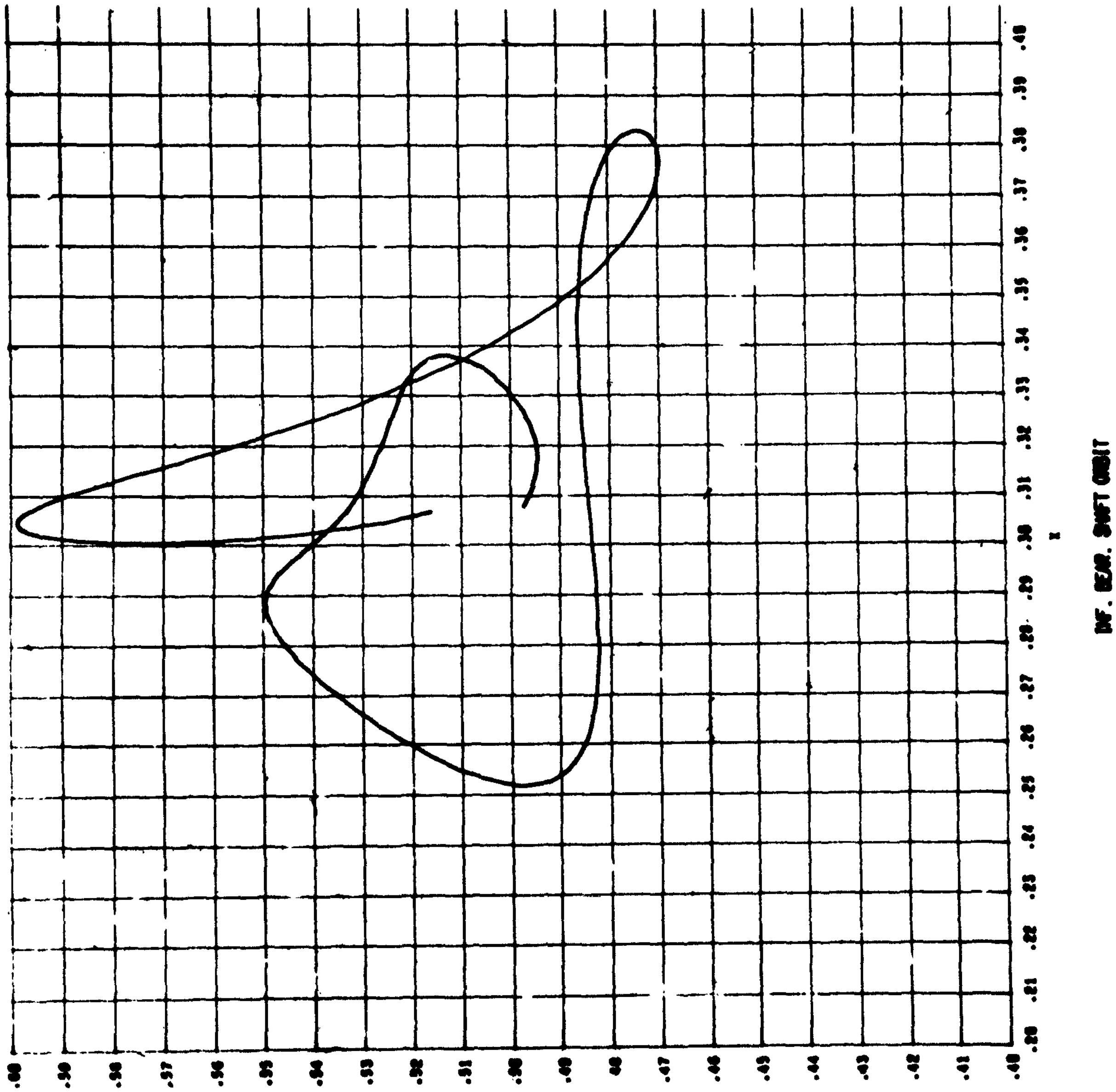

Fig. 30b
Run 8
B = .8;
ΔT = .011
2nd 1000 steps

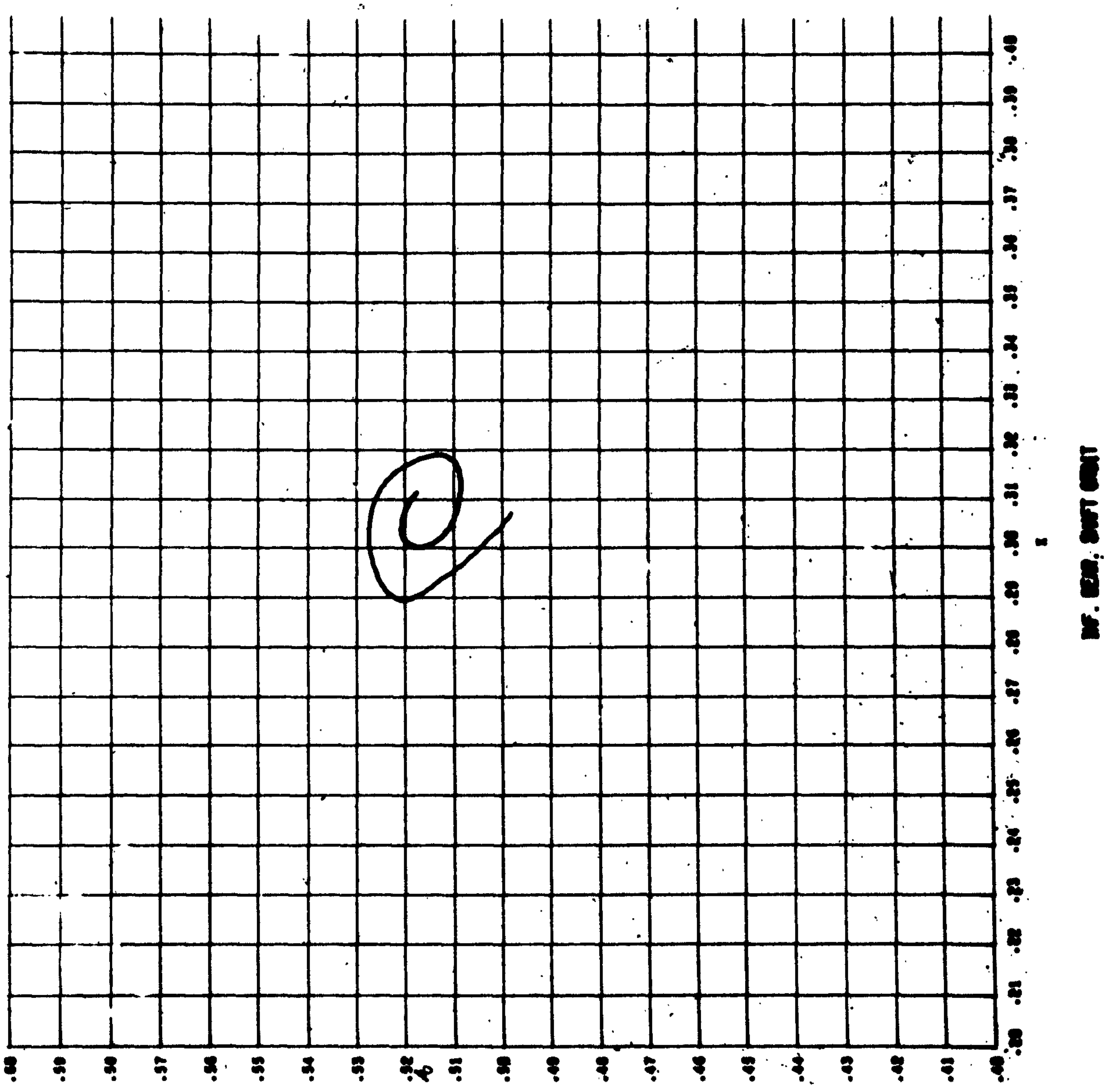

Fig. 31a
Run 8
B = 0.2;
$\Delta T = 0.011$
1st 1000 steps

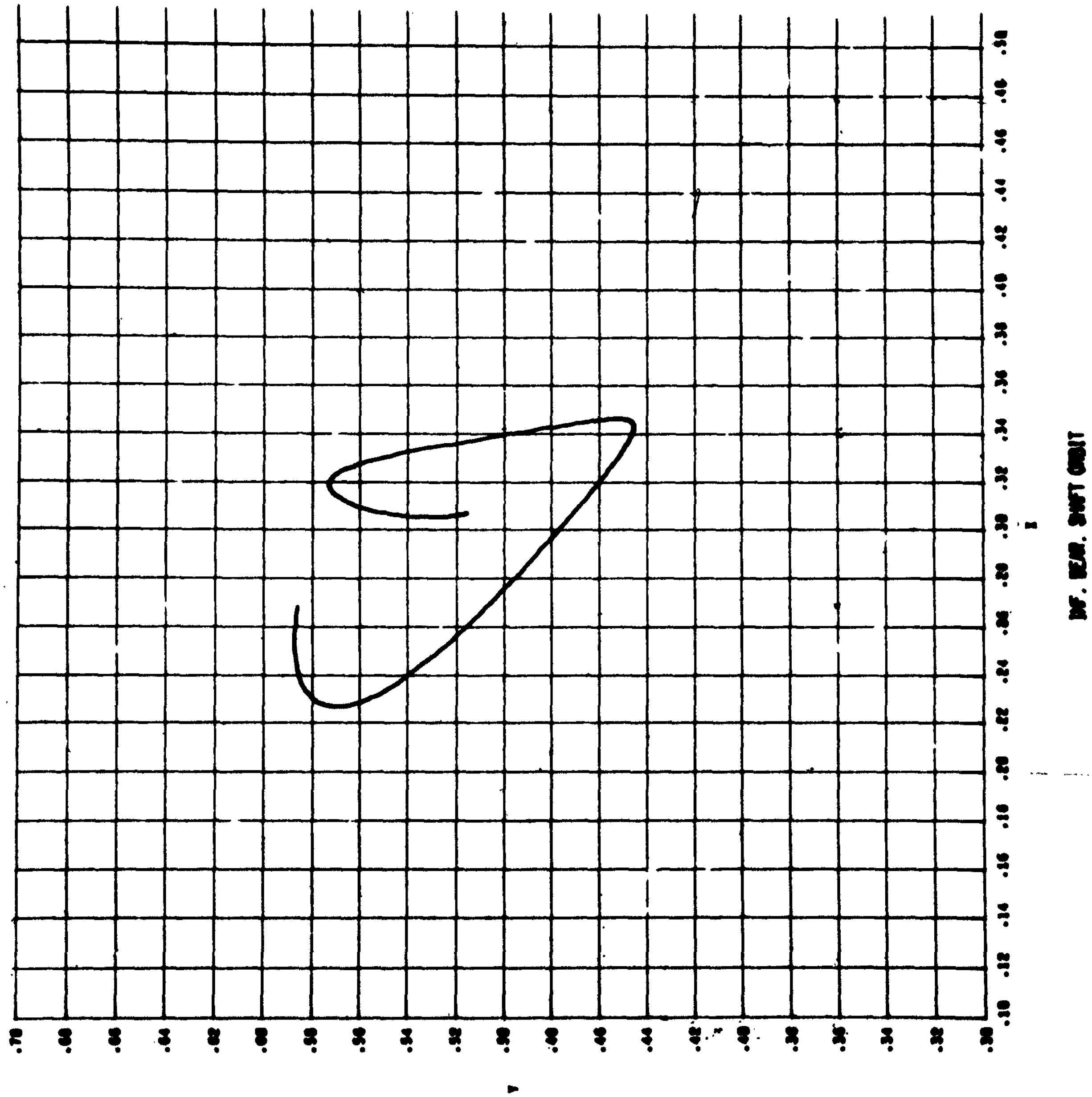

Fig. 31b
Run 8
B = 0.2;
ΔT = 0.011
2nd 1000 steps

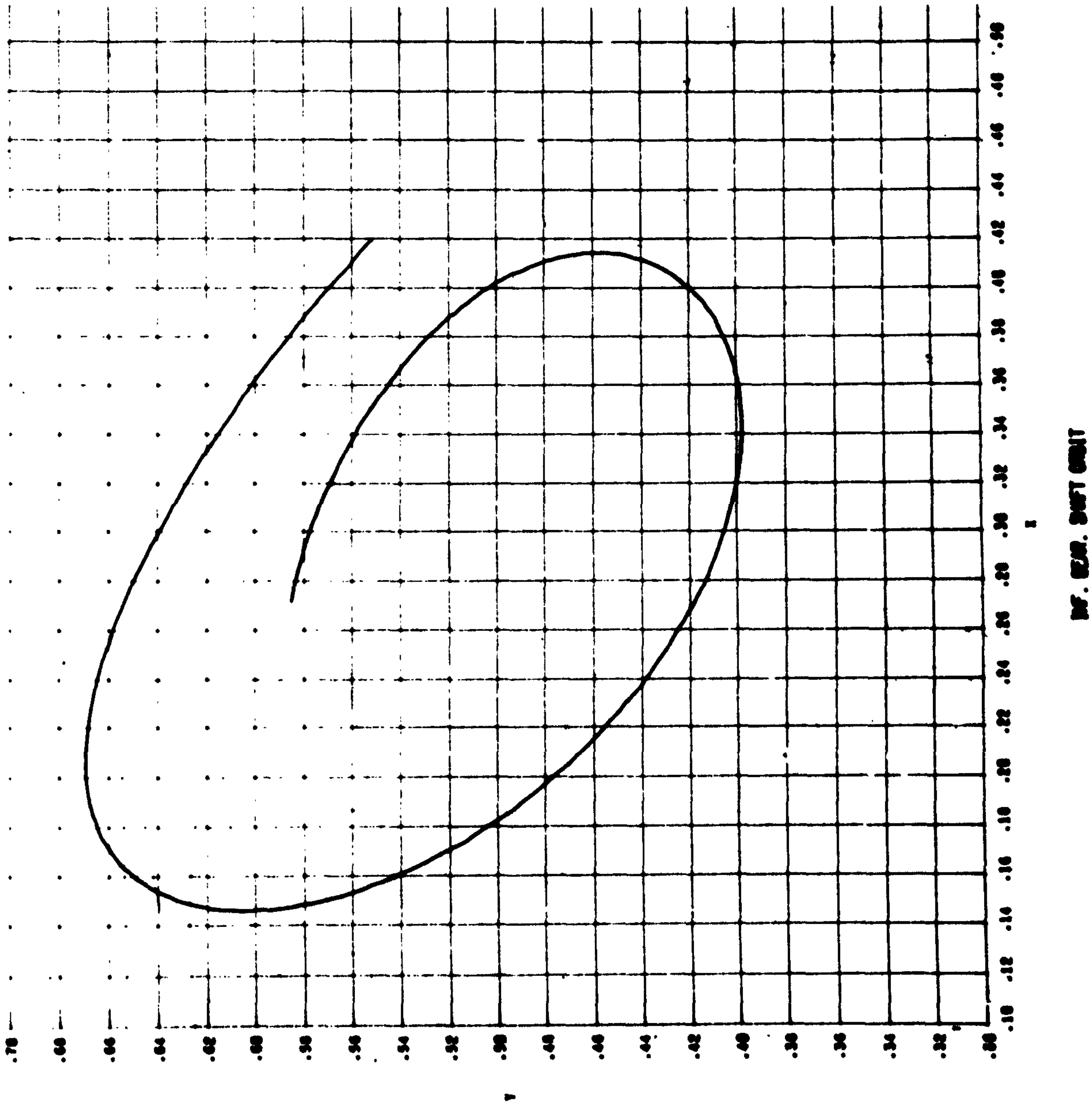

Fig. 32a
Run 12
B = 1.5
$\Delta T = 0.026$
1st 1000 steps
Sample Orbit
Value of B
Slightly Larger
Than Threshold

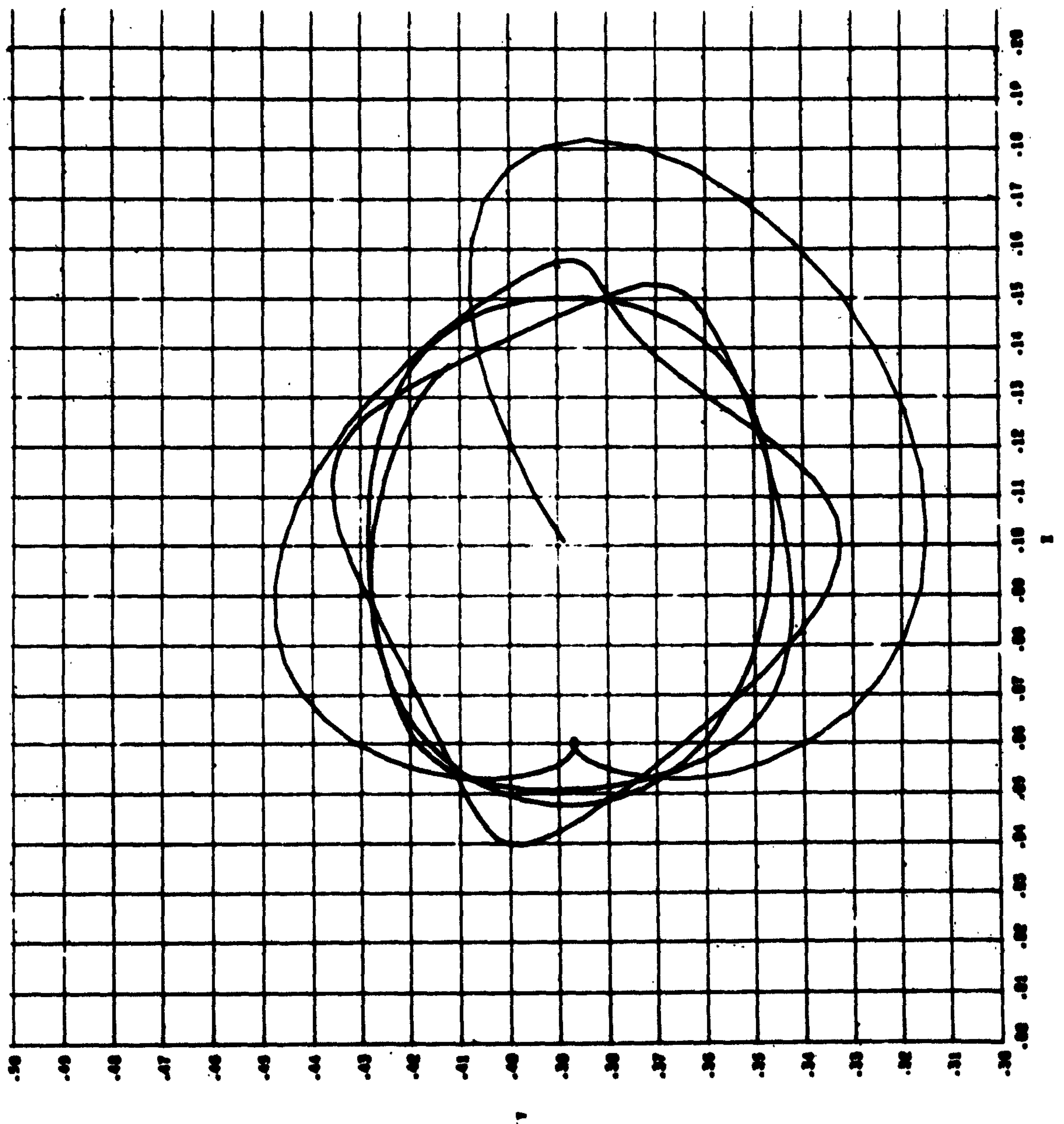

Fig. 32b
Run 12
B = 1.5
$\Delta T = 0.026$
2nd 1000 steps
Sample Orbit
Value of B
Slightly Larger
Than Threshold

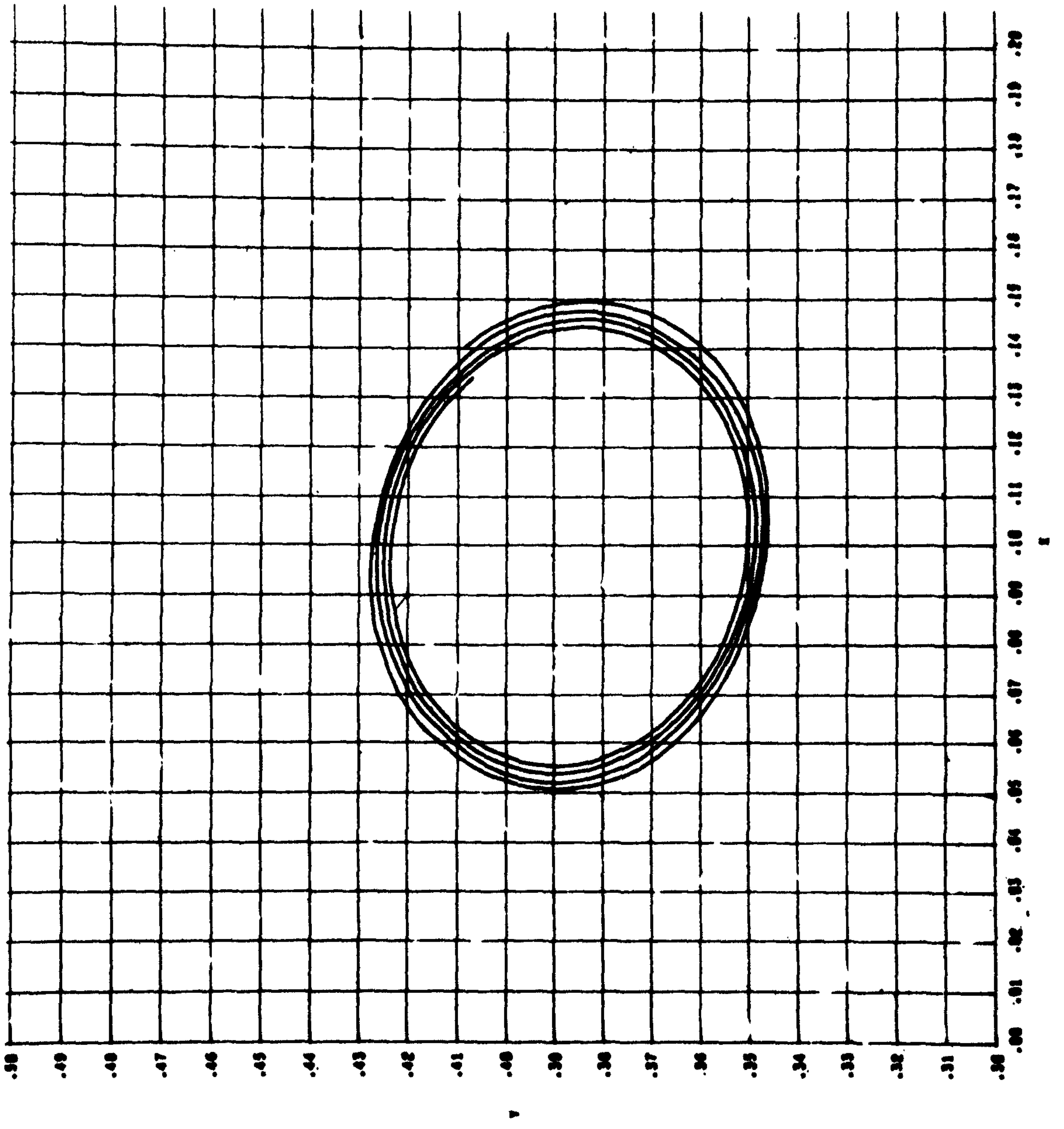

Fig. 33a
Run 12
$B = 1.2$
$\Delta T = 0.026$
1st 1000 steps
Sample Orbit
Value of B
Slightly Smaller
Than Threshold

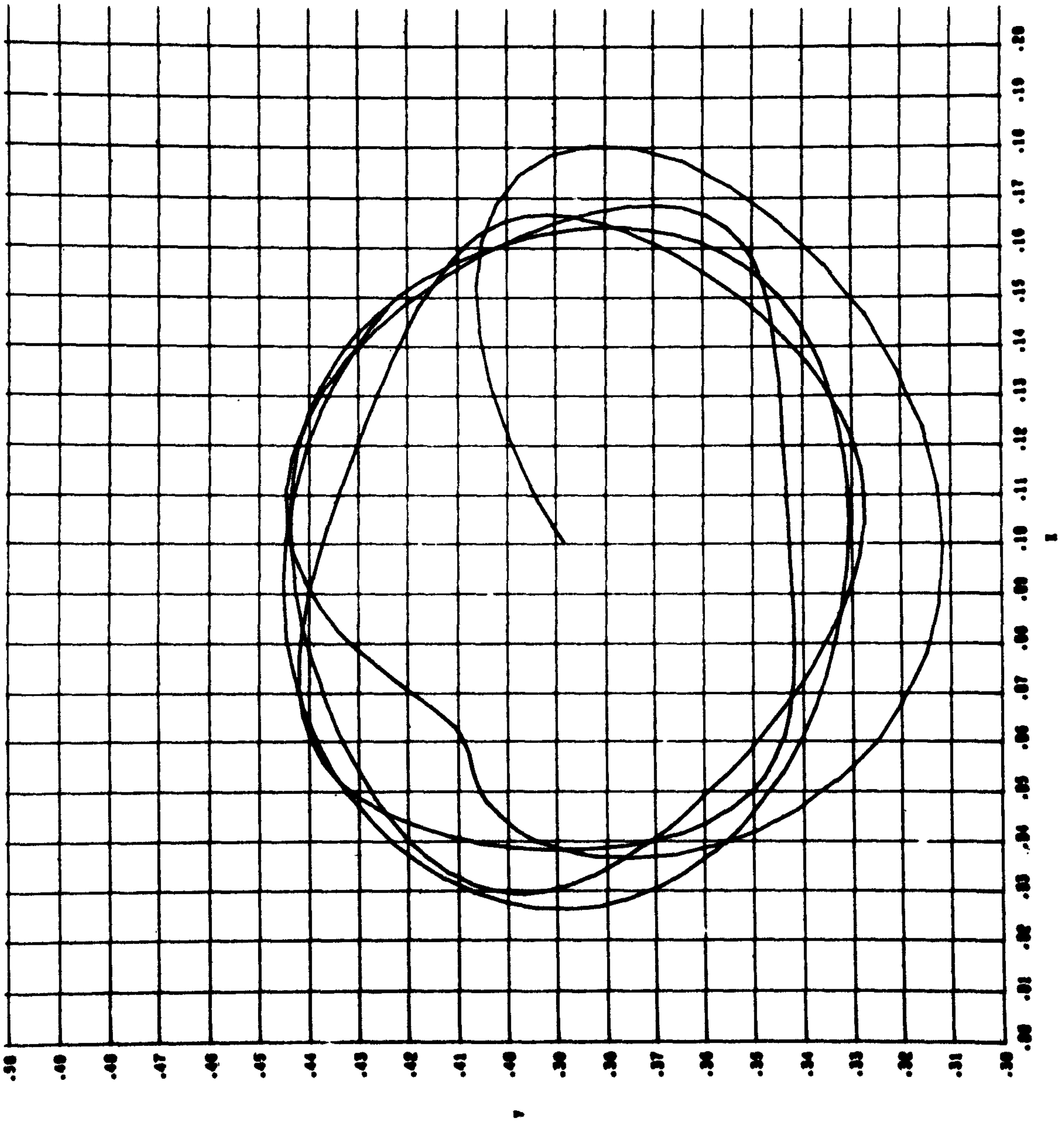

Fig. 33b
Run 12
B = 1.2
$\Delta T = 0.026$
2nd 1000 steps
Sample Orbit
Value of B
Slightly Smaller
Than Threshold

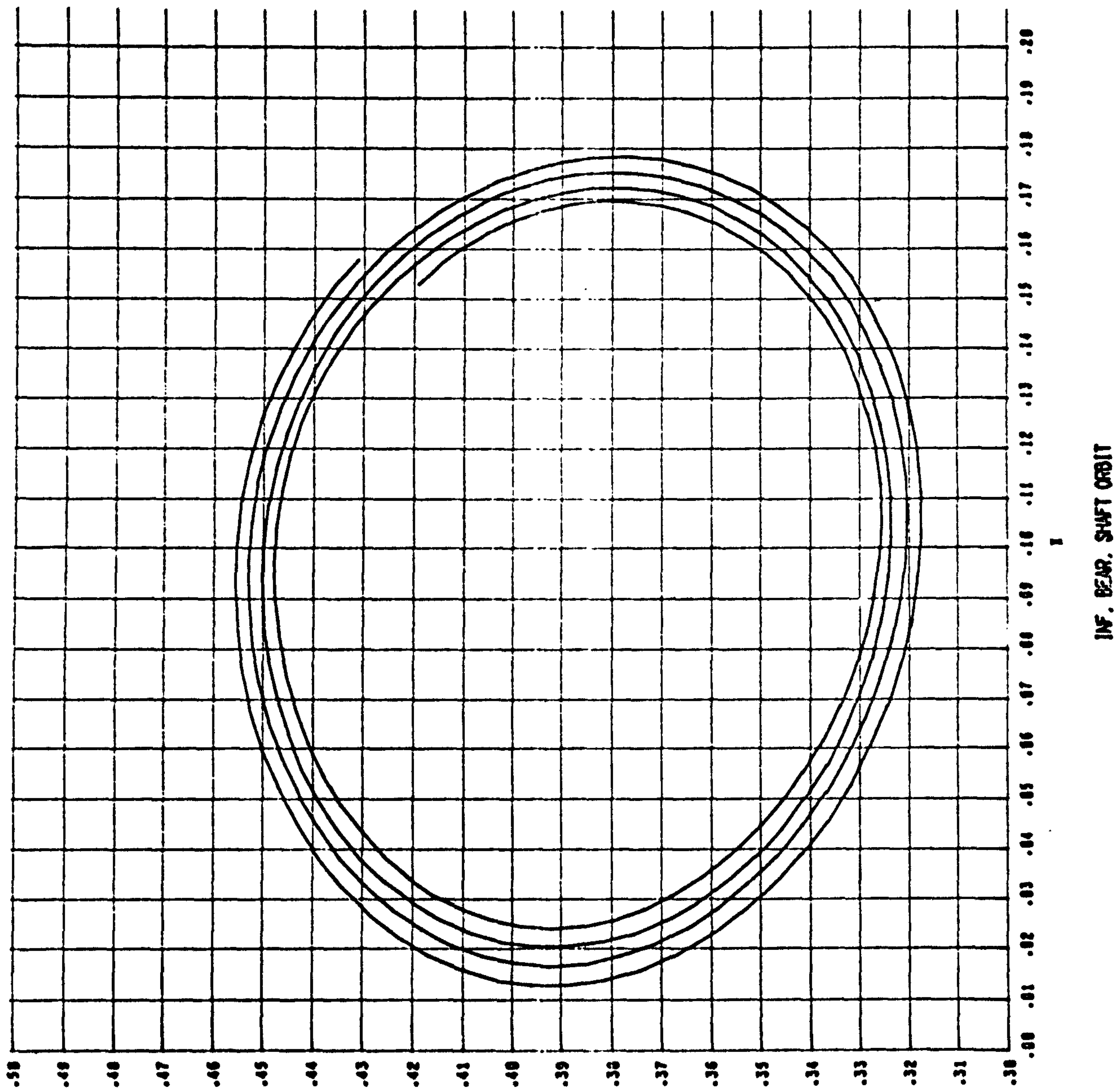

Fig. 34a
Run 12
B = 1.0
$\Delta T = 0.026$
1st 1000 Steps
Sample Orbit
Value of B
Smaller Than
Threshold

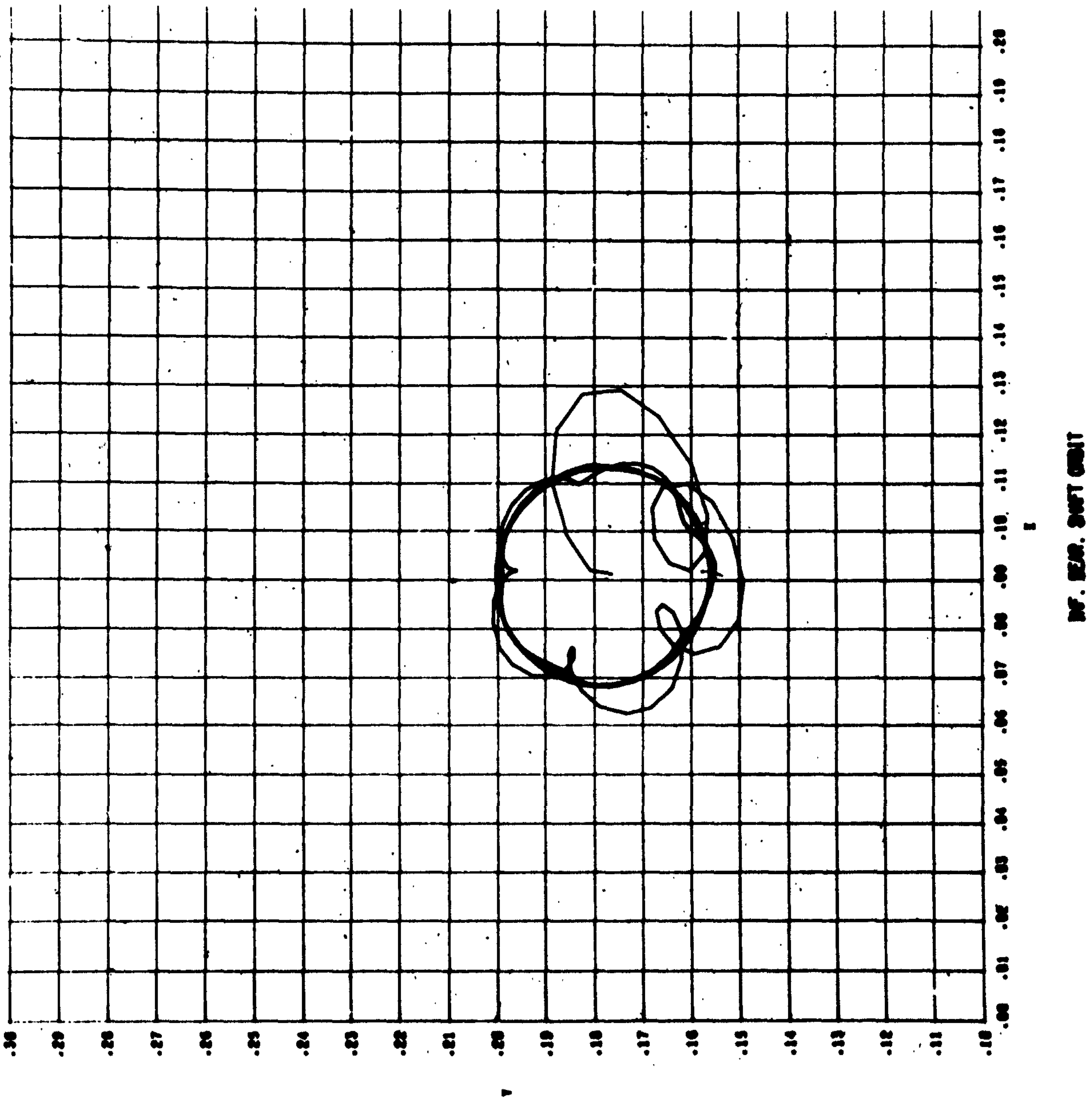

Fig. 34b
Run 12
B = 1.0
$\Delta T = 0.026$
2nd 1000 Steps
Sample Orbit
Value of B
Smaller Than
Threshold

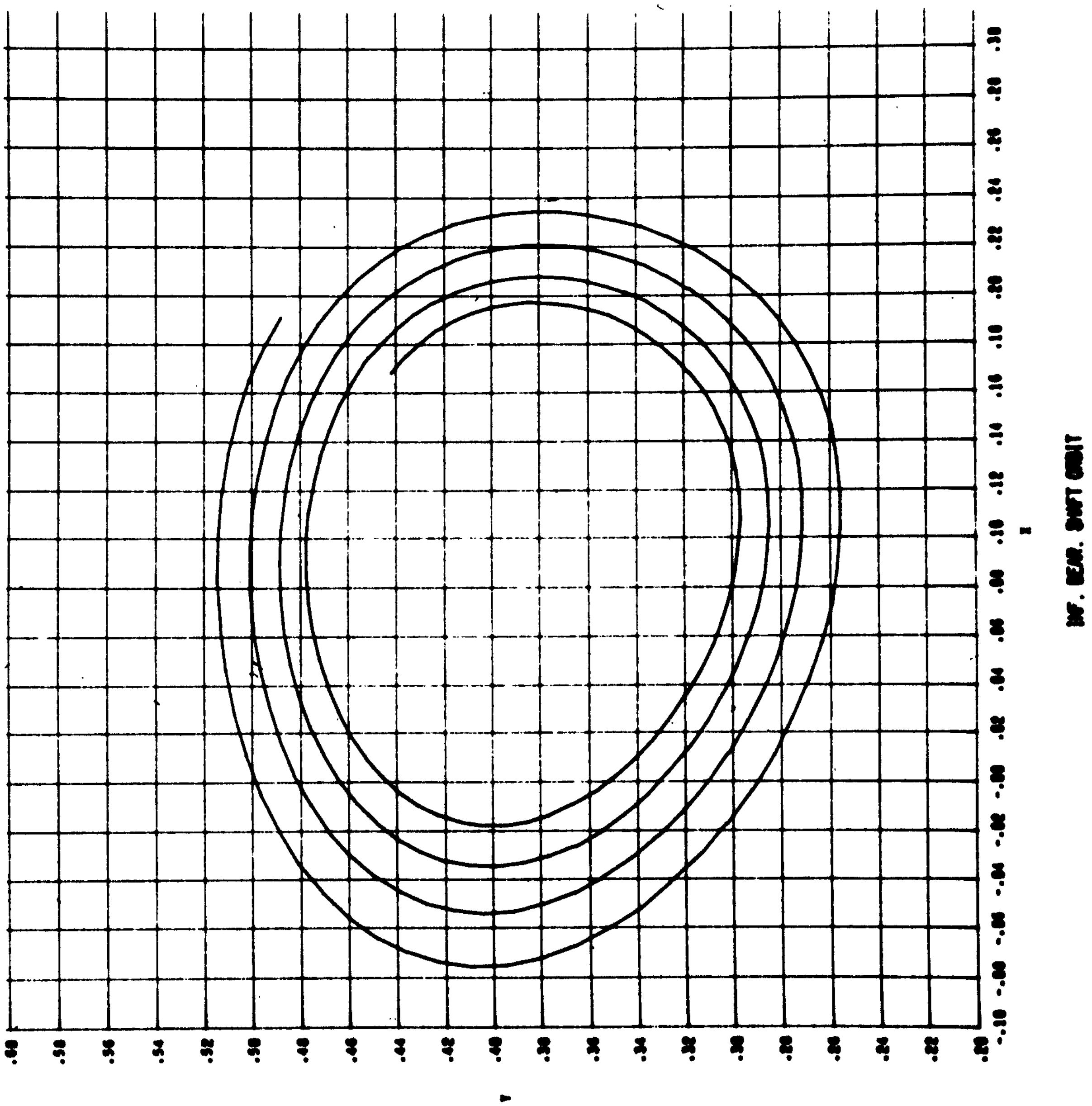

Fig. 35a
Illustration
of
Transients
Run 17
B = 6.0;
ΔT = 0.026
1st 1000 Steps

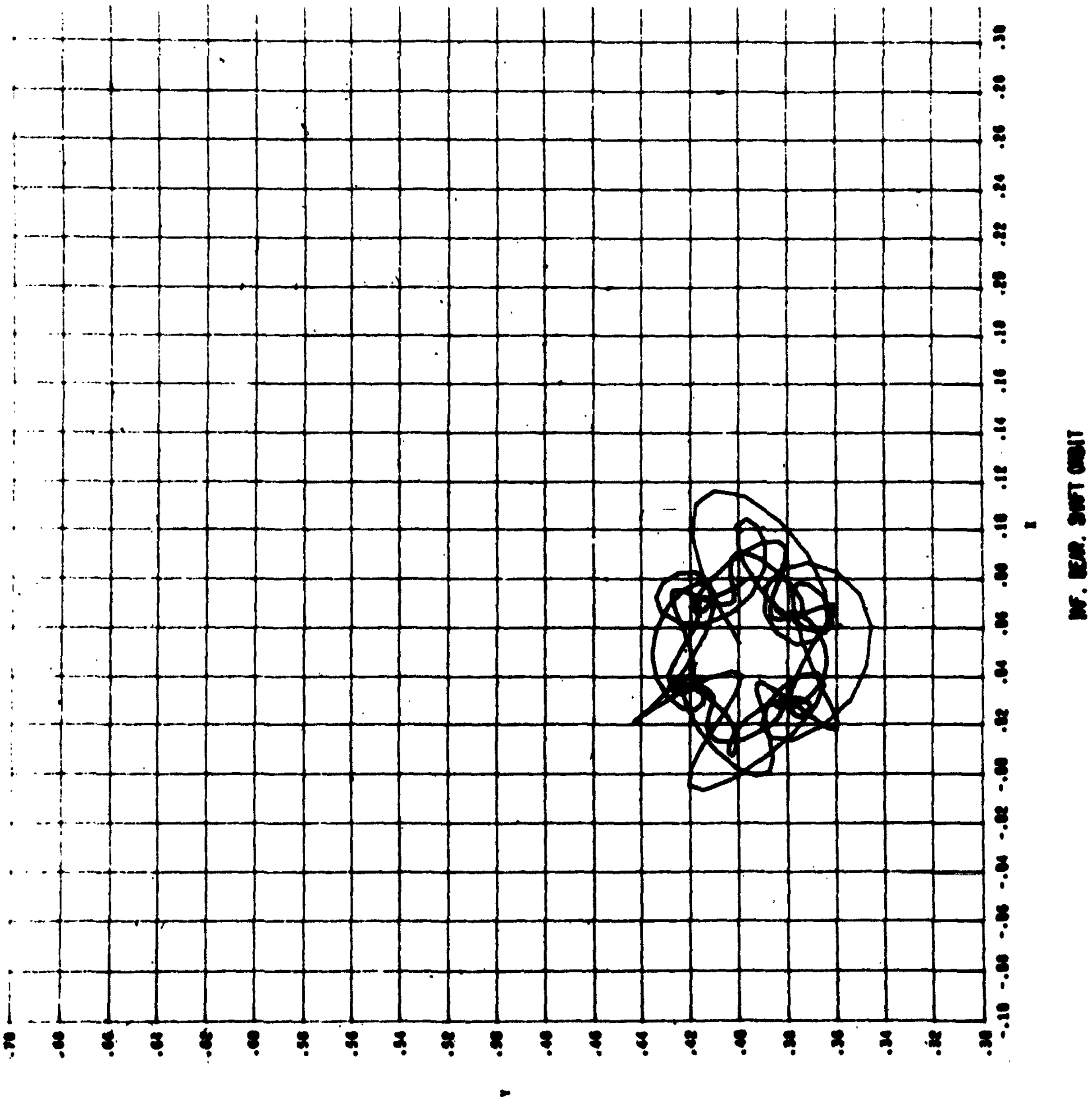

Fig. 35b
Illustration
of
Transients
Run 17
B = 6.0;
ΔT = 0.026
2nd 1000 Steps

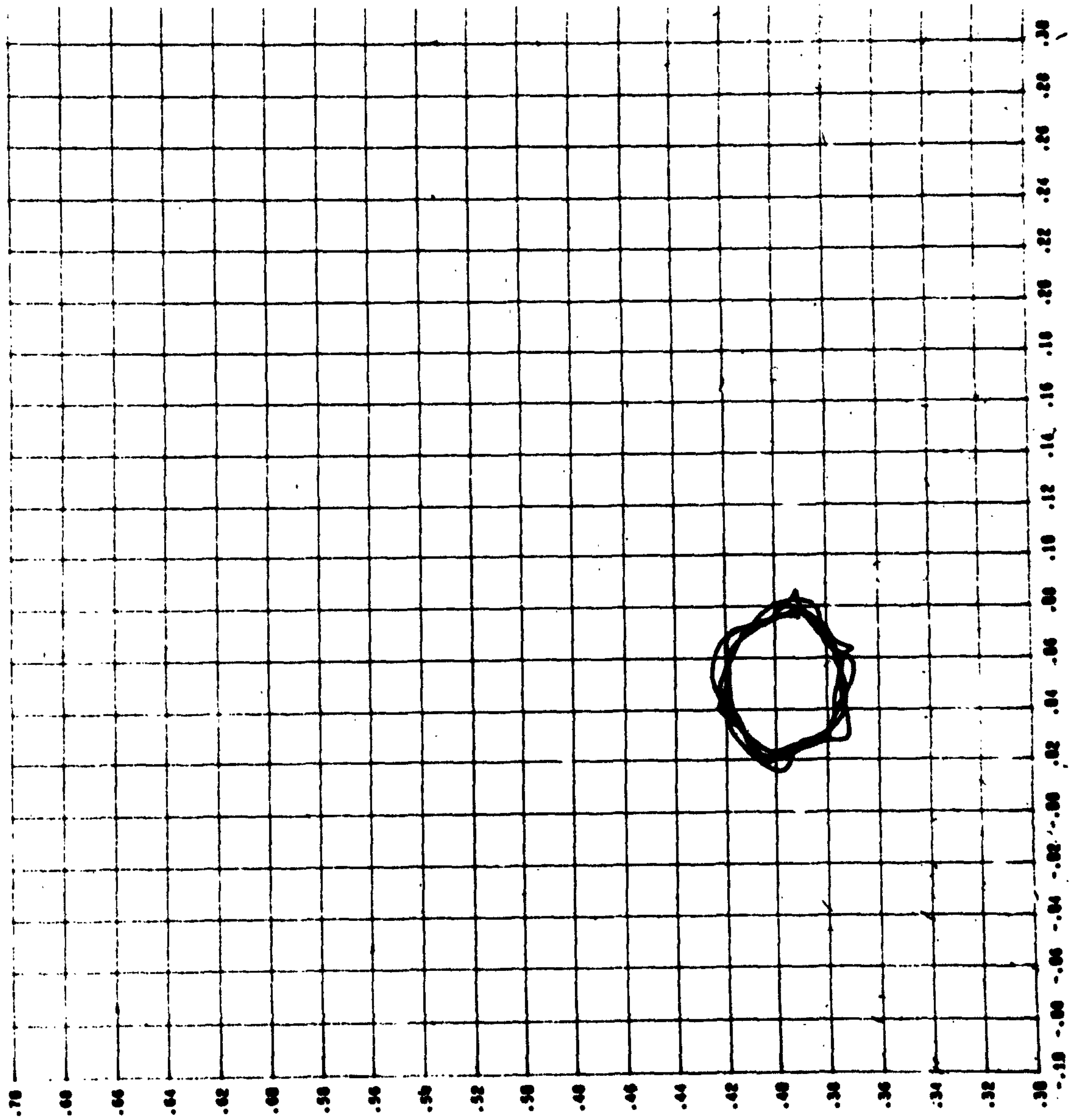

Fig. 36a
Illustration
of
Transients
Run 16
B = 8.0;
$\Delta T = 0.026$
1st 1000 Steps

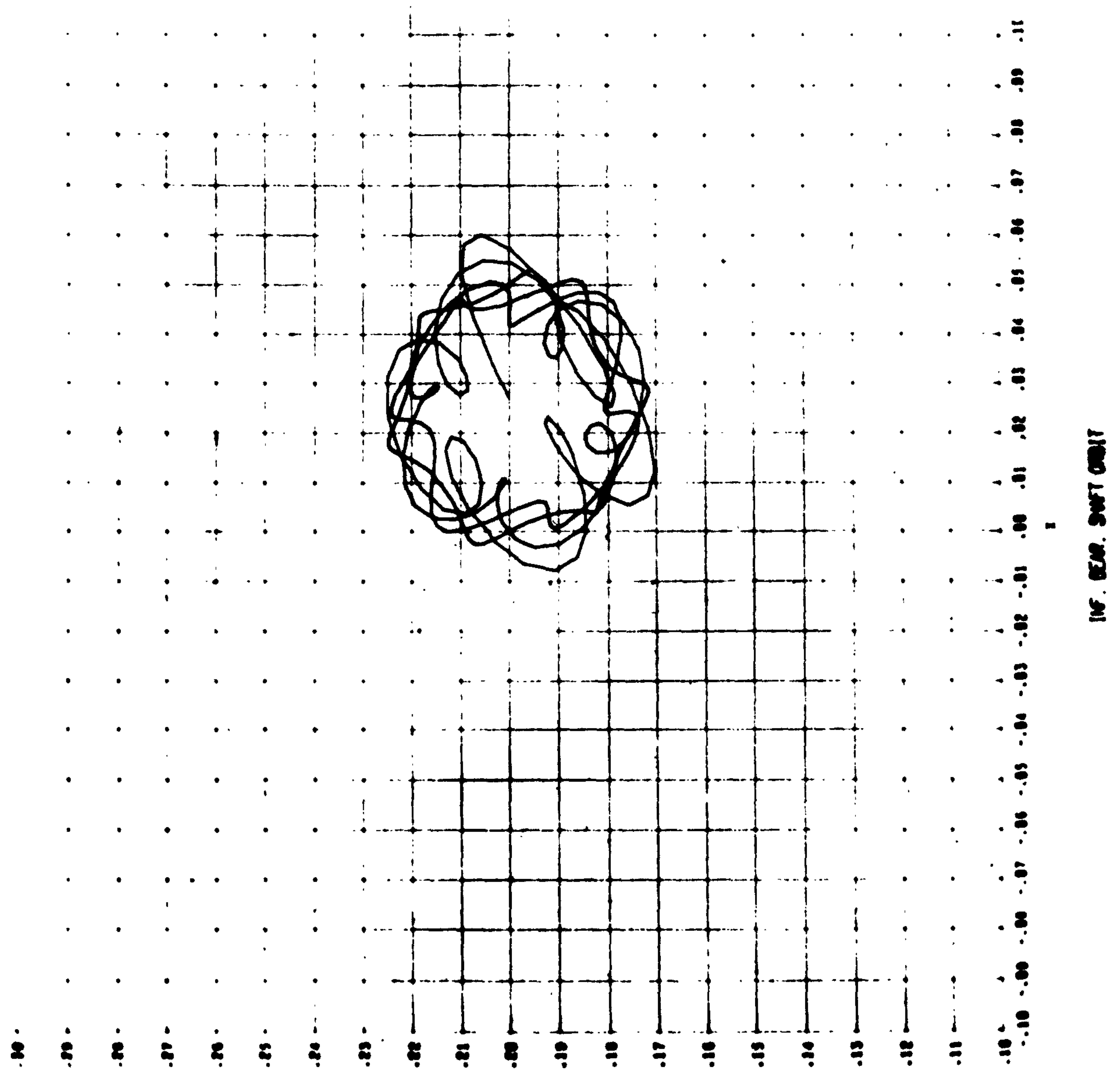

Fig. 36b
Illustration
of
Transients
Run 16
B = 8.0;
$\Delta T = 0.026$
2nd 1000 Steps

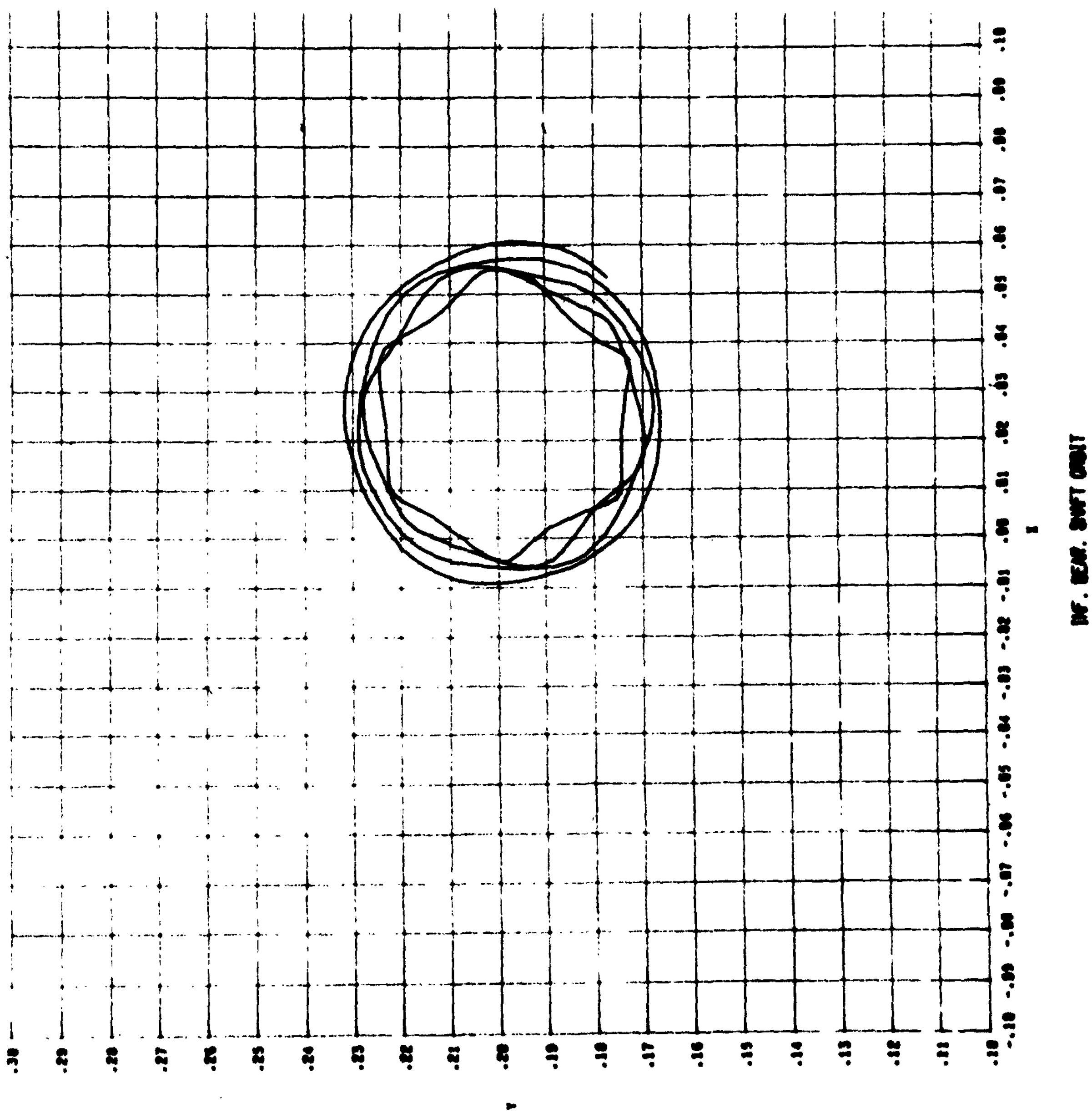

Fig. 37a
Illustration
of
Transients
Run 16
$B = 5.0$;
$\Delta T = 0.026$
1st 1000 Steps

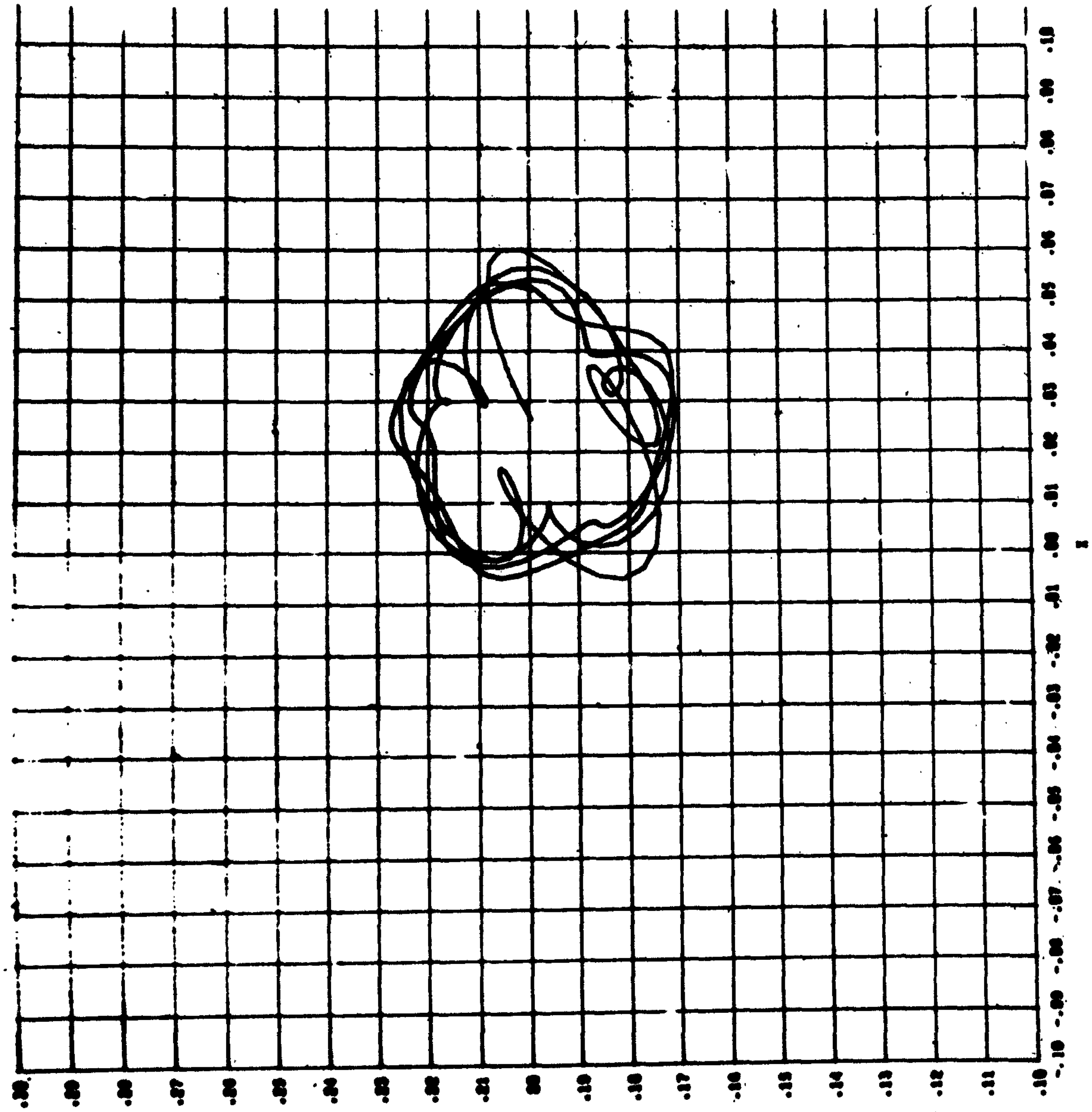

Fig. 37b
Illustration
of
Transients
Run 16
B = 5.0;
$\Delta T = 0.026$
2nd 1000 Steps

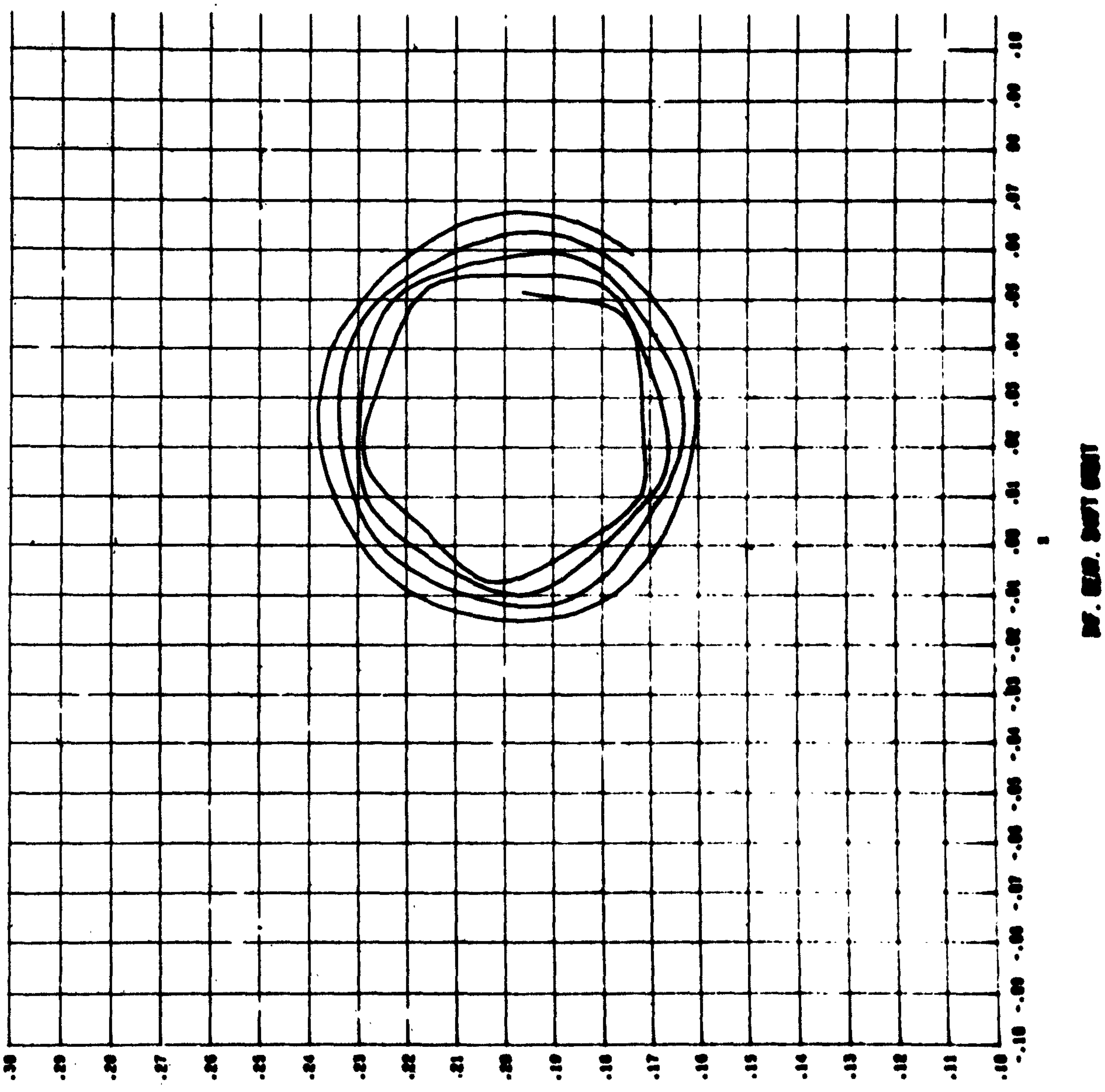

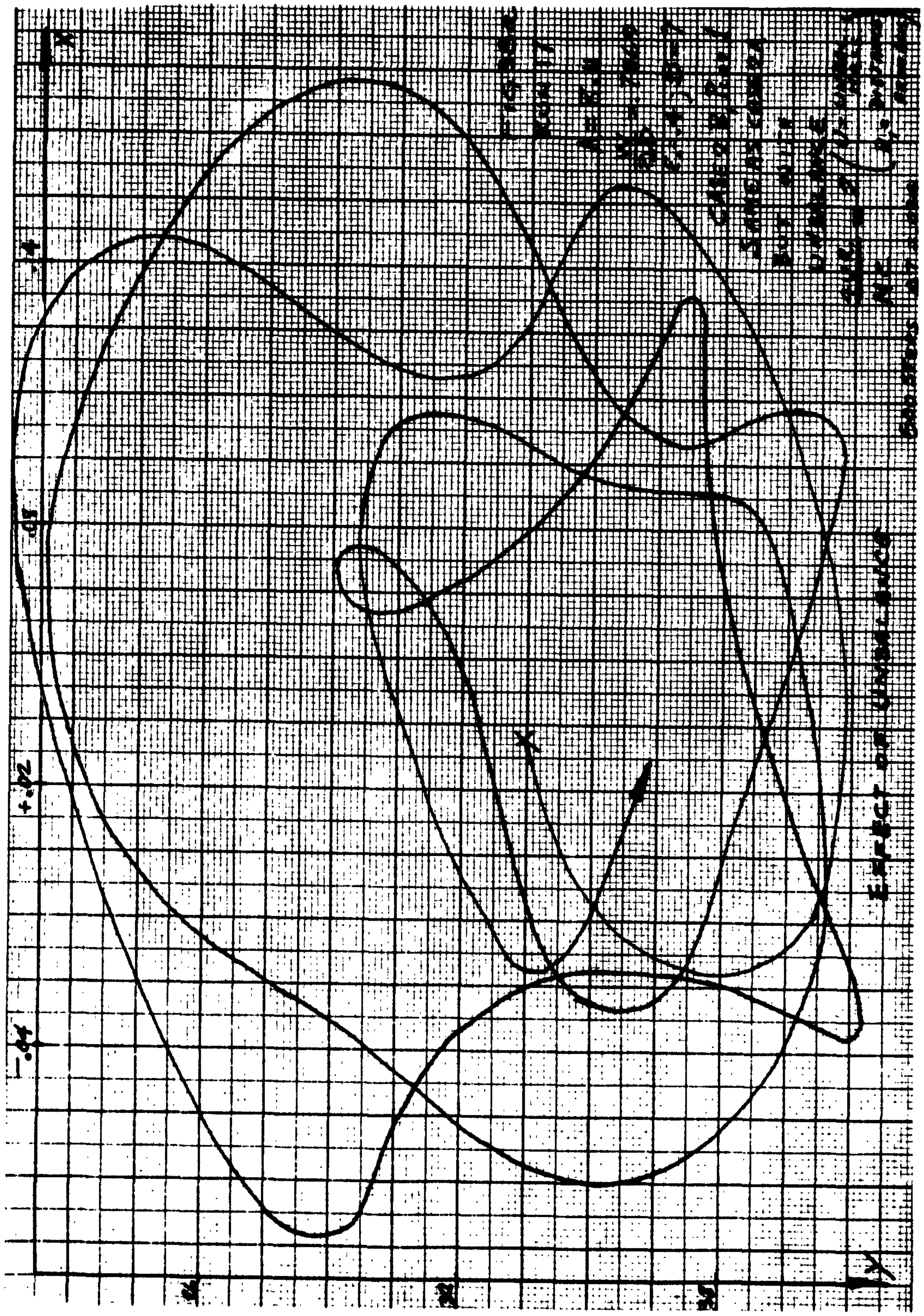

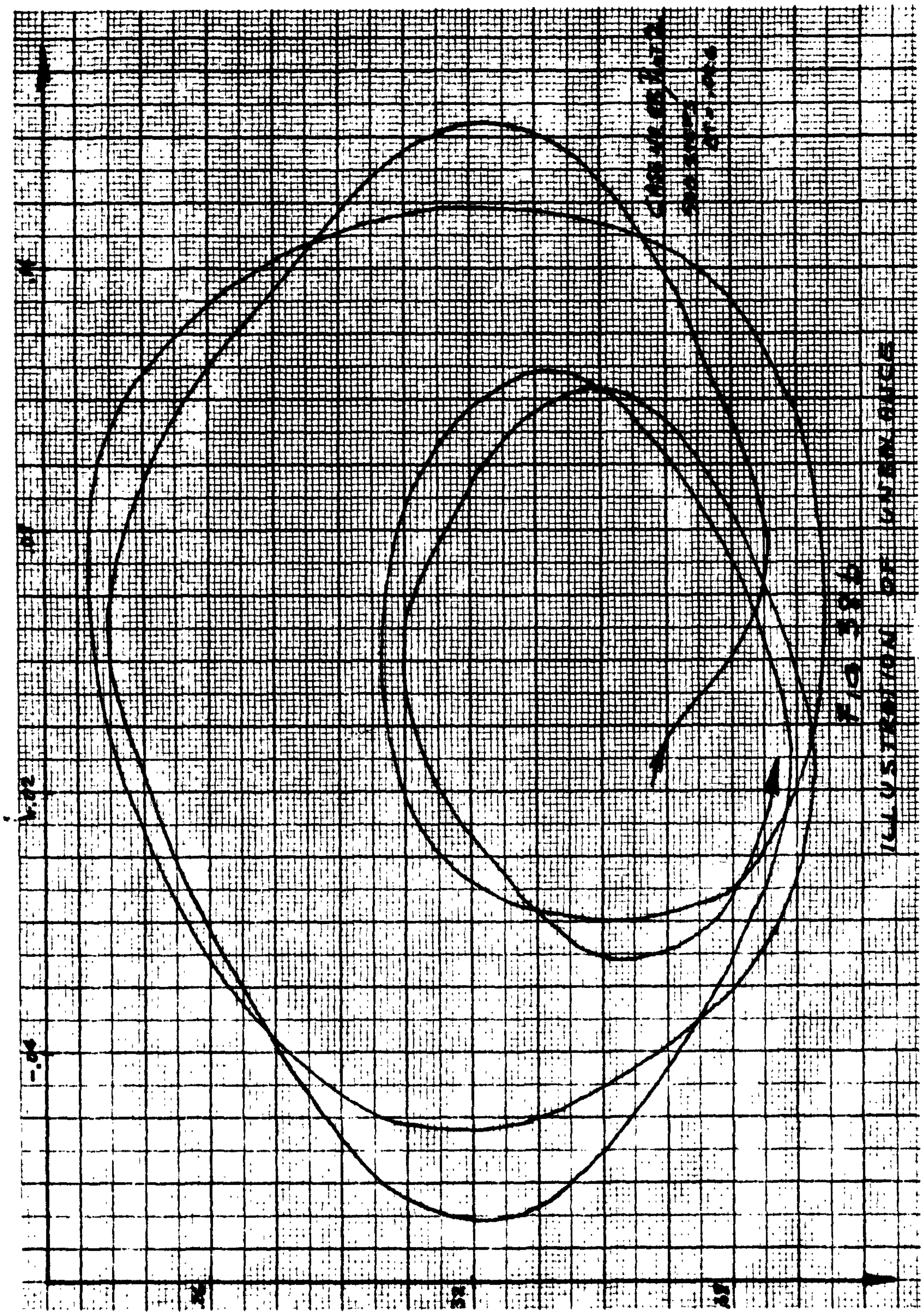
FIG 38b
ILLUSTRATION OF UNBALANCE

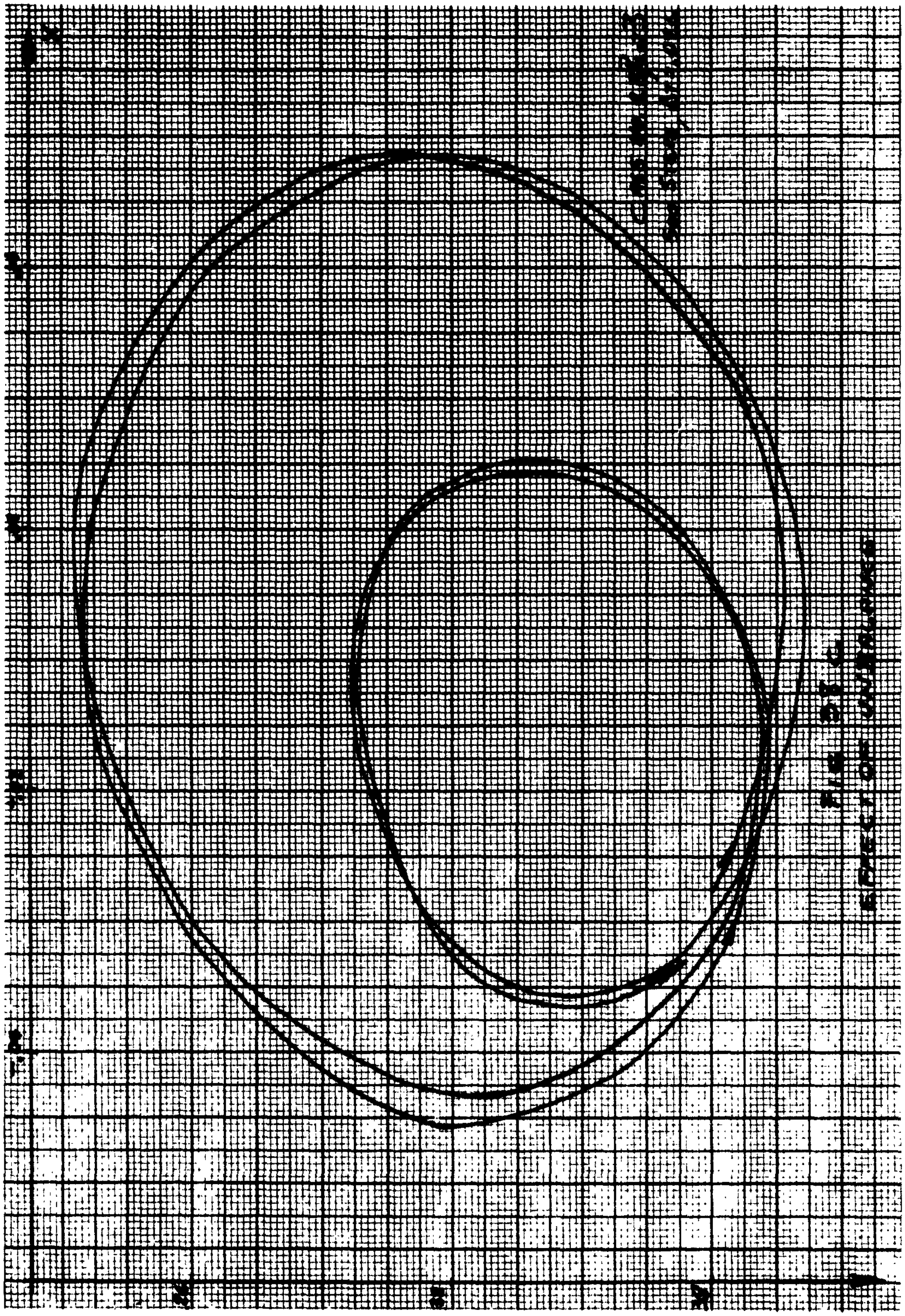

FIG. 25 C
EFFECT OF UNBALANCE

Fig. 39a
Possible
Limit
Cycle
Run 6
B = 10;
$\Delta T = 0.026$
1st 1000 Steps

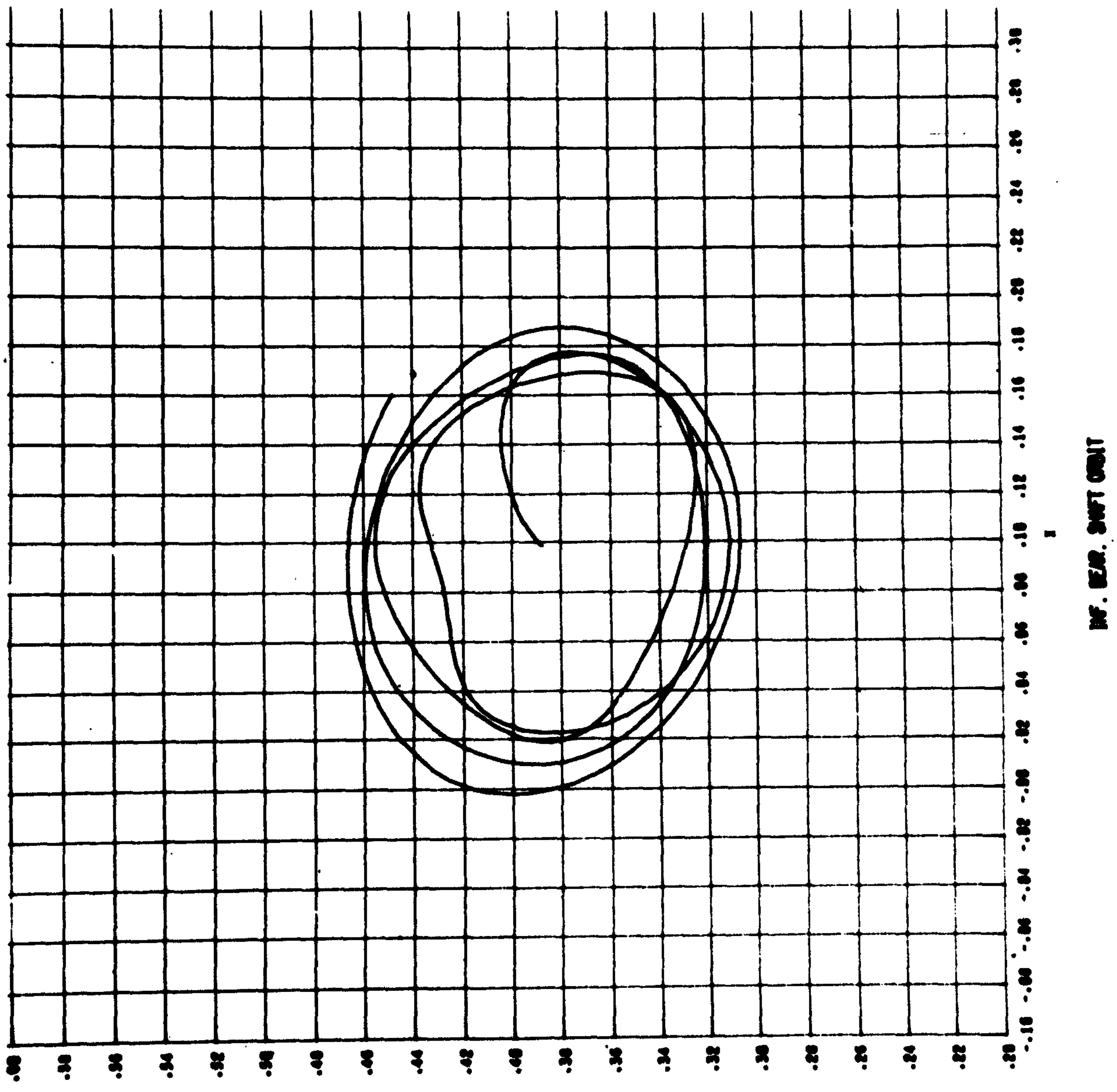

Fig. 39b
Possible
Limit
Cycle
Run 6
B = 10;
$\Delta T = 0.026$
2nd 1000 Steps

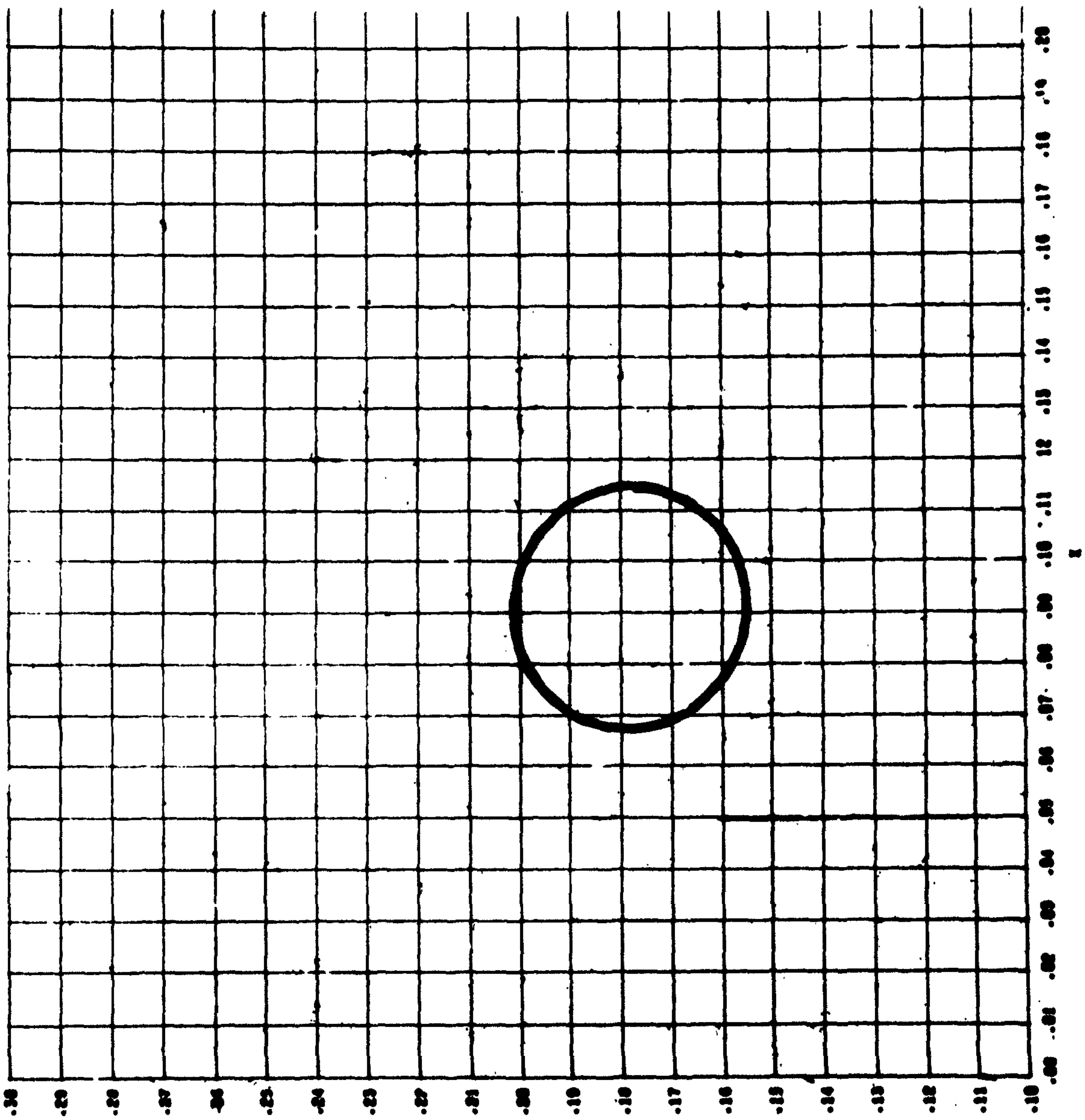

Fig. 40a
Possible
Limit Cycle
Run 6
$B = 8$; $\Delta T = 0.013$
1st 1000 steps

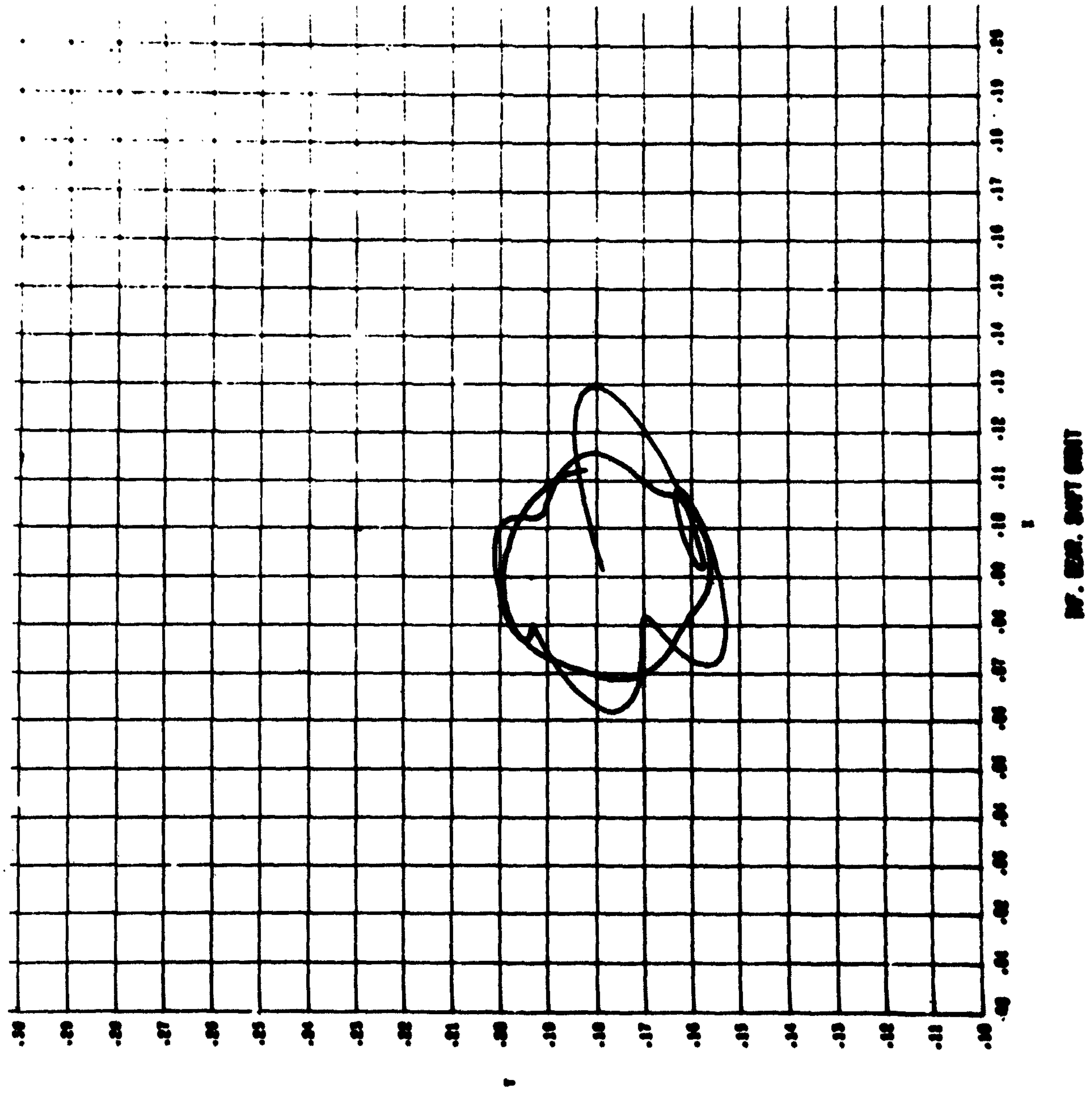

Fig. 40b
Possible
Limit Cycle
Run 6
B = 8; $\Delta T = 0.013$
2nd 1000 steps

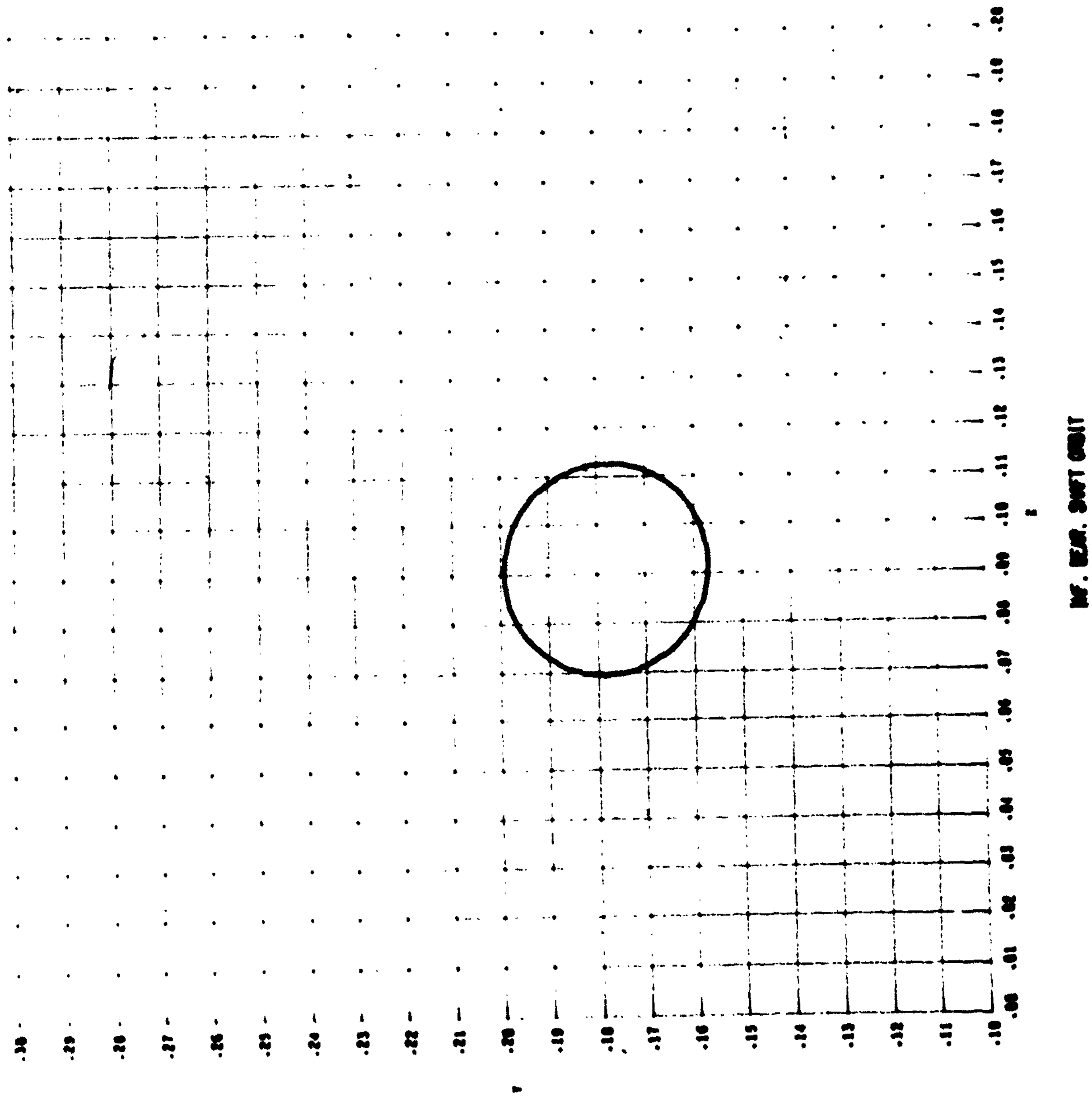

Fig. 40c
Possible
Limit Cycle
Run 6
$B = 8;\ \Delta T = 0.013$
3rd 1000 steps

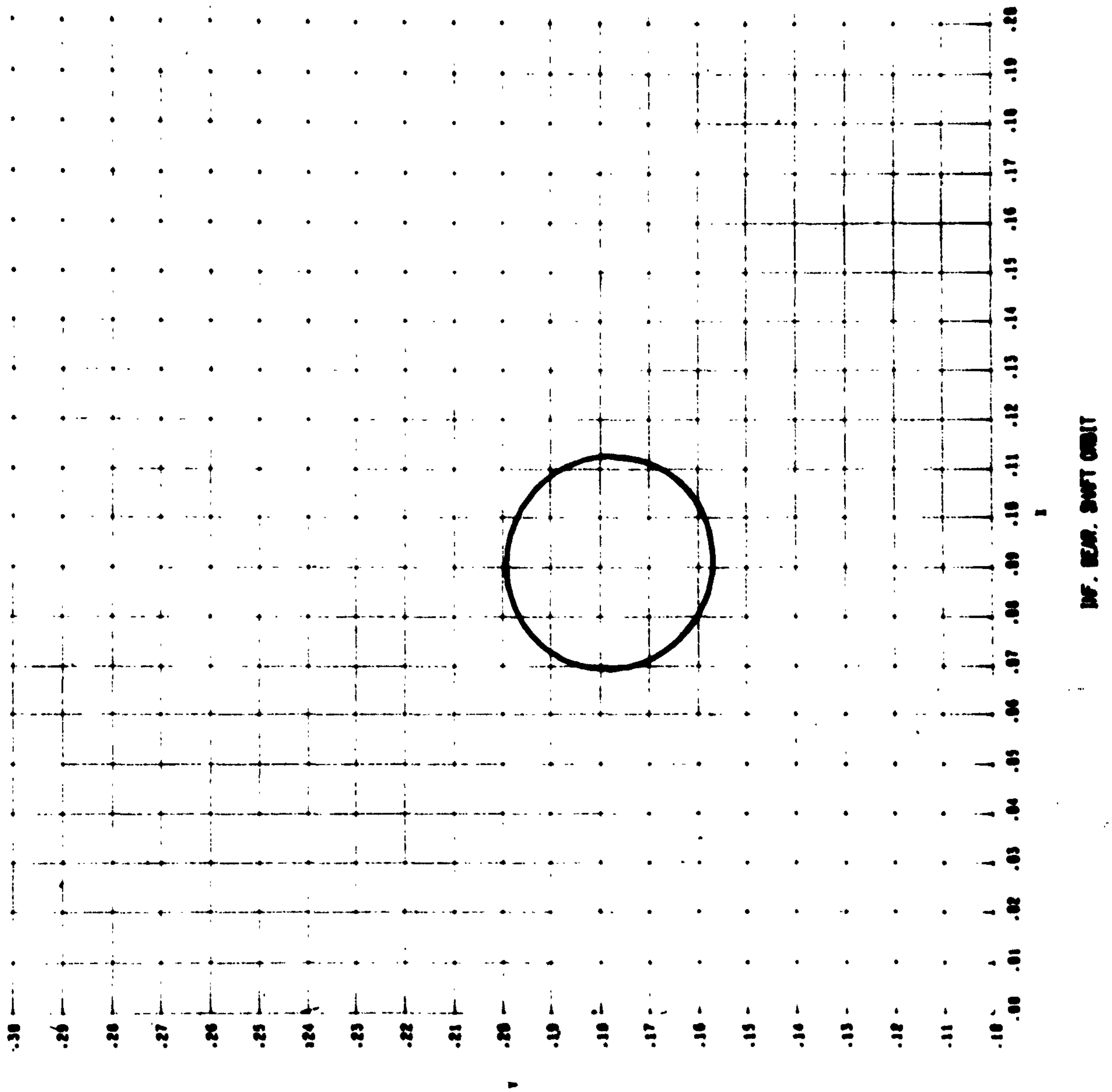

Fig. 41a
Large Amplitude
Orbit
Run 6
B = 1; $\Delta T = 0.026$
1st 1000 steps

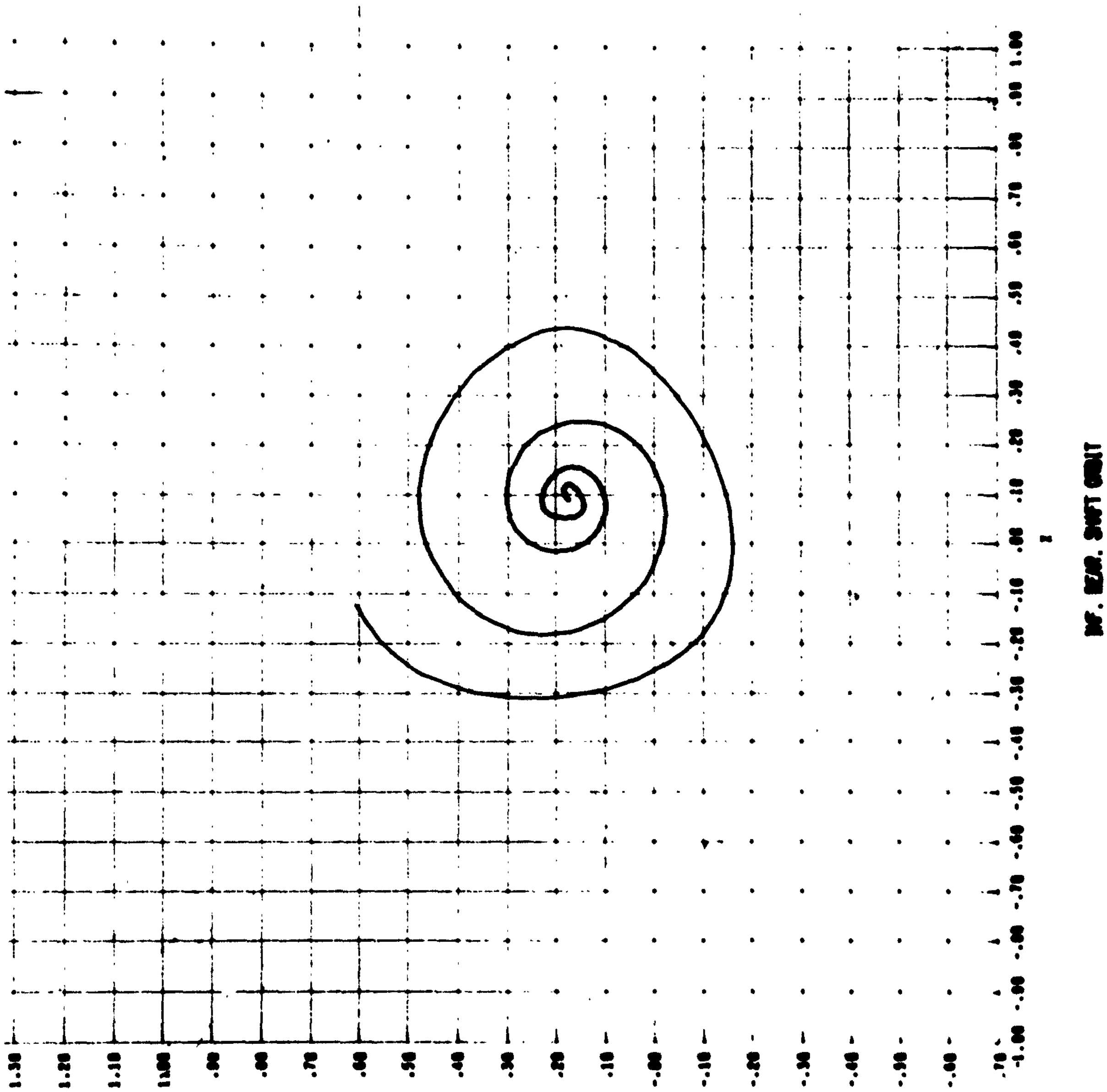

Fig. 41b
Large Amplitude
Orbit
Run 6
B = 1; ΔT = 0.026
2nd 1000 steps

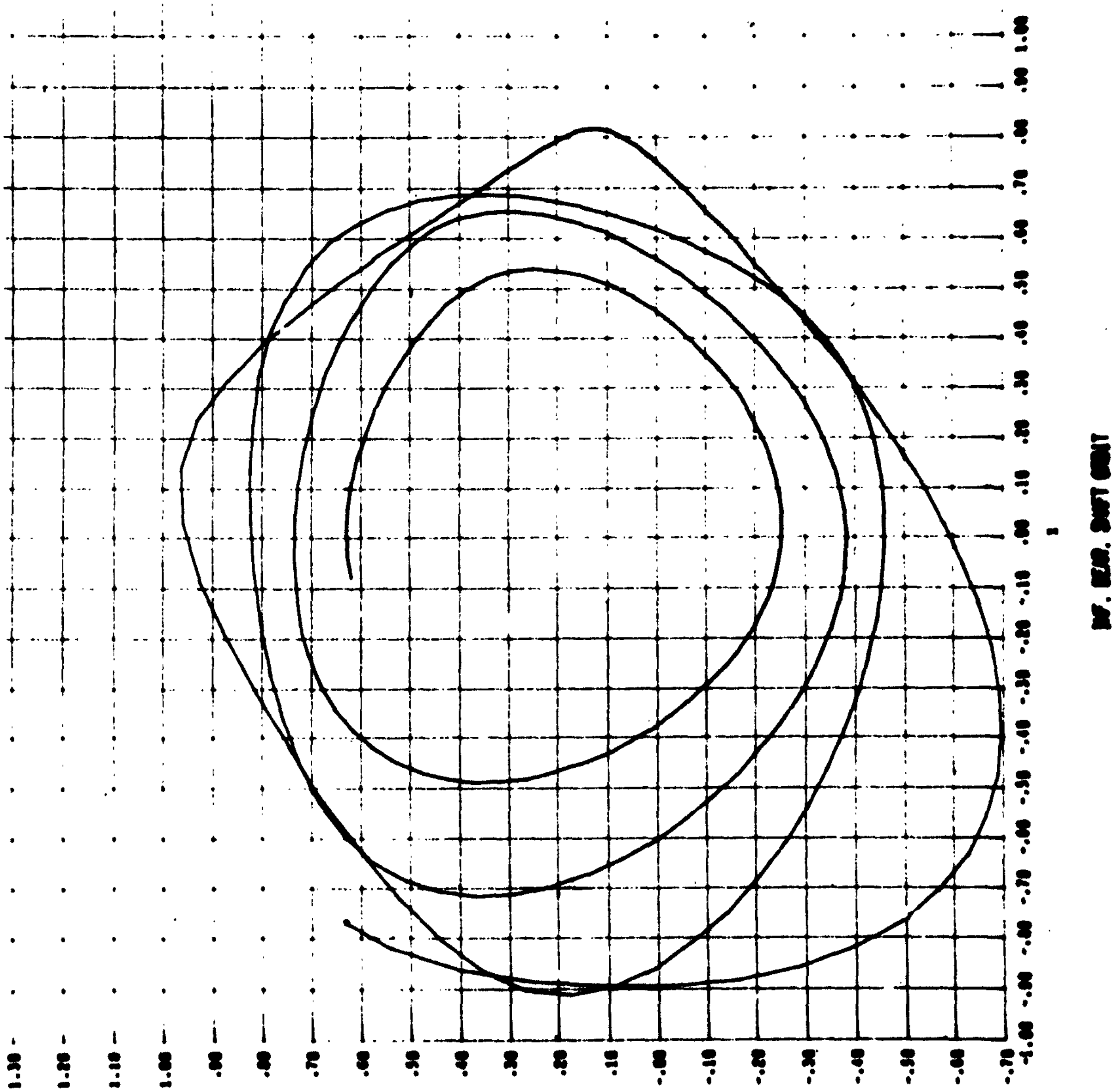

```
CASE    2, STEP 6100, B= 0.1000000E 02, TIME=0.58634070E 02, X= 0.05081908, Y= 0.39760687, DT=0.26000000E-01
 LAMBDA=0.81099999E 01            W = PH  DISTRIBUTION
  1.1538813  1.1732943  1.1899080  1.2028308  1.2113788  1.2151227  1.2139125  1.2078795  1.1974171  1.1831431
  1.1658480  1.1464343  1.1258538  1.1050486  1.0849011  1.0661981  1.0496102  1.0356849  1.0243529  1.0174397
  1.0136790  1.0137214  1.0176334  1.0253857  1.0368292  1.0516660  1.0694225  1.0894356  1.1108603  1.1327034

CASE    2, STEP 6101, B= 0.1000000E 02, TIME=0.58660070E 02, X= 0.05244562, Y= 0.39877538, DT=0.26000000E-01
 LAMBDA=0.81099999E 01            W = PH  DISTRIBUTION
  1.1529126  1.1724903  1.1893099  1.2024685  1.2112693  1.2152692  1.2143047  1.2084947  1.1982222  1.1840969
  1.1669036  1.1475422  1.1269647  1.1061155  1.0858814  1.0670549  1.0503128  1.0362096  1.0251823  1.0175625
  1.0135900  1.0134211  1.0171287  1.0246906  1.0359658  1.0506654  1.0683246  1.0882881  1.1097167  1.1316198

CASE    2, STEP 6102, B= 0.1000000E 02, TIME=0.58686069E 02, X= 0.05494550, Y= 0.40044066, DT=0.26000000E-01
```

FIG. 42a
RUN 17;
B=10 ; ΔT= .026
PH DISTRIB'S

FIG. 42b
RUN 17
B = 10 ; ΔT = .026
PH DISTRIB'S

```
LAMBDA=0.81099999E 01                W = PH  DISTRIBUTION
 1.1519361  1.1716741  1.1886958  1.2020873  1.2111388  1.2153936  1.2146747  1.2090887  1.1990079  1.1850338
 1.1679457  1.1486407  1.1280705  1.1071817  1.0868654  1.0679194  1.0510270  1.0367491  1.0255292  1.0177049
 1.0135218  1.0131421  1.0166450  1.0240153  1.0351202  1.0496795  1.0672376  1.0871472  1.1085750  1.1305332

CASE    2, STEP 6103, B= 0.1000000E 02, TIME=0.58712069E 02, X= 0.05796308, Y= 0.40252017, DT=0.26000000E-01
LAMBDA=0.81099999E 01                W = PH  DISTRIBUTION
 1.1509547  1.1708492  1.1880697  1.2016912  1.2109914  1.2154998  1.2150261  1.2096643  1.1997763  1.1859553
 1.1689748  1.1497291  1.1291696  1.1082449  1.0878501  1.0687885  1.0517493  1.0372998  1.0259899  1.0178633
 1.0134711  1.0128814  1.0161797  1.0233577  1.0342908  1.0487077  1.0661616  1.0860137  1.1074367  1.1294459

CASE    2, STEP 6104, B= 0.1000000E 02, TIME=0.58738068E 02, X= 0.06172255, Y= 0.40491646, DT=0.26000000E-01
LAMBDA=0.81099999E 01                W = PH  DISTRIBUTION
 1.1499711  1.1700187  1.1874350  1.2012642  1.2108310  1.2155916  1.2153622  1.2102244  1.2005297  1.1868626
 1.1699914  1.1508072  1.1302609  1.1093034  1.0888333  1.0696592  1.0524764  1.0378584  1.0262611  1.0180343
 1.0134348  1.0126363  1.0157304  1.0227160  1.0334763  1.0477490  1.0650965  1.0848881  1.1063030  1.1283596

CASE    2, STEP 6105, B= 0.1000000E 02, TIME=0.58764068E 02, X= 0.06602997, Y= 0.40752013, DT=0.26000000E-01
LAMBDA=0.81099999E 01                W = PH  DISTRIBUTION
 1.1489871  1.1691851  1.1867947  1.2008693  1.2106609  1.2156723  1.2156860  1.2107717  1.2012700  1.1877574
 1.1709963  1.1518749  1.1313439  1.1103558  1.0898131  1.0705294  1.0532058  1.0384220  1.0266399  1.0182152
 1.0134101  1.0124041  1.0152948  1.0220881  1.0326751  1.0468025  1.0640417  1.0837706  1.1051747  1.1272760

CASE    2, STEP 6106, B= 0.1000000E 02, TIME=0.58790068E 02, X= 0.07077564, Y= 0.41021347, DT=0.26000000E-01
LAMBDA=0.81099999E 01                W = PH  DISTRIBUTION
 1.1480042  1.1683503  1.1861510  1.2004490  1.2104838  1.2157444  1.2160002  1.2113085  1.2019992  1.1886410
 1.1719903  1.1529327  1.1324182  1.1114013  1.0907881  1.0713972  1.0539353  1.0389883  1.0270239  1.0184034
 1.0133947  1.0121827  1.0148710  1.0214724  1.0318860  1.0458672  1.0629969  1.0826612  1.1040523  1.1261959

CASE    2, STEP 6107, B= 0.1000000E 02, TIME=0.58816067E 02, X= 0.07583710, Y= 0.41287437, DT=0.26000000E-01
LAMBDA=0.81099999E 01                W = PH  DISTRIBUTION
 1.1470234  1.1675156  1.1855056  1.2000253  1.2103017  1.2158102  1.2163068  1.2118366  1.2027192  1.1895148
 1.1729746  1.1539809  1.1334838  1.1124594  1.0917575  1.0722615  1.0546637  1.0395557  1.0274114  1.0185973
 1.0133868  1.0119703  1.0144574  1.0208675  1.0311076  1.0449422  1.0619612  1.0815595  1.1029360  1.1251198

CASE    2, STEP 6108, B= 0.1000000E 02, TIME=0.58842067E 02, X= 0.08108242, Y= 0.41538053, DT=0.26000000E-01
LAMBDA=0.81099999E 01                W = PH  DISTRIBUTION
 1.1460447  1.1665814  1.1848591  1.1995992  1.2101158  1.2158710  1.2166074  1.2123578  1.2034313  1.1903801
 1.1739500  1.1550205  1.1345413  1.1134704  1.0927211  1.0731216  1.0553899  1.0401233  1.0278011  1.0187955
 1.0133852  1.0117657  1.0140527  1.0202721  1.0303390  1.0440266  1.0609341  1.0804651  1.1018253  1.1240477

CASE    2, STEP 6109, B= 0.1000000E 02, TIME=0.58868066E 02, X= 0.08637384, Y= 0.41761380, DT=0.26000000E-01
LAMBDA=0.81099999E 01                W = PH  DISTRIBUTION
 1.1450680  1.1658476  1.1842117  1.1991708  1.2079267  1.2159276  1.2169028  1.2128729  1.2041367  1.1912382
 1.1749178  1.1560524  1.1355914  1.1144947  1.0936792  1.0739779  1.0561140  1.0406906  1.0281926  1.0189975
 1.0133890  1.0115681  1.0136560  1.0196855  1.0295793  1.0431195  1.0599147  1.0793772  1.1007196  1.1229790

CASE    2, STEP 6110, B= 0.1000000E 02, TIME=0.58894066E 02, X= 0.09157173, Y= 0.41746455, DT=0.26000000E-01
LAMBDA=0.81099999E 01                W = PH  DISTRIBUTION
 1.1440922  1.1650133  1.1835625  1.1987397  1.2097339  1.2159798  1.2171933  1.2133826  1.2048360  1.1920898
 1.1758769  1.1570777  1.1366351  1.1155135  1.0946327  1.0748309  1.0568365  1.0412581  1.0285861  1.0192032
 1.0133982  1.0113772  1.0132671  1.0191071  1.0288279  1.0422202  1.0589022  1.0782949  1.0996181  1.1219129

CASE    2, STEP 6111, B= 0.1000000E 02, TIME=0.58920065E 02, X= 0.09653854, Y= 0.42083591, DT=0.26000000E-01
LAMBDA=0.81099999E 01                W = PH  DISTRIBUTION
 1.1431158  1.1641770  1.1829101  1.1983045  1.2095364  1.2160268  1.2174783  1.2138866  1.2055297  1.1929357
 1.1768344  1.1580975  1.1376740  1.1165277  1.0955830  1.0756820  1.0575586  1.0418269  1.0289826  1.0194135
 1.0134134  1.0111934  1.0128860  1.0185370  1.0280845  1.0413284  1.0578960  1.0772173  1.0985195  1.1208479

CASE    2, STEP 6112, B= 0.1000000E 02, TIME=0.58946065E 02, X= 0.10114295, Y= 0.42164759, DT=0.26000000E-01
```

FIG. 42c
RUN 17
B = 10; ΔT = .026
PH DISTRIB'S

```
LAMBDA=0.81099999E 01                W = PH  DISTRIBUTION
 1.1421370  1.1633366  1.1822523  1.1978631  1.2093323  1.2160672  1.2177568  1.2143844  1.2062175  1.1937763
 1.1777851  1.1591131  1.1387093  1.1175397  1.0965319  1.0765329  1.0582820  1.0423985  1.0293834  1.0196296
 1.0134356  1.0110175  1.0123134  1.0179753  1.0273492  1.0404435  1.0568952  1.0761434  1.0974225  1.1197824

CASE    2, STEP 6113, B= 0.1000000E 02, TIME=0.58972064E 02, X= 0.10526376, Y= 0.42183927, DT=0.26000000E-01
 LAMBDA=0.81099999E 01                W = PH  DISTRIBUTION
 1.1411535  1.1624896  1.1815866  1.1974129  1.2091190  1.2160987  1.2180270  1.2148747  1.2068989  1.1946115
 1.1787316  1.1601257  1.1397429  1.1185510  1.0974815  1.0773861  1.0590091  1.0429753  1.0297907  1.0198533
 1.0134664  1.0108510  1.0121503  1.0174229  1.0266222  1.0395656  1.0558995  1.0750722  1.0963257  1.1187145

CASE    2, STEP 6114, B= 0.1000000E 02, TIME=0.58998064E 02, X= 0.10879355, Y= 0.42137315, DT=0.26000000E-01
 LAMBDA=0.81099999E 01                W = PH  DISTRIBUTION
 1.1401628  1.1615330  1.1809097  1.1969506  1.2088936  1.2161184  1.2182864  1.2153558  1.2075727  1.1954409
 1.1796742  1.1611363  1.1407762  1.1195639  1.0984344  1.0782442  1.0597426  1.0435599  1.0302072  1.0200872
 1.0135082  1.0106957  1.0117983  1.0168809  1.0259043  1.0386949  1.0549084  1.0740027  1.0952275  1.1176421

CASE    2, STEP 6115, B= 0.1000000E 02, TIME=0.59024063E 02, X= 0.11164188, Y= 0.42023571, DT=0.26000000E-01
 LAMBDA=0.81099999E 01                W = PH  DISTRIBUTION
 1.1391622  1.1607638  1.1802182  1.1964726  1.2086522  1.2161229  1.2185321  1.2158252  1.2082373  1.1962639
 1.1806130  1.1621458  1.1418109  1.1205804  1.0993931  1.0791099  1.0604855  1.0441553  1.0306357  1.0203341
 1.0135633  1.0105538  1.0114593  1.0163507  1.0251966  1.0378317  1.0539219  1.0729343  1.0941265  1.1165633

CASE    2, STEP 6116, B= 0.1000000E 02, TIME=0.59050063E 02, X= 0.11373805, Y= 0.41843843, DT=0.26000000E-01
 LAMBDA=0.81099999E 01                W = PH  DISTRIBUTION
 1.1381490  1.1598787  1.1795083  1.1959749  1.2083910  1.2161095  1.2187609  1.2162803  1.2088909  1.1970795
 1.1815479  1.1631547  1.1428484  1.1216028  1.1003602  1.0799863  1.0612411  1.0447650  1.0310795  1.0205971
 1.0136349  1.0104281  1.0111356  1.0158343  1.0245002  1.0369770  1.0529401  1.0718662  1.0930215  1.1154760

CASE    2, STEP 6117, B= 0.1000000E 02, TIME=0.59076063E 02, X= 0.11503305, Y= 0.41601749, DT=0.26000000E-01
 LAMBDA=0.81099999E 01                W = PH  DISTRIBUTION
 1.1371207  1.1589744  1.1787762  1.1954534  1.2081057  1.2160711  1.2189689  1.2167179  1.2095309  1.1978955
 1.1824781  1.1641635  1.1438898  1.1226328  1.1013383  1.0808765  1.0620125  1.0453922  1.0315422  1.0208796
 1.0137261  1.0103215  1.0108297  1.0153337  1.0238169  1.0361317  1.0519633  1.0707983  1.0919113  1.1143783

CASE    2, STEP 6118, B= 0.1000000E 02, TIME=0.59102062E 02, X= 0.11550082, Y= 0.41303229, DT=0.26000000E-01
 LAMBDA=0.81099999E 01                W = PH  DISTRIBUTION
 1.1360748  1.1583478  1.1780184  1.1949041  1.2077921  1.2160065  1.2191521  1.2171345  1.2101546  1.1986807
 1.1834027  1.1651721  1.1449361  1.1236722  1.1023296  1.0817832  1.0628031  1.0460406  1.0320273  1.0211850
 1.0138402  1.0102370  1.0105444  1.0148515  1.0231487  1.0352973  1.0509924  1.0697305  1.0907952  1.1132687

CASE    2, STEP 6119, B= 0.1000000E 02, TIME=0.59128062E 02, X= 0.11513879, Y= 0.40956318, DT=0.26000000E-01
 LAMBDA=0.81099999E 01                W = PH  DISTRIBUTION
 1.1350094  1.1570962  1.1772314  1.1943230  1.2074460  1.2159104  1.2193066  1.2175266  1.2107590  1.1994626
 1.1843204  1.1661800  1.1459877  1.1247223  1.1033363  1.0827091  1.0636160  1.0467134  1.0325381  1.0215169
 1.0139805  1.0101779  1.0102828  1.0143901  1.0224976  1.0344753  1.0500282  1.0686632  1.0896727  1.1121459

CASE    2, STEP 6120, B= 0.1000000E 02, TIME=0.59154061E 02, X= 0.11396755, Y= 0.40570814, DT=0.26000000E-01
 LAMBDA=0.81099999E 01                W = PH  DISTRIBUTION
 1.1339228  1.1561172  1.1764122  1.1937065  1.2070634  1.2157786  1.2194283  1.2178902  1.2113408  1.2002287
 1.1852295  1.1671865  1.1470447  1.1257841  1.1043600  1.0836564  1.0644537  1.0474136  1.0330780  1.0218785
 1.0141505  1.0101474  1.0100477  1.0139522  1.0218660  1.0336677  1.0490723  1.0675970  1.0885439  1.1110091

CASE    2, STEP 6121, B= 0.1000000E 02, TIME=0.59180061E 02, X= 0.11202978, Y= 0.40157889, DT=0.26000000E-01
 LAMBDA=0.81099999E 01                W = PH  DISTRIBUTION
 1.1328139  1.1551089  1.1755580  1.1930515  1.2066405  1.2156073  1.2195132  1.2182219  1.2118968  1.2009762
 1.1861278  1.1681903  1.1481067  1.1268578  1.1054018  1.0846270  1.0653186  1.0481439  1.0336500  1.0222731
 1.0143533  1.0101485  1.0098422  1.0135408  1.0212564  1.0328765  1.0481262  1.0665331  1.0874091  1.1098580

CASE    2, STEP 6122, B= 0.1000000E 02, TIME=0.59206060E 02, X= 0.10938863, Y= 0.39729652, DT=0.26000000E-01
```

```
LAMBDA=0.81099799E 01                W = PH  DISTRIBUTION
  1.1316822  1.1540700  1.1746670  1.1923553  1.2061744  1.2153929  1.2195576  1.2185176  1.2124234  1.2017021
  1.1870131  1.1691898  1.1491728  1.1279434  1.1064624  1.0856220  1.0662126  1.0489067  1.0342565  1.0227053
  1.0145917  1.0101842  1.0096691  1.0131584  1.0206714  1.0321041  1.0471916  1.0654728  1.0862692  1.1086927

CASE    2, STEP 6123, B= 0.1000000E 02, TIME=0.59232060E 02, X= 0.10612537, Y= 0.39298682, DT=0.26000000E-01
 LAMBDA=0.81099999E 01               W = PH  DISTRIBUTION
  1.1305279  1.1530000  1.1737379  1.1916159  1.2056624  1.2151324  1.2195581  1.2187741  1.2129173  1.2024033
  1.1878827  1.1701826  1.1502416  1.1290402  1.1075417  1.0866421  1.0671368  1.0497034  1.0343995  1.0231714
  1.0148685  1.0102571  1.0095311  1.0128078  1.0201134  1.0313528  1.0462712  1.0644179  1.0851256  1.1075141

CASE    2, STEP 6124, B= 0.1000000E 02, TIME=0.59258059E 02, X= 0.10233676, Y= 0.38877565, DT=0.26000000E-01
 LAMBDA=0.81099999E 01               W = PH  DISTRIBUTION
  1.1293515  1.1518967  1.1727700  1.1908320  1.2051025  1.2148233  1.2195119  1.2189883  1.2133754  1.2030768
  1.1887338  1.1711671  1.1513114  1.1301470  1.1086391  1.0876874  1.0680918  1.0505353  1.0355807  1.0236793
  1.0151852  1.0103696  1.0094306  1.0124914  1.0195852  1.0306252  1.0453668  1.0633706  1.0839798  1.1063235

CASE    2, STEP 6125, B= 0.1000000E 02, TIME=0.59284059E 02, X= 0.09813196, Y= 0.38478437, DT=0.26000000E-01
 LAMBDA=0.81099999E 01               W = PH  DISTRIBUTION
  1.1281546  1.1507675  1.1717635  1.1900031  1.2044935  1.2144637  1.2194167  1.2191573  1.2137945  1.2037195
  1.1895633  1.1721399  1.1523797  1.1312620  1.1097535  1.0887571  1.0690775  1.0514027  1.0363009  1.0242283
  1.0155439  1.0105234  1.0093698  1.0122117  1.0190890  1.0299236  1.0444811  1.0623332  1.0828341  1.1051225

CASE    2, STEP 6126, B= 0.1000000E 02, TIME=0.59310059E 02, X= 0.09362928, Y= 0.38112568, DT=0.26000000E-01
 LAMBDA=0.81099999E 01               W = PH  DISTRIBUTION
  1.1269389  1.1496073  1.1707193  1.1891294  1.2038351  1.2140526  1.2192705  1.2192789  1.2141720  1.2043283
  1.1903684  1.1730983  1.1534439  1.1323830  1.1108830  1.0898500  1.0700931  1.0523054  1.0370602  1.0248191
  1.0159455  1.0107201  1.0093503  1.0119705  1.0186272  1.0292506  1.0436166  1.0613082  1.0816911  1.1039135

CASE    2, STEP 6127, B= 0.1000000E 02, TIME=0.59336058E 02, X= 0.08895276, Y= 0.37789984, DT=0.26000000E-01
 LAMBDA=0.81099999E 01               W = PH  DISTRIBUTION
  1.1257071  1.1484204  1.1696390  1.1882119  1.2031275  1.2135895  1.2190724  1.2193511  1.2145055  1.2049006
  1.1911460  1.1740393  1.1545011  1.1335071  1.1120253  1.0909642  1.0711372  1.0532424  1.0378583  1.0254516
  1.0163906  1.0109605  1.0093736  1.0117696  1.0182017  1.0286095  1.0427759  1.0602985  1.0805534  1.1026993

CASE    2, STEP 6128, B= 0.1000000E 02, TIME=0.59362058E 02, X= 0.08422882, Y= 0.37519148, DT=0.26000000E-01
 LAMBDA=0.81099999E 01               W = PH  DISTRIBUTION
  1.1244621  1.1472096  1.1685250  1.1872525  1.2023719  1.2130748  1.2188218  1.2193729  1.2147931  1.2054339
  1.1918931  1.1749596  1.1555481  1.1346314  1.1131774  1.0920972  1.0722078  1.0542121  1.0386941  1.0261253
  1.0168790  1.0112450  1.0094405  1.0116103  1.0178143  1.0279994  1.0419616  1.0593068  1.0794240  1.1014329

CASE    2, STEP 6129, B= 0.1000000E 02, TIME=0.59388057E 02, X= 0.07958286, Y= 0.37306697, DT=0.26000000E-01
 LAMBDA=0.81099999E 01               W = PH  DISTRIBUTION
  1.1232072  1.1459781  1.1673801  1.1862536  1.2015699  1.2125095  1.2185191  1.2193436  1.2150335  1.2059260
  1.1926071  1.1758562  1.1565814  1.1357523  1.1143361  1.0932458  1.0733021  1.0552124  1.0395656  1.0268390
  1.0174101  1.0115736  1.0095514  1.0114936  1.0174665  1.0274253  1.0411759  1.0583359  1.0783063  1.1002676

CASE    2, STEP 6130, B= 0.1000000E 02, TIME=0.59414057E 02, X= 0.07513602, Y= 0.37157254, DT=0.26000000E-01
 LAMBDA=0.81099999E 01               W = PH  DISTRIBUTION
  1.1219463  1.1447296  1.1662080  1.1852183  1.2007243  1.2118955  1.2181650  1.2192633  1.2152256  1.2063751
  1.1932855  1.1767259  1.1575977  1.1368662  1.1154978  1.0944068  1.0744170  1.0562406  1.0404713  1.02759[illegible]
  1.0179827  1.0119456  1.0097061  1.0114198  1.0171594  1.0268879  1.0404213  1.0573887  1.0772032  1.0990569

CASE    2, STEP 6131, B= 0.1000000E 02, TIME=0.59440056E 02, X= 0.07100217, Y= 0.37073296, DT=0.26000000E-01
 LAMBDA=0.81099999E 01               W = PH  DISTRIBUTION
  1.1206831  1.1434681  1.1650124  1.1841501  1.1998380  1.2112350  1.2177612  1.2191325  1.2153691  1.2067800
  1.1939260  1.1775660  1.1585935  1.1379695  1.1166587  1.0955753  1.0755490  1.0572933  1.0414076  1.0283789
  1.0185950  1.0123597  1.0099043  1.0113893  1.0168936  1.0263885  1.0396996  1.0564677  1.0761182  1.0978546

CASE    2, STEP 6132, B= 0.1000000E 02, TIME=0.59466056E 02, X= 0.06728505, Y= 0.37055100, DT=0.26000000E-01
```

FIG. 42d
RUN 17
B=10 ; ΔT=.026
PH DISTRIB'S

```
 LAMBDA=0.81099999E 01              W = PH  DISTRIBUTION
  1.1194219  1.1421979  1.1637978  1.1830532  1.1989147  1.2105311  1.2173098  1.2189524  1.2154642  1.2071398
  1.1945269  1.1783737  1.1595656  1.1390584  1.1178147  1.0967502  1.0766942  1.0583669  1.0423716  1.0292000
  1.0192448  1.0128144  1.0101447  1.0114014  1.0166696  1.0259282  1.0390128  1.0555755  1.0750541  1.0966642

CASE     2, STEP 6133, B= 0.1000000E 02, TIME=0.59492055E 02, X= 0.06407575, Y= 0.37100752, DT=0.26000000E-01
 LAMBDA=0.81099999E 01              W = PH  DISTRIBUTION
  1.1181665  1.1409234  1.1625685  1.1819320  1.1979585  1.2097873  1.2168135  1.2187249  1.2155116  1.2074542
  1.1950869  1.1791469  1.1605109  1.1401292  1.1189618  1.0979244  1.0778484  1.0594576  1.0433597  1.0300512
  1.0199295  1.0133077  1.0104261  1.0114555  1.0164872  1.0255076  1.0383621  1.0547141  1.0740140  1.0954893

CASE     2, STEP 6134, B= 0.1000000E 02, TIME=0.59518055E 02, X= 0.06145055, Y= 0.37206218, DT=0.26000000E-01
 LAMBDA=0.81099999E 01              W = PH  DISTRIBUTION
  1.1169209  1.1396490  1.1613293  1.1807911  1.1969736  1.2090074  1.2162756  1.2184520  1.2155127  1.2077233
  1.1956051  1.1798835  1.1614266  1.1411786  1.1200963  1.0990948  1.0790074  1.0605611  1.0443679  1.0309289
  1.0206460  1.0138369  1.0107465  1.0115504  1.0163459  1.0251271  1.0377487  1.0538855  1.0730004  1.0943332

CASE     2, STEP 6135, B= 0.1000000E 02, TIME=0.59544054E 02, X= 0.05946900, Y= 0.37365490, DT=0.26000000E-01
 LAMBDA=0.81099999E 01              W = PH  DISTRIBUTION
  1.1156888  1.1383788  1.1600846  1.1796350  1.1959647  1.2081956  1.2156995  1.2181368  1.2154691  1.2079479
  1.1960810  1.1805822  1.1623105  1.1422034  1.1212142  1.1002572  1.0801670  1.0616733  1.0453923  1.0318294
  1.0213911  1.0143993  1.0111036  1.0116845  1.0162450  1.0247865  1.0371732  1.0530912  1.0720157  1.0931989

CASE     2, STEP 6136, B= 0.1000000E 02, TIME=0.59570054E 02, X= 0.05817258, Y= 0.37570774, DT=0.26000000E-01
 LAMBDA=0.81099999E 01              W = PH  DISTRIBUTION
  1.1144738  1.1371169  1.1588389  1.1784686  1.1949365  1.2073563  1.2150891  1.2177822  1.2153831  1.2081292
  1.1965147  1.1812421  1.1631605  1.1432008  1.1223123  1.1014079  1.0813230  1.0627900  1.0464288  1.0327489
  1.0221612  1.0149920  1.0114951  1.0118559  1.0161830  1.0244852  1.0366359  1.0523322  1.0710617  1.0920893

CASE     2, STEP 6137, B= 0.1000000E 02, TIME=0.59596054E 02, X= 0.05758363, Y= 0.37812743, DT=0.26000000E-01
 LAMBDA=0.81099999E 01              W = PH  DISTRIBUTION
  1.1132787  1.1358670  1.1575964  1.1772963  1.1938933  1.2064940  1.2144485  1.2173917  1.2152573  1.2082687
  1.1969070  1.1818626  1.1639752  1.1441686  1.1233875  1.1025431  1.0824714  1.0639071  1.0474733  1.0336834
  1.0229527  1.0156115  1.0119181  1.0120623  1.0161585  1.0242225  1.0361367  1.0516092  1.0701400  1.0910065

CASE     2, STEP 6138, B= 0.1000000E 02, TIME=0.59622053E 02, X= 0.05770490, Y= 0.38080839, DT=0.26000000E-01
 LAMBDA=0.81099999E 01              W = PH  DISTRIBUTION
  1.1121062  1.1346324  1.1563609  1.1761223  1.1928398  1.2056129  1.2137818  1.2169689  1.2150947  1.2083687
  1.1972589  1.1824440  1.1647538  1.1451048  1.1244372  1.1036598  1.0836088  1.0650208  1.0485218  1.0346291
  1.0237619  1.0162546  1.0123696  1.0123014  1.0161696  1.0239971  1.0356750  1.0509224  1.0692516  1.0899523

CASE     2, STEP 6139, B= 0.1000000E 02, TIME=0.59648053E 02, X= 0.05851945, Y= 0.38363639, DT=0.26000000E-01
 LAMBDA=0.81099999E 01              W = PH  DISTRIBUTION
  1.1109584  1.1334158  1.1551359  1.1749504  1.1917800  1.2047173  1.2130930  1.2165175  1.2148983  1.2084314
  1.1975719  1.1829867  1.1654960  1.1460084  1.1254593  1.1047553  1.0847319  1.0661275  1.0495707  1.0355823
  1.0245853  1.0169180  1.0128467  1.0125704  1.0162141  1.0238073  1.0352499  1.0502717  1.0683970  1.0889282

CASE     2, STEP 6140, B= 0.1000000E 02, TIME=0.59674052E 02, X= 0.05999118, Y= 0.38649081, DT=0.26000000E-01
 LAMBDA=0.81099999E 01              W = PH  DISTRIBUTION
  1.1098368  1.1322195  1.1539241  1.1737842  1.1907177  1.2038112  1.2123861  1.2160413  1.2146716  1.2084597
  1.1978480  1.1834920  1.1662018  1.1468787  1.1264526  1.1058273  1.0858381  1.0672241  1.0506166  1.0365396
  1.0254194  1.0175983  1.0133463  1.0128667  1.0162897  1.0236513  1.0348601  1.0496563  1.0675762  1.0879349

CASE     2, STEP 6141, B= 0.1000000E 02, TIME=0.59700052E 02, X= 0.06206577, Y= 0.38925155, DT=0.26000000E-01
 LAMBDA=0.81099999E 01              W = PH  DISTRIBUTION
  1.1087424  1.1310450  1.1527279  1.1726263  1.1896562  1.2028982  1.2116648  1.2155440  1.2144178  1.2084564
  1.1980896  1.1839614  1.1668722  1.1477155  1.1274160  1.1068745  1.0869251  1.0683080  1.0516566  1.0374977
  1.0262611  1.0182923  1.0138653  1.0131674  1.0163938  1.0235271  1.0345040  1.0490752  1.0667889  1.0869726

CASE     2, STEP 6142, B= 0.1000000E 02, TIME=0.59726051E 02, X= 0.06467218, Y= 0.39180012, DT=0.26000000E-01
```

FIG. 42 e
RUN 17
B = 10 ; ΔT = .026
PH DISTRIB'S

Fig. 42 f
RUN 17
B=10 ; ΔT=.026
PH DISTRIB'S

```
 LAMBDA=0.81099999E 01              W = PH  DISTRIBUTION
  1.1076754  1.1298935  1.1515488  1.1714791  1.1885983  1.2019815  1.2109327  1.2150290  1.2141405  1.2084247
  1.1982992  1.1843967  1.1675083  1.1485195  1.1283494  1.1078957  1.0879914  1.0693773  1.0526883  1.0384541
  1.0271073  1.0189971  1.0144009  1.0145298  1.0165240  1.0234323  1.0341797  1.0485273  1.0663342  1.0860410

CASE    2, STEP 6143, B= 0.1000000E 02, TIME=0.59752051E 02, X= 0.06772459, Y= 0.39402524, DT=0.26000000E-01
 LAMBDA=0.81099999E 01              W = PH  DISTRIBUTION
  1.1066356  1.1287653  1.1503881  1.1703442  1.1875461  1.2010637  1.2101925  1.2144994  1.2138427  1.2083675
  1.1984797  1.1848007  1.1681120  1.1492916  1.1292531  1.1088908  1.0890362  1.0704302  1.0537096  1.0394063
  1.0279557  1.0197101  1.0149502  1.0138912  1.0166776  1.0233646  1.0338852  1.0480099  1.0653106  1.0851393

CASE    2, STEP 6144, B= 0.1000000E 02, TIME=0.59778050E 02, X= 0.07112479, Y= 0.39582635, DT=0.26000000E-01
 LAMBDA=0.81099999E 01              W = PH  DISTRIBUTION
  1.1056223  1.1276601  1.1492458  1.1692225  1.1865011  1.2001468  1.2094469  1.2139583  1.2135275  1.2082881
  1.1986338  1.1851756  1.1686853  1.1500335  1.1301282  1.1098600  1.0900590  1.0714662  1.0547194  1.0403526
  1.0288041  1.0204289  1.0155110  1.0142690  1.0168523  1.0233217  1.0336181  1.0475220  1.0646166  1.0842663

CASE    2, STEP 6145, B= 0.1000000E 02, TIME=0.59804050E 02, X= 0.07476500, Y= 0.39711732, DT=0.26000000E-01
 LAMBDA=0.81099999E 01              W = PH  DISTRIBUTION
  1.1046543  1.1265771  1.1481219  1.1681143  1.1854644  1.1992323  1.2086979  1.2134079  1.2131978  1.2081892
  1.1987645  1.1855242  1.1692307  1.1507472  1.1309760  1.1108043  1.0910605  1.0724848  1.0557167  1.0412919
  1.0296510  1.0211517  1.0160809  1.0146610  1.0170455  1.0233010  1.0333761  1.0470610  1.0639502  1.0834204

CASE    2, STEP 6146, B= 0.1000000E 02, TIME=0.59830049E 02, X= 0.07853088, Y= 0.39782951, DT=0.26000000E-01
 LAMBDA=0.81099999E 01              W = PH  DISTRIBUTION
  1.1036697  1.1255151  1.1470154  1.1670193  1.1844359  1.1983210  1.2079467  1.2128501  1.2128557  1.2080735
  1.1988747  1.1858494  1.1697509  1.1514350  1.1317986  1.1117251  1.0920409  1.0734864  1.0567314  1.0422234
  1.0304951  1.0219769  1.0166584  1.0150652  1.0172551  1.0233003  1.0331569  1.0466246  1.0633092  1.0825994

CASE    2, STEP 6147, B= 0.1000000E 02, TIME=0.59856049E 02, X= 0.08230483, Y= 0.39791442, DT=0.26000000E-01
 LAMBDA=0.81099999E 01              W = PH  DISTRIBUTION
  1.1027266  1.1244722  1.1459249  1.1659365  1.1834155  1.1974131  1.2071943  1.2122865  1.2125032  1.2079434
  1.1989670  1.1861539  1.1702486  1.1520995  1.1325982  1.1126242  1.0930022  1.0744719  1.0576739  1.0431470
  1.0313361  1.0226036  1.0172419  1.0154799  1.0174791  1.0233175  1.0329563  1.0462105  1.0626913  1.0818012

CASE    2, STEP 6148, B= 0.1000000E 02, TIME=0.59882049E 02, X= 0.08596940, Y= 0.39734552, DT=0.26000000E-01
 LAMBDA=0.81099999E 01              W = PH  DISTRIBUTION
  1.1018026  1.1234464  1.1448486  1.1648646  1.1824021  1.1965083  1.2064408  1.2117177  1.2121419  1.2078008
  1.1990438  1.1864405  1.1707267  1.1527436  1.1333774  1.1135041  1.0939461  1.0754429  1.0586351  1.0440633
  1.0321737  1.0233313  1.0178307  1.0159038  1.0177161  1.0233507  1.0327780  1.0458165  1.0620940  1.0810234

CASE    2, STEP 6149, B= 0.1000000E 02, TIME=0.59908048E 02, X= 0.08941068, Y= 0.39611953, DT=0.26000000E-01
 LAMBDA=0.81099999E 01              W = PH  DISTRIBUTION
  1.1008952  1.1224351  1.1437842  1.1638014  1.1813941  1.1956054  1.2056859  1.2111441  1.2117725  1.2076474
  1.1991072  1.1867116  1.1711878  1.1533701  1.1341391  1.1143672  1.0948750  1.0764010  1.0595865  1.0449730
  1.0330086  1.0240599  1.0184242  1.0163360  1.0179646  1.0233983  1.0326143  1.0454403  1.0615152  1.0802636

CASE    2, STEP 6150, B= 0.1000000E 02, TIME=0.59934048E 02, X= 0.09252148, Y= 0.39425566, DT=0.26000000E-01
 LAMBDA=0.81099999E 01              W = PH  DISTRIBUTION
  1.1000019  1.1214358  1.1427293  1.1627448  1.1803897  1.1947031  1.2049285  1.2105654  1.2113954  1.2074840
  1.1991587  1.1869694  1.1716346  1.1539817  1.1348860  1.1152164  1.0957912  1.0773485  1.0605298  1.0458776
  1.0338415  1.0247900  1.0190224  1.0167761  1.0182239  1.0234590  1.0324655  1.0450801  1.0609524  1.0795192

CASE    2, STEP 6151, B= 0.1000000E 02, TIME=0.59960047E 02, X= 0.09520445, Y= 0.39179686, DT=0.26000000E-01
 LAMBDA=0.81099999E 01              W = PH  DISTRIBUTION
  1.0991202  1.1204459  1.1416811  1.1616921  1.1793864  1.1937992  1.2041672  1.2099807  1.2110105  1.2073112
  1.1991996  1.1872156  1.1720693  1.1545810  1.1356209  1.1160543  1.0966976  1.0782880  1.0614673  1.0467789
  1.0346738  1.0255224  1.0196259  1.0172241  1.0184935  1.0235319  1.0323304  1.0447341  1.0604039  1.0787881

CASE    2, STEP 6152, B= 0.1000000E 02, TIME=0.59986047E 02, X= 0.09737464, Y= 0.38880640, DT=0.26000000E-01
```

```
 LAMBDA=0.81099999E 01              W = PH  DISTRIBUTION
  1.0982478  1.1194628  1.1406369  1.1606408  1.1783818  1.1928916  1.2034002  1.2093885  1.2106171  1.2071291
  1.1992306  1.1874516  1.1724937  1.1551703  1.1363464  1.1168837  1.0975968  1.0792219  1.0624012  1.0476789
  1.0355073  1.0262584  1.0202354  1.0176805  1.0187734  1.0236168  1.0322080  1.0444012  1.0598678  1.0780682

CASE     2, STEP 6153, B= 0.1000000E 02, TIME=0.600120846E 02, X= 0.09896184, Y= 0.38536648, DT=0.26000000E-01
 LAMBDA=0.81099999E 01              W = PH  DISTRIBUTION
  1.0973825  1.1184841  1.1395942  1.1595879  1.1773730  1.1919777  1.2026252  1.2087873  1.2102138  1.2069369
  1.1992516  1.1876781  1.1729092  1.1557515  1.1370648  1.1177073  1.0984915  1.0801530  1.0633341  1.0485799
  1.0363439  1.0269996  1.0208522  1.0181461  1.0190641  1.0237134  1.0320979  1.0440804  1.0593428  1.0773577

CASE     2, STEP 6154, B= 0.1000000E 02, TIME=0.600380846E 02, X= 0.09991223, Y= 0.38157508, DT=0.26000000E-01
 LAMBDA=0.81099999E 01              W = PH  DISTRIBUTION
  1.0965226  1.1175077  1.1385505  1.1585309  1.1763573  1.1910547  1.2018396  1.2081746  1.2097991  1.2067336
  1.1992624  1.1878954  1.1733168  1.1563262  1.1377781  1.1185273  1.0993843  1.0810837  1.0642686  1.0494843
  1.0371858  1.0277480  1.0214779  1.0186220  1.0193663  1.0238223  1.0320002  1.0437713  1.0588281  1.0766554

CASE     2, STEP 6155, B= 0.1000000E 02, TIME=0.600640845E 02, X= 0.10018971, Y= 0.37754243, DT=0.26000000E-01
 LAMBDA=0.81099999E 01              W = PH  DISTRIBUTION
  1.0956668  1.1165316  1.1375036  1.1574673  1.1753321  1.1901198  1.2010407  1.2075481  1.2093707  1.2065176
  1.1992618  1.1881031  1.1737168  1.1568952  1.1384878  1.1193457  1.1002774  1.0820170  1.0652072  1.0503946
  1.0380354  1.0285058  1.0221144  1.0191100  1.0196813  1.0239443  1.0319152  1.0434738  1.0583253  1.0759603

CASE     2, STEP 6156, B= 0.1000000E 02, TIME=0.600900845E 02, X= 0.09977643, Y= 0.37338708, DT=0.26000000E-01
 LAMBDA=0.81099999E 01              W = PH  DISTRIBUTION
  1.0948141  1.1155547  1.1364516  1.1563947  1.1742946  1.1891704  1.2002257  1.2069051  1.2089263  1.2062869
  1.1992485  1.1883004  1.1741089  1.1574591  1.1391949  1.1201640  1.1011727  1.0829545  1.0661521  1.0513132
  1.0388950  1.0292751  1.0227637  1.0196117  1.0200107  1.0240806  1.0318439  1.0431886  1.0578284  1.0752721

CASE     2, STEP 6157, B= 0.1000000E 02, TIME=0.601160844E 02, X= 0.09867302, Y= 0.36923178, DT=0.26000000E-01
 LAMBDA=0.81099999E 01              W = PH  DISTRIBUTION
  1.0939641  1.1145760  1.1353932  1.1553113  1.1732426  1.1882036  1.1993918  1.2062427  1.2084631  1.2060390
  1.1992204  1.1884858  1.1744923  1.1580175  1.1398998  1.1209831  1.1020716  1.0838982  1.0671057  1.0522424
  1.0397669  1.0300582  1.0234281  1.0201293  1.0203563  1.0242329  1.0317876  1.0429166  1.0573440  1.0745908

CASE     2, STEP 6158, B= 0.1000000E 02, TIME=0.601420844E 02, X= 0.09689816, Y= 0.36519928, DT=0.26000000E-01
 LAMBDA=0.81099999E 01              W = PH  DISTRIBUTION
  1.0931172  1.1135952  1.1343274  1.1542158  1.1721743  1.1872173  1.1985363  1.2055580  1.2079783  1.2057713
  1.1991751  1.1886574  1.1748656  1.1585698  1.1406024  1.1218035  1.1029752  1.0848495  1.0680695  1.0531842
  1.0406534  1.0303575  1.0241098  1.0206651  1.0207202  1.0244031  1.0317480  1.0426591  1.0568711  1.0739172

CASE     2, STEP 6159, B= 0.1000000E 02, TIME=0.601680844E 02, X= 0.09448766, Y= 0.36140817, DT=0.26000000E-01
 LAMBDA=0.81099999E 01              W = PH  DISTRIBUTION
  1.0922740  1.1126124  1.1332540  1.1531070  1.1710880  1.1862093  1.1976568  1.2048483  1.2074689  1.2054807
  1.1991100  1.1888128  1.1752270  1.1591145  1.1413019  1.1226251  1.1038839  1.0858095  1.0690450  1.0541404
  1.0415565  1.0316752  1.0248113  1.0212213  1.0211048  1.0245934  1.0317271  1.0424180  1.0564114  1.0732524

CASE     2, STEP 6160, B= 0.1000000E 02, TIME=0.601940843E 02, X= 0.09149324, Y= 0.35796911, DT=0.26000000E-01
 LAMBDA=0.81099999E 01              W = PH  DISTRIBUTION
  1.0914357  1.1116285  1.1321731  1.1519847  1.1699827  1.1851780  1.1967510  1.2041110  1.2069320  1.2051643
  1.1990219  1.1889492  1.1755740  1.1596498  1.1419969  1.1234471  1.1047976  1.0867785  1.0700332  1.0551123
  1.0424780  1.0325132  1.0255345  1.0218003  1.0215123  1.0248062  1.0317272  1.0421956  1.0559666  1.0725980

CASE     2, STEP 6161, B= 0.1000000E 02, TIME=0.602200843E 02, X= 0.08798082, Y= 0.35498115, DT=0.26000000E-01
 LAMBDA=0.81099999E 01              W = PH  DISTRIBUTION
  1.0906041  1.1106447  1.1310854  1.1508489  1.1688579  1.1841222  1.1958171  1.2033435  1.2063648  1.2048190
  1.1989077  1.1890636  1.1759038  1.1601733  1.1426857  1.1242682  1.1057156  1.0877565  1.0710345  1.0561010
  1.0434191  1.0333734  1.0262817  1.0224043  1.0219454  1.0250440  1.0317510  1.0419942  1.0555393  1.0719562

CASE     2, STEP 6162, B= 0.1000000E 02, TIME=0.602460842E 02, X= 0.08402857, Y= 0.35252877, DT=0.26000000E-01
```

FIG. 42g
RUN 17
B=10 ; ΔT=.026
PH DISTRIB'S

```
LAMBDA=0.81099999E 01              W = PH  DISTRIBUTION
 1.0897814  1.1096629  1.1299923  1.1497004  1.1677136  1.1830411  1.1948536  1.2025439  1.2057646  1.2044418
 1.1987642  1.1891526  1.1762133  1.1606822  1.1433659  1.1250867  1.1066366  1.0887429  1.0720489  1.0571069
 1.0443810  1.0342571  1.0270547  1.0230354  1.0224062  1.0253093  1.0318009  1.0418166  1.0551320  1.0713293

CASE    2, STEP 6163, B= 0.1000000E 02, TIME=0.60272042E 02, X= 0.07972473, Y= 0.35067918, DT=0.26000000E-01
 LAMBDA=0.81099999E 01             W = PH  DISTRIBUTION
 1.0889703  1.1086853  1.1288957  1.1485404  1.1665503  1.1819346  1.1938596  1.2017104  1.2051291  1.2040297
 1.1985881  1.1892129  1.1764991  1.1611732  1.1440345  1.1259002  1.1075589  1.0897364  1.0730759  1.0581301
 1.0453642  1.0351656  1.0278549  1.0236957  1.0228970  1.0256047  1.0318799  1.0416655  1.0547475  1.0707204

CASE    2, STEP 6164, B= 0.1000000E 02, TIME=0.60298041E 02, X= 0.07516517, Y= 0.34949039, DT=0.26000000E-01
 LAMBDA=0.81099999E 01             W = PH  DISTRIBUTION
 1.0881736  1.1077147  1.1277977  1.1473706  1.1653691  1.1808029  1.1928347  1.2008418  1.2044564  1.2035802
 1.1983764  1.1892411  1.1767578  1.1616431  1.1446886  1.1267060  1.1084802  1.0907355  1.0741144  1.0591701
 1.0463690  1.0360994  1.0286836  1.0243867  1.0234200  1.0259325  1.0319904  1.0415440  1.0543890  1.0701322

CASE    2, STEP 6165, B= 0.1000000E 02, TIME=0.60324041E 02, X= 0.07045097, Y= 0.34895974, DT=0.26000000E-01
 LAMBDA=0.81099999E 01             W = PH  DISTRIBUTION
 1.0873945  1.1067540  1.1267011  1.1461933  1.1641717  1.1796471  1.1917789  1.1999374  1.2037448  1.2030910
 1.1981262  1.1892339  1.1769857  1.1620881  1.1453246  1.1275009  1.1093980  1.0917380  1.0751629  1.0602261
 1.0473949  1.0370589  1.0295416  1.0251099  1.0239770  1.0262950  1.0321351  1.0414547  1.0540595  1.0695682

CASE    2, STEP 6166, B= 0.1000000E 02, TIME=0.60350040E 02, X= 0.06568578, Y= 0.34912318, DT=0.26000000E-01
 LAMBDA=0.81099999E 01             W = PH  DISTRIBUTION
 1.0866364  1.1058065  1.1256090  1.1450111  1.1629601  1.1784685  1.1906928  1.1989970  1.2029934  1.2025602
 1.1978350  1.1891882  1.1771794  1.1625047  1.1459390  1.1282815  1.1103091  1.0927414  1.0762194  1.0612967
 1.0484413  1.0380439  1.0304294  1.0258661  1.0245693  1.0266941  1.0323164  1.0414006  1.0537619  1.0690314

CASE    2, STEP 6167, B= 0.1000000E 02, TIME=0.60376040E 02, X= 0.06097327, Y= 0.34995508, DT=0.26000000E-01
 LAMBDA=0.81099999E 01             W = PH  DISTRIBUTION
 1.0859027  1.1048757  1.1245246  1.1438271  1.1617370  1.1772690  1.1895777  1.1980208  1.2022015  1.2019865
 1.1975006  1.1891011  1.1773357  1.1628894  1.1465282  1.1290444  1.1112103  1.0937428  1.0772815  1.0623800
 1.0495069  1.0390539  1.0313470  1.0266560  1.0251981  1.0271315  1.0325364  1.0413842  1.0534994  1.0685252

CASE    2, STEP 6168, B= 0.1000000E 02, TIME=0.60402039E 02, X= 0.05641458, Y= 0.35141876, DT=0.26000000E-01
 LAMBDA=0.81099999E 01             W = PH  DISTRIBUTION
 1.0851966  1.1039650  1.1234514  1.1426444  1.1605050  1.1760509  1.1884351  1.1970097  1.2013692  1.2013689
 1.1971212  1.1889704  1.1774516  1.1632388  1.1470885  1.1297859  1.1120982  1.0947390  1.0783465  1.0634739
 1.0505900  1.0400876  1.0322937  1.0274796  1.0258642  1.0276084  1.0327969  1.0414076  1.0532745  1.0680525

CASE    2, STEP 6169, B= 0.1000000E 02, TIME=0.60428039E 02, X= 0.05210588, Y= 0.35345759, DT=0.26000000E-01
 LAMBDA=0.81099999E 01             W = PH  DISTRIBUTION
 1.0845214  1.1030778  1.1223929  1.1414665  1.1592675  1.1748170  1.1872672  1.1959652  1.2004971  1.2007073
 1.1966959  1.1887941  1.1775246  1.1635497  1.1476165  1.1305025  1.1129692  1.0957268  1.0794114  1.0645756
 1.0516886  1.0411437  1.0332688  1.0283366  1.0265677  1.0281256  1.0330992  1.0414729  1.0530897  1.0676163

CASE    2, STEP 6170, B= 0.1000000E 02, TIME=0.60454039E 02, X= 0.04813597, Y= 0.35599674, DT=0.26000000E-01
 LAMBDA=0.81099999E 01             W = PH  DISTRIBUTION
 1.0838802  1.1022176  1.1213526  1.1402970  1.1580279  1.1735705  1.1860766  1.1948891  1.1995862  1.2000019
 1.1962239  1.1885708  1.1775524  1.1638195  1.1481091  1.1311907  1.1138198  1.0967026  1.0804730  1.0656825
 1.0528003  1.0422201  1.0342709  1.0292262  1.0273084  1.0286835  1.0334444  1.0415816  1.0529470  1.0672191

CASE    2, STEP 6171, B= 0.1000000E 02, TIME=0.60480038E 02, X= 0.04458418, Y= 0.35894544, DT=0.26000000E-01
 LAMBDA=0.81099999E 01             W = PH  DISTRIBUTION
 1.0832756  1.1013873  1.1203340  1.1391395  1.1567897  1.1723145  1.1848661  1.1937838  1.1986383  1.1992535
 1.1957054  1.1882996  1.1775334  1.1640459  1.1485634  1.1318473  1.1146465  1.0976630  1.0815278  1.0667913
 1.0539222  1.0433146  1.0352980  1.0301471  1.0280856  1.0292820  1.0338528  1.0417346  1.0528482  1.0668632

CASE    2, STEP 6172, B= 0.1000000E 02, TIME=0.60506038E 02, X= 0.04151840, Y= 0.36219983, DT=0.26000000E-01
```

FIG. 42 h
RUN 17
B= 10; ΔT=.026
PH DISTRIB'S

```
LAMBDA=0.81099999E 01              W = PH  DISTRIBUTION
 1.0827099  1.1005900  1.1193404  1.1379975  1.1555564  1.1710526  1.1836392  1.1926522  1.1976556  1.1984638
 1.1951410  1.1879805  1.1774668  1.1642270  1.1489771  1.1324694  1.1154462  1.0986046  1.0825727  1.0678989
 1.0550515  1.0444245  1.0363481  1.0310977  1.0288982  1.0299204  1.0342644  1.0419327  1.0527944  1.0665503

CASE     2, STEP 6173, B= 0.1000000E 02, TIME=0.60532037E 02, X= 0.03899343, Y= 0.36564616, DT=0.26000000E-01
 LAMBDA=0.81099999E 01              W = PH  DISTRIBUTION
 1.0821851  1.0998280  1.1183746  1.1368742  1.1543318  1.1697885  1.1823992  1.1914974  1.1966407  1.1976345
 1.1945319  1.1876138  1.1773520  1.1643617  1.1493481  1.1330545  1.1162160  1.0995242  1.0836041  1.0690019
 1.0561849  1.0455470  1.0374186  1.0320756  1.0297444  1.0305975  1.0347387  1.0421758  1.0527861  1.0662816

CASE     2, STEP 6174, B= 0.1000000E 02, TIME=0.60558037E 02, X= 0.03704954, Y= 0.36916449, DT=0.26000000E-01
 LAMBDA=0.81099999E 01              W = PH  DISTRIBUTION
 1.0817027  1.0991034  1.1174393  1.1357729  1.1531191  1.1685258  1.1811499  1.1903228  1.1955968  1.1967685
 1.1938802  1.1872006  1.1771893  1.1644495  1.1496753  1.1336006  1.1169551  1.1004189  1.0846189  1.0700970
 1.0573192  1.0466789  1.0385066  1.0330786  1.0306222  1.0313119  1.0352545  1.0424634  1.0528237  1.0660581

CASE     2, STEP 6175, B= 0.1000000E 02, TIME=0.60584036E 02, X= 0.03571153, Y= 0.37263253, DT=0.26000000E-01
 LAMBDA=0.81099999E 01              W = PH  DISTRIBUTION
 1.0812634  1.0984178  1.1165368  1.1346962  1.1519218  1.1672681  1.1798948  1.1891322  1.1945273  1.1958686
 1.1931880  1.1867426  1.1769797  1.1644905  1.1499577  1.1341062  1.1176556  1.1012863  1.0856140  1.0711809
 1.0584511  1.0478170  1.0396089  1.0341036  1.0315290  1.0320613  1.0358103  1.0427944  1.0527065  1.0658798

CASE     2, STEP 6176, B= 0.1000000E 02, TIME=0.60610036E 02, X= 0.03498805, Y= 0.37592974, DT=0.26000000E-01
 LAMBDA=0.81099999E 01              W = PH  DISTRIBUTION
 1.0808677  1.0977722  1.1156688  1.1336467  1.1507427  1.1660187  1.1786376  1.1879294  1.1934359  1.1949382
 1.1924585  1.1862422  1.1767247  1.1644850  1.1501954  1.1345703  1.1183217  1.1021231  1.0865867  1.0722506
 1.0595771  1.0489578  1.0407224  1.0351476  1.0324621  1.0328433  1.0364040  1.0431674  1.0530338  1.0657465

CASE     2, STEP 6177, B= 0.1000000E 02, TIME=0.60636035E 02, X= 0.03487132, Y= 0.37894141, DT=0.26000000E-01
 LAMBDA=0.81099999E 01              W = PH  DISTRIBUTION
 1.0805154  1.0971674  1.1146367  1.1326265  1.1495847  1.1647811  1.1773825  1.1867181  1.1923264  1.1939812
 1.1916949  1.1857022  1.1764263  1.1644346  1.1503887  1.1349927  1.1189502  1.1029285  1.0875346  1.0733032
 1.0606942  1.0500980  1.0418435  1.0362072  1.0334181  1.0336550  1.0370332  1.0435803  1.0532039  1.0656574

CASE     2, STEP 6178, B= 0.1000000E 02, TIME=0.60662035E 02, X= 0.03533748, Y= 0.38156260, DT=0.26000000E-01
 LAMBDA=0.81099999E 01              W = PH  DISTRIBUTION
 1.0802059  1.0966033  1.1140413  1.1316370  1.1484499  1.1635580  1.1761323  1.1855023  1.1912029  1.1930013
 1.1909010  1.1851256  1.1760873  1.1643416  1.1505388  1.1353734  1.1195406  1.1037007  1.0884556  1.0743360
 1.0617994  1.0512344  1.0429689  1.0372790  1.0343939  1.0344933  1.0376948  1.0440306  1.0534149  1.0656110

CASE     2, STEP 6179, B= 0.1000000E 02, TIME=0.60688034E 02, X= 0.03634708, Y= 0.38370185, DT=0.26000000E-01
 LAMBDA=0.81099999E 01              W = PH  DISTRIBUTION
 1.0799380  1.0960794  1.1132830  1.1306795  1.1473404  1.1623521  1.1748905  1.1842856  1.1900694  1.1920027
 1.1900806  1.1845163  1.1757106  1.1642079  1.1506472  1.1357133  1.1200928  1.1044389  1.0893480  1.0753468
 1.0628898  1.0523637  1.0440951  1.0383595  1.0353859  1.0353547  1.0383859  1.0445155  1.0536645  1.0656056

CASE     2, STEP 6180, B= 0.1000000E 02, TIME=0.60714034E 02, X= 0.03784630, Y= 0.38528441, DT=0.26000000E-01
 LAMBDA=0.81099999E 01              W = PH  DISTRIBUTION
 1.0797101  1.0955950  1.1125615  1.1297545  1.1462575  1.1611658  1.1736600  1.1830715  1.1889296  1.1909895
 1.1892378  1.1838760  1.1752996  1.1640363  1.1507161  1.1360137  1.1206072  1.1051427  1.0902107  1.0763337
 1.0639631  1.0534831  1.0452190  1.0394452  1.0363905  1.0362358  1.0391030  1.0450319  1.0539500  1.0656390

CASE     2, STEP 6181, B= 0.1000000E 02, TIME=0.60740034E 02, X= 0.03976841, Y= 0.38625494, DT=0.26000000E-01
 LAMBDA=0.81099999E 01              W = PH  DISTRIBUTION
 1.0795202  1.0951486  1.1118764  1.1288625  1.1452025  1.1600007  1.1724434  1.1818632  1.1877874  1.1899657
 1.1883768  1.1832147  1.1748585  1.1638303  1.1507479  1.1362753  1.1210848  1.1058121  1.0910430  1.0772953
 1.0650170  1.0545899  1.0463374  1.0405328  1.0374041  1.0371330  1.0398427  1.0455766  1.0542683  1.0657086

CASE     2, STEP 6182, B= 0.1000000E 02, TIME=0.60766033E 02, X= 0.04203565, Y= 0.38657950, DT=0.26000000E-01
```

FIG. 42 i
RUN 17
B=10 ; ΔT=.026
PH DISTRIB's

Fig 42j
Run 17
B=10 ; ΔT=.026
PH Distrib's

```
 LAMBDA=0.81099999E 01            W = PH  DISTRIBUTION
  1.0793660  1.0947386  1.1112266  1.1280030  1.1441757  1.1588584  1.1712429  1.1806636  1.1866460  1.1889350
  1.1875015  1.1825304  1.1743904  1.1635930  1.1507455  1.1365032  1.1215268  1.1064477  1.0919445  1.0782305
  1.0660499  1.0555817  1.0474475  1.0416189  1.0384235  1.0380427  1.0406013  1.0461461  1.0546163  1.0658115

CASE    2, STEP 6183, B= 0.1000000E 02, TIME=0.60772033E 02, X= 0.04456147, Y= 0.38624673, DT=0.26000000E-01
 LAMBDA=0.81099999E 01            W = PH  DISTRIBUTION
  1.0792449  1.0943630  1.1106108  1.1271755  1.1431775  1.1577397  1.1700601  1.1794751  1.1855087  1.1879009
  1.1866159  1.1818292  1.1738996  1.1633282  1.1507121  1.1366970  1.1219351  1.1070503  1.0926154  1.0791386
  1.0670603  1.0567567  1.0485468  1.0427009  1.0394453  1.0389616  1.0413755  1.0467370  1.0549908  1.0659450

CASE    2, STEP 6184, B= 0.1000000E 02, TIME=0.60818032E 02, X= 0.04725296, Y= 0.38526825, DT=0.26000000E-01
 LAMBDA=0.81099999E 01            W = PH  DISTRIBUTION
  1.0791544  1.0940195  1.1100273  1.1263791  1.1422075  1.1566453  1.1688964  1.1782998  1.1843780  1.1868668
  1.1857234  1.1811146  1.1733896  1.1630393  1.1506507  1.1368603  1.1223116  1.1076214  1.0933563  1.0800195
  1.0680475  1.0578132  1.0496332  1.0437760  1.0404667  1.0398864  1.0421619  1.0473459  1.0553886  1.0661059

CASE    2, STEP 6185, B= 0.1000000E 02, TIME=0.60844032E 02, X= 0.05001350, Y= 0.38367813, DT=0.26000000E-01
 LAMBDA=0.81099999E 01            W = PH  DISTRIBUTION
  1.0790917  1.0937060  1.1094745  1.1256125  1.1412652  1.1555752  1.1677526  1.1771391  1.1832561  1.1858353
  1.1848271  1.1803903  1.1728641  1.1627298  1.1505647  1.1369958  1.1226586  1.1081626  1.0940682  1.0808735
  1.0690109  1.0588501  1.0507051  1.0448422  1.0414851  1.0408143  1.0429574  1.0479697  1.0558064  1.0662913

CASE    2, STEP 6186, B= 0.1000000E 02, TIME=0.60870031E 02, X= 0.05274545, Y= 0.38153163, DT=0.26000000E-01
 LAMBDA=0.81099999E 01            W = PH  DISTRIBUTION
  1.0790541  1.0934199  1.1089502  1.1248741  1.1403496  1.1545290  1.1666291  1.1759940  1.1821446  1.1848086
  1.1839299  1.1796591  1.1723265  1.1624030  1.1504570  1.1371065  1.1229785  1.1086757  1.0947521  1.0817010
  1.0699505  1.0598668  1.0517612  1.0458976  1.0424982  1.0417428  1.0437594  1.0486056  1.0562414  1.0664984

CASE    2, STEP 6187, B= 0.1000000E 02, TIME=0.60896031E 02, X= 0.05535282, Y= 0.37890309, DT=0.26000000E-01
 LAMBDA=0.81099999E 01            W = PH  DISTRIBUTION
  1.0790392  1.0931591  1.1084524  1.1241625  1.1394597  1.1535063  1.1655258  1.1748652  1.1810448  1.1837884
  1.1830339  1.1789237  1.1717790  1.1620619  1.1503307  1.1371949  1.1232738  1.1091626  1.0954096  1.0825030
  1.0708666  1.0608630  1.0528006  1.0469410  1.0435045  1.0426698  1.0445654  1.0492510  1.0566911  1.0667245

CASE    2, STEP 6188, B= 0.1000000E 02, TIME=0.60922030E 02, X= 0.05774396, Y= 0.37588321, DT=0.26000000E-01
 LAMBDA=0.81099999E 01            W = PH  DISTRIBUTION
  1.0790445  1.0929212  1.1079791  1.1234757  1.1385939  1.1525060  1.1644422  1.1737526  1.1799570  1.1827758
  1.1821406  1.1781861  1.1712246  1.1617089  1.1501884  1.1372638  1.1235467  1.1096254  1.0960425  1.0832807
  1.0717598  1.0618389  1.0538232  1.0479716  1.0445026  1.0435938  1.0453737  1.0499038  1.0571530  1.0669673

CASE    2, STEP 6189, B= 0.1000000E 02, TIME=0.60948030E 02, X= 0.05983388, Y= 0.37257583, DT=0.26000000E-01
 LAMBDA=0.81099999E 01            W = PH  DISTRIBUTION
  1.0790682  1.0927042  1.1075285  1.1228122  1.1377508  1.1515269  1.1633774  1.1726558  1.1788815  1.1817713
  1.1812511  1.1774477  1.1706648  1.1613462  1.1500322  1.1373154  1.1237995  1.1100663  1.0966523  1.0840355
  1.0726313  1.0627951  1.0548289  1.0489891  1.0454920  1.0445137  1.0461828  1.0505624  1.0576254  1.0672248

CASE    2, STEP 6190, B= 0.1000000E 02, TIME=0.60974029E 02, X= 0.06154649, Y= 0.36909430, DT=0.26000000E-01
 LAMBDA=0.81099999E 01            W = PH  DISTRIBUTION
  1.0791085  1.0925064  1.1070986  1.1221700  1.1369287  1.1505675  1.1623304  1.1715740  1.1779177  1.1807749
  1.1803656  1.1767092  1.1701008  1.1609752  1.1498640  1.1373516  1.1240342  1.1104871  1.0972410  1.0847691
  1.0734823  1.0637325  1.0558185  1.0499938  1.0464724  1.0454291  1.0469919  1.0512257  1.0581070  1.0674956

CASE    2, STEP 6191, B= 0.1000000E 02, TIME=0.61000029E 02, X= 0.06281651, Y= 0.36555759, DT=0.26000000E-01
 LAMBDA=0.81099999E 01            W = PH  DISTRIBUTION
  1.0791642  1.0923265  1.1066881  1.1215477  1.1361262  1.1496264  1.1612996  1.1705059  1.1767646  1.1797858
  1.1794840  1.1759709  1.1695333  1.1605970  1.1496852  1.1373740  1.1242526  1.1108896  1.0978103  1.0854830
  1.0743143  1.0646524  1.0567928  1.0509862  1.0474441  1.0463398  1.0478007  1.0518931  1.0585970  1.0677785

CASE    2, STEP 6192, B= 0.1000000E 02, TIME=0.61026029E 02, X= 0.06359101, Y= 0.36208636, DT=0.26000000E-01
```

```
 LAMBDA=0.81099999E 01              W = PH  DISTRIBUTION
  1.0792343  1.0921632  1.1062956  1.1209439  1.1353415  1.1487019  1.1602835  1.1694500  1.1757209  1.1788031
  1.1786054  1.1752324  1.1689621  1.1602119  1.1494964  1.1373838  1.1244560  1.1112755  1.0983620  1.0861789
  1.0751289  1.0655562  1.0577531  1.0519674  1.0484081  1.0472465  1.0486096  1.0525645  1.0590949  1.0680730

CASE     2, STEP 6193, B= 0.1000000E 02, TIME=0.61052028E 02, X= 0.06383061, Y= 0.35879900, DT=0.26000000E-01
 LAMBDA=0.81099999E 01              W = PH  DISTRIBUTION
  1.0793187  1.0920160  1.1059202  1.1203572  1.1345732  1.1477924  1.1592802  1.1684045  1.1746847  1.1778250
  1.1777285  1.1744924  1.1683866  1.1598197  1.1492979  1.1373816  1.1246456  1.1116461  1.0988976  1.0868586
  1.0759278  1.0664457  1.0587011  1.0529389  1.0493654  1.0481501  1.0494191  1.0532405  1.0596010  1.0683789

CASE     2, STEP 6194, B= 0.1000000E 02, TIME=0.61078028E 02, X= 0.06351030, Y= 0.35580792, DT=0.26000000E-01
 LAMBDA=0.81099999E 01              W = PH  DISTRIBUTION
  1.0794172  1.0918846  1.1055612  1.1197867  1.1338201  1.1468962  1.1582880  1.1673674  1.1736541  1.1768495
  1.1768514  1.1737496  1.1678056  1.1594197  1.1490894  1.1373675  1.1248218  1.1120024  1.0994183  1.0875236
  1.0767128  1.0673226  1.0596386  1.0539024  1.0503178  1.0490521  1.0502306  1.0539220  1.0601160  1.0686967

CASE     2, STEP 6195, B= 0.1000000E 02, TIME=0.61104027? 02, X= 0.06261991, Y= 0.35321597, DT=0.26000000E-01
 LAMBDA=0.81099999E 01              W = PH  DISTRIBUTION
  1.0795305  1.0917691  1.1052184  1.1192317  1.1330811  1.1460118  1.1573050  1.1663365  1.1726267  1.1758744
  1.1759718  1.1730018  1.1672175  1.1590105  1.1488702  1.1373414  1.1249849  1.1123451  1.0999254  1.0881754
  1.0774855  1.0681888  1.0605675  1.0548599  1.0512671  1.0499544  1.0510458  1.0546105  1.0606412  1.0690273

CASE     2, STEP 6196, B= 0.1000000E 02, TIME=0.61130027E 02, X= 0.06116415, Y= 0.35111341, DT=0.26000000E-01
 LAMBDA=0.81099999E 01              W = PH  DISTRIBUTION
  1.0796595  1.0916701  1.1048919  1.1186920  1.1323552  1.1451381  1.1563295  1.1653098  1.1716003  1.1748970
  1.1750872  1.1722465  1.1666200  1.1585904  1.1486387  1.1373022  1.1251348  1.1126744  1.1004195  1.0888152
  1.0782476  1.0690463  1.0614898  1.0558135  1.0522156  1.0508590  1.0518665  1.0553078  1.0611780  1.0693719

CASE     2, STEP 6197, B= 0.1000000E 02, TIME=0.61156026E 02, X= 0.05916232, Y= 0.34957511, DT=0.26000000E-01
 LAMBDA=0.81099999E 01              W = PH  DISTRIBUTION
  1.0798055  1.0915884  1.1045821  1.1181675  1.1316420  1.1442737  1.1553597  1.1642851  1.1705722  1.1739147
  1.1741949  1.1714812  1.1660105  1.1581571  1.1483934  1.1372490  1.1252706  1.1129903  1.1009013  1.0894440
  1.0790005  1.0698967  1.0624077  1.0567656  1.0531656  1.0517683  1.0526952  1.0560161  1.0617285  1.0697322

CASE     2, STEP 6198, B= 0.1000000E 02, TIME=0.61182026E 02, X= 0.05664767, Y= 0.34865838, DT=0.26000000E-01
 LAMBDA=0.81099999E 01              W = PH  DISTRIBUTION
  1.0799703  1.0915255  1.1042899  1.1176581  1.1309410  1.1434179  1.1543944  1.1632606  1.1695401  1.1729247
  1.1732917  1.1707027  1.1653863  1.1577081  1.1481321  1.1371800  1.1253914  1.1132924  1.1013708  1.0900624
  1.0797454  1.0707418  1.0633231  1.0577183  1.0541195  1.0526849  1.0535344  1.0567378  1.0622948  1.0701103

CASE     2, STEP 6199, B= 0.1000000E 02, TIME=0.61208025E 02, X= 0.05366646, Y= 0.34840122, DT=0.26000000E-01
 LAMBDA=0.81099999E 01              W = PH  DISTRIBUTION
  1.0801556  1.0914828  1.1040164  1.1171648  1.1302524  1.1425700  1.1534321  1.1622343  1.1685017  1.1719244
  1.1723750  1.1699081  1.1647444  1.1572407  1.1478525  1.1370933  1.1254959  1.1135799  1.1018279  1.0906711
  1.0804834  1.0715830  1.0642380  1.0586738  1.0550797  1.0536112  1.0543866  1.0574754  1.0628795  1.0705083

CASE     2, STEP 6200, B= 0.1000000E 02, TIME=0.61234025E 02, X= 0.05027673, Y= 0.34882125, DT=0.26000000E-01
 LAMBDA=0.81099999E 01              W = PH  DISTRIBUTION
  1.0803638  1.0914621  1.1037630  1.1166884  1.1295764  1.1417298  1.1524722  1.1612043  1.1674550  1.1709112
  1.1714416  1.1690943  1.1640817  1.1567519  1.1475517  1.1369867  1.1255823  1.1138518  1.1022722  1.0912700
  1.0812150  1.0724214  1.0651539  1.0596342  1.0560486  1.0545498  1.0552544  1.0582316  1.0634850  1.0709287

CASE     2, STEP 6201, B= 0.1000000E 02, TIME=0.61260024E 02, X= 0.04654671, Y= 0.34991510, DT=0.26000000E-01
 LAMBDA=0.81099999E 01              W = PH  DISTRIBUTION
  1.0805970  1.0914654  1.1035312  1.1162300  1.1289137  1.1408972  1.1515138  1.1601708  1.1663980  1.1698829
  1.1704891  1.1682585  1.1633952  1.1562388  1.1472273  1.1368579  1.1256488  1.1141066  1.1027029  1.0918591
  1.0819407  1.0732582  1.0660722  1.0606013  1.0570282  1.0555030  1.0561403  1.0590090  1.0641140  1.0713739

CASF     2, STEP 6202, B= 0.1000000E 02, TIME=0.61286024E 02, X= 0.04255319, Y= 0.35165851, DT=0.26000000E-01
```

FIG. 42k
RUN 17
B=10; ΔT=.026
PH DISTRIB'S

CASE NUMBER 2, B= 0.09999999E 02

STEP	X	Y	DX/DT	DY/DT		STEP	X	Y	DX/DT	DY/DT
6100	0.0508191	0.3976069	0.3150345E-01	0.2334129E-01	**	6150	0.0925215	0.3942557	0.1176464E-00	-0.7167983E-01
6101	0.0524456	0.3987754	0.6255902E-01	0.4494296E-01	**	5151	0.0952045	0.3917969	0.1031909E-00	-0.9456887E-01
6102	0.0548455	0.4004407	0.9230326E-01	0.6404877E-01	**	6152	0.0973746	0.3888064	0.8346905E-01	-0.1150177E-00
6103	0.0579631	0.4025202	0.1199068E-00	0.7998167E-01	**	6153	0.0989618	0.3853665	0.6104590E-01	-0.1323046E-00
6104	0.0617226	0.4049165	0.1445952E-00	0.9216484E-01	**	6154	0.0999122	0.3815751	0.3655388E-01	-0.1458231E-00
6105	0.0660300	0.4075201	0.1656697E-00	0.1001411E-00	**	6155	0.1001897	0.3775424	0.1067198E-01	-0.1551020E-00
6106	0.0707756	0.4102135	0.1825258E-00	0.1035901E-00	**	6156	0.0997764	0.3733871	-0.1589526E-01	-0.1598211E-00
6107	0.0758371	0.4128744	0.1946717E-00	0.1023426E-00	**	6157	0.0986730	0.3692318	-0.4243862E-01	-0.1598191E-00
6108	0.0810824	0.4153805	0.2017431E-00	0.9639086E-01	**	6158	0.0968982	0.3651993	-0.6826414E-01	-0.1550964E-00
6109	0.0863738	0.4176138	0.2035164E-00	0.8589496E-01	**	6159	0.0944877	0.3614082	-0.9271144E-01	-0.1458114E-00
6110	0.0915717	0.4194646	0.1999184E-00	0.7118288E-01	**	6160	0.0914932	0.3579691	-0.1151700E-00	-0.1322717E-00
6111	0.0965385	0.4208359	0.1910312E-00	0.5274460E-01	**	6161	0.0879808	0.3549812	-0.1350931E-00	-0.1149211E-00
6112	0.1011430	0.4216476	0.1770929E-00	0.3121878E-01	**	6162	0.0840286	0.3525288	-0.1520094E-00	-0.9432249E-01
6113	0.1052638	0.4218393	0.1584928E-00	0.7372274E-02	**	6163	0.0797247	0.3506792	-0.1655325E-00	-0.7113800E-01
6114	0.1087935	0.4213732	0.1357608E-00	-0.1792776E-01	**	6164	0.0751652	0.3494804	-0.1753674E-00	-0.4610744E-01
6115	0.1116419	0.4202357	0.1095514E-00	-0.4374767E-01	**	6165	0.0704510	0.3489597	-0.1813155E-00	-0.2002473E-01
6116	0.1137381	0.4184384	0.8062195E-01	-0.6912580E-01	**	6166	0.0656858	0.3491232	-0.1832767E-00	0.6286275E-02
6117	0.1150330	0.4160175	0.4980740E-01	-0.9311333E-01	**	6167	0.0609733	0.3499551	-0.1812504E-00	0.3199633E-01
6118	0.1155008	0.4130323	0.1799136E-01	-0.1148150E-00	**	6168	0.0564146	0.3514188	-0.1753340E-00	0.5629540E-01
6119	0.1151388	0.4095632	-0.1392397E-01	-0.1334272E-00	**	6169	0.0521059	0.3534576	-0.1657195E-00	0.7841665E-01
6120	0.1139676	0.4057081	-0.4504786E-01	-0.1482708E-00	**	6170	0.0481360	0.3559967	-0.1526889E-00	0.9765957E-01
6121	0.1120298	0.4015789	-0.7452939E-01	-0.1588172E-00	**	6171	0.0445842	0.3589454	-0.1366073E-00	0.1134117E-00
6122	0.1093886	0.3972965	-0.1015829E-00	-0.1647066E-00	**	6172	0.0415184	0.3621998	-0.1179144E-00	0.1251687E-00
6123	0.1061254	0.3929668	-0.1255098E-00	-0.1657575E-00	**	6173	0.0389934	0.3656462	-0.9711449E-01	0.1325514E-00
6124	0.1023368	0.3887756	-0.1457156E-00	-0.1619681E-00	**	6174	0.0370495	0.3691645	-0.7476475E-01	0.1353203E-00
6125	0.0981320	0.3847844	-0.1617230E-00	-0.1535106E-00	**	6175	0.0357115	0.3726325	-0.5146171E-01	0.1333861E-00
6126	0.0936293	0.3811257	-0.1731803E-00	-0.1407187E-00	**	6176	0.0349880	0.3759297	-0.2792653E-01	0.1268159E-00
6127	0.0889528	0.3778998	-0.1798661E-00	-0.1240706E-00	**	6177	0.0348713	0.3789414	-0.4489086E-02	0.1158335E-00
6128	0.0842288	0.3751915	-0.1816899E-00	-0.1041678E-00	**	6178	0.0353375	0.3815626	0.1792889E-01	0.1008152E-00
6129	0.0795829	0.3730670	-0.1786909E-00	-0.8171171E-01	**	6179	0.0363471	0.3837018	0.3883086E-01	0.8227889E-01
6130	0.0751360	0.3715725	-0.1710321E-00	-0.5747809E-01	**	6180	0.0378463	0.3852844	0.5766238E-01	0.6086781E-01
6131	0.0710022	0.3707330	-0.1589942E-00	-0.3229141E-01	**	6181	0.0397684	0.3862549	0.7392718E-01	0.3732823E-01
6132	0.0672850	0.3705510	-0.1429662E-00	-0.6998276E-02	**	6182	0.0420356	0.3865795	0.8720158E-01	0.1248301E-01
6133	0.0640758	0.3710075	-0.1234343E-00	0.1755835E-01	**	6183	0.0445615	0.3862467	0.9714688E-01	-0.1279874E-01
6134	0.0614505	0.3720622	-0.1009695E-00	0.4056432E-01	**	6184	0.0472530	0.3852682	0.1035189E-00	-0.3763388E-01
6135	0.0594690	0.3736549	-0.7621336E-01	0.6125847E-01	**	6185	0.0500135	0.3836781	0.1061746E-00	-0.6115810E-01
6136	0.0581726	0.3757077	-0.4986258E-01	0.7895516E-01	**	6186	0.0527454	0.3815316	0.1050747E-00	-0.8255754E-01
6137	0.0575836	0.3781274	-0.2265181E-01	0.9306512E-01	**	6187	0.0553528	0.3789031	0.1002839E-00	-0.1010979E-00
6138	0.0577049	0.3808084	0.4664102E-02	0.1031139E-00	**	6188	0.0577440	0.3758832	0.9196681E-01	-0.1161493E-00
6139	0.0585194	0.3836361	0.3132906E-01	0.1087580E-00	**	6189	0.0598339	0.3725758	0.8038134E-01	-0.1272068E-00
6140	0.0599912	0.3864908	0.5660511E-01	0.1097968E-00	**	6190	0.0615465	0.3690943	0.6586971E-01	-0.1339049E-00
6141	0.0620658	0.3892515	0.7979201E-01	0.1061822E-00	**	6191	0.0628165	0.3655576	0.4884704E-01	-0.1360270E-00
6142	0.0646722	0.3918001	0.1002464E-00	0.9802235E-01	**	6192	0.0635910	0.3620864	0.2978845E-01	-0.1335088E-00
6143	0.0677246	0.3940252	0.1174002E-00	0.8558146E-01	**	6193	0.0638306	0.3587990	0.9215289E-02	-0.1264366E-00
6144	0.0711248	0.3958264	0.1307773E-00	0.6927388E-01	**	6194	0.0635103	0.3558079	-0.1231945E-01	-0.1150419E-00
6145	0.0747650	0.3971173	0.1400081E-00	0.4965255E-01	**	6195	0.0626199	0.3532160	-0.3424572E-01	-0.9969010E-01
6146	0.0785309	0.3978295	0.1448413E-00	0.2739196E-01	**	6196	0.0611641	0.3511134	-0.5599087E-01	-0.8086763E-01
6147	0.0823048	0.3979144	0.1451520E-00	0.3265699E-02	**	6197	0.0591623	0.3495751	-0.7699360E-01	-0.5916514E-01
6148	0.0859694	0.3973455	0.1409453E-00	-0.2188077E-01	**	6198	0.0566477	0.3486584	-0.9671716E-01	-0.3525892E-01
6149	0.0894107	0.3961193	0.1323567E-00	-0.4716084E-01	**	6199	0.0536665	0.3484012	-0.1146616E-00	-0.9890512E-02

FIG. 43
RUN 17
B=10; ΔT=.026
ORBIT
COÖRDINATES

Fig. 44
Run 17
B = 10; $\Delta T = 0.026$
400 Steps

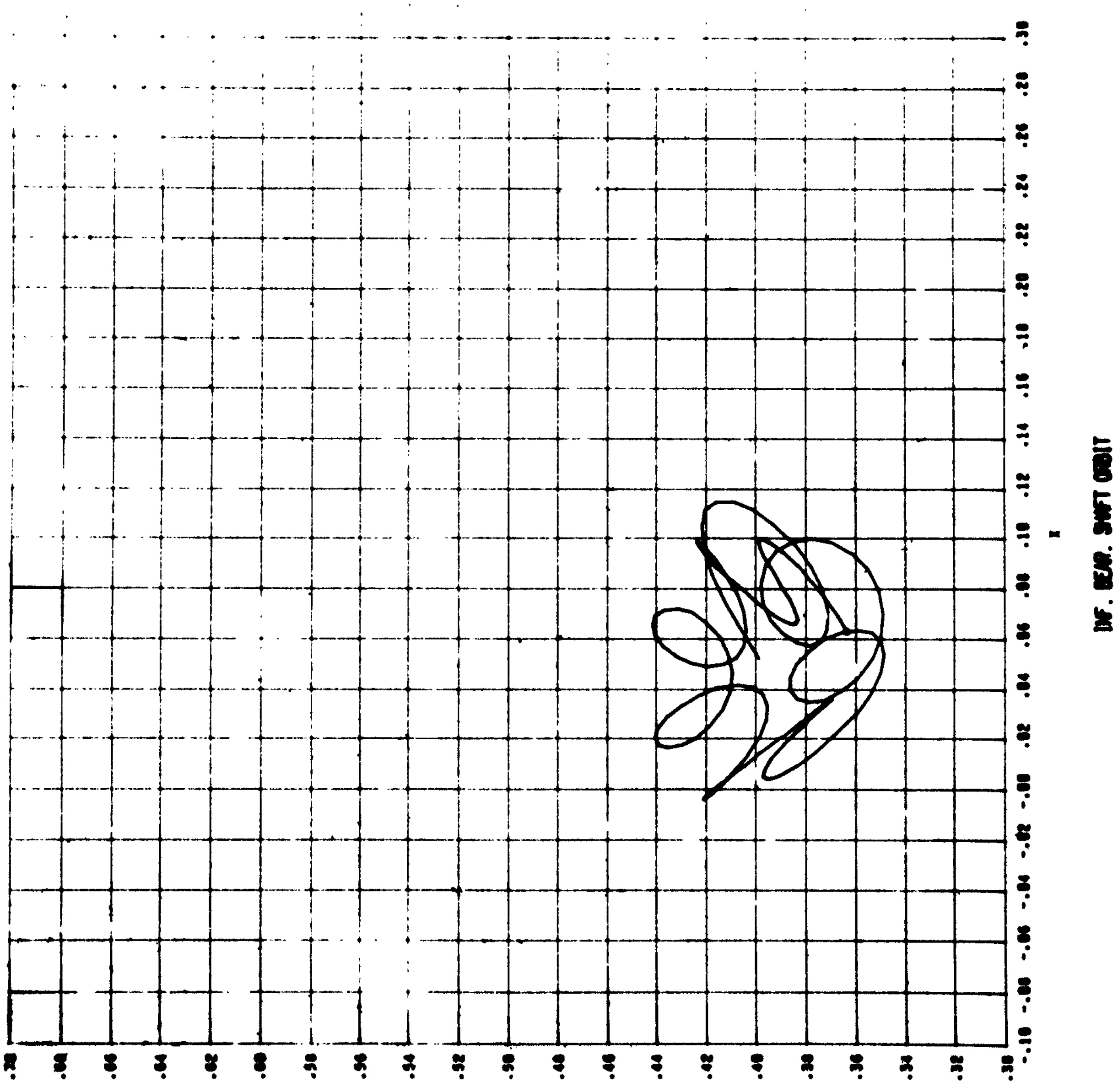

APPENDIX I

DERIVATION OF LUBRICATION EQUATIONS

Let u, v, w be the velocity $\vec{V}$ component in the α, β, γ directions respectively. Then the equation of continuity is

$$\frac{\partial \rho}{\partial t} + \nabla \cdot \rho \vec{V} = 0 \qquad \text{(I-1)}$$

The Naviet-Stokes equations for a Newtonian fluid are

$$\rho \frac{Du}{Dt} = -\frac{\partial p}{\partial \alpha} + \frac{\partial}{\partial \alpha}\left[\mu\left(2\frac{\partial u}{\partial \alpha} - \frac{2}{3}\nabla \cdot \vec{V}\right)\right] + $$

$$+ \frac{\partial}{\partial \beta}\left[\mu\left(\frac{\partial u}{\partial \beta} + \frac{\partial v}{\partial \alpha}\right)\right] + \frac{\partial}{\partial \gamma}\left[\mu\left(\frac{\partial w}{\partial \alpha} + \frac{\partial u}{\partial \gamma}\right)\right], \qquad \text{(I-2)}$$

$$\rho \frac{Dv}{Dt} = -\frac{\partial p}{\partial \beta} + \frac{\partial}{\partial \beta}\left[\mu\left(2\frac{\partial v}{\partial \gamma} - \frac{2}{3}\nabla \cdot \vec{V}\right)\right] + $$

$$+ \frac{\partial}{\partial \alpha}\left[\mu\left(\frac{\partial v}{\partial \gamma} + \frac{\partial w}{\partial \beta}\right)\right] + \frac{\partial}{\partial \alpha}\left[\mu\left(\frac{\partial u}{\partial \beta} + \frac{\partial v}{\partial \alpha}\right)\right], \qquad \text{(I-3)}$$

$$\rho \frac{Dw}{Dt} = -\frac{\partial p}{\partial \alpha} + \frac{\partial}{\partial \alpha}\left[\mu\left(2\frac{\partial w}{\partial \gamma} - \frac{2}{3}\nabla \cdot \vec{V}\right)\right] + $$

$$+ \frac{\partial}{\partial \alpha}\left[\mu\left(\frac{\partial w}{\partial \alpha} + \frac{\partial u}{\partial \gamma}\right)\right] + \frac{\partial}{\partial \beta}\left[\mu\left(\frac{\partial w}{\partial \beta} + \frac{\partial v}{\partial \gamma}\right)\right]. \qquad \text{(I-4)}$$

With the assumption of a perfect gas the equation of state is

$$p = \rho R T_1 \qquad \text{(I-5)}$$

where R is the gas constant and T_1 the absolute temperature.

Assuming an isothermal film

$$T_1 = \text{const.}$$

and the energy equation reduces to

$$p \;\alpha\; \rho \qquad \text{(I-6)}$$

For very thin films fully developed laminar flow exists in the bearing gap. Components of velocity normal to the bearing surface (w) can be neglected with respect to the horizontal component because the ratio W/u is of the same order as the angle between the bearing and journal surfaces. Observing that variations of velocity in the γ-direction are of order U/δ and U/δ^2, and are of larger magnitude than variations in other directions, we have from I-2, 3, 4:

$$\rho\left(\frac{\partial u}{\partial t} + u\frac{\partial u}{\partial \alpha} + v\frac{\partial u}{\partial \beta}\right) = -\frac{\partial p}{\partial \alpha} + \frac{\partial}{\partial \gamma}\,\mu\,\frac{\partial u}{\partial \gamma}, \qquad \text{(I-7)}$$

$$\rho\left(\frac{\partial v}{\partial t} + u\frac{\partial v}{\partial \alpha} + v\frac{\partial v}{\partial \beta}\right) = -\frac{\partial p}{\partial \beta} + \frac{\partial}{\partial \gamma}\,\mu\,\frac{\partial v}{\partial \gamma}, \qquad \text{(I-8)}$$

$$0 = \frac{\partial p}{\partial \gamma} \qquad \text{(I-9)}$$

The left-hand sides of these equations represent the acceleration terms which can generally be neglected in comparison to the viscous forces since their ratio is

a) Convective Terms

$$\frac{\text{Inertia Forces}}{\text{Viscous Forces}} \approx \frac{\rho\,\dfrac{R^2 c\ U}{R/U}}{\mu\,\dfrac{U}{c}\,R^2} = \frac{\rho\ U\ c^2}{\mu R} = \frac{\rho\ U\ R}{\mu}\left(\frac{c}{R}\right)^2$$

This ratio is much lower than unity in most normal applications.

b) Fluctuation Terms

$$\frac{\text{Inertia Force}}{\text{Viscous Force}} \simeq \frac{\rho\,U'\,\omega_1}{\mu\,\dfrac{U\,R^2}{c}} = \frac{U'}{U}\,\frac{c}{\nu R^2}\quad\omega_1$$

Using commonly net values, frequencies higher than 10^3 and full amplitude ($u^1 = v$) fluctuations are needed to make this ratio of order unity.

Then the Navier-Stokes equations reduce to:

$$\frac{\partial p}{\partial \alpha} = \frac{\partial}{\partial \gamma}\left(\mu\,\frac{\partial u}{\partial \gamma}\right), \qquad \text{(I-10)}$$

$$\frac{\partial p}{\partial \beta} = \frac{\partial}{\partial \xi}\left(\mu\,\frac{\partial v}{\partial \gamma}\right), \qquad \text{(I-11)}$$

$$\frac{\partial p}{\partial \gamma} = 0 \qquad \text{(I-12)}$$

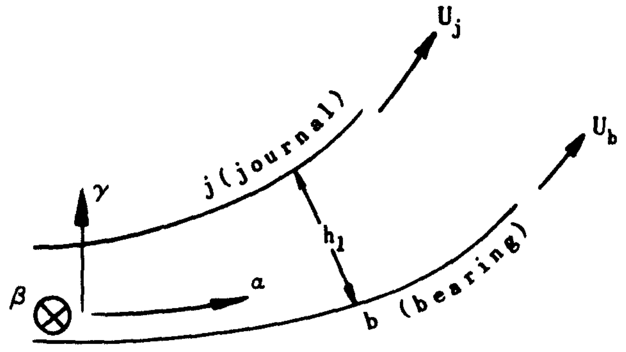

Integrating the equations of motion, we get:

$$u = \frac{1}{2\mu}\frac{\partial p}{\partial \alpha}\gamma(\gamma - h_1) + \frac{h_1 - \gamma}{h_1} U_b + \frac{\gamma}{h_1} U_j \tag{I-13}$$

$$v = \frac{1}{2\mu}\frac{\partial p}{\partial \beta}\gamma(\gamma - h_1) \tag{I-14}$$

From the equation of continuity, there results:

$$\frac{\partial(\rho w)}{\partial \gamma} = -\frac{\partial \rho}{\partial t} - \frac{\partial(\rho u)}{\partial \alpha} - \frac{\partial(\rho v)}{\partial \beta} = -\frac{\partial \rho}{\partial t} - \frac{1}{2}\left\{\frac{\partial}{\partial \alpha}\left[\frac{\rho}{\mu}\frac{\partial p}{\partial \alpha}(\gamma - h_1)\gamma\right] + \right.$$

$$\left. + \frac{\partial}{\partial \beta}\left[\frac{\rho}{\mu}\frac{\partial p}{\partial \beta}(\gamma - h_1)\gamma\right]\right\} + - \frac{\partial}{\partial \alpha}\left\{\left[\rho\frac{(h_1 - \gamma)}{h_1}U_b\right] + \frac{\rho\gamma U_j}{h_1}\right\} \tag{I-15}$$

Integration over the clearance h_1 and use of the boundary condition of no slip, gives:

$$\int_0^h \frac{\partial(\rho w)}{\partial \gamma} d\gamma = -h\frac{\partial \rho}{\partial t} + \frac{1}{2}\left[\frac{\partial}{\partial \alpha}\left(\frac{\rho h_1^3}{6\mu}\frac{\partial p}{\partial \alpha}\right) + \frac{\partial}{\partial \beta}\left(\frac{\rho h_1^3}{6\mu}\frac{\partial p}{\partial \beta}\right)\right] +$$

$$- \frac{1}{2}\frac{\partial}{\partial \alpha}(\rho h U_b) - \left\{\frac{1}{2}\frac{\partial}{\partial \alpha}(\rho h_1 U_j) - \rho U_j \frac{\partial h_1}{\partial \alpha}\right\} \tag{I-16}$$

or:

$$\frac{\partial}{\partial \alpha}\left(\frac{\rho h_1^3}{\mu}\frac{\partial}{\partial \alpha}p\right) + \frac{\partial}{\partial \beta}\left(\frac{\rho h_1^3}{\mu}\frac{\partial p}{\partial \beta}\right) = 6\left\{2h_1\frac{\partial p}{\partial t} + 2\rho(w_j - w_b) + \right.$$

$$\left. - \rho(u_j - u_b)\frac{\partial h}{\partial \alpha} + h\frac{\partial}{\partial \alpha}(\rho[u_j + u_b])\right\} \tag{I-17}$$

Now, if Ω denotes angular velocity:

$$u_b = R\,\Omega_b$$

$$\omega_b = 0$$

$$u_j = R\,\Omega_j - \frac{\partial}{\partial t}\,\frac{\partial h_1}{\partial \theta}$$

$$\omega_j = R\,\Omega_j\,\frac{\partial h_1}{\partial \alpha} + \frac{\partial h_1}{\partial T} \qquad \text{(I-18)}$$

Then the right hand side of (I-17) becomes

$$\begin{aligned}
6 \Bigg\{ & 2\,h_1\,\frac{\partial \rho}{\partial t} + 2\,\rho \left[R\,\Omega_j\,\frac{\partial h_1}{\partial \alpha} + \frac{\partial h_1}{\partial t} \right] + \\
& - \rho \left(R\,\Omega_j - \frac{\partial}{\partial t}\,\frac{\partial h_1}{\partial \theta} - R\,\Omega_b \right) \frac{\partial h_1}{\partial \alpha} + \\
& + h_1 \left(R\,[\Omega_j + \Omega_b] - \frac{\partial}{\partial t}\,\frac{\partial h}{\partial \theta} \right) \frac{\partial \rho}{\partial \alpha} + \\
& + h_1\,\rho\,\frac{\partial}{\partial \alpha} \left(- \frac{\partial}{\partial t}\,\frac{\partial h_1}{\partial \theta} \right) \Bigg\} = \rho\,R(\Omega_j + \Omega_b)\,\frac{\partial h_1}{\partial \alpha} + \\
& + h_1\,R(\Omega_j + \Omega_b)\,\frac{\partial \rho}{\partial \alpha} + 2 h_1\,\frac{\partial \rho}{\partial t} + 2\rho\,\frac{\partial h_1}{\partial t} + \rho\,\frac{\partial}{\partial t} \left(\frac{\partial h_1}{\partial \theta} \right) \cdot \frac{\partial h_1}{\partial \alpha} - \\
& - h_1\,\frac{\partial}{\partial t} \left(\frac{\partial h_1}{\partial \theta} \right) \cdot \frac{\partial \rho}{\partial \alpha} - h_1\,\rho\,\frac{\partial}{\partial \alpha}\,\frac{\partial}{\partial t}\,\frac{\partial h_1}{\partial \theta}
\end{aligned} \qquad \text{(I-19)}$$

But

$$\frac{\dfrac{\partial}{\partial t}\,\dfrac{\partial h_1}{\partial \theta}}{R(\Omega_j + \Omega_b)} = \frac{\dot{x}_1 \cos\theta - \dot{y}_1 \sin\theta}{R(\Omega_j + \Omega_b)} = 0\left(\frac{C}{R}\right) \qquad \text{(I-20)}$$

and

$$\frac{\dot{h}_1\,\dfrac{\partial}{\partial \alpha}\,\dfrac{\partial}{\partial t}\,\dfrac{\partial h_1}{\partial \theta}}{2\dfrac{\partial h_1}{\partial t}} = \frac{h_1}{R}\,\frac{(-\,\dot{x}_1 \sin\theta - \dot{y}_1 \cos\theta)}{2\,\dot{h}_1} = -\,\frac{h_1}{2R} \qquad \text{(I-21)}$$

Then, letting $\alpha = R\theta$, and neglecting terms of order $\frac{c}{R}$, we obtain

$$\frac{1}{R^2}\frac{\partial}{\partial\theta}\left(\rho\, h_1{}^3\frac{\partial p}{\partial\theta}\right)+\frac{\partial}{\partial\beta}\left(\rho\, h_1{}^3\frac{\partial p}{\partial\beta}\right)=$$

$$=6\mu(\Omega_j+\Omega_b)\left\{\frac{2}{(\Omega_j+\Omega_b)}\frac{\partial(\rho\, h_1)}{\partial t}+\frac{\partial(\rho\, h_1)}{\partial\theta}\right\} \tag{I-22}$$

where $\omega_b + \omega_j$ can be replaced by Ω

APPENDIX II

DERIVATION OF EXPRESSION FOR FRICTIONAL FORCES

From Appendix I we have:

$$u = \frac{1}{2\mu R}\frac{\partial p}{\partial \theta}\gamma(\gamma - h_1) + \frac{(h_1 - \gamma)}{h_1}U_b + \frac{\gamma}{h_1}U_j \tag{II-1}$$

Therefore,

$$S_f = \mu\frac{\partial u}{\partial \gamma}\Bigg|_{\gamma = h_1} \tag{II-2}$$

becomes:

$$S_f = \frac{cHP_a}{2R}\frac{\partial p}{\partial \theta} + \frac{\mu R\Omega}{cH} + \mu\frac{\frac{\partial \dot{H}}{\partial \theta}}{H} \tag{II-3}$$

Then

$$K_x = \int_o^{2\pi} S_f R\cos\theta\, d\theta;\quad Ky = -\int_o^{2\pi} S_f R\sin\theta\, d\theta \tag{II-4}$$

Using the complete expression for S, we get:

$$K_x = \oint \frac{h_1}{2}\frac{\partial p}{\partial \theta}\cos\theta\, d\theta + \oint \frac{\mu R^2\Omega}{h_1}\cos\theta\, d\theta +$$

$$+ \oint \frac{\mu Rc}{h_1}[\dot{Y}\sin\theta - \dot{X}\cos\theta]\cos\theta\, d\theta = I_1 + I_2 + I_3 + I_4 \tag{II-5}$$

Let us evaluate the integrals in (5) one at the time using $H = 1 - x\sin\theta + y\cos\theta = 1 + \epsilon\cos(\theta - \theta_1)$

$$I_1 = \frac{1}{2}\oint h_1 p'\cos\theta\, d\theta = \frac{1}{2}\oint \frac{\partial}{\partial \theta}(ph_1\cos\theta)\, d\theta +$$

$$- \frac{1}{2}\oint ph_1'\cos\theta\, d\theta + \frac{1}{2}\oint ph\sin\theta\, d\theta =$$

$$= \frac{1}{2}[ph\cos\theta]\Big|_o^{2\pi} - \frac{1}{2}\oint pc[X\cos\theta - Y\sin\theta]\cos\theta\, d\theta +$$

$$+ \frac{1}{2}\oint cp[1 + X\sin\theta + Y\cos\theta]\sin\theta\, d\theta =$$

$$I_1 = \frac{c}{2}\oint p\sin\theta\, d\theta - \frac{c}{2}\oint p[X\cos 2\theta - Y\sin 2\theta]\, d\theta \tag{II-6}$$

$$I_2 = \mu\Omega R^2 \oint \frac{\cos\theta}{h_1} d\theta = \frac{\mu\Omega R^2}{\epsilon\, c \cos\theta_1} \oint \frac{\cos\theta\cos\theta_1}{1 + \epsilon\cos(\theta - \theta_1)} d\theta =$$

$$= \frac{\mu\Omega R^2}{\epsilon\, c\cos\theta_1}\left[\oint \frac{\cos(\theta - \theta_1)}{1 + \epsilon\cos(\theta - \theta_1)} d\theta - \oint \frac{\epsilon\sin\theta\sin\theta_1}{1 + \epsilon\cos(\theta - \theta_1)} d\theta\right] =$$

$$= \frac{\mu\Omega R^2}{\epsilon\, c\cos\theta_1}\left\{\oint \frac{\epsilon\cos(\theta - \theta_1)}{1 + \epsilon\cos(\theta - \theta_1)} d(\theta - \theta_1) + \right.$$

$$- \tan\theta_1 \left[\oint \frac{\epsilon\sin(\theta - \theta_1)}{1 + \epsilon\cos(\theta - \theta_1)} d(\theta - \theta_1) + \right.$$

$$\left.\left. + \oint \frac{\epsilon\cos\theta\sin\theta_1}{1 + \epsilon\cos(\theta - \theta_1)} d\theta\right]\right\}$$

Bringing the last term to the left hand side, we have:

$$\frac{\mu R\,\Omega}{c}\left[\oint \frac{\cos\theta}{1 + \epsilon\cos(\theta - \theta_1)} d\theta\right][1 + \tan^2 Q_1] =$$

$$= \frac{\mu\Omega R^2}{\epsilon\, c\cos\theta_1}\left[\oint \frac{\epsilon\cos(\theta - \theta_1)}{1 + \epsilon\cos(\theta - \theta_1)} d(\theta - \theta_1)\right] -$$

$$- \tan\theta_1 \oint \frac{\epsilon\sin(\theta - \theta_1)}{1 + \epsilon\cos(\theta - \theta_1)} d(\theta - \theta_1)$$

Therefore:

$$I_2 = \frac{\mu\Omega R^2}{\epsilon c}\cos\theta_1\left[\oint d\theta - \oint \frac{d\theta}{1 + \epsilon\cos(\theta - \theta_1)} + \right.$$

$$\left. + \tan\theta_1 \oint d\ln[1 + \epsilon\cos(\theta - \theta_1)]\right] = \frac{\mu\Omega R^2}{\epsilon c}\cos\theta_1$$

$$\left\{\left[2\pi - \frac{2\pi}{\sqrt{1 - \epsilon^2}}\right] + \tan\theta\,[\ln[1 + \epsilon\cos(\theta - \theta_1)]]_o^{2\pi}\right\} =$$

$$I_2 = \frac{2\pi\,\mu\Omega R^2}{\epsilon\, c}\left[1 - \frac{1}{\sqrt{1 - \epsilon^2}}\right] Y. \tag{II-7}$$

$$I_3 = R\mu\oint\dot{Y} \frac{\sin\theta\cos\theta}{1 + \epsilon\cos(\theta - \theta_1)} d\theta =$$

$$= \mu\frac{R}{2}\dot{Y}\oint \frac{\sin 2\theta}{1 + \epsilon\cos(\theta - \theta_1)} d\theta =$$

$$= \frac{R\mu\dot{Y}}{2}\oint \frac{\sin 2(\xi + Q_1)}{1 + \epsilon\cos\xi} d\xi$$

where

$$\xi = \theta - \theta_1$$

$$I_3 = \mu R\dot{Y}\left[\cos 2\theta_1 \oint \frac{\sin\xi\cos\xi}{1 + \epsilon\cos\xi} d\xi + \right.$$

$$\left. + \frac{\sin 2\theta_1}{2}\oint \frac{\cos^2\xi - \sin^2\xi}{1 + \epsilon\cos\xi} d\xi\right]$$

But

$$\int_{-\theta_1}^{2\pi - \theta_1} \frac{\sin\xi\cos\xi}{1 + \epsilon\cos\xi} d\xi = 0$$

because if

$$\frac{\sin\xi\cos\xi}{1 + \epsilon\cos\xi} = f_1(\xi)$$

$$f_1(\xi) = - f_1(-\xi) \quad \text{(odd)}$$

Then:

$$I_3 = \mu\frac{R}{2}\dot{Y}\sin 2\theta_1\left[\oint \frac{d\xi}{1 + \epsilon\cos\xi} - 2\oint \frac{\sin^2\xi}{1 + \epsilon\cos\xi} d\xi\right] =$$

$$= \frac{\mu R\dot{Y}}{2}\sin 2\theta_1\left[\oint \frac{d\xi}{1 + \epsilon\cos\xi} - 2\left\{\frac{1}{\epsilon^2}\oint d\xi + \right.\right.$$

$$\left.\left. - \frac{1}{\epsilon}\oint\cos\xi\, d\xi + \left(1 - \frac{1}{\epsilon^2}\right)\oint \frac{d\xi}{1 + \epsilon\cos\xi}\right\}\right] =$$

$$= \mu\frac{R}{2}\dot{Y}\sin 2\theta_1\left[\left(\frac{2 - \epsilon}{\epsilon^2}\right)^2 \frac{2\pi}{\sqrt{1 - \epsilon^2}} - \frac{4\pi}{\epsilon^2}\right] =$$

$$I_3 = \frac{\mu R\pi\ 2XY}{\epsilon^2 \sqrt{1-\epsilon^2}} \left[\frac{1-\sqrt{1-\epsilon^2}}{\epsilon}\right]^2 \dot{Y} \tag{II-8}$$

$$I_4 = -\mu R\dot{X} \oint \frac{\cos^2\theta}{1+\epsilon\cos(\theta-\theta_1)}\, d\theta = -\mu R\dot{X} \oint \frac{\cos 2\theta + 1 - \cos^2\theta}{1+\epsilon\cos(\theta-\theta_1)}\, d\theta$$

the last term to the left hand side, we get:

$$2I_4 = -\mu R\dot{X} \oint \frac{\cos 2\theta + 1}{1+\epsilon\cos(\theta-\theta_1)}\, d\theta =$$

$$= -\mu R\dot{X} \left[\oint \frac{\cos 2(\xi+\theta_1)}{1+\epsilon\cos\xi}\, d\xi + \oint \frac{d\xi}{1+\epsilon\cos\xi}\right]$$

$$I_4 = -\frac{\mu R\dot{X}}{2} \left[\cos 2\theta_1 \oint \frac{\cos^2\xi - \sin^2\xi}{1+\epsilon\cos\xi}\, d\xi + \right.$$

$$\left. - 2\sin(2\theta_1) \oint \frac{\sin\xi\cos\xi}{1+\epsilon\cos\xi}\, d\xi\right] - \mu R\dot{X} \frac{\pi}{\sqrt{1-\epsilon^2}} =$$

$$= -\mu R\dot{X} \left[\frac{\pi\cos 2\alpha}{\epsilon^2\sqrt{1-\epsilon^2}} (1-\sqrt{1-\epsilon^2})^2 + \frac{\pi}{\sqrt{1-\epsilon^2}}\right] =$$

$$I_4 = \mu R\dot{X} \frac{\pi}{\sqrt{1-\epsilon^2}} \left\{ \left(\frac{1-\sqrt{1-\epsilon^2}}{\epsilon}\right)^2 \frac{Y^2 - X^2}{\epsilon^2} + 1 \right\} \tag{II-9}$$

Concluding:

$$K_x = \frac{c}{2R} \left\{ R\, P_a \oint P \sin\theta\, d\theta + R\, P_a \oint P(Y\sin 2\theta - X\cos 2\theta)\, d\theta + \right.$$

$$+ \frac{\pi}{3} \frac{\Lambda R\, P_a}{\sqrt{1-\epsilon^2}^2} \left[-2\left(\frac{1-\sqrt{1-\epsilon^2}}{\epsilon^2}\right) Y + \right.$$

$$\left.\left. + \left(\frac{c}{R}\right) \left\{ -\frac{X}{\Omega} + \left(\frac{1-\sqrt{1-\epsilon^2}}{\epsilon}\right)^2 \left(\frac{2\, XY\, \dot{y} - Y^2\, \dot{x} + X^2\, \dot{x}}{\epsilon^2\, \Omega}\right) \right\} \right] \right\} \tag{II-10}$$

Now, for ky

$$K_y = -\oint \frac{h_1}{2} \frac{\partial p}{\partial\theta} \sin\theta\, d\theta + \oint \frac{\mu R^2\Omega}{h_1} \sin\theta\, d\theta + -\mu RC \oint \left[\frac{\dot{Y}\sin\theta - \dot{X}\cos\theta}{h_1}\right]$$

$$\sin\theta\, d\theta = I_1' + I_2' + I_3' + I_4' \tag{II-11}$$

The results of the integrations are:

$$I_1' = \frac{c}{2} P_a \oint P \cos\theta \, d\theta + \frac{c}{2} P_a \oint P[X \sin 2\theta + Y \cos 2\theta] \, d\theta \tag{II-12}$$

$$I_2' = \frac{c}{R} \frac{\pi\Lambda}{3} \frac{RP_a}{\sqrt{1-\epsilon^2}} \frac{(1-\sqrt{1-\epsilon^2})}{\epsilon^2} X \tag{II-13}$$

$$I_3' = \mu R\dot{Y} \frac{\pi}{\epsilon^2} \left[(Y^2 - X^2) \left(\frac{1-\sqrt{1-\epsilon^2}}{\epsilon} \right) - \epsilon^2 \right] \tag{II-14}$$

$$I_4' = \mu R\dot{X} \frac{2\pi}{\epsilon^2} \frac{X\,Y}{\sqrt{1-\epsilon^2}} \frac{(1-\sqrt{1-\epsilon^2})}{\epsilon^2} \tag{II-15}$$

Therefore:

$$K_y = \frac{c}{2R} \Bigg\{ R\,P_a \oint P \cos\theta \, d\theta + R\,P_a \oint P\,[Y \cos 2\theta + X \sin 2\theta] \, d\theta + \\ + \frac{\pi}{3} \frac{\Lambda R\,P_a}{\sqrt{1-\epsilon^2}} \Bigg[2\,X \left(\frac{1-\sqrt{1-\epsilon^2}}{\epsilon^2} \right) + \\ + \frac{c}{R} \Bigg\{ \left(\frac{1-\sqrt{1-\epsilon^2}}{\epsilon} \right)^2 \left(\frac{[Y^2 - X^2]\dot{Y} + 2\,XY\dot{X}}{\Omega\,\epsilon^2} - \frac{\dot{Y}}{\Omega} \right) \Bigg\} \Bigg] \Bigg\} \tag{II-16}$$

Considering that $\frac{c}{r} << 1$, $\frac{x}{\omega} \sim 0(1)$, $\frac{y}{\omega} \sim 0(1)$ the expressions for k_x and k_y become:

$$K_x = R\,P_a \left(\frac{c}{2R} \right) \Bigg\{ \oint P \sin\theta \, d\theta + \oint_0^{2\pi} P\,[Y \sin 2\theta - X \cos 2\theta] \, d\theta + \\ - \frac{2\pi}{3} \Lambda \frac{(1-\sqrt{1-\epsilon^2})}{\epsilon^2 \sqrt{1-\epsilon^2}} Y \Bigg\} \tag{II-17}$$

$$K_y = R\,P_a \left(\frac{c}{2R} \right) \Bigg\{ \oint P \cos\theta \, d\theta + \oint P\,[Y \cos 2\theta + X \sin 2\theta] \, d\theta + \\ + \frac{2\pi}{3} \Lambda \frac{(1-\sqrt{1-\epsilon^2})}{\epsilon^2 \sqrt{1-\epsilon^2}} X \Bigg\} \tag{II-18}$$

APPENDIX III

SOLUTION OF TRIDIAGONAL SET OF N SYSTEMS OF TWO EQUATIONS

Consider the system:

$$\begin{cases} a_i\, x_{i-1} + b_i\, x_i + c_i\, x_{i+1} + d_i\, y_i = e_i \\ f_i\, y_{i-1} + g_i\, y_i + h_i\, y_{i+1} + i_i\, x_i = j_i \end{cases} \qquad \text{(III-1)}$$

$i = 1 \rightarrow N$

Since the terms x_o, y_o are known, in general we have relations of the type:

$$\begin{cases} x_{i-1} = A_i\, x_i + B_i\, y_i + C_i \\ y_{i-1} = D_i\, x_i + E_i\, y_i + F_i \end{cases} \qquad \text{(III-2)}$$

Then, by substitution:

$$x_i(b_i + A_i a_i) + C_i x_{i+1} + y_i(d_i + B_i a_i) = e_i - C_i a_i$$

$$y_i(g_i + E_i f_i) + h_i y_{i+1} + x_i(i_i + f_i D_i) = j_i - F_i f_i \qquad \text{(III-3)}$$

These equations can be expressed as

$$x_i\, W_i + y_i\, Z_i = R_i - c_i\, x_{i+1}$$

$$x_i\, X_i + y_i\, Y_i = S_i - h_i\, y_{i+1} \qquad \text{(III-4)}$$

Or:

$$x_i = \frac{\begin{vmatrix} R_i - c_i\, x_{i+1} & Z_i \\ S_i - h_i\, y_{i+1} & Y_i \end{vmatrix}}{\begin{vmatrix} W_i & Z_i \\ X_i & Y_i \end{vmatrix}} \quad ; \quad y_i = \frac{\begin{vmatrix} W_i & R_i - c_i\, x_{i+1} \\ X_i & S_i - h_i\, y_{i+1} \end{vmatrix}}{\begin{vmatrix} W_i & Z_i \\ X_i & Y_i \end{vmatrix}}$$

Therefore:

$$\begin{cases} x_i = \dfrac{Y_i R_i - Y_i c_i x_{i+1} - Z_i S_i + Z_i h_i y_{i+1}}{W_i Y_i - X_i Z_i} \\[2ex] y_i = \dfrac{W_i S_i - W_i h_i y_{i+1} - R_i X_i + X_i c_i x_{i+1}}{W_i Y_i - X_i Z_i} \end{cases} \qquad \text{(III-5)}$$

Comparing with III-2, we have

$$\begin{cases} A_{i+1} = -Y_i c_i/L_i; & D_{i+1} + X_i c_i/L_i \\ B_{i+1} = Z_i h_i/L_i; & E_{i+1} = -W_i h_i/L_i \\ C_{i+1} = (R_i Y_i - Z_i S_i)/L_i; & F_{i+1} = (W_i S_i - R_i X_i)/L_i \end{cases} \qquad \text{(III-6)}$$

where

$$\left.\begin{aligned} W_i &= b_i + a_i A_i \\ Z_i &= d_i + a_i B_i \\ R_i &= e_i - a_i C_i \\ Y_i &= g_i + f_i E_i \\ X_i &= i_i + f_i D_i \\ S_i &= j_i - f_i F_i \end{aligned}\right\}$$

$$L_i = W_i Y_i - X_i Z_i \qquad \text{(III-7)}$$

After evaluation of A_i, B_i, C_i, D_i, E_i, F_i, for $i = 1 \rightarrow N + 1$, use of (III-2) for $i = (N + 1) \rightarrow 1$ will give the answer to the problem.

APPENDIX IV

FINITE ORBIT PROGRAM

The programmed equations were:

$$
\left\{
\begin{aligned}
\frac{\partial\psi}{\partial T} &= \frac{1}{\Lambda}\left[H\psi\,\frac{\partial^2\psi}{\partial\theta^2} - \psi^2(1 - H) + H\left(\frac{\partial\psi}{\partial\theta}\right)^2 - \psi\,\frac{\partial\psi}{\partial\theta}\,\frac{\partial H}{\partial\theta}\right] - \frac{\partial\psi}{\partial\theta} \\
\frac{dX}{dT} &= x \\
\frac{dX}{dT} &= B \oint P \sin\theta\, d\theta + \frac{4U_1R_1}{Mc}\cos\Omega T + \frac{2K_1}{\Omega M}\left(-X + \frac{a_1}{b_1}\,[Y - Y_o]\right) \\
\frac{dY}{dT} &= \theta \\
\frac{d\,\theta}{dT} &= B \oint P \cos\theta\, d\theta + BL - \frac{4U_1R_1}{Mc}\sin\Omega T + \\
&\quad + \frac{2\,K_2}{\Omega M}\left(-\,\theta - \frac{b_1}{a_1}\,[X - X_o]\right)
\end{aligned}
\right.
$$

K_1 and K_1 are the artificial damping coefficients in the X and Y directions respectively.
a_1 and b_1 major axes of assumed elliptical whirl.

```
C       INF. JOUR. BRG. V. CASTELLI FRANKLIN INST.
     10 DIMENSION W(100), W1(100), H(100), DT(20), STHETA(100)
        DIMENSION  CTHETA(100), DHDTHE(100), W2(100)
     21 DIMENSION DXDT1(120),DYDT1(120),X1(120),Y1(120),NST(120)
        DIMENSION X2(6000),Y2(6000),LP(51,51)
        FREQUENCY 90(30),340(30),420(1,10),460(1,10),510(30,1,0),550(30),
       1630(30),660(0,1,100),670(0,1,1),730(100,1,0),740(0,0,1),763(30),
       1810(20,1,0),850(1,100),900(1,1,0),920(1,1,0)
      1 CALL LGCHAR(5,4HUX03)
     30 READ 40,N,NDT,L1,L2,L3,L4,LNSTEP,LKOUNT,NPO,NSPA,TRUNC,DXDTO,DYDTO
       1,NCASE
     40 FORMAT(2I3,I2,3I1,I4,I3,I5,I2,3E14.8,I5)
     50 FN = N
     60 DTHETA = 3.14159265*2.0/FN
     70 THETA = DTHETA
     80 N1 = N + 1
     90 DO 120 I = 2, N1
    100 STHETA(I) = SINF(THETA)
    110 CTHETA(I) = COSF(THETA)
    120 THETA = THETA + DTHETA
    121 DTHE2 = DTHETA*DTHETA
    122 D2THE = 2.0*DTHETA
    130 SENSE LIGHT 0
    140 IF(L1) 160, 160, 150
    150 SENSE LIGHT 1
    160 IF(L2) 180, 180, 170
    170 SENSE LIGHT 2
    180 IF(L3) 200, 200, 190
    190 SENSE LIGHT 3
    200 IF(L4) 220, 220, 210
    210 SENSE LIGHT 4
    220 READ 230, (DT(K), K = 1, NDT)
    230 FORMAT (5E14.8)
    240 READ 230, PLAMDA, B, PL, X0, Y0, UNBAL, DAMP1, DAMP2, ABRTIO,BNUMB
    250 READ 230, (W(I), I = 2, N1)
C       PRELIMINARY CALCULATIONS OVER. NOW SET VARIABLES
    260 T = 0.0
    261 L=0
    262 LL=0
    270 X = X0
    280 Y = Y0
    290 K = 1
    291 ASSIGN 661 TO M1
    292 NSTEP = 0
    293 ASSIGN 525 TO M2
    294 KOUNT = 0
    295 BN = 0.0
    300 DXDT = DXDTO
    310 DYDT = DYDTO
    311 BPL = B * PL
C       END OF SETTING. ENTER MAJOR LOOP
    320 SUM1 =0.0
    330 SUM2 = 0.0
    340 DO 390 I = 2, N1
    350 H(I) = 1.0 + X*STHETA(I) + Y*CTHETA(I)
    360 DHDTHE(I) = X*CTHETA(I) -Y*STHETA(I)
    370 P = W(I)/H(I)
    380 SUM1 = SUM1 + P*STHETA(I)
    390 SUM2 = SUM2 + P*CTHETA(I)
```

A 18

```
 400 G = SUM1*DTHETA*B
 410 Q = SUM2*DTHETA*B +BPL
 420 IF(SENSE LIGHT 1) 430, 460
 430 SENSE LIGHT 1
 440 G = G + UNBAL*COSF(2.0*T)
 450 Q = Q - UNBAL*SINF(2.0*T)
 460 IF(SENSE LIGHT 2) 470, 500
 470 SENSE LIGHT 2
 480 G = G + DAMP1*(ABRTIO*(Y - Y0) - DXDT)
 490 Q = Q - DAMP2*((X - X0)/ABRTIO + DYDT)
 500 T = T + DT(K)
 510 IF(T - 97.3893722) 521, 520, 520
 520 T = T - 97.3893722
 521 DXDT = DXDT + G*DT(K)
 522 DYDT = DYDT + Q*DT(K)
 523 X = X + DXDT*DT(K)
 524 Y = Y + DYDT*DT(K)
5241 L = L + 1
     LL = LL+1
5242 DXDT1(L) = DXDT
5243 DYDT1(L) = DYDT
5244 X1(L) = X
     X2(LL)=X
5245 Y1(L) = Y
     Y2(LL)=Y
     NST(L) = NSTEP + 1
5246 IF(L-100)525,5247,5247
5247 WRITE OUTPUT TAPE 15,5248,NCASE,B,(NST(L),X1(L),Y1(L),DXDT1(L),DYD
    1T1(L),NST(L+50),X1(L+50),Y1(L+50),DXDT1(L+50),DYDT1(L+50),L=1,50)
5248 FORMAT(12H1CASE NUMBER I5,4H, B= E15.8/6H0 STEP 5X 1HX 10X 1HY 10X
    15HDX/DT 10X 5HDY/DT 11X 5HSTEP 5X 1HX 10X 1HY 10X 5HDX/DT 10X
    15HDY/DT//(I6,2F11.7,2E15.7,5H **   I5,2F11.7,2E15.7))
5249 L = 0
     GO TO 525
 525 SUM3 = 0.0
 526 SUM4 = 0.0
 530 W(1) = W(N1)
 540 W(N + 2) = W(2)
 550 DO 620 I = 2, N1
 560 GAMMA = (W(I+1) + W(I-1) - 2.0*W(I))/DTHE2
 570 CSI = (W(I+1) - W(I-1))/D2THE
 580 FDT =(-(W(I)*(W(I) + CSI * DHDTHE(I))) - H(I)*(CSI*CSI + W(I)*(
    1GAMMA + W(I))))/PLAMDA - CSI)*DT(K)
 600 SUM3 = SUM3 + ABSF(FDT)
 610 W1(I) = W(I) + FDT
 620 SUM4 = SUM4 + W1(I)
 629 NSTEP = NSTEP + 1
 630 DO 640 I = 2, N1
 640 W(I) = W1(I)
 650 CONIND = SUM3/SUM4
 660 GO TO M1, (661, 665, 800)
 661 ASSIGN 665 TO M1
 662 GO TO 730
 665 WRITE OUTPUT TAPE 16,666,NCASE,NSTEP,CONIND
 666 FORMAT(9H CASE NO. I5,9H,STEP NO. I5,5H, M = E15.8)
 670 IF(CONIND - PRECM) 730, 680, 680
 680 IF(SENSE LIGHT 3) 710, 690
 690 SENSE LIGHT 3
 700 GO TO 730
```

A19

```
 710 IF(K - NDT) 720,1320,1320
 720 K = K + 1
 730 IF(NSTEP - LNSTEP) 740,750, 750
 740 IF(CONIND - TRUNC) 750, 750, 770
 750 ASSIGN 800 TO M1
 760 ASSIGN 890 TO M2
 761 WRITE OUTPUT TAPE 99, 762, NSTEP, NSTEP
 762 FORMAT(26H0 START OF ORBIT, STEP NO. I5/10H2 IN ORBIT  I5)
 763 DO 764 I = 2, N1
 764 W2(I) = W(I)
 765 GO TO 820
 770 PRECM = CONIND
 800 KCUNT = KOUNT + 1
 810 IF(KOUNT - LKOUNT) 850, 820, 820
 820 KOUNT = 0
 830 WRITE OUTPUT TAPE 16,840,NCASE,NSTEP,B,T,X,Y,DT(K),PLAMDA,(W(I),I=
    12,N1)
 840 FORMAT(6HOCASE I4,6H, STEP I5,4H, B= E14.7,7H, TIME=E14.8,4H, X=
    1F11.8,4H, Y=F11.8, 5H, DT= E14.8/9H  LAMBDA=E14.8,10X 22H  W = PH
    1 DISTRIBUTION/(1H 10F11.7))
 850 GO TO M2,(525,890)
 890 EPSIL2 = X*X + Y*Y
 900 IF(EPSIL2 - 0.98) 910, 910, 1110
 910 BN = BN + 1.0
 920 IF(BN-BNUMB)320,930,930
 930 BN = 0.0
 931 IF(SENSE LIGHT 3) 9310,9310
9310 IF(SENSE SWITCH 2)9398,9311
9311 BIGX=X2(1)
9312 DO 9315 LL1=2,LL
9313 IF(BIGX -X2(LL1))9314,9315,9315
9314 BIGX = X2(LL1)
9315 CONTINUE
9316 SMALLX=X2(1)
9317 DO 9320 LL1=2,LL
9318 IF(X2(LL1)-SMALLX) 9319,9320,9320
9319 SMALLX = X2(LL1)
9320 CONTINUE
9321 BIGY=Y2(1)
9322 DO 9325 LL1= 2,LL
9323 IF(BIGY-Y2(LL1))9324,9325,9325
9324 BIGY = Y2(LL1)
9325 CONTINUE
9326 SMALLY =Y2(1)
9327 DO 9330 LL1=2,LL
9328 IF(Y2(LL1) - SMALLY)9329,9330,9330
9329 SMALLY = Y2(LL1)
9330 CONTINUE
9331 IF(SMALLX) 9332,9333,9333
9332 SMALLX =SMALLX - 0.1
9333 LOWX = SMALLX * 10.0
     IF(SMALLY)9334,9335,9335
9334 SMALLY=SMALLY-0.1
9335 LOWY = SMALLY*10.0
9336 SMALLX = LOWX
9337 SMALLY=LOWY
9338 SMALLX =SMALLX/10.0
9339 SMALLY = SMALLY/10.0
9340 LANGEX= (BIGX-SMALLX)/0.2 +1.0
```

A20

```
      LANGEY= (BIGY-SMALLY)/0.20+1.0
      IF(LANGEX-LANGEY)9343,9344,9344
 9343 RANGE = LANGEY
      LANGE=LANGEY
      GO TO 9345
 9344 RANGE=LANGEX
      LANGE=LANGEX
 9345 RANGEY=0.20*RANGE
      RANGEX=0.20*RANGE
      BIGX=SMALLX+RANGEX
      BIGY=SMALLY+RANGEY
 9347 NPLO=(LL+NPO-1)/NPO
 9348 LLIM=NPLO*NPO
 9349 DO 9351 I=LL,LLIM
 9350 X2(I) = X2(LL)
 9351 Y2(I) = Y2(LL)
      DO 9362 NPL=1,NPLO                                      (3H X)     3H
      CALL FNPLOT(29H(24H  INF. BEAR. SHAFT ORBIT) , 8H( 3H  X) ,8H( 3H
     1Y*),SMALLX,BIGX,SMALLY,BIGY,20,1,20,1,6H(F5.2),6H(F5.2))
      L2L=NPL*NPO
      XXXXX=SPACEF(NSPA)
      CALL CURVE(X2(L2L),Y2(L2L),NPO,6H      )
      WRITE OUTPUT TAPE 99,9361,NCASE,B,NPL
 9361 FORMAT(9H CASE NO. I4,4H, B= E15.8,9H,PLOT NO. I4)
 9362 CONTINUE
 9398 LL=0
 9399 BN=0.0
  940 READ 950 , B, BNUMB, INDEX, L1, L2, L4
  950 FORMAT(2E14.8, I5, 3I2)
  960 IF(SENSE LIGHT 1)961,961
  961 IF(SENSE LIGHT 2)962,962
  962 IF(SENSE LIGHT 4)970,970
  970 IF(L1) 990, 990, 980
  980 SENSE LIGHT 1
  990 IF(L2) 1010, 1010, 1000
 1000 SENSE LIGHT 2
 1010 IF(L4) 1021,1021,1020
 1020 SENSE LIGHT 4
 1021 WRITE OUTPUT TAPE 15, 1023, INDEX, L1,L2, L4
 1022 WRITE OUTPUT TAPE 99, 1023, INDEX, L1,L2, L4
 1023 FORMAT(9H INDEX = I3, 3I2)
 1024 BPL = B*PL
 1030 GO TO(1031,1031,1091,1031),INDEX
 1031 IF(L)1033,1033,1032
 1032 WRITE OUTPUT TAPE 15,5248,NCASE,B,(NST(IN),X1(IN),Y1(IN),DXDT1(IN)
     1,DYDT1(IN), IN = 1, L)
      L=0
 1033 GO TO(1040,30,1091,1260),INDEX
 1040 DO 1050 I = 2, N1
 1050 W(I) = W2(I)
 1060 X = X0
 1070 Y = Y0
 1080 DXDT = DXDT0
 1090 DYDT = DYDT0
 1091 IF(SENSE LIGHT 4)1092,1100
 1092 READ 40,N,NDT,L1,L2,L3,L4,LNSTEP,LKOUNT,NPO,NSPA,TRUNC,DXDT0,
     1DYDT0,NCASE
 1100 IF(SENSE LIGHT 3)1340,320                                          A21
C     FAILURE PROCEDURE.SIGNAL ON THE PRINTER AND READ NEW INPUT DATA.
```

```
 1110 WRITE OUTPUT TAPE 15,1130,NCASE, B, NSTEP
 1120 WRITE OUTPUT TAPE 99,1130, NCASE, B, NSTEP
 1130 FORMAT(26H BEARING FAILURE. CASE NO.I5,4H, B= E14.7,9H,STEP NO.
     1I5/1H2)
 1140 DO 1150 I = 2, N1
 1150 W(I) = W2(I)
 1160 X = X0
 1170 Y = Y0
 1180 DXDT = DXDT0
 1190 DYDT = DYDT0
 1200 GO TO 931
C    TERMINATION PROCEDURE FOR END OF JOB. REWIND AND PAUSE.
 1260 WRITE OUTPUT TAPE 99, 1270
 1270 FORMAT(29H JOB FINISHED, MACHINE PAUSE.)
 1280 END FILE 15
 1281 END FILE 16
 1282 CALL LSCHAR(5,4HUXC3)
      END FILE 5
 1290 REWIND 15
 1291 REWIND 16
 1292 REWIND 5
 1300 PAUSE
 1310 CALL ENDJOB
C    PROCEDURE FOR CASE WHEN LIST OF DELTA T IS TERMINATED.RESTART.
 1320 WRITE OUTPUT TAPE 99, 1330
 1330 FORMAT(45H-EXHAUSTED LIST OF DELTA T.LOOK FOR NEW CASE./1H2)
 1340 SENSE LIGHT 3
 1350 GO TO 940
      END
```

A22

INFINITE JOURNAL BEARING.
FINITE SHAFT ORBIT PROGRAM

GLOSSARY

N = no. of points around shaft
NDT = no. of input values of ΔT
LNSTEP = go in orbit after LNSTEP steps
LKOUNT = print pressure profiles after LKOUNT steps
NPO = number of X-Y pairs per picture
NSPA = plot every NSPAth point
TRUNC = go in orbit when ΔP is less than TRUNC
DXDTO = $\dot{X}_0$
DYDTO = $\dot{Y}_0$
NCASE = case number
PLAMB = Λ
B = B
X0 = X_0
Y0 = Y_0
UNBAL = $\frac{4 U_1 R_1}{M C}$
DAMP1 = $2 k_1/(\Omega M)$
DAMP2 = $2 K_2/(\Omega M)$
ABRTIO = ratio of axes of assumed ellipse
BNWNB = no. of T steps before new instruction
W = PH

A23

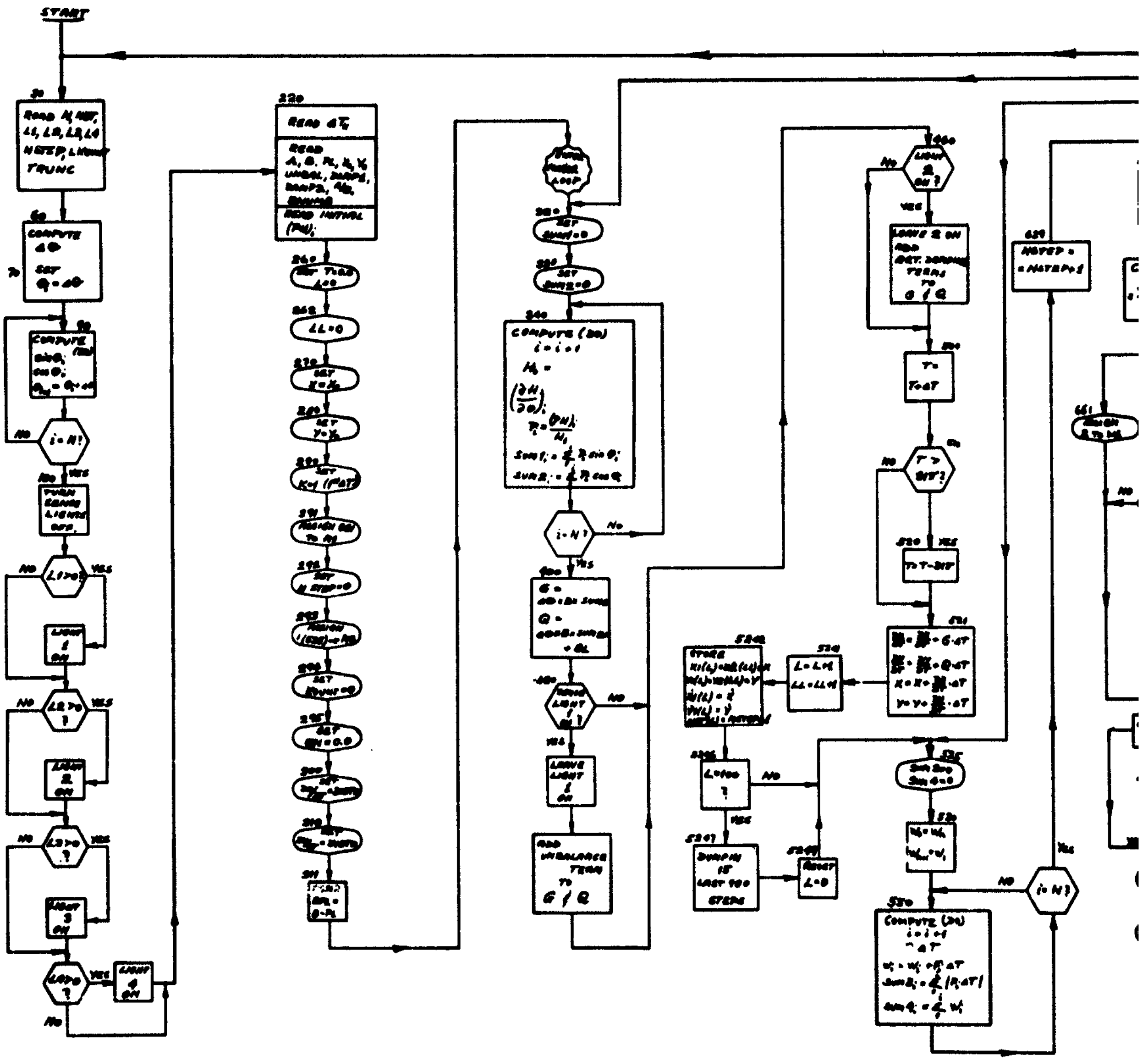
START

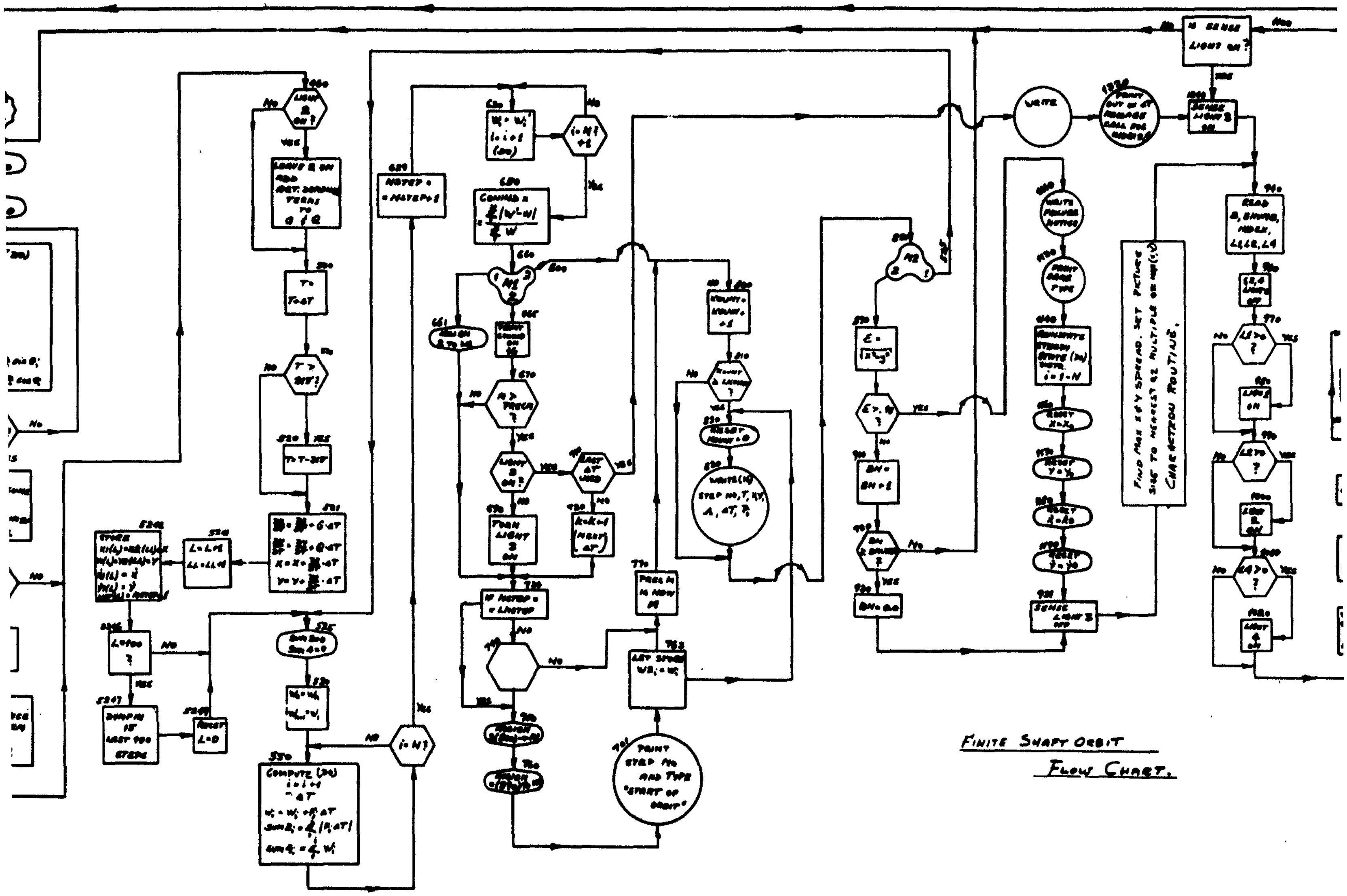

FINITE SHAFT ORBIT

FLOW CHART.

2049-20

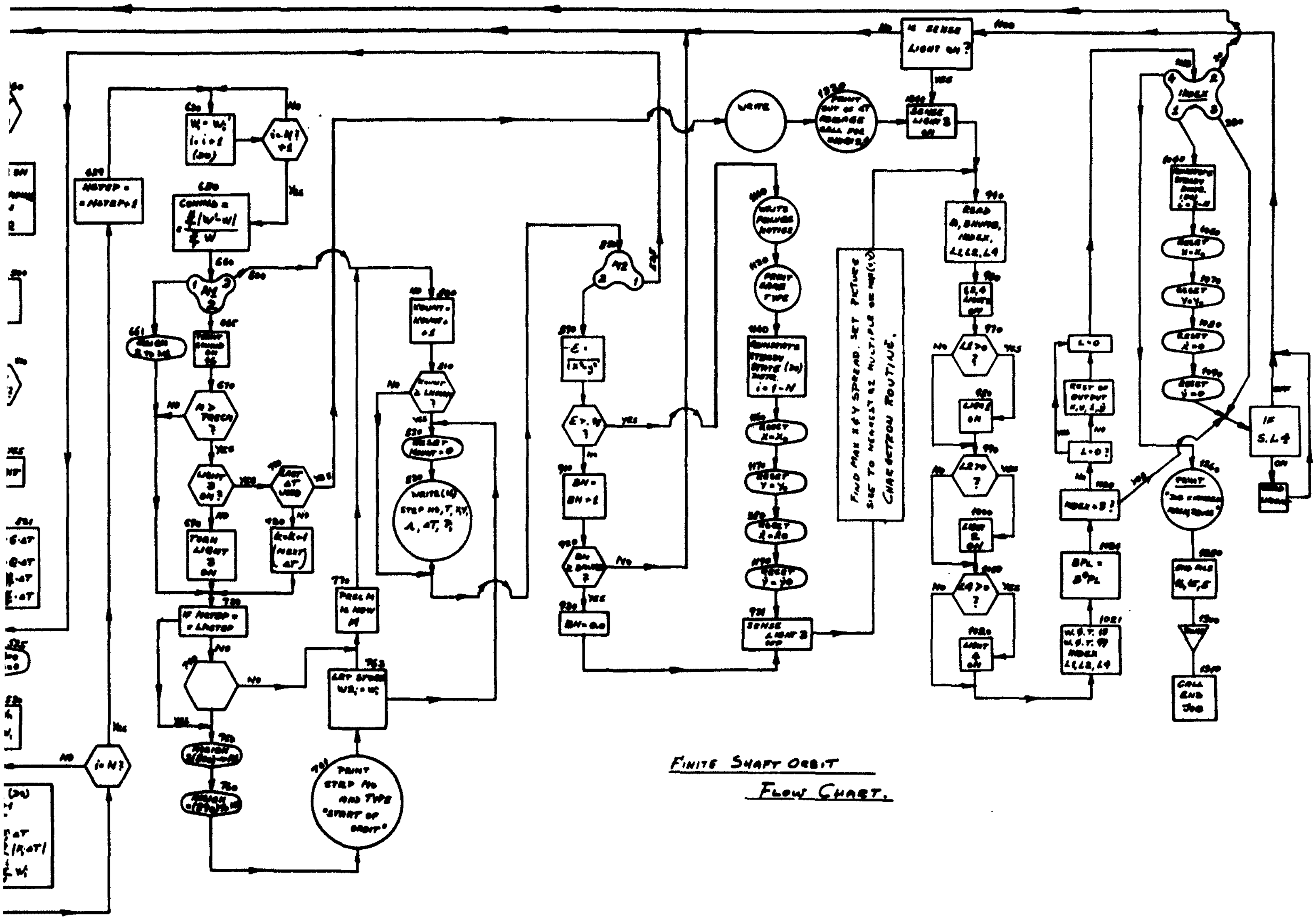

Finite Shaft Orbit

Flow Chart.

3

Auth: Letter of 3/18/63
Nonr 2342(00)
320-A2049-00

UNCLASSIFIED
W. W. Shugarts
ONR

	Technical
Chief of Naval Research Department of the Navy Washington 25, D.C. Attn: Code 438 Attn: Code 429 Attn: Code 461 Attn: Code 463 Attn: Code 466	 5 1 1 1 1
Commanding Officer Office of Naval Research Branch Office 495 Summer Street Boston 10, Massachusetts	1
Commanding Officer Office of Naval Research Branch Office 86 East Randolph Street Chicago 1, Illinois	1
Commanding Officer Office of Naval Research Branch Office 207 West 24th Street New York 11, N.Y.	1
Commanding Officer Office of Naval Research Branch Office 1000 Geary Street San Francisco 9, California	1
Commanding Officer Office of Naval Research Branch Office 1030 East Green Street Pasadena 1, California	1
Commanding Officer Office of Naval Research Branch Office Box 39, Navy #100 Fleet Post Office New York, New York	10
Chief, Bureau of Ships Department of the Navy Washington 25, D.C. Attn: Code 644B (James C. Reid, Jr.) Attn: Code 342 (E. A. Bukzin) Attn: Code 634 (E. A. Vagman)	 1 1 1

	Technical
Chief, Bureau of Naval Weapons Department of the Navy Washington 25, D.C. Attn: Codes RRMA-431 (J. W. Case) RADF-4 (S. Collegeman)	 1 1
Director Naval Research Laboratory Washington 25, D.C. Attn: Code 2000 5230	 6 1
Special Projects Office Department of the Navy Washington 25, D.C. Attn: Code SP23-A (D. Gold)	1
Head, Bearings and Seals Branch U.S. Naval Engineering Experiment Station Annapolis, Maryland Attn: Code 851 (Watt V. Smith) Mr. Robert Belt	 1 1
Material Laboratory Library Building 291, Code 912B New York Naval Shipyard Brooklyn 1, New York	1
Library Technical Reports Section U.S. Naval Postgraduate School Monterey, California	1
Commanding Officer U.S. Naval Avionics Facility Indianapolis 18, Indiana Attn: J.G. Weir	1
Director U.S. Naval Boiler & Turbine Lab. Naval Base Philadelphia 12, Pennsylvania	1
Office of Chief of Ordnance Research and Development Div. Dept. of the Army Washington 25, D.C. Attn: Norman L. Klein	1

	Technical
Fuels & Lubricants Section Research Branch Research & Development Division Office, Chief of Ordnance 4th Floor, Pentagon Annex #2 Washington 25, D.C. Attn: Mr. Ronald E. Streets	1
Chief of Research and Development Office, Chief of Staff Department of the Army Pentagon Building Washington 25, D.C.	1
Commanding General U.S. Army Engineer R&D Laboratories Fort Belvoir, Virginia Attn: W.M. Crim, Nuclear Power Field Office	2
Director U.S. Army Engineer Research and Development Laboratory Fort Belvoir, Virginia Attn: Technical Documents Center	1
Commander Army Rocket & Guided Missile Agency Redstone Arsenal, Alabama Attn: Technical Library	1
ESD - AROD Box CM, Duke Station Durham, North Carolina	1
Chief of Staff, U.S. Air Force The Pentagon Washington 25, D.C. Attn: AFRDR-AS/M	1
Commander Air Force Office of Scientific Research Washington 25, D.C. Attn: SRHM	1
Commander Aeronautical Systems Division of the Air Force Systems Command Wright-Patterson AF Base, Ohio Attn: ASRCNL-2, J.L. Morris ASRMDD, P.D. Hanlon ASRMFP-1, B.L. McFadden, Jr. ASRNCCO-1, R.W. McAdory Mr. G.A. Beane	 2 1 1 1 1

	Technical
Armed Services Technical Information Agency (TIPCR) Arlington Hall Station Arlington 12, Virginia	10
Office of Assistant Director (Army Reactors) Division of Reactor Development U.S. Atomic Energy Commission Washington 25, D.C. Attn: Mr. Clarence E. Miller, Jr.	2
Mr. N. Grossman, Chief Engineering Development Branch Reactor Development Division U.S. Atomic Energy Commission Washington 25, D.C.	1
Headquarters Library U.S. Atomic Energy Commission Washington 25, D.C.	1
Chief, Division of Engineering Maritime Administration GAO Building Washington 25, D.C.	1
Cryogenic Engineering Laboratory National Bureau of Standards Boulder, Colorado Attn: Library	1
Mr. Harold Hessing National Aeronautics and Space Administration 1512 H. Street, N.W. Washington 25, D.C.	2
Mr. Edmund E. Bisson Chief, Lubrication & Wear Branch Lewis Research Center National Aeronautics and Space Administration 21000 Brookpark Road Cleveland, Ohio	1
Mr. Rudolph Beyer George C. Marshall Space Flight Center National Aeronautics and Space Administration Guidance and Control Division Gyro-Stabilizer Branch Huntsville, Alabama	12
Mr. H.W. Savage Oak Ridge National Laboratory Post Office Box Y Oak Ridge, Tennessee	1

Technical

Chief, Technical Information
Service Extension
P.O. Box 62
Oak Ridge, Tennessee
Attn: Melvin S. Day — 1

Applied Physics Laboratory
Johns Hopkins University
Silver Spring, Maryland
Attn: George L. Seielstad,
Supr., Tech., Reports Group — 1

Department of Chemical Engineering
New York University
New York 53, New York
Attn: James J. Barker, Assoc, Prof.
of Nuclear Engineering — 1

Professor A. Charnes
The Technological Institute
Northwestern University
Evanston, Illinois — 1

Resident Representative
Office of Naval Research
c/o University of Pennsylvania
3438 Walnut Street
Philadelphia 4, Penna. — 1

Professor P. R. Trumpler
Towne School of Civil and Mechanical
Engineering
University of Penna.
Philadelphia, Penna. — 1

Jet Propulsion Laboratory
California Institute of Technology
4800 Oak Grove Ave.
Pasadena, California
Attn: Mr. Henri Sirri — 1
Attn: Library — 1

Illinois Institute of Technology
Chicago 16, Illinois
Attn: Professor L.N. Tao — 1

Professor M.C. Shaw, Head
Department of Mechanical Engineering
Carnegie Institute of Technology
Pittsburgh 13, Pennsylvania — 1

Engineering Projects Laboratory
Massachusetts Institute of Technology
Cambridge 39, Massachusetts
Attn: Dr. R.W. Mann (Room 3-459 A) — 1

Technical

Massachusetts Institute of Technology
Instrumentation Laboratory
68 Albany Street
Cambridge 39, Massachusetts
Attn: Library, W1-109 — 1

Professor P.F. Martinuzzi
Stevens Institute of Technology
Hoboken, New Jersey — 1

Battelle Memorial Institute
505 King Avenue
Columbus 1, Ohio
Attn: Dr. Russell Dayton — 1

Franklin Institute
Laboratory for Research and Development
Philadelphia, Pennsylvania
Attn: Professor D.D. Fuller — 3

Library Institute of Aerospace Sciences
2 East 64th Street
New York, New York — 1

Mr. O.B. Spoon
Sr. Member, Technical Staff
ITT Federal Laboratories
Division of International Telephone
and Telegraph Corporation
15151 Bledsoe Street
San Fernando, California — 1

Aerojet-General Nucleonics
P.O. Box 86
San Ramon, California
Attn: Barbara M. Probert — 1

Aerospace Corporation
P.O. Box 95085
Los Angeles 45, California
Attn: Aerospace Library — 1
Attn: Technical Reports Group — 1

AiResearch Manufacturing Company
Sky Harbor Airport
402 South 36th Street
Phoenix, Arizona
attn: Librarian — 1

Mr. William D. Stimmel
Research Laboratories Library
Allis-Chalmers Manufacturing Co.
Milwaukee 1, Wisconsin — 1

J.W. Fecker Division
American Optical Co.
4709 Baum Blvd.
Pittsburgh 13, Pennsylvania — 1

No. of Copies		Technical
1	American Society of Lubrication Engineers 5 North Wabash Avenue Chicago 2, Illinois	1
2	Chairman Research Committee on Lubrication The American Society of Mechanical Engineers United Engineering Center 345 East 47th Street New York 17, New York	2
1	Mr. James R. Kerr, President Lycoming Division AVCO Stratford, Connecticut	1
1	Research Precision Mechanisms Division of the Barden Corporation 4 Old Newtown Road Danbury, Connecticut Attn: B.L. Mims, Vice President General Manager	1
1	Beemer Engineering Company Industrial Park Fort Washington, Pennsylvania	1
1	Utica Division The Bendix Corporation 211 Seward Avenue Utica, New York Attn: Mr. Russell T. DeMuth Supervisory Engineer	1
1	Bendix Aviation Corporation Research Laboratories Division Southfield, Michigan Attn: Mr. Ralph H. Larson	1
1	Mr. C.R. Adams Physics Technology Department Aero-Space Division The Boeing Company Seattle 24, Washington	1
1	Bryant Chucking Grinder Company 60 Clinton Avenue Springfield, Vermont Attn: Mr. Roald Cann	1
1	Cadillac Gage Company P.O. Box 3806 Detroit 5, Michigan Attn: Mr. J. Taylor, Project Engineer	1

No. of Copies		Technical
1	Dr. Dewey J. Sandell Director of Development Carrier Research and Development Co. Carrier Parkway Syracuse, New York	1
1	Chance Vought Corporation P.O. Box 5907 Dallas, Texas Attn: Mr. R.C. Blaylock Vice President (Engineering)	1
1	Chrysler Corporation Defense Operations P.O. Box 757 Detroit 31, Michigan Attn: Mr. C.W. Snider	1
1	J.D. Mamarchev & Associates Consulting Engineers 3908 Main Street Houston 2, Texas	1
2	Mr. B.W. Birmingham Cryogenic Engineering Laboratory National Bureau of Standards Boulder, Colorado	2
1	Curtiss Wright Corporation Wright Aeronautical Division Department 8332 Wood Ridge New Jersey Attn: W.J. Derner Chief Project Engineer	1
1	Daystrom Pacific 9320 Lincoln Boulevard Los Angeles 45, California Attn: Robert H. Smith Special Project Engineer	1
1	Ford Instrument Company 31-10 Thomson Avenue Long Island City 1, New York Attn: Mr. Jarvis	1
1	Mr. Adolf Egli Ford Motor Company Engineering and Research Staff P.O. Box 2053 Dearborn, Michigan	1
1	Dr. John E. Mayer, Jr. Non-Metallics Section Applied Science Department Scientific Laboratory Ford Motor Company P.O. Box 2053 Dearborn, Michigan	1

Technical

AiResearch Manufacturing Division
The Garrett Corporation
9851 S. Sepulveda Boulevard
Los Angeles, Calif.
Attn: Jerry Glaser, Supervisor
Mechanical Lab-Dept. 93-17 — 1

General Atomics Division
General Dynamics Corporation
P.O. Box 608
San Diego 12, California
Attn: Mr. F.W. Simpson — 1

Bearing and Lubricant Center
General Engineering Laboratory
General Electric Company
1 River Road
Schenectady, New York
Attn: G.R. Fox, Manager — 2

Mr. L.W. Winn
General Electric Company
Aircraft Accessory Turbine Department
950 Western Avenue Bldg. 3-74
Lynn, Massachusetts — 1

Research Laboratories
General Motor Corporation
General Motors Technical Center
12 Mile and Mound Roads
Warren, Michigan
Attn: Mr. E. Roland Maki,
Mechanical Development Dept. — 1

A.C. Spark Plug Division
General Motors Corporation
Milwaukee 1, Wisconsin
Attn: Allen Knudsen — 1

Mr. Walter Carow
Kearfott Division
General Precision Inc.
1150 McBride Avenue
Little Falls, New Jersey — 1

Grumman Aircraft Engineering Corp.
Bethpage, Long Island, New York
Attn: Mr. David W. Craig, Jr.
Mechanical Design Section
Engineering Department — 1

Hydronautics, Incorporated
Pindell School Road
Howard County
Laurel, Maryland — 1

Technical

International Business Machine Corp.
Research Laboratory
San Jose, California
Attn: Dr. W.E. Langlois — 2

Mr. B.A. Napier, Engr. Div. Mgr.
Lear, Incorporated
110 Ionia Avenue NW
Grand Rapids, Michigan — 1

Mr. L.R. Barr, V.P.
Lear-Romec Division
Abbe Road
Elyria, Ohio — 1

Dr. Calus G. Goetzel, D/53-30
Bldg. 201, Plant 2, Palo Alto
Lockheed Missiles & Space Co.
P.O. Box 504
Sunnyvale, California — 1

Dr. J. S. Ausman
Litton Systems, Inc.
5500 Canoga Avenue
Woodland Hills, California — 2

Mr. Don Moore
Litton Systems
5500 Canoga Avenue
Woodland Hills, California — 1

Mr. A. N. Thomas
Astra Division
The Marquardt Corporation
16555 Saticoy Street
Van Nuys, California — 1

Mr. Krendall Perkins
Vice President (Engr)
McDonnell Aircraft Corporation
Lambert St. - St. Louis
Municipal Airport
Box 516
St. Louis 3, Missouri — 1

Dr. Beno Sternlicht
Mechanical Technology Incorporated
1 Herbert Drive
Latham, New York — 3

Mr. J. W. Lower
Chief, Engineer-Inertial Components
Honeywell Aero Division
2600 Ridgway Road
Minneapolis, Minnesota — 1

Technical

Mr. Carl F. Graesser, Jr.
Director of Research
New Hampshire Ball Bearings, Inc.
Peterborough, New Hampshire — 1

Mrs. Alice Ward, Librarian
Norden Division of United Aircraft Corp.
Helen Street
Norwalk, Connecticut — 1

Northrop Corporation
Norair Division
1001 East Broadway
Hawthorne, California
Attn: Technical Information, 3125 — 1

Mr. N. L. Simmons
Nortronics
A Division of Northrop Corp.
500 East Orangethorpe Avenue
Anaheim, California — 1

Nortronics
A Division of Northrop Corp.
100 Morse Street
Norwood, Massachusetts
Attn: Mr. E. L. Swainson, Tech. Asst.
Precision Products Department — 1

Pratt & Whitney Aircraft
Division of UAC - CANEL
P. O. Box 611
Middletown, Connecticut
Attn: Librarian — 1

Library, Bldg. 10-2-5
Radio Corporation of America
Camden 2, New Jersey — 1

Mr. Robert S. Siegler
Rocketdyne
Nucleonics Subdivision
6633 Canoga Ave.
Canoga Park, California — 2

Ryan Aeronautical Company
Lindberg Field
San Diego 12, California
Attn: Engineering Library — 1

Mr. M. A. Vreeland
Sanderson & Porter
72 Wall Street
New York 5, New York — 1

Technical

Jack & Heintz, A Division of
The Siegler Corporation
1725 Eye Street
Suite 505
Washington 6, D. C. — 1

Mr. Paul A. Pitt, Vice President
Engineering & Research
Solar Aircraft Company
2200 Pacific Highway
San Diego 12, California — 1

Mr. W. G. Wing
Sperry Gyroscope Company
C-2
Great Neck, New York — 1

Mrs. Florence Turnbull
Engineering Librarian
Sperry Gyroscope Company
Great Neck, New York — 1

Sundstrand Aviation-Denver
2480 West 70th Avenue
Denver 21, Colorado — 1

Mr. James W. Salassi, President
Turbocraft, Inc.
1946 S. Myrtle Avenue
Monrovia, California — 1

Universal Match Corporation
Avionics Dept. Technical Library
4407 Cook Avenue
St. Louis 15, Missouri — 1

Waukesha Bearings Corporation
P.O. Box 346
Waukesha, Wisconsin
Attn: Mr. J. M. Gruber, Ch. Engr. — 1

Mr. John Boyd
Westinghouse Electric Corporation
Research Laboratories
East Pittsburg, Pennsylvania — 1

Mr. H. Walter
Director of Research
Worthington Corporation
Harrison, New Jersey — 1

Dr. W. A. Gross
Ampex Corporation
934 Charter Blvd.
Redwood City, California — 2

	Technical
Professor J. Medrey Department of Mechanical Engineering Union College Schenectady 6, New York	2
Stratos Division Fairchild Stratos Corporation Bayshore, L. I., New York Attn: Mr. John Meacher	1
A. C. Spark Plug Division General Motors Corporation Route 128 Wakefield, Massachusetts Attn: Technical Library	1
The Cleveland Graphite Bronze Company 17000 St. Clair Avenue Cleveland 10, Ohio Attn: Mr. R. H. Josephson	1
Mr. Richard J. Matt, Manager Bearing Development & Contract New Departure Division General Motors Corporation Bristol, Connecticut	1
Mr. James J. Barker 10 Walden Avenue Jericho, New York	1
Thomson Ramo Wooldridge TAPCO Group New Devices Laboratories 7209 Platt Ave. Cleveland 4, Ohio Attn: Mr. O. Decker	1
Dr. L. Licht International Business Machines Corp. Thomas J. Watson Research Center P.O. Box 218 Yorktown Heights, New York	1
Mr. E. A. Babley Union Carbide Nuclear Co. Post Office Box P Oak Ridge, Tennessee	1
Lockheed Aircraft Corporation Missiles and Space Division Technical Information Center 3251 Hanover Street Palo Alto, California	1
Office of Technical Services Department of Commerce Washington 25, D.C.	1